Optimisation and characterisation of human corneal stromal models

Samantha Louise Wilson

Submitted for the award of Doctor of Philosophy in Biomedical Engineering

October 2013

Keele University

Abstract

The native corneal structure is highly organised and unified in architecture with structural and functional integration which mediates its transparency and mechanical strength. Two of the most demanding challenges in corneal tissue engineering are the replication of the native corneal stromal architecture and the preservation of stromal cell phenotype which prevents scar-like tissue formation. A concerted effort in this thesis has been devoted to the generation of a functional human corneal stromal model by the manipulation of chemical, topographical and cellular cues. To achieve this, previously built non-destructive, online, real-time monitoring techniques, micro-indentation and optical coherence tomography (OCT), which allow for the mechanical and contraction properties of corneal equivalents to be monitored, have been improved. These macroscopic parameters have been cross-validated by histological, imunohistochemical, morphological and genetic expression analysis.

It has been demonstrated that chemical and topographical cues can be used to manipulate the phenotype of cultured (fibroblastic) stromal cells. Tailoring the culture niche encourages stromal cells towards keratocyte, fibroblast or myofibroblast lineages. The removal of serum from media and the introduction of stiff, orthogonally arranged nanofibres caused fibroblastic cells to revert to quiescent, non-proliferative, elongated keratocyte-like cells with increased cell organisation. Through the use of cellular cues, *via* epithelial co-culturing, it has been observed that it is possible to de-differentiate fibroblastic cells to a native keratocyte phenotype *in vitro.* Importantly, it demonstrates that despite *in vitro* culturing, corneal stromal cells retain their plasticity. Furthermore, this thesis has investigated and revealed the correlation of naturally altered collagen structure caused by the ageing process and the corresponding biomechanical and cellular properties of the resulting hydrogel constructs since collagen was used as a scaffold intensively and

exclusively throughout this work. Ageing caused lower collagen viscoelasticity and cellular contractibility. All together, these studies pave a foundation for full thickness functional corneal tissue engineering.

Acknowledgements

I would like to acknowledge the help of my supervisors Dr Ying Yang and Professor Alicia El Haj. Ying, you have constantly pushed me to achieve my full potential and to achieve the best I possibly can. Your enthusiasm, dedication and hard work has allowed be to progress and become independent in my research and thinking. Alicia, you have calmed me down when things started to get too much, put things back into perspective and made once scary tasks seem more manageable.

A huge thank-you to my cornea guru, original mentor and "honouree supervisor" Dr Mark Ahearne. Your endless patience and advice has been fundamental to this work and my sanity! I hope to continue to work with you in the future, because we know corneas are the way to go!

A huge thank-you to Dr Divya Chandri, Stuart Jenkins, Professor Bill O'Farrell, Dr Andrew Hopkinson and Dr Paul Roach for your invaluable advice and time regarding my successful ETERM fellowship application. Thanks to you, I am staying in the cornea game for a least another two years! I would also like to acknowledge the Doctoral Training Centre and the people that saw something in me all those years back and gave me this unique opportunity to escape from teaching and into a career which challenges me daily.

A big thank-you to SMP, in particular to Wendy for your cooperation, assistance and endless supply of eyes!

I would like to acknowledge my colleagues whom I have had the pleasure of working with at the ISTM, whose friendship and support have made my PhD experience more enjoyable. So thank-you Hari, I dread to think of the kgs of Haribo's we have consumed...;

Kiren- my PCR princess; Khondoker, for the endless pep talks; the beautiful Angeliki; Abbie, Anto (potato!), Tina, Mikey, Kim and Rups.

I could not go without mentioning my brother from another mother, coconut and Kutti Deepz. You have been a brother to me in so many ways, through the good times and the bad, making my PhD experience at the ISTM enjoyable and manageable. From practically the first week you have indisputably offered me your support, opinion and friendship. A friendship that has carried me through my PhD and that I hope will last into the future.

I would like to acknowledge my family and parents, and apologise for becoming a bit of a hermit, particularly in the last 6 months or so of my thesis. I hope that I have done you proud. O, and thanks for the free bits of kit Dad! I will put KMF on the scientific radar! Also, thank-you to Sue and Ian for welcoming me into your home and lives. Thank-you to my brother Paul for all your technical help, don't know how you do it, but you have kept my computers working despite my endless attempts to kill them; also thanks to Kerry for the use of printing facilities- you have saved me a fortune!

Finally, I would like to thank my Alex. You have seen the best and worst of me; coped with the tears, tantrums, rants and endless presentation practices. If it wasn't for you I would have never had the confidence to apply in the first place. You have been behind me all the way, never holding me back and I love you with all of my heart for it.

I would like to dedicate this thesis to my grandparents. Grandad, without realising it you continue to keep me grounded, our Monday night coffees always put things back into perspective, make me realise what's really important and enable me to face the rest of the week. Nana, I know you are still helping me, because I have asked you for strength so many times and you have given it to me. I miss you. Forget-me-not.

Table of contents

List of Figures

List of tables

Abbreviation List

A+A	Antibiotic and antimitotic solution
AGEs	Advanced glycation end-products
AHDCS	Adult human derived corneal stromal cells
ALDH	Aldehyde dehydrogenase
ANOVA	Analysis of variance
bFGF	Basic fibroblast growth factor
BSA	Bovine serum albumin
CCD	Charge coupled device
cDNA	Complementary deoxyribonucleic acid
CEET	Chicken enucleated eye tests
CK	Conductive keratoplasty
CO_2	Carbon dioxide
DEPC	Diethyl pyrocarbonate
DMEM	Dulbecco's modified eagle medium
DMF	Dimethylformaide solvent
DMSO	Dimethyl sulfoxide solvent
DNA	Doxyribonecleic acid
ECM	Extracellular matrix
EGF	Epidermal growth factor
ELISA	Enzyme-linked immunosorbent assay

Epi-LASIK	Epipolis laser *in situ* keratomileusis
F media	Fibroblast media (serum containing)
FCS	Foetal calf serum
FGF	Basic fibroblast growth factor
FGF-2	Basic fibroblast growth factor
FITC	Fluorecein isothiocyante
Fn	Fibronectin
GAGs	Glycoaminoglycans
HCGS	Human corneal growth supplement
HCl	Hydrochloric acid
hCSSC	Human corneal stromal stem cells
HFP	1,1,1,3,3,3-hexafluro-2-propanol
HGF	Hepatocyte growth factor
HPLC	High performance liquid chromatography
HSV	Herpes simplex virus
HVPS	High voltage power supply
IGF	Insulin-like growth factor
Il-1	Interleukin-1
K media	Keratocyte media (serum free, insulin supplemented)
K* media	Advanced keratocyte media (FGF supplemented)
KGF	Keratinocyte growth factor
KS-GAGs	Keratan sulphate glycoaminoglycans
KSPGs	Keratan sulphate proteoglycans
LASEK	Laser subepithelial keratomileusis
LASIK	Laser *in situ* keratomileusis
LED	Light emitting diode

L-Glut	L-glutamine
LSCD	Limbal stem cell deficiency
LSCs	Limbal stem cell
LTK	Thermalkeratoplasty
MEM	Minimum essential medium
MMPs	Matrix metalloproteinases
mRNA	Messenger ribonucleic acid
MTT	3-(4,5-dimethythiazol-2-yl)-2,5-diphenyl tetrazolium bromide
NaHCO3	Sodium bicarbonate
NaOH	Sodium hydroxide
NSAIDS	Non steroidal anti-inflammatories
NTC	Non template control
OCT	Optical coherence tomography
PBS	Phosphate buffered saline
PCR	Polymerase chain reaction
PDGF	Platelet derived growth factor
PEO	Poly ethylene oxide
PGA	Polyglycolic acid
PHEMA	Poly(methyl methacrylate)
PK	Penetrating keratoplasty
PLDLA	Poly(L,D lactic acid)
PMMA	Poly(methy methacrylate)
PRK	Photorefractive keractomy
PTFE	Polytetrafluoroethlene
PVA	Poly(vinal alcohol)
PVC	Polyvinal chloride

qPCR	Quantitative polymerase chain reaction
RAGE	Receptor for advanced glycation end-products
RCE	Rabbit corneal epithelium
RCF	Relative centrifugal force
RK	Radial keratotmy
RNA	Ribonucleic acid
RT-PCR	Real-time quantitative polymerase chain reaction
SJS	Steven's-Johnson syndrome
SPARC	Secreted protein, acidic and rich in cystine
TACs	Transient amplifying cells
TCP	Tissue culture plastic
TEN	Toxic epidermal necrosis
TGF-β	Transforming growth factor-beta
TNA-α	Tumour necrosis factor-alpha
TRITC	Tetramethyl rhodamine isothiocyanate
TKT	Transkelotase
UV	Ultraviolet
WHO	World health organisation
α-SMA	Alpha-smooth muscle actin
2D	Two dimensional
3D	Three dimensional

Symbols list

a	Radius of the clamped portion of a hydrogel construct
C	Viscometer constant
E	Elastic modulus
h	Thickness of construct
H	The degree of alignment in a magnetic field
k	Boltzmann's constant
R	Radius of sphere/indenter
t	Time
T	Absolute temperature
v	Kinematic viscosity
δ	Vertical indentation displacement
$\Delta\chi$	Diamagnetic anisotropy of an ensemble
$\Delta\chi p$	Diamagnetic anisotropy of a single peptide bond

1. Introduction

1.1. Background

The biomechanical and viscoeleastic characteristics of tissues are vital to their integrity and function. Such characteristics vary dependent upon the tissue function and the forces that they undergo. The mechanical function of tissues operates at both macro and cellular levels as the cells within a tissue are able to create and manipulate their surrounding extracellular matrix (ECM) and thus alter the mechanical properties (Brown 2006). In corneal tissue, the overall biomechanical properties are very complex in comparison to other tissues due to the anisotropic nature of the tissue, i.e. different mechanical properties in different directions (Ruberti et al. 2007). It is the unique highly organised and unified architecture, with structural and cellular functional integration that is pivotal to tissue function with regards to transparency and vision.

The majority of corneal diseases, injuries and refractive surgery techniques can all cause changes to the corneal shape and structure, often due to a disruption of the complex tissue organisation (Anderson et al. 2004, Fullwood 2004) specifically the alteration of the fibril arrangement in the stromal layer (Fullwood 2004). This can lead to corneal scarring and opacities caused by an activation and differentiation of the native cell types which ultimately alter the mechanical properties of the cornea, resulting in vision loss. Currently, when corneal damage is excessive, the only truly successful treatment is corneal transplantation. However, although the cornea is immune privileged, transplantation still carries many risk factors and as a result, 1 in 6 full thickness transplants experience some degree of rejection (Khodadoust 2008). Arguably, the biggest current limitation to corneal transplantation is the supply of high quality donor tissue (Amano et. al 2008). This shortfall differs drastically between territories, with westernised nations generally well

provided for (Esker et al. 2012, Hara and Cooper, 2011), and demand in Africa and Asia considerably outstripping supply (Hara and Cooper, 2011, Shao et al. 2012). The increasing worldwide trend for refractive surgery procedures (Esker et al. 2012, Hara and Cooper, 2011), cultural and religious concerns related to the use of cadaver corneas (Hara and Cooper, 2011), and the short shelf-life of suitable corneas (Stevenson et al. 2012), all add to tissue shortages, resulting in over 10 million untreated patients globally (Fagerholm et al. 2010).

The current and projected donor shortages are a driver for many to develop feasible long-term alternatives to cadaveric donor tissue (Amano et al. 2008); amongst these are xenografts, keratoprostheses and tissue engineered corneas. Tissue engineered corneas offer a promising alternative capable of closely mimicking the morphological, physiological and biomechanical properties of healthy, native human corneas.

Two fundamental challenges in corneal tissue engineering are the replication of the corneal collagen architecture and the maintenance of phenotype in isolated stromal cells. If both factors are not satisfied, the result is often a regenerated tissue mimicking that of scarred native tissue. Thus far, advances in the development of a fully bioengineered cornea are still at an analytical stage (Ruberti et al. 2007). It has already been shown that the three main corneal layers can be recreated *in vitro* using collagen-based scaffolds (Griffith et al. 1999). As the native corneal environment primarily comprises of type I collagen, the use of type I collagen hydrogels are a sensible starting material.

Collagen type I hydrogels commonly used in tissue engineered tissues as scaffolds formed by conventional thermal gelation often have poor mechanical strength and lack organisation (Ruberti et al. 2007), which is contrary to the characteristics of native stroma (Kotecha 2007). Thus the biomechanical and optical properties of the tissue engineered

corneal equivalents are compromised (Boote et al. 2005). Much research has focused upon mimicking the native tissue architecture in both two-dimensional (2D) and three-dimensional (3D) cultures. Contact guidance techniques have been extensively researched as they are able to affect many cell characteristics including orientation, morphology, differentiation and secretion of ECM proteins (Vrana et al. 2007). Micro- and nano-patterned surfaces, magnetic alignment and electrospinning techniques are amongst a variety of techniques that have been explored.

The ability to construct a scaffold that has orthogonal lamellae of aligned collagen fibrils is desirable in the development of tissue-engineered corneas (Torbet et al. 2007) and has yet to be successfully achieved. Scaffolds able to mimic the native corneal organisation may be beneficial as they create a strong tissue substrate that may accelerate the healing process, aid orientation of the subsequent secreted ECM, increase the tensile strength of the construct (Wilson et al. 2012a), and potentially be used to control cell differentiation.

Retaining the native phenotype of corneal stromal cells which prevent scar-like tissue formation remains a challenge to tissue engineered corneal equivalents. It has already been established that the native keratocytes differ in a variety of ways from the injury subtypes: fibroblasts and myofibroblasts. Cell morphology, proliferation and the expression of gene products are identifiable as being significantly different (Berryhill et al. 2002). Phenotypical changes occur when a cell becomes fibroblastic and it has proven difficult to reverse such changes when attempting to culture keratocytes *in vitro*. For tissue engineered constructs to be more accurate and useful, particularly with regards to wound healing response following surgeries and exogenous factors, the phenotype of the cells, particularly the cells of the stromal layer need to be of the native healthy (uninjured) cell phonotype, i.e. the keratocytes. Currently we and other groups recognise that the culture of pure corneal cells is problematic (Schneider et al. 1999), and that removal of serum from media

alone is insufficient. Chemical cues supplied by culture media and supplementation can influence cell phenotype *in vitro*. This is not specific to corneal cells but is true for most cell types. Supplementation is required in serum-free media that can promote cell growth and proliferation of keratocytes without encouraging fibroblastic differentiation (Wilson, et al. 2012a). The optimal culture conditions of isolated corneal cells still needs to be defined as the list of biochemical components in current literature is extensive and often contradictory. Previous investigations have claimed that it is possible to de-differentiate corneal myofibroblasts back to their fibroblast phenotype (Berryhill et al. 2002). However, the main challenge still remains for researchers to de-differentiate fibroblasts to a keratocyte phenotype. Multiple growth factor and ECM signals are important to keratocyte differentiation *in vivo*. Often studies that look at the effect of biochemical cues are performed under simplified 2D tissue culture conditions, and so interactions between the keratocytes and competing environmental stimuli are not considered (Jester, Jin 2003). Thus a 3D environment in combination with chemical stimulation may be more suitable in order to more closely mimic the environmental stimuli required to successfully culture and differentiate keratocytes *in vitro*. Transparency can be restored to corneal scar tissue *in vivo* suggesting that fibroblasts are capable of returning to the keratocyte phenotype and replacing the disorganised ECM of the scarred tissue. Careful manipulation of *in vitro* culture environments are under investigation to determine a suitable niche environment that simulates native keratocyte migration and generation.

Most tissues consist of more than one cell type and it is the organisation and cross-talk of the cells within the tissue that is essential to normal development, homeostasis and in the case of corneal tissue, transparency. *In vivo,* epithelial cells are in close contact with keratocytes (Du et al. 2007, Kawakita et al. 2005) in the stromal layer; they are connected both anatomically and functionally (Wilson et al. 1999). Co-culture studies aim to

recapture this cellular anatomy and functionality by bringing together two or more cell types within the same culture environment, enabling them to interact and communicate which can act as a very powerful *in vitro* tool (Hendriks et al. 2007). The influence of cellular interactions is of particular interest to tissue engineers because the tissue formation of one or all cell types can be regulated by simulating and stimulating the natural physiology and differentiation of cells.

It has been suggested that growth factors and cytokines secreted by epithelial cells regulate keratocyte cell function and *vice versa* (Gabison et al. 2009, Nakamura et al. 2002) in a reciprocal, bidirectional manner that aid and stimulate normal migration and the secretion of proteoglycans and glycoaminoproteins in a simultaneous, highly coordinated manner which changes dependent upon development, homeostasis and wound healing; although direct cell-cell communications do occur in some situations (Wilson et al. 2003) that are vital to cell response (Kamma-Lorger et al. 2009). These interactions are critical in *in vivo* wound healing and may have important connotations for *in vitro* co-cultures. Although much work still needs to be done, it is apparent that cell-cell communication is fundamental in ensuring that the cells in the stromal layer maintain their keratocyte phenotype. Specifically, the cellular communication aids in the restoration of activated keratocytes (fibroblasts) back to a quiescent keratocyte phenotype following injury, and restoring tissue transparency which avoids excessive scarring that is detrimental to vision.

There are numerous cell based approaches that have been reported, all with the similar aim to manipulate the cells to create their own ECM so that they behave the way that they would in a natural, healthy cornea. There is a great deal of information in the cells themselves that needs to be understood as is the cells that contribute to the transparency and strength of the cornea. When developing co-culture models, it is important to balance the ability to observe, measure and manipulate cell behaviour when constructing *in vitro*

3D environments (Hendriks et al. 2007), which often results in the use of simplified models. These include the use of conditioned media (Hibino et al. 1998), transwell cultures which utilise a semi-permeable membrane (Nakamura et al. 2002, Nakazawa et al. 1997) and direct explant cultures.

Every mechanical or biological reaction to disease and/or injury has an impact on visual acuity (Dupps, Wilson 2006). The ability to mechanically characterise both the cellular and mechanical properties of tissue engineered corneal equivalents is important to understanding corneal healing mechanisms following refractive surgery techniques and changes following disease and/or injury due to wound healing responses. The tensile mechanical strength of the cornea is vital to its function (Dupps, Wilson 2006, Ahearne et al. 2010a, Ahearne et al. 2009, Ahearne et al. 2007), as cellular interactions within the collagen matrix are decided partially by the cell-matrix tension state (Grinnell 2008).

Lui and Ju (2001, 2002) initially developed an experimental technique that allowed for the non-destructive measurement of thin, circular, fragile membrane-like materials including latex and egg membranes. The technique involved the central indentation of a circumferentially clamped construct using a sphere of known weight. The central displacement is then measured. This technique was modified by Ahearne (Ahearne et al. 2007, Ahearne et al. 2008) to allow for the characterisation of cell-seeded hydrogel constructs under sterile cell culture conditions whilst fully immersed in solution and at elevated temperatures. This allows for on-line, real-time and non-destructive measurements to be taken over prolonged culture periods. The instrumentation developed to measure deformation consisted of a circular sample holder with a spherical indenter and an image acquisition system. This system has been further modified to allow for more convenient clamping of constructs allowing for faster measuring of the constructs and reduced contamination/infection risk. The mechanical properties can then be corroborated

to the changes in cellular behaviour by qPCR gene expression analysis, immunohistochemistry and morphological analysis. This confirms that the mechanical properties can act as a biomarker to determine the behaviour of the cell.

By producing more accurate corneal models that incorporate the corneal fibril organisation and the native cell phenotype whilst accounting for cellular communications into the design could potentially act as a model to be used by corneal surgeons to more accurately predict the outcome of surgical procedures; or alternatively as a more relevant human cornea substitute for drug and irritant testing in order to refine, reduce and replace animal work. Currently no reliable human corneas (or substitutes) exist for drug and toxicity testing. Often pathogens are species specific and thus human models are essential and more relevant.

1.2. Objectives

The first objective of this study is to build complexity into the current collagen corneal stromal layer model (Ahearne et al. 2010b) *via* the introduction of aligned elsctrospun nanofibre meshes. The benefit of nanofibre incorporation is threefold in that it improves the inherently weak mechanical properties and disorganised architecture of the starting scaffold material whilst having an additional effect regarding stromal cell phenotype and genotype. The development and refinement of existing non-destructive monitoring techniques (Ahearne et al. 2007, Ahearne et al. 2008) which utilise the application of optical coherence tomography (OCT), a low coherence interferometric imaging technique (Yang et al. 2007), in conjunction with a spherical indentation technique allow us to more efficiently measure corneal equivalents non-destructively under cell culture conditions with reduced construct damage and infection risks.

The second objective is to further utilise the aforementioned non-destructive imaging tools to reveal how the combined effect of biochemical ingredients and topographical features of scaffolds can be used to manipulate culture stromal cell differentiation in 2D, semi-3D and 3D culture environments in terms of cell migration, protein expression, construct contraction, mechanical properties and gene expression. The combination of non-destructive imaging tools and analysis of protein and gene expression provide important feedback mechanisms for the optimisation of cell culture conditions not previously achieved in 3D corneal stromal equivalents.

The third objective of this research is to more closely elucidate the complex mechanisms that control stromal cell phenotype, genotype and differentiation in order to restore cultured stromal cells to the native keratocyte cell lineage. The introduction of an additional epithelial culture not only allows for a more complete stromal model, but also provides a greater understanding of wound healing mechanisms and the way that cell-cell interactions are mediated. This allows us to further understand, accelerate and enhance the corneal wound healing restorative process.

The forth objective of this research is to investigate the effects that the ageing process has with regards to collagen structural changes and the subsequent effect that this has on collagen fibrillogenesis, which ultimately alters the biomechanical properties of reconstituted collagen hydrogel matrices. Intra- and intermolecular cross linking due to the accumulation of advanced glycation end-products (AGEs), with advanced ageing have been characterised *via* the measurement and monitoring of the mechanical properties of the collagen constructs; which ultimately determine cellular behaviour with regards to matrix remodelling and re-organisation.

1.3. Structure of thesis

Chapter 2 is a comprehensive review of existing literature related to this field of work. The complex structure of the cornea which is fundamental to transparency and tissue function and homeostasis are described. Medical conditions that can specifically alter the stromal architecture and biomechanical function, often detrimentally, are detailed. Corneal treatments and alternative approaches including current tissue engineering concepts and solutions are then critically evaluated. The different wound healing mechanisms which are vital to either repair or restoration of corneal transparency and function and the effectors that control such outcomes are reviewed. An examination of the fundamental challenges that are associated with tissue engineering strategies including the replication of the tissue architecture and maintenance of cell phenotype are discussed; the importance and ways of mimicking the native intrinsic and extrinsic factors are then evaluated. The potential avenue of tissue engineered corneal constructs for the use in toxicity testing and ocular drug development is explored. Finally, a thorough examination of the different approaches of mechanical characterisation of corneal tissue (and equivalents) and their pitfalls is covered.

Chapter 3 describes the fabrication and characterisation methods employed to manufacture and observe corneal stromal equivalent models. The production and optimised incorporation of aligned elctrospun nanofibres into collagen hydrogel constructs is investigated. Improvements to previous non-destructive imaging techniques and optimised procedures required to interpret and corroborate the mechanical findings are examined.

Chapter 4 studies the influence of topographical and chemical cues on the phenotypical, genotypical and mechanical behaviour of cultured adult human derived corneal stromal (AHDCS) cells in 2D, semi-3D and 3D culture environments respectively. The optimised 3D multi-layered organised collagen scaffolds determined from the previous

chapter are cellularised and examined. The effects of topographical cues provided *via* orthogonally aligned electospun nanofibres and the influence of chemical cues provided *via* media supplementation are examined. The changes in contractility and elastic modulus over time have been measured and the corresponding gene and protein expression changes are examined using immunochemical and quantitative- or real time PCR techniques (q-PCR/ RT-PCR). The potential use of macroscopic changes to act as a biomarker of cell activity is discussed. The results suggested that de-differentiation and restoration of the native keratocyte phenotype in cultured stromal cells is achievable by careful tailoring of culture environments.

Chapter 5 further builds upon the work described in the previous chapter by investigating the influence of cellular interactions *via* the utilisation of different epithelial-stromal co-culture systems. In order to more closely mimic the native niche environment three different co-culture methods have been examined; epithelial explant; transwell; the use of conditioned media and their effects on stromal cell function were studied. The different co-culture models help us to determine as to whether cell-cell interactions are due to direct cell contact or not, and as to whether the cells themselves have to be present to elicit a response. The effects of the addition of transforming growth factor beta-1 (TGF-β1) and wortmannin to the culture medias was also investigated to examine cell plasticity within the corneal model.

Chapter 6 describes the structure of collagen and the importance of this protein in tissue engineering applications. The structural changes that occur during the process of ageing which subsequently alter its biomechanical properties are discussed. The influence of different aged collagens on the mechanical and contractile properties of cell-seeded reconstituted hydrogel constructs are examined. This chapter describes how the use of non-destructive imaging modalities and the measurement of macroscopic parameters enables us

to predict microscopic differences which ultimately affect cellular behaviour and function within the construct. This provides valuable insights into the relationship between collagen molecular structure and their biomechanical properties which should be considered when manipulating and constructing *in vitro* tissues.

Chapter 7 describes the final conclusions that can be drawn from this research and summarises the main findings and achievements. In addition, recommendations regarding how this work could be explored and developed further are discussed.

2. Literature Review

This literature review is based upon the review article entitled "**Control of Scar Tissue Formation in the Cornea: Strategies in Clinical and Corneal Tissue Engineering**" which has been published in the Journal of Functional Biomaterials, volume 3, pages 642-687, 2012, doi: 10.3390/jfb3030642. In addition the review article **"Keeping an Eye on Decellularized Corneas: A Review of Methods, Characterization and Applications"** which is based on the latter half of this section has been published in the Journal of Functional Biomaterials, volume 4, pages 114-161, 2013, doi:10.3390/jfb40x000x.

2.1. Anatomy and physiology of the cornea

2.1.1. The structure and function of the cornea

The cornea comprises one-sixth of the total ocular globe (Ruberti et al. 2007) (**Figure 2.1**) with a structure described as "*the epitome of efficiently unified structure and function*" (Levin et al. 2011) due to its complexity and extracellular organisation. The avascular (Griffith et al. 1999, McLaughlin et al. 2009), sparsely populated, viscoeleastic (Glass et al. 2008, Ahearne 2007), multilaminar structure (Naylor 1953) forms a barrier to protect the intraocular contents, is transparent to visible light and forms an almost perfect optical boundary to refract light onto the retina (Aurell and Holgren, 1953), providing two-thirds of the optical power of the eye (West-Mays, Dwivedi 2006). As corneal avascularity is essential for optical clarity, oxygen and nutrient transfer are achieved *via* the corneas unique structural features. Instead of traversing red blood cells, oxygen is derived from the tear film and the aqueous humour, providing much of the corneas nutritional requirements (Levin et al. 2011). The peripheral cornea is supplied with oxygen from limbal circulation (Sutphin 2007).

In humans, corneal tissue is approximately 500 µm thick (Wray, Orwin 2009), with a diameter of approximately 12 mm (Ruberti, Zieske 2008). The integrity and transparency of the cornea are essential for preserving vision (Qu et al. 2009) and are controlled by both tissue structure and cellular tissue expression.

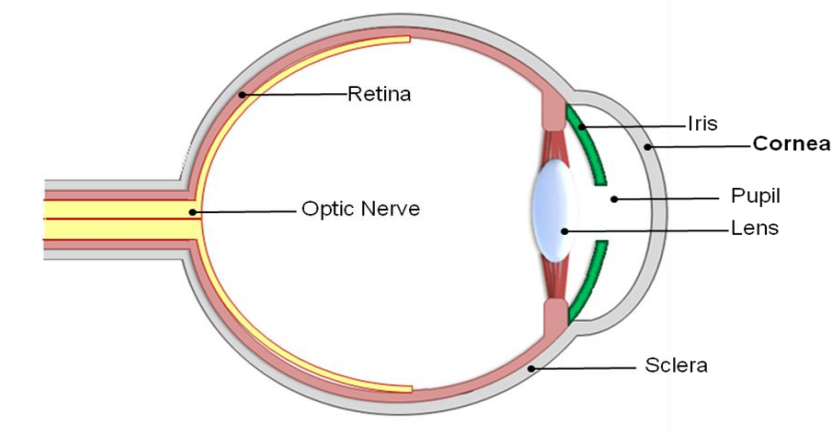

Figure 2.1: Basic anatomy of the human eye and location of the cornea.

The corneal tissue consists of five distinct layers: epithelial; Bowman's; stromal; Descemet's; and endothelial layers with the three cellular functional layers being the epithelium, stroma and the endothelium (**Figure 2.2**).

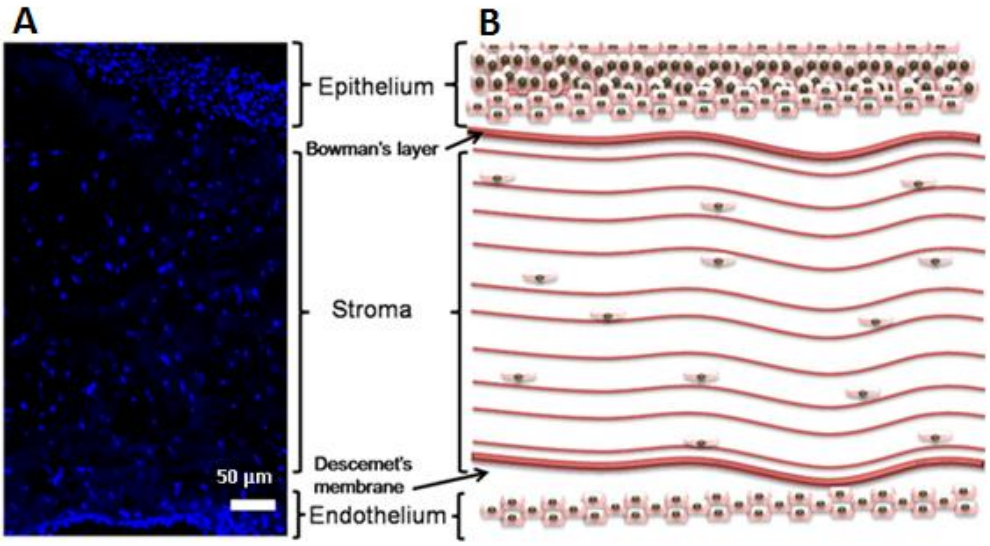

Figure 2.2: (A) DAPI stained cross section of the cornea detailing the three distinct cellular layers of the cornea; epithelium, stroma and endothelium; (B) schematic representation of the corneal layers with the additional Bowman's layer and Descemet's membrane detailed.

2.1.1.1. The epithelial layer

The epithelial layer and the tear film form the optically smooth outermost layer of the cornea that make up approximately 10% (50 µm) of the total corneal thickness (Sutphin 2007). A healthy epithelium has 5-7 layers of cells, resting on a basement membrane comprising of laminin, type IV collagen, identifiable hemidesmosomes (specialised structures linked to cell adhesion) and anchoring fibrils. The corneal epithelium has one of the body's highest densities of nerve endings (Sutphin 2007) that are sensitive to pain, i.e. when rubbed or scratched. The epithelium's main role is to protect the stroma from invasion as it restricts foreign material from entering the eye. The epithelial layer absorbs oxygen and cell nutrients from tears and then distributes them to the rest of the cornea.

The cells of the epithelial layer are highly differentiated and self-renewing, with a turnover of the entire epithelium occurring approximately every 7 days (Levin et al. 2011) thus stem cells are essential for epithelial replacement and migration. The stem cells are located in the limbal basal layer (Schermer at al. 1986). When examined microscopically

the epithelial surface of the cornea is seen as an irregular array of polygonal cells which can be divided into populations of smaller and larger cells. The smaller cells are young cells that have recently reached the surface, whilst the larger cells are more mature cells waiting to be sloughed from the surface (Levin et al. 2011).

2.1.1.2. The Bowman's layer

The Bowman's layer is a transparent sheet of tissue that lies just below the basement membrane of the epithelium. It is less complex in comparison to the other layers as the collagen fibres are randomly arranged (Germain et al. 2000). It is a dense felt-like sheet characterised by thin collagen fibrils and high levels of collagen type V (Musselmann, 2006). It aids in maintaining corneal shape and curvature and is involved in tissue remodelling following disease and/or injury (Gabison et al. 2009). It scars when damaged, resulting in vision loss if the scars are large and centrally located. The Bowman's layer is approximately 8-12 μm thick and contains collagen types I, III and V (Musselmann, 2006). It also contains collagen type IV, laminin and perlecan- a heparin sulfate proteoglycan.

2.1.1.3. The stromal layer

The stromal layer occupies approximately 90% (450 μm) of the total thickness of the cornea. It comprises of 78% water, 16% collagen and is avascular. The stroma has the most organised ECM in the body (Musselmann, 2006) and this helps to maintain corneal transparency. The ECM is made up of collagen fibres and proteoglycans. The collagen fibres are a heterogeneous mix of collagen type I (80%) and collagen type V (20%) (Wray, Orwin 2009). Collagen type VI is also present but forms a separate filamentous network that may help negotiate the interaction between collagen types I and V fibres, and proteoglycans (Nakamura et al. 1997). The stroma is responsible for the overall strength

and shape of the cornea (Fullwood 2004). Disruption to the stromal layer by disease or injury is often the cause of permanent blindness.

Corneal transparency is heavily dependent upon the highly complex levels of organisation and regular spatial order of the thin collagen fibrils within the stromal layer (Fullwood 2004, Meek, Boote 2009, Kim et al. 2012). The collagen fibrils are approximately 25-35 nm (Wray, Orwin 2009, Meek, Boote 2009) in diameter and are closely arranged (Bron 2001) parallel to each other in 200-250 nm thick layers (or lamellae) (Maurice 1956) (**Figure 2.3**). The collagen fibrils themselves are weak light scatterers as their diameters are less than the wavelength of light with a refractive index close to that of the corneal ground substances (Bron 2001). Fibril packing is denser in the anterior two-thirds and axial cornea, in comparison to the peripheral cornea (Skuta et al. 2011). The ground substances of the lamellae are a hydrated matrix rich in proteoglycans, glycoproteins, salts and keratocytes (Boote et al. 2005). Keratocytes that reside between the lamellae are responsible for the secretion of these components (Lim, Ye et al. 2007). Within the central cornea there are approximately 200-400 lamellae (Maurice, 1956) that span from limbus to limbus (Dupps, Wilson 2006). Lamellae organisation and distribution is believed to control the corneal shape and curvature.

The collagen fibrils are almost monomised in diameter (same shape and size) (Ruberti et al. 2007) across the majority of the cornea (Meek, Boote 2009), but raise abruptly from approximately 4 nm from the centre to nearly 50 nm at the limbus (Meek, Boote 2009). Fibril diameter (Meek, Boote 2009) and local interfibrillar spacing (Ruberti et al. 2007) does not alter with corneal depth, but has been shown to increase slightly with age (Meek, Boote 2004). The proteoglycans are thought to be responsible for the spatial distribution and organisation of the collagen fibrils (Fullwood 2004, Meek, Boote 2004). Electron microscopy and X-ray diffraction studies (Maurice 1988) indicate that the fibrils in

adjacent stromal lamellae are predominantly orthogonal in arrangement (Torbet et al. 2007). It is the nanoscale organisation of the stromal layer that is responsible for the corneas strength, clarity and its ability to refract light.

2.1.1.4. The Descemet's membrane

The Descemet's membrane is a thin (approximately 15 µm thick) but strong barrier against infection and injury and helps to maintain the curvature of the cornea (Ahearne 2007, Jakus 1956). The Descemet's membrane is derived from secretions of endothelial cells (Kaufman et al. 2001) and has the ability to regenerate after infection.

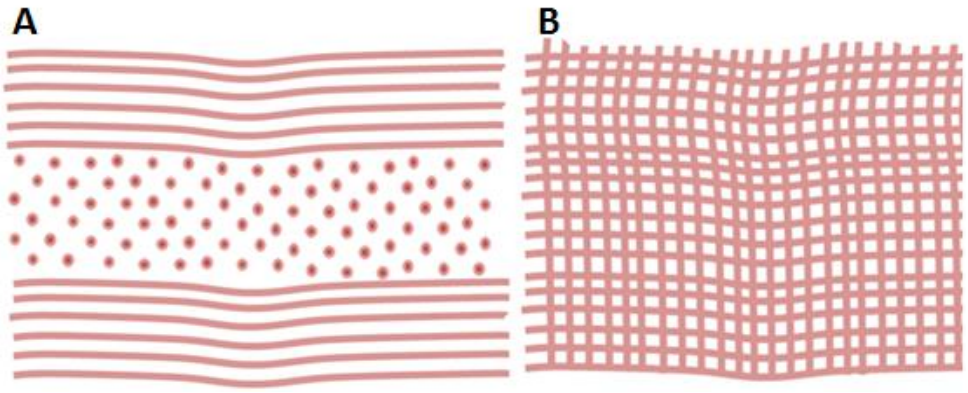

Figure 2.3: A schematic representation of (A) a cross sectional view; (B) a top view of the microstructural arrangement of parallel collagen fibrils; the collagen fibrils within the stromal layer are arranged parallel to each other in regularly spaced lamellae sheets.

2.1.1.5. The endothelium

The endothelium is a very thin, innermost layer of the cornea. It is made up of closely interdigitated cells arranged in a mosaic pattern of mostly hexagonal shapes (Sutphin 2007). It is essential for keeping the cornea clear as it pumps excess fluid out of the stroma. This prevents stromal swelling, hazing and ultimately the occurrence of an opaque stromal layer. Human endothelial cells do not proliferate *in vivo*, but they can divide *in vitro*.

Endothelial cell loss results in enlargement and spread of neighbouring cells to cover the defective area (Sutphin 2007). Therefore, damage to the endothelial cells results in permanent destruction which leads to corneal edema (swelling) and blindness.

2.2. Corneal diseases

Corneal diseases are vast and diverse with epidemiologies encompassing an array of infectious and inflammatory diseases. Corneal diseases are the second most common cause of vision loss and irreversible blindness to cataracts (Huang, Li 2007, Allan 1999) globally affecting over 10 million patients (Huang, Li 2007, Carlsson et al. 2003a) usually manifesting as a badly damaged ocular surface (Allan 1999) and/or changes to the shape and thickness of the cornea (Anderson et al. 2004). 180 million people worldwide are acutely visually disabled (although not classed as blind) discounting the further hundreds of millions affected by monocular visual loss (Whitcher et al. 2001). The occurrence of corneal blindness is variable from country to country and between populations (Whitcher et al. 2001). The prevalence is also accustomed to the availability and standards of eye care. For example, in some parts of Africa and Asia, corneal scarring is 20 times more likely than in industrialised countries.

A great deal of research is focused upon diseases of the cornea as they are often responsible for changes in shape and thickness of the cornea (Anderson et al. 2004) which may lead to permanent opacities which ultimately lower visual acuity (Miller 2002). Historically, corneal blindness has been caused by disease including, although not exclusive to, trachoma, onchocerciasis, leprosy, opthalmia neonatotrum, xerophthalmia and opthalmia neonatorum. However, blindness due to ocular trauma, corneal ulceration and complications from using traditional medicines are becoming more commonplace. A

summary of corneal diseases specifically linked to scar tissue formation is provided in **Table 2.1**.

Table 2.1: Corneal diseases linked to scar tissue formation; their epidemiology, causes and treatment.

Disease	Epidemiology	Causes	Treatment	Further information
Fuchs' dystrophy	Deterioration of endothelial cells. Loss in efficiency of pumping water from stroma. Swelling and distortion of cornea. Changes in the cornea's curvature. Hazing. Tiny blisters on corneal surface. Glare and light sensitivity. Bilateral blindness.	Thought to be inherited, autosomal dominant trait (Gottsch et al. 2003). Gene mutation strongly suspected.	Salt solutions such as sodium chloride drops or ointment are often prescribed to draw fluid from the cornea and reduce swelling. Contact lenses. Hair dryer to dry out corneal blisters.	Short-term success with transplantation, but long-term survival is a problem. Incurable.
Leprosy	Blindness. Chronic uveitis. Cataract formation. Exposure keratitis. Reoccurring corneal ulcers. Corneal scarring. Vascularisation.	*Mycobacterium laprae* usually affects the anterior segment of the eye (Whitcher et al. 2001).	Multi-drug therapy using dapsone, rifampicin and clofazamine.	Corneal complications caused by leprosy are a significant cause of corneal blindness globally affecting 250,000 people, predominantly in Africa and Southern India.
Ocular trauma and ulceration	Unilateral vision loss. Ulceration. Corneal perforation. Endophthalmitis. Phthisis. Blindness. Hyphaemas (Thylefors 1992). Ruptured globes.	Mechanical trauma, debris entering the eye, chemical and thermal burns. Workplace activities, such as mining injuries, agriculture and warfare. Road accidents. Domestic accidents (Thylefors 1992).	Corneal transplant. Antibiotic and antifungal treatments although visual outcome usually poor (Whitcher, Srinivasan et al. 2001).	Ocular traumas are becoming more prevalent causes of scarring and blindness. Worldwide, half a million people are blind as the result of trauma (Whitcher et al. 2001, Thylefors 1992).

Disease	Epidemiology	Causes	Treatment	Further information
Onchocerciasis (river blindness)	Destructive chorioretinitis. Blinding keratitis Acute corneal scarring. Vascularisation.	Caused by a parasite *Onchocerca volvulus* (Whitcher, Srinivasan et al. 2001). .	Invermectin kills the microfilaria (larval form) and sterilises the adult worm to prevent spread in infected individuals.	Incidences of onchoceriasis have decreased since the introduction of invermectin in the 1980s.
Opthalmia Neonatorum (conjunctivitis of the newborn)	Bilateral scarring. Blindness.	Infection caused by *Neisseria gonorrhoeae.* Herpes simplex virus (HSV) can also cause childhood corneal blindness by causing opthalmia and xerophthalmia, although such infections are infrequent in infants.	Saline washes. Antibacterial eye ointments. Treatments with tetracyanite/ erythromycin/ silver nitrate ointments.	Blindness risk is reduced when opthalmia neonatorum is caused by less virulent pathogens such as *Chlamydia trachomatis* (Whitcher, et al. 2001).
Stevens-Johnson Syndrome (SJS) also known as Erytheme multiform	Subepithelial bullae. Scarring. Keratinocyte apoptosis of the surrounding skin and epidermal necrolysis. Erosion of mucous membranes (Roujeau et al. 1995). Bilateral blindness (Koizumi et al. 2001).	Drugs including sulphonamide, anticonvulsants, salicytes, non-steroidal anti-inflammatory drugs (NSAIDs) and penicillin (Roujeau, et al. 1995). Infection, such as Herpes Simplex virus (HSV). *Streptociocci*, adenovirus and microplasma (Koizumi et al. 2001).	Withdrawal of all potential causative drugs (Koizumi et al. 2001). Intravenous fluid replacement. Immunosupressive therapy. Corneal stem cell transplant. Corneal transplant.	<100 drugs associated with SJS (Roujeau et al. 1995). Most severe cases referred to as toxic epidermal necrolysis (TEN). Transplanted tissue often rejected.

Disease	Epidemiology	Causes	Treatment	Further information
Trachoma	Vascularisation. Ocular surface problems. Entropion. Trichiasis.	Bacterial infection trachoma caused by *Chlamydia trachomatis* (Whitcher et al. 2001). Infection can be transmitted from eye to eye *via* contaminated fingers, clothes, make-up and flies.	Corneal transplant. The disease is preventable *via* antibiotic treatment with azithromycin; however more antibiotic treatment is still required to prevent further progression of the infection to corneal blindness in previously infected individuals (Whitcher et al. 2001).	World's leading cause of ocular morbidity and blindness (Whitcher et al. 2001).
Xerophthalmia (dry eye syndrome).	Night blindness. Xerosis. Corneal perforation. Scarring. Irreversible blindness (Pirie 1976).	Collagenase secretion, caused by the influx of inflammatory cells is believed to be responsible for the rapid destruction of the xerophthalmic cornea (Pirie 1976). 70% of cases are due to a vitamin A deficiency (Whitcher et al. 2001, Pirie 1976).	Artificial tears. Increase humidity of surroundings. Vitamin A supplementation.	Xerophthalmia patients are predominantly infants or young children, with a peak age of approximately 2.5 years (Pirie 1976).

The majority of corneal diseases are the result of some form of disruption to the fibril arrangement in the stromal layer (Fullwood 2004) and are a major cause of blindness worldwide. Unfortunately, many of the current treatments are not cost effective and can only alleviate, or treat secondary symptoms of the disease and fail to cure the underlying cause. Prevention, in the case of most diseases, would be more cost effective and successful in eliminating corneal blindness. However, extensive investigation is still required to help us to understand the underpinning mechanisms that lead to permanent scarring in diseased and injured corneas.

2.3. Current corneal treatments

2.3.1. Refractive surgery techniques

With the trend occurring that most individuals will at some stage in their life go on to develop some form of refractive error, ophthalmic surgery needs to develop and progress in order to provide sufficient treatment for preserving or restoring vision. José Barraquer first recognised that small changes in the curvature of the cornea can dramatically affect its refractive ability, and in 1976 introduced the first lamellar refractive surgery techniques (O'Keefe, Kirwan 2010). Photoablation of corneal tissue was reported by Trokel *et. al.* (1983) and showed evidence of changes to the refractive power of damaged corneas. Since then, variations of refractive surgery techniques have come into practice, with the common aim to alter and improve the refractive power of the cornea.

Thermalkeratoplasty (LTK) and conductive keratoplasty (CK) involve the heating the cornea to a critical temperature of 58–76°C inducing collagen shrinkage, thus altering the corneal curvature to make it steeper (Skuta et al. 2011). LTK is a non-contact treatment whereby a holmium laser is used to heat the corneal collagen. CK is a contact treatment involving the use of a radiofrequency diathermy probe inserted directly into the cornea (Skuta et al. 2011). Both techniques have problems associated with local necrosis if the temperature is too high and if the heat source is not consistent or uniformly administered, resulting in variable astigmatism (unequal corneal curvature) (Skuta et al. 2011).

Radial keratotomy (RK) is an incisional technique used to treat myopia and hyperopia. However, the technique is often superseded by excimer laser treatments. The procedure includes making tiny cuts in the cornea, which flattens it, reducing the curvature of the cornea (Newall 1981) and decreasing the refractive power (Skuta et al. 2011).

Photorefractive keratectomy (PRK) was the first form of laser ablation (Trokel et al. 1983) that permanently alters the refractive power of the eye using an argon fluoride laser

with predictable outcomes and is commonly used to treat myopia. In corrective PRK a wound is created *via* mechanical epithelial debridement and surgical removal of the corneal disc (Tuft et al. 1993), followed by laser ablation of the basement membrane and anterior stroma (West-Mays, Dwivedi 2006, Gabison et al. 2009), leaving a smooth wound remaining. This encourages corneal flattening as most of the corneal tissue is removed centrally, with less removed around the peripheral area (O'Keefe, Kirwan 2010). Initially, the technique was favourable over RK, as it appeared that following the PRK procedure that corneal mechanical properties are maintained and an increased reproducibility between patients was observed (Tuft et al. 1993).

Laser *in situ* keratomileusis (LASIK) or Epipolis LASIK (Epi-LASIK) is currently the prevailing refractive surgery (Camelin 2003). During LASIK the epithelium is mechanically separated below the basement membrane and just above the Bowman's layer. It is favourable to PRK as the epithelial layer and cells are well preserved and so act as a protective layer preventing exposure to tears and the ablated stroma. This is important as tears contain growth factors and cytokines associated with fibrotic response and scarring.

Laser subepitheial keratomileusis *(*LASEK) was originally called alcohol assisted flap PRK as it is a combination of PRK and LASIK techniques (Azar et al. 2001, Camelin 2003). The technique involves the chemical reduction of the adhesion molecules that attach the epithelium to the Bowman's layer. A marking trephine (cylindrical blade) 8-9mm in diameter is placed onto the surface of the cornea and a dilute alcohol solution is added to loosen the epithelium (Azar et al. 2001). The epithelium is lifted and peeled back as a complete flap and the surface of the cornea is dried and ablated with an eximer laser. The epithelial layer is then repositioned and a bandage contact lens covers the wound for 3-5 days allowing for re-epithelialsation (Azar et al. 2001). LASEK is sometimes preferred by

patients over LASIK as it has a lower risk of corneal estacsia (O'Keefe, Kirwan 2010) and a faster healing and rehabilitation period (O'Keefe, Kirwan 2010).

The change in corneal curvature elicited by external surgeries or removal of corneal issue, no matter how small or procedure, inevitably provokes a wound healing response. Currently, the only truly successful treatment available for many corneal diseases is corneal allografting. Although the cornea is immune privileged, transplantation carries many risk factors. There are numerous alternatives that are being investigated in order to replace donated tissue (Vrana et al. 2007), or to possibly suppress the demand for donated tissue (Pang et al. 2010). Amongst these are xenografts, keratoprostheses, decellularised/acellular matrices and Tissue Engineered corneas.

2.3.2. Corneal allografting

Corneal allografting is often referred to as corneal transplant, keratoplasty or penetrating keratoplasty (PK). The graft replaces the damaged central corneal tissue with healthy corneal tissue from the same species. Unlike other forms of tissue transplantation, corneal allografting is routinely performed without the aid of prior tissue typing or systemic immunosuppressive drugs unless the patient has had prior problems regarding rejection. The cornea and corneal allografts are often referred to as immune privileged due to its avascular nature (Niederkorn 2003), however clinicians often object to this proposition as immune rejection is the leading cause of corneal graft failure and remains as a barrier to successful transplantation (Niederkorn 2003). Corneal allografts are in fact immunogenic (capable of inducing alloimmune responses) and antigenic (susceptible to antigen specific responses by alloimmune effectors). The rate of corneal graft rejection is variable amongst studies and may be due to differences in patient population, diagnostic rejection criteria and immunosuppressive treatments (Baradaran-Rafii et al. 2007). Grafts onto inflamed

recipient corneas reject most frequently and rapidly (Coster et al. 2009). Once inflamed, a cornea is never the same with regards to immune privileges. Rejection of the donor endothelium is the principal source of transplant failure. Rejection of allograft materials most commonly occurs within 4-18 months post transplantation, but can be seen anytime following surgery (Baradaran-Rafii et al. 2007) sometimes years after surgery (Niederkorn 2003). Risk factors that lead to graft rejection involve surgery technique (loose sutures and premature suture removal), the extent and severity of vascularisation in the recipient, the number of regrafts, bilateral grafting, inflammation, glaucoma, dermatitis and dry eye conditions (Baradaran-Rafii et al. 2007).

2.3.3. Xenografts

Xenografts are when tissue(s) from one species are transplanted into a different species. They are advantageous in that they offer a virtually unlimited tissue source and scheduling is independent of the availability of a human donor (Boneva, Folks 2004). Porcine corneas are commonly used as they have a similar physiology to human corneas and are relatively easy to obtain (Pan et al. 2007). The prevailing problem concerning xenografts is interspecies differences leading to graft failure and disease transmission (Ahearne 2007, Boneva, Folks 2004). Reports of corneal xenotranplantation models often show different results in different species, so the mean survival time varies from days to months (Pan et al. 2007), but all eventually fail due to immune response. Glucocorticoids are often used as immune suppressants as they block inflammatory mediator release and inhibit cytokine production. However, more research into immune suppression following surgery is still required as the precise mechanism of corneal xenografts rejection is still unknown (Pan et al. 2007).

Commonly, the rhesus monkey is used in xenotransplantation studies as it shares anatomical, histological and immunological responses to humans, thus can act as a predictor of clinical performance. However they may not faithfully represent what would happen if a porcine cornea was transplanted into a human subject because non-human primates may develop immunity against human proteins expressed in pigs (Pan et al. 2007). Ultimately, it is the risk of cross-species disease transmission that has given the public a poor perception of xenografts; which prevents technique from developing further than pre-clinical stage research.

2.3.4. Keratoprostheses

Keratoprostheses were essentially the first form of artificial corneas (McLaughlin et al. 2009) and offer hope to patients with dry eye conditions such as severe ocular surface disease, chemical burns or corneal vascularisation (Zerbe et al. 2006). Surgery is usually only offered to patients with bilateral corneal blindness or those unsuitable for allografting (Allan 1999).

A keratoprosthesis is an acellular artificial implant that ideally should be biologically, mechanically and functionally anchored to the eye tissues without biological and mechanical adverse side-effects (Pintucci et al. 1995), permit light transmission in the visible range and protect the retina from ultraviolet (UV) damage (Ruberti et al. 2007). The majority of keratoprostheses are based upon a transparent central optic, surrounded by an anchoring "skirt" that promotes cellular integration from the host (McLaughlin et al. 2009, Allan 1999) (**Figure 2.4**). A keratoprosthesis that has undergone clinical trials is AlphaCor™ originally known as the Chirilia Keratoprosthesis (Hicks et al. 1997, Eguchi et al. 2004, Chirila 2001). AlphaCor™ comprises of cross linked poly(2-hydroxethyl methacrylate) (pHEMA), which is one of the most extensively examined materials for

keratoprostheses. AlphaCor™ has been implanted into human patients with promising results achieved (Eguchi, Hicks et al. 2004); however, patient maintenance of the device is principle to its success post-surgery (Ruberti et al. 2007).

The Boston Type 1 (Zerbe et al. 2006) is another commonly used keratoprosthesis in the United States that has undergone clinical trials. It consists of two plates made from poly(methyl methacrylate) (PMMA) with a titanium locking ring to hold the back plate in place. PMMA is the most frequently used keratoprosthesis material and can be made in UV absorbing forms for intraocular lenses. It can be shaped and preserves clarity whilst having low toxicity (Ruberti et al. 2007), but its rigidity and hydrophobicity mean diffusion (of corneal essential nutrients, growth factor, cytokines and oxygen) is often poor.

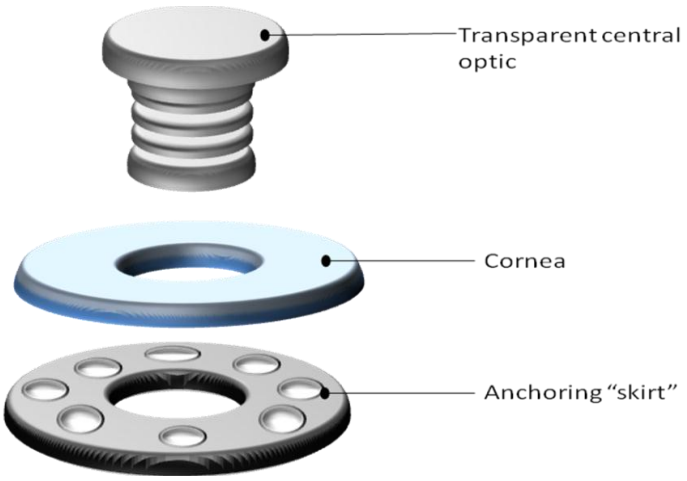

Figure 2.4: A schematic diagram of an atypical keratoprosthesis.

Advances in implantable synthetic optical materials have been prolonged and labour intensive (Ruberti et al. 2007). The procedure to implant a keratoprosthesis is complicated and to date, clinical use of keratoprostheses is limited.

2.3.5. Decellularised scaffolds

Acelular corneal matrices have been examined (Xu et al. 2008, Tegtmeyer et al. 2001) as a possible scaffold material for *in vitro* corneal reconstruction as they can potentially provide an ideal structure for corneal epithelial and endothelial adhesion and proliferation (Xu et al. 2008). Porcine corneal acellular matrix is regularly used by researchers due to its relative anatomic similarity to human corneas and easy availability. Rabbit limbal epithelial cells, keratocytes and endothelial cells have all reportedly been grown on a porcine acellular corneal matrix (Xu et al. 2008). The rationale behind this study was that if corneal cells from another species (i.e. a rabbit) could be supported by a porcine decellularised scaffold then it could potentially be used to facilitate the restoration of the human cornea in certain corneal diseases. Decellularisation of porcine tissue has been detailed by Gonzalez-Andrades *et. al.* (2010), however reproductions of such techniques are often variable in efficacy and difficult to reproduce. There is currently no reliable or standardised protocol for decellularisation of human corneas. In order to be a viable technique it needs to be determined that the decellularisation process is successful in eliminating all cells and debris without disrupting the tissue architecture which is vital to corneal integrity, optical behaviour and transparency. Additionally a technique needs to be established whereby infiltration of the cell types is successful with regards to cell phenotype and that they adopt the native phenotypes rather than an injury, fibroblastic or myofibroblastic phenotypes. The future challenge of corneal research is to move away from animal models and into human tissues. This avoids xenogenetic, infection and rejection problems associated with using animal tissues. To date decellularised corneas have only been implanted into rabbits. Although the results for this model suggest that the implants were well integrated with the host after a month, interspecies differences may mean that this is not necessarily the case in humans.

2.3.6. Tissue engineered corneas

Tissue engineering (TE) can be described as "*the production of biological or semi-synthetic living tissue for use as replacement tissues for damaged or diseased tissues*" (Suuronen et al. 2004). Technically speaking, it is the generation of a tissue by seeding isolated, specific cells into or onto a template (often referred to as a scaffold) and culturing it in a dynamic environment with the aim to eventually form a tissue which mimics the morphological, physiological and biochemical properties of the natural tissue as closely as possible. With respect to corneal TE there are many challenges that need to be addressed, not least the fact that the structure of the cornea is unique and difficult to replicate. Two fundamental challenges in corneal TE are the maintenance of phenotype in isolated stromal cells and the replication of the collagen architecture. If both factors are not satisfied, the result is often a regenerated tissue mimicking that of scarred native tissue. Thus far, advances in the development of a fully bioengineered cornea are still at an analytical stage (Ruberti et al. 2007). However, recently there have been reports related to the success of acellular corneal matrices in Phase I clinical trials (Fagerholm et al. 2010). Furthermore, at the time of this review, there were a further three registered clinical trials involving the use of decellularised corneal tissue (NIH, 2013), which is a promising outlook with regards to corneal tissue engineering. At present when attempting to construct a TE-cornea tissue strength and transparency are the main areas of focus as these are lacking in current models (Guo et al. 2007). A more in-depth review of TE corneas and their challenges can be found in **section 2.6.**

2.4. Mechanisms of wound healing in the cornea

The ability of the cornea to remain transparent can become compromised when the cornea is exposed to trauma, infection, ulceration or chronic inflammation (Etheredge et al. 2009). Much of the knowledge concerning corneal wound healing is derived from animal studies (Steele 1999), and although they are scientifically valuable, anatomical differences (such as the lack of a Bowman's layer in rabbit eyes) mean that some caution should be exercised when extrapolating animal models to human clinical findings (Steele 1999). Corneal wound healing and the mechanisms involved are complex and include a cascade of cytokine mediated interactions between epithelial, stromal and endothelial cells, corneal nerves, lacrimal glands, tear film and cells of the immune system (Agrawal, Tsai 2003, Eraslan, Toker 2009). Activation of these mechanisms attracts immune cells which are responsible for eliminating debris and microbes that penetrate into the stroma (Agrawal, Tsai 2003). However, it should be noted that most of the mechanisms that occur during wound healing are similar to those that occur during normal homeostasis (Agrawal, Tsai 2003). In general, corneal wound repair occurs in 3 overlapping phases including re-epithlisation and migration; cell proliferation and synthesis; and the remodelling of the underlying ECM (Agrawal, Tsai 2003, Zieske et al. 2000) with many growth factors and cytokines stimulating one or more of these phases during repair (Zieske et al. 2000). The interaction of the cytokines leading to a network-like action is pivotal to the final outcome of wound healing (Agrawal, Tsai 2003). The wound healing response and resulting tissue changes are dependent upon the size, depth (Steele 1999, Agrawal, Tsai 2003, Mulholland et al. 2005), the species of animal (West-Mays, Dwivedi 2006), and inciting injury, with the severity of the response affecting the overall outcome (Eraslan, Toker 2009). Tear quality and integrity is also of importance as tear deficiencies can compromise the wound healing process (Steele 1999). The principal purpose of any wound healing response is to

regain anatomical and functional capacity in the fastest and most perfect way. Elsewhere in the body, wound healing often ends in scar formation and vascularisation, where as one of the most vital aspects of corneal wound healing is the minimisation of such results which would otherwise have serious visual consequences (Steele 1999). Healing of corneal tissue is slower than other connective tissues; possibly due to its avascularity (Steele 1999).

The remodelling process of the injured stroma is vital to the resulting architecture of the tissue deposited following injury (Eraslan, Toker 2009). The synthesis, breakdown and cross-linking of collagen are all involved in the strengthening and stabilisation of the wound and such processes can last for months or years. The remodelling process is able to alter the architecture of the initial repaired tissue so that it reverts to that of a non-injured state. Understanding these mechanisms and the factors involved may aid in the development of therapeutic agents which can speed up this process.

In mammals when a tissue is damaged a fibrotic response is usually activated which heals the tissue, but fails to restore full function (Fini 1999). However, in some instances such as during foetal wounding or some corneal wounding healing takes on a regenerative capacity whereby full function is restored. A theory of "activation" has been suggested by Fini (1999) where upon cells that undergo fibroblastic differentiation in response to injury will *repair* tissue; whereas cells that are able to proliferate in response to injury without activation will *regenerate* the damaged tissue. The subtle difference between the two could be the difference between an opaque tissue and a functioning transparent tissue. One of the most demanding challenges of corneal biology is to assist tissue repair *via regeneration* rather than *fibrosis* (Wang et al. 2011).

2.4.1. Regeneration

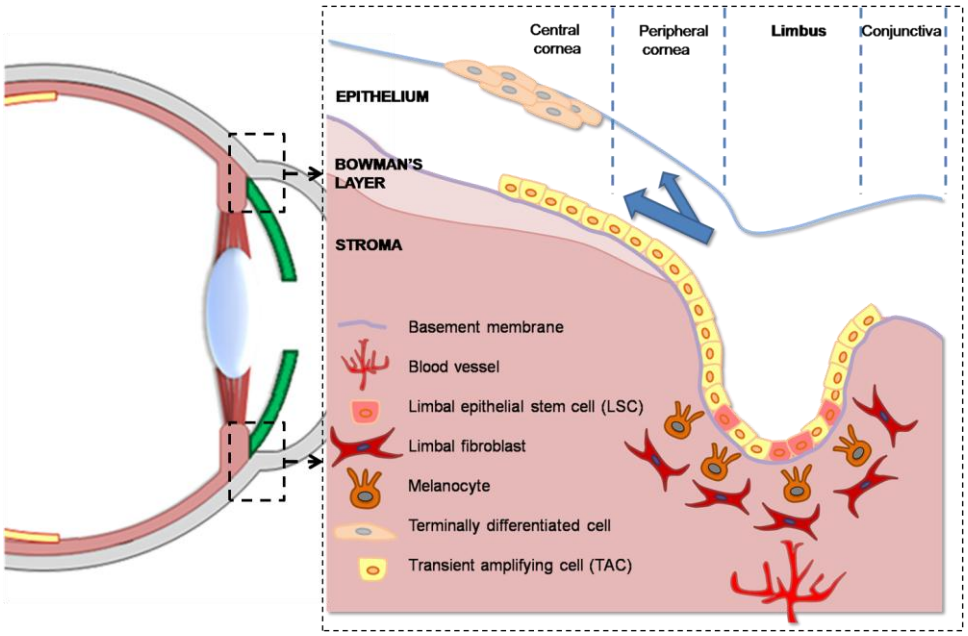

Figure 2.5: Schematic representation of the limbal area of the cornea and its location.

There are a number of stem niches in ocular tissue that are vital to maintenance, repair and regeneration (Ruberti et al. 2007); these include limbal stem cells (LSCs). LSCs are capable of self-renewal and generate daughter cells that can continue to differentiate until they are eventually shed (Scheremer 1986). *In vivo* the epithelium is regularly renewed from a population of relatively undifferentiated cells found in the basal layer of the corneal limbus (**Figure 2.5**). LSCs are normally slow-cycling, self-renewing cells that produce transient amplifying cells (TACs). TACs are capable of multiple rounds of division, although this does not usually occur during normal homeostasis (Agrawal, Tsai 2003). Proliferation to generate more TACs occurs dependent upon the necessity, i.e. more proliferation occurs during regeneration (it can increase up to nine-fold) following a corneal wound. Epithelial repair is critical to the healing process (Mulholland et al. 2005) and regeneration. Re-epithelialsation does not occur one layer at a time; there is a gradient

of basal and suprabasal cells from opposite directions that meet in the centre (Agrawal, Tsai 2003).

The adjoining stromal layer is important to stem cell density, although the exact mechanism controlling this remains elusive. Complex intercommunications between the stem cells and their surrounding microenvironment are pivotal to this role (Ruberti et al. 2007). Stromal regeneration, as opposed to repair, is dependent upon highly coordinated cellular interactions between epithelial and keratocyte cells (Tuft et al. 1993). As keratocytes originate from a population of neural crest cells, it has been postulated that some of the regenerative properties exhibited by these cells following corneal wounding could be attributed to their stem-like properties retained from their cell of origin (West-Mays, Dwivedi 2006). An example of keratocyte regeneration is the healing of epithelial debridement wounds. In these cases, where the epithelium has been scraped away exposing the basement membrane, the keratocytes beneath the membrane undergo apoptosis. Mitosis of the adjacent cells occurs, which replace the cells, and no additional response occurs (West-Mays, Dwivedi 2006). The initial cell apoptosis is thought to occur to prevent an inflammatory response occurring which may affect corneal transparency, which effectively protects the cornea from self-harm.

Preservation of the basement membrane has also been attributed to the difference between regeneration and scarring (Gabison et al. 2009, Ainscough et al. 2011) as it is important in the regulation of epithelial-stromal interactions (Gabison et al. 2009). An intact basement membrane hinders epithelial pro-fibrotic cytokines and growth factors (Gabison et al. 2009), preventing their production whilst promoting re-epithilisation, which provides effective anti-fibrotic protection to both the epithelium and stroma.

2.4.2. Scar formation

Scaring of the cornea occurs for many reasons; debris and/or chemicals entering the eye, infection, inflammation and diseases of the cornea can all lead to permanent scarring. Injuries to the cornea manifest as changes in cell phenotype particularly in the stromal layer. The disruption of the Bowman's layer and Descemets's membrane are also both key steps in initiating tissue remodelling (Gabison et al. 2009). A fibrotic response usually involves rapid contraction and closing of the wound space by activated keratocytes (fibroblasts) followed by scarring. However, keratocyte activity does not manifest until the corneal surface has been fully re-epithelialised (Steele 1999). In the case of a fibrotic response in corneal wound healing opaque scar tissue will ultimately interfere with vision and the strength of the corneal scar tissue will never match that of uninjured tissue (Steele 1999). The primary stages of wound healing involve removal of the injured tissue, followed by cell proliferation and migration to the wound site. Here repair and replacement occurs before the wound healing procedure has ended (Baldwin, Marshall 2002).

During scarring a change in collagen or proteoglycan structure alters the usually highly organised lattice structure, thus decreasing the optical properties of the cornea. Corneal scar tissue is hazier, lass elastic, with lower mechanical properties than a normal, healthy adult cornea (Tuft et al. 1993). Increased cellularity of the scar (Etheredge et al. 2009), vacuolation (an increased number of vacuoles present), or light scattering occurring due to a modified collagen fibril arrangement have all been linked to corneal haziness. Transparency can improve over time as the fibril arrangement nears normal, although vacuoles remain. Even after prolonged periods of healing (up to 18 months), original collagen structure and cross linking is not restored, thus scar remodelling is never perfect and remains incomplete, i.e. it never returns to its pre-injured state.

Endothelial integrity is also pivotal to the maintenance of corneal transparency (Steele 1999). The endothelial cells are often disrupted during corneal, trauma, disease and surgeries which leads to stromal dehydration and hazing (Zieske et al. 2000). Over hydration of the endothelium can also cause corneal opacity, due to the loss of the tight junctions and integrity of the epithelium during wounding, which consequently affects cell membrane permeability leaving the cornea vulnerable to infections by microbes (Agrawal, Tsai 2003). The invasion of microbes disrupts cytokine-mediated control of healing which decreases endothelial fluid transport, thus increasing stromal hydration (Agrawal, Tsai 2003). As many as 80% of endothelial cells can be lost before decomposition occurs (Steele 1999). Endothelial cells in humans and primates have minimal or no capacity to proliferate and thus endothelial wound healing is dependent upon the enlargement and migration of the surrounding cells to cover the wound site (Schultz et al. 1994). Endothelial cells *in vitro* have limited proliferative capacity (Zieske et al. 2000) and so the use of growth factors may have a key role in regulation and stimulation of the healing endothelial layer.

In some contexts scar formation represents foetal corneal synthesis in that the fibrils secreted in the initial stages of a scar are comparable to the diameter of the parallel bundles of fibrils secreted during embryogenesis (Tuft et al. 1993, Kamma-Lorger et al. 2009). However, differences are apparent with respect to the reduction in the ratio of interfibrillar type VI collagen to type I collagen in scar tissue compared to the developing cornea, and lack of the original organised template in foetal tissue.

2.5. Effectors to control the outcome of corneal wound healing

2.5.1. Phenotype differentiation in the corneal stroma

Quiescent keratocytes inhabit the stromal layer in a healthy cornea *in vivo* (Fini 1999, Jester, Jin 2003, Builles et al. 2006, Berryhill et al. 2002, Pei et al. 2004). When viewed in cross section they appear as sparsely populated flattened cells located between the collagen lamellae. However, when viewed *en face* they appear as broad cells that form an elaborate network (Fini 1999) interconnected by long dendritic processes (West-Mays, Dwivedi 2006) (**Figure 2.6B)** joined by gap junctions (Ainscough et al. 2011). The main function of the keratocyte is to maintain the balance of stromal substances by synthesising new collagens and proteoglycans, whilst secreting collagenase amongst other enzymes to degrade old stromal matrix (Pei et al. 2004). Keratocytes contain highly expressed proteins known as crystallins, which contribute to the transparent nature of the cornea.

During wound healing, an epithelial slide is initiated at the wound edge. This is independent of cell division and cell migration is achieved *via* a migration of slow cycling stem cells situated in the basal layer of the limbus (Tuft et al. 1993). The epithelial layer thins over protruding areas of the wound and thickens over the wound area, effectively producing an even, smooth corneal surface (Tuft et al. 1993). The epithelial cells co-ordinate with the keratocytes in the stromal layer below *via* cytokine release mechanisms, which aid and stimulate migration and proliferation. The cytokine release attracts inflammatory cells (such as macrophages and T-cells) into the stroma, resulting in an inflammatory response (Wang et al. 2011).

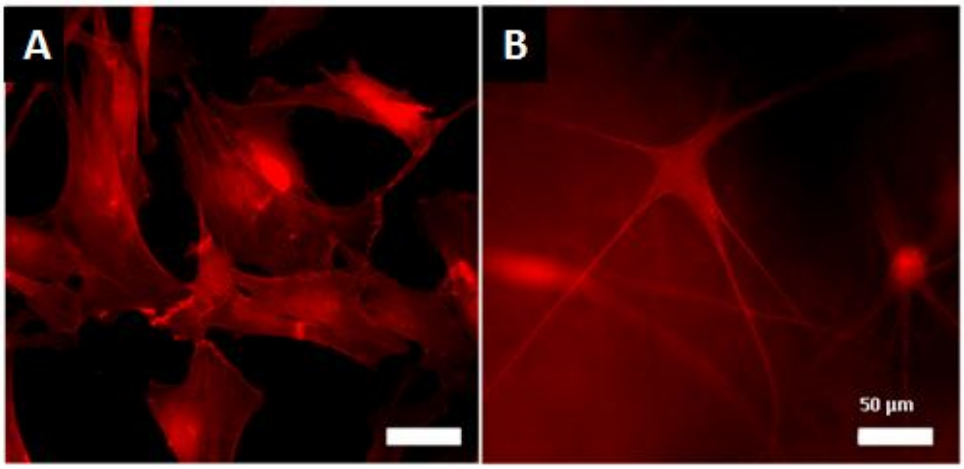

Figure 2.6: F-actin stained fluorescent images showing differences in morphology of a fusiform fibroblast (A) compared to the smaller, more dendritic shaped keratocyte (B), scale bar = 50 µm.

This inflammatory response initiates phenotypical changes to the keratocyte. Previous *in vivo* studies on rats (Fini 1999), cats (Jester et al. 1995) and rabbits (Fini 1999, Matsuda et al. 2009) have enabled the changes of a keratocyte into an activated repair fibroblast to be observed (Fini 1999). Keratocytes in close proximity to the wound edge undergo apoptosis and disappear within a few hours, leaving an acellular area. This activates the keratocytes flanking the acellular area within 6–24 hrs after the initial injury. Ultrastructural and biochemical studies demonstrate that keratocytes are markedly different from fibroblasts (**Figure 2.6**) with regards to intracellular distribution of filamentous actin and form stress fibers characteristic of myofibroblast-like cells (Garana et al. 1992). These changes allow usually quiescent cells to migrate to the injured area and proliferate. This process can last up to 7 days. Corneal fibroblasts are greater in size than keratocytes with a fusiform shape. They secrete higher levels of ECM proteins and enzymes (Beales et al. 1999, Funderburgh et al. 2003) and so are able to reconstruct and repair the injured tissue. The differences in composition of ECM synthesised by corneal fibroblasts in comparison to keratocytes may account for the opacity of the resulting repair tissue (Fini 1999), as the resulting scar tissue has a different composition compared to healthy tissue. Epithelial cells are gradually

moved upwards and their remaining attachments are combined into the resulting scar. Keratocyte activity reverts to normal usually after 3 months (Tuft et al. 1993), although hypercellularity (an abnormally large number of cells) can remain for years.

During wound closure a subpopulation of corneal fibroblasts appears: the myofibroblast. Myofibroblasts are greater in size, less mobile and exert greater contractile forces on a tissue in comparison to fibroblasts (Helary et al. 2006). Myofibroblasts are fundamental to wound contraction and scarring (Bernstein et al. 2007, Nakamura et al. 2002). They are characterised by the presence of actin fibers, including α-smooth muscle actin (α-SMA) (Jester et al. 1995, Helary et al. 2006) which helps to convey contractile properties of the cell (Fini 1999, Jester et al. 1995). Optical transparency may return with time, but even after 6 months the cells in the scar are not normal keratocytes, although they may share many similar characteristics (Fini 1999). Corneal fibroblasts and myofibroblasts have been identified *in vivo* many weeks after the injury has occurred (Ahearne 2007, Netto et al. 2006). It is still not fully explained if the fibroblasts and myofibroblasts ever fully revert back to the uninjured keratocyte phenotype both morphologically and biochemically. It has been hypothesised that corneal fibroblasts can partially return to the original keratocyte phenotype but some fibroblastic characteristics are retained (Berryhill et al. 2002, Wilson, et al. 2012a). It has been suggested that myofibroblastic differentiation is not activated by stromal injury alone and it is in fact a consequence of both stromal and epithelial injury (Nakamura et al. 2002). The precise involvement of the corneal epithelium in corneal stromal wound healing is not known, although deviations of its barrier function render it permeable to cytokines and growth factors from the tear film. These may then penetrate into the stromal layer, thus causing activation of the residing keratocytes (Ainscough et al. 2011).

2.5.2. Growth factors

In a healthy, uninjured cornea cell generation and loss, and the quantities of growth factors that stimulate and inhibit, are balanced. Injured cells generate cytokines- powerful peptide or glycoprotein regulatory factors that serve as autocrine or paracrine agents to control cell communication, migration, proliferation, protein synthesis (Tuft et al. 1993) inflammation, differentiation and angiogenesis (Baldwin, Marshall 2002). Cytokines regulate both epithelial and stromal wound healing responses (Ruberti et al. 2007). The cytokines are thought to originate from the lacrimal gland, conjunctiva and conjunctival vessel that are secreted into the tear film during would healing with differing concentrations measured in accordance to different corneal pathologies (Baldwin, Marshall 2002).

Wound healing is regulated by a vast assortment of growth factors, including but not exclusive to platelet derived growth factor (PDGF), epidermal growth factor (EGF), transforming growth factor beta (TGF-β), basic fibroblast growth factor (FGF, also known as bFGF, βFGF and FGF-2), the interleukins (Il-1, Il-6, Il-8), tumor necrosis factor alpha (TNF-α) (Tuft et al. 1993), insulin-like growth factor (IGF) (Lakshman, Petroll 2012), keratinocyte growth factor (KGF) and hepatocyte growth factor (HGF) (Nakamura et al. 2002). *In vivo* all these growth factors differentiately co-ordinate keratocyte proliferation, cytoskeletal organisation and ECM synthesis (Lakshman, Petroll 2012) *via* complex cascade mechanisms (Eraslan, Toker 2009). Growth factors are able to act on corneal tissues through autocrine (self-acting, the growth factor acts upon the cell that produces it; e.g. TGF-β), paracrine (growth factor acts upon cells in the vicinity of the emitting cell; e.g. KGF and HGF) or juxtacrine (affecting both emitting cells and cells in the vicinity; e.g. PDGF) fashions (Imanishi et al. 2000, Klenkler, Sheardown 2004) and the presence of multiple growth factors have varying responses dependent upon their relative

concentrations (Klenkler, Sheardown 2004). The effects of growth factors on a cell type can vary dependent upon ECM environment (Klenkler, Sheardown 2004). The binding of growth factors to ECM leads to sequestration or controlled release that may regulate or enhance the growth factor effect (Klenkler, Sheardown 2004). Upon binding, integrin signaling, shape and cytoskeletal tension, which control cell cycle progression initiated by growth factors are changed (Klenkler, Sheardown 2004). Cells stimulated by growth factors cause them to produce or alter ECM and promote migration *via* enhanced integrin expression, affinity or cytoskeletal interactions (Klenkler, Sheardown 2004).

Epithelial cells secrete type I cytokines including TGF-β, Il-1, and PDGF (Ruberti et al. 2007). TGF-β and PDGF in particular are powerful chemotactic agents and mitogens (stimulate mitosis) for fibroblasts and can initiate wound contraction (Kim, Zhou et al. 2012, Nakamura et al. 2002). TGF-β is arguably the most documented growth factor associated with corneal wound healing in literature and recent investigations into molecular therapy have been focused upon the inhibition of myofibroblast differentiation *via* the targeting of TGF-β isoforms (Eraslan, Toker 2009).

TGF-β1 is the most commonly documented isoform that induces fibroblastic and myofibroblastic differentiation. In addition, TGF-β2 has been established as the primary mediator of fibrosis and scarring as it is believed to play a role in the development of excessive ECM build up (Petroll et al. 1998) and along with TGF-β1 increases fibrotic gene marker expression (Karamichos et al. 2011) such as α-SMA and collagen type III. Both TGF-β1 and –β2 are very potent growth factors that are capable of blocking epithelial, lymphocyte and hepatocyte cell proliferation promoted by KGF, EGF and HGF (Imanishi et al. 2000, Klenkler, Sheardown 2004), whilst stimulating the proliferation of mesenchymal originating cells such as fibroblasts. Interestingly, the TGF-β3 isoform has

been shown to act as an inhibitor of fibrosis and scar development (Karamichos et al. 2011), and has been shown to promote scar-free healing.

PDGF exists as a dimeric glycoprotein comprised of two A (AA) and two B (BB) chains, or a combination of the two (AB) (Imanishi et al. 2000). PDGF can facilitate TGF-β myofibroblast differentiation *via* an autocrine feedback loop (Lakshman, Petroll 2012). PDGF-BB stimulates keratocyte proliferation, upregulation of the secretion of normal stromal ECM and migration of both keratocytes and fibroblasts (Lakshman, Petroll 2012, Grinnell 2008). PDGF-AB on the other hand has been shown to differentiate keratocytes to fibroblasts, evident *via* the development of stress fibers, local adhesions and contraction in 3D collagen matrices (Lakshman, Petroll 2012). Similarly, PDGF-BB is able to significantly increase the growth of endothelial cells *in vivo* where as PDGF-AA does not (Imanishi et al. 2000). However neither TGF-β, Il-1, nor PDGF will exert their proliferation, chemotaxis or differentiation effects on stromal cells under normal homeostatic conditions (Gabison et al. 2009).

Il-1α and soluble Fas ligand are cytokines released by epithelial cells in response to injury (Wilson et al. 1999) and have been associated to the upregulation of HGF (Eraslan, Toker 2009) and KGF (Agrawal, Tsai 2003), and acting in synergy with EGF to accelerate epithelial wound closure (Agrawal, Tsai 2003). Il-1α is a master modulator of the wound healing cascade (Eraslan, Toker 2009). However, unwounded keratocytes do not produce Il-1α (Wilson et al. 1999). Keratocytes only produce Il-1 when exposed to the cytokine following epithelial injury as it cannot pass into the stromal layer as the epithelial barrier function blocks it. Keratocytes exposed to Il-1 enter a self-perpetuating autocrine loop (Eraslan, Toker 2009) that controls the production of HGF and KGF by keratocytes which effectively regulates epithelial healing and keratocyte proliferation and apoptosis (Imanishi et al. 2000, Wilson, Liu et al. 1999). Il-1 also initiates the synthesis of collagenases, matrix

metalloproteinases (MMPs) and other enzymes by keratocytes which are involved in collagen remodelling during healing. Il-1 and PDGF are usually only secreted by epithelial cells under physiological conditions, where as their corresponding receptors are expressed by stromal cells (Gabison et al. 2009), demonstrating the need for cross-talk between cell types.

Type II cytokines moderate both epithelial and fibroblast cells and include IGF and FGF. IGF stimulates keratocyte proliferation and migration (Imanishi et al. 2000) whilst maintaining cell morphology, cytoskeletal organisation, and keratocan sulphate synthesis.

Fibroblasts produce type III cytokines including KGF and HGF which are important signalling molecules in regulating epithelial-mesenchymal interactions (Baldwin, Marshall 2002). KGF and HGF (also known as scatter factor (Klenkler, Sheardown 2004, Bussolino et al. 1992) both stimulate epithelial cell proliferation. KGF (a member of the FGF family; Imanishi et al. 2000) stimulates growth of limbal and conjunctival epithelial cells where as HGF is involved in the proliferation and control of peripheral epithelial cells, with the dominant factor dependent upon the wound site (Agrawal, Tsai 2003); EGF has similar effects and is a known potent mitogen of epithelial cells (Klenkler, Sheardown 2004). It is thought that EGF acts as a basic facilitator for epithelial proliferation where as KGF and HGF are up-regulated dependent upon the amount of damage (Agrawal, Tsai 2003). HGF also promotes epithelial motility, aiding in the spatial arrangement of the cells (Bussolino et al. 1992) and prevents epithelial terminal differentiation (Gabison et al. 2009).

2.5.3. Matrix components

The majority of the corneal stroma is comprised of collagen I, V, VI and XII, along with dermatan sulphate proteoglycan decorin and keratan sulphate proteoglycans (KSPGs) lumican, keratocan and osteoglycin (mimican) (Bron 2001, Carlson et al. 2003) which form the ground substances of the stroma. Keratan sulphate comprises of approximately 50% of all the stromal glycoaminoglycans (GAGs) present in the stroma (Bron 2001). Keratocytes are the major cell type in a healthy cornea. As of yet there is no single defined molecular marker for the keratocytes cell type although they do express lumican and keratocan to develop and maintain collagen interfibrilliar spacing and fibril diameter (Carlson et al. 2003).

Keratocan is a cornea specific protein only expressed in healthy corneas and keratocytes (Carlson et al. 2003). *In vivo*, following initial injury keratocan expression is not detectable. It may return during and following the healing process, albeit in significantly lower levels than in an uninjured cornea (Carlson et al. 2003). Similarly, *in vitro* keratocan expression is lost when stromal cells are cultured in the presence of serum (Carlson et al. 2003, Wilson et al. 2012a).

Lumican belongs to a small leucine-rich proteoglycan family and is a major KSPG (Hayashi et al. 2010). The non-glycanated lumican core protein is distributed extensively in numerous interstitial connective tissues including the sclera, aorta, cartilage and liver (Hayashi et al. 2010). However, in the cornea it is found in a glycanated form, meaning keratan sulfate GAGs (KS-GAGs) have bound to the central protein. This binding is thought to be involved in the control of fibril diameter, with the extended KS-GAG side chains controlling fibril spacing and corneal hydration required for tissue integrity and transparency. In studies on lumican knock-out mice, abnormally large collagen fibrils and disorganised interfibrillar spacing occurs (Hayashi et al. 2010), confirming that the key role

of lumican is concerned with maintenance of fibril architecture *via* fibril assembly arrangement and balancing the KS-GAG levels required for transparency. It may also act as a regulatory molecule for cellular functions including proliferation, migration and prevention of apoptosis in injured epithelium, and modulation of keratocan and aldehyedehydrogenase (ALDH, an important modulator of corneal metabolism) expression *via* keratocytes (Hayashi et al. 2010).

Decorin is a small leucine rich protein that plays a key role in many cellular tissues in a variety of tissues including the cornea (Mohan et al. 2011). It is the predominant dermatan sulphate proteoglycan in the cornea (Funderburgh et al. 1998) but is also found in the majority of connective tissues. Decorin is expressed in both healthy and injured corneas (Funderburgh et al. 1998) where it interacts with growth factors such as EGF and TGF-β to mediate processes such as fibrillogenesis (Mohan et al. 2010), ECM metabolism, cell-cycle progression (Mohan et al. 2011) and remodelling following injury. Decorin expression increases significantly in response to injury which has led to it often been associated as a marker for corneal fibrosis and scarring (Funderburgh et al. 1998).

Healing corneas share many characteristics of the developing cornea in that they both appear to have unusually thick collagen fibrils and irregular spacing and primarily synthesise collagen types I and V (Kamma-Lorger et al. 2009). Heavily opaque corneal scarring has also demonstrated the phenomenon of abnormally large fibril diameters. The increase in collagen fibril diameter in response to injury prevents normal swelling in the subsequent scar tissue from developing, causing disruption of corneal homeostasis (Kamma-Lorger et al. 2009). As proteoglycans are hydrophilic molecules, their presence may increase spacing between the fibrils making them appear larger (Kamma-Lorger et al. 2009). However, studies performed on bovine corneas (Kamma-Lorger et al. 2009) demonstrate that intermolecular spacing between collagen fibrils is similar in both injured

and uninjured corneas. Thus the increase in fibril diameter is not necessarily caused by the swelling usually observed during healing that may push the collagen molecules apart. The increased fibril diameters may be due to a fusion of adjacent collagen fibrils, caused by a deficit of proteoglycans in the newly synthesised tissue (Kamma-Lorger et al. 2009).

2.5.4. Mechanical stress

The tensile mechanical strength of the cornea is vital to its function and the mechanical properties are essential for linking morphology to mechanical behavior (Dupps, Wilson 2006, Ahearne et al. 2010a, Ahearne et al. 2009, Ahearne et al. 2007) as cellular interactions within the collagen matrix are decided partially by the cell-matrix tension state (Grinnell 2008). It is the biomechanical and wound healing capacity of the cornea that determines the reproducibility and stability of many refractive surgery techniques (Dupps, Wilson 2006). The anatomical and regenerative characteristics of the cornea are vital to its function as a strong, transparent structure able to protect against intraocular injury (Dupps, Wilson 2006) without rupture (Ruberti et al. 2007). The highly organised and ordered collagen fibril network accounts for the corneas mechanical strength (Skuta et al. 2011, Vrana et al. 2007) and load bearing element within the tissue (Vrana et al. 2007). The interweaving collagen bundles between adjacent lamellae supply vital structural foundations for shear (sliding) resistance and transference of tensile loads among lamellae (Dupps, Wilson 2006). Collagen fibrils are only found in the stroma and Bowman's layer; hence it is these layers that are vital in provision of the cornea's tensile strength (Dupps, Wilson 2006). Stripping of the epithelium, although has biological ramifications, has little to no effect on the anterior corneal curvature (Dupps, Wilson 2006), thus attributes very little to the corneas overall tensile strength. The Descemets's membrane has a relatively low stiffness and so accommodates for fluctuations in intraocular pressure which may

attribute to the absence of stromal stresses experienced by the adjoining endothelium (Dupps, Wilson 2006). Extensiometry testing whereupon the Bowman's layer was removed resulted in negligible mechanical changes of the cornea, thus the mechanical properties of the cornea are stromal layer dominant (Dupps, Wilson 2006).

In a healthy or edematous (swollen) cornea, the anterior lamellae assume nearly all of the strain (Skuta et al. 2011). Additionally cell matrix tension state is controlled by collagen density, matrix restraint and growth factor environment (Grinnell 2008). Keratorefactive treatments and corneal disease may alter the biomechanical properties directly or indirectly (Skuta et al. 2011). Biomechanical deviations become apparent with changes in corneal shape, shape instability, enhanced sensitivity, changes in hydration, hypoxia and injury as a consequence (Dupps, Wilson 2006). During scarring, deposition of abnormal tissue reduces transparency whilst disorganised loss of the remaining tissue causes a loss of tensile strength (Baldwin, Marshall 2002).

During healing, the initial matrix is less dense, disorganised and more flexible than uninjured tissue. ECM composition, stress and stiffness can all alter the cell phenotype both *in vivo* and *in vitro*. For example, increasing ECM stiffness *in vitro* is known to up regulate myofiroblastic transformation, mimicking what occurs *in vivo* as myofibroblasts develop towards the end of the wound healing process when cell density is high and the wound environment is stiffer (Lakshman, Petroll 2012). The increased cell-matrix tension causes fibroblasts to display stress fibers, focal adhesions and activate focal adhesion signaling *via* phosphorylation of focal adhesion kinase (Lakshman, Petroll 2012, Grinnell 2008). This response is absent when cell-matrix tension is low, i.e. in a healthy cornea as from a mechanical point of view quiescent non-activated keratocytes do not generate stress fibers or vast contractile forces (Kim et al. 2012). The dynamic mechanical feedback existing between cells and the surrounding matrices in 3D *in vitro* cultures occurs due to

time-dependent ECM remodelling, and may facilitate patterning during embryonic development as well as during wound healing (Kim et al. 2012).

2.6. Tissue engineered corneas and their challenges

The design of any tissue replacement requires a comprehensive knowledge and understanding of the capacity of the native tissue (Ruberti et al. 2007). There have been compelling advances in the development of synthetic corneal replacements and culture of human corneal cells onto and within supporting natural substrates. However, the gross results of these developments are poor and there are currently no transplantable TE corneal equivalents to date (Ruberti et al. 2007, Vrana et al. 2007). Mimicking the complex organisation of the corneal architecture is a current stumbling block. Two specific hurdles in particular need to be elucidated before appropriate TE corneas can be accomplished: (i) replacement or replication of the ultrastructure of the ECM; (ii) production of a dependable supply of untransformed proliferative corneal endothelial cells. Additionally, lack of tensile strength to permit surgical manipulation and attachment of the corneal equivalent along with the correct formation of appropriate surface curvature (Roujeau et al. 1995) are problems that need addressing.

Currently, a significant deal of research, including this thesis, is primarily focussed upon addressing the first hurdle. The regeneration of the native ECM involves two separate but interlinked issues: the maintenance of the keratocyte phenotype and neo-ECM formation, as opposed to scar tissue formation. The capacity to successfully culture corneal stromal cells is progressing and the ability to determine differentiation state, contractile behaviour and secretion of matrix components *via* manipulation of factors including but not limited to TGF-β, insulin and ascorbic acid derivatives are all encouraging. Controlling the assembly and/or remodelling of the collagen ECM through guiding stromal cell migration and ECM

synthesis *via* nanoscale topographical aligned features are current strategies employed to address the aforementioned first hurdle as the principle functions of the cornea (strength, transparency and refraction) are all directly connected to the nanoscale organisation.

2.6.1. Current strategies in tissue engineered corneas

The cornea is a layered structure, with the stromal layer occupying over 90% of the cornel structure. Due to this, the most prevalent strategies in corneal tissue engineering are focussed upon the stromal layer and the control of the stromal cell phenotype. Currently we and other groups recognise that the culture of pure corneal cells is problematic (Schneider et al. 1999), and that the optimal culture conditions of the isolated cells need to be defined and optimised, in particular the control and maintenance of the keratocyte phenotype. It has already been established that keratocytes differ in a variety of ways from fibroblasts and myofibroblasts. Cell morphology, proliferation and the expression of protein and gene products are identifiable as being significantly different (Berryhill et al. 2002). Keratocytes are quiescent, transparent cells which do not scatter light *in situ* (Jester et al. 2005). They synthesise a few cytosolic enzymes in abundance, including aldehyde dehydrogenase (ALDH) and transkelotase (TKT), which are often referred to collectively as the corneal crystallins (Jester et al. 2005). The crystallins are thought to play a role in the development and maintenance of tissue transparency through their effects on light scattering and adsorption. They also have metabolic roles in mitigating oxidative and UV light stress (Jester et al. 2005). Phenotypical changes occur when a cell becomes fibroblastic and it has proven difficult to reverse such changes when attempting to culture keratocytes *in vitro*. Fibroblastic cells are very different to keratocytes in that they are motile, highly proliferative, contractile cells able to synthesise ECM. If corneal fibroblasts are not controlled and guided the resulting tissue equivalent can become disorganised and opaque,

characteristic of scar tissue. Previous investigations have claimed that it is possible to differentiate corneal myofibroblasts back to their fibroblast phenotype (Berryhill et al. 2002). However, the main challenge still remains for researchers to differentiate fibroblasts to a keratocyte phenotype. The successful differentiation would be hugely significant with regards to corneal tissue transparency *in vivo* and *in vitro*. Transparency can be restored in corneal scar tissue *in vivo,* suggesting that fibroblasts are capable of returning to the keratocyte phenotype and replacing the disorganised ECM of the scarred tissue (Berryhill et al. 2002). The suppression of scar tissue formation is the general strategy employed for functional corneal tissue formation. *In vitro* manipulation of chemical, topographical, extracellular and cellular environments may enable us to mimic the conditions required to do this.

2.6.1.1. Choice of scaffold material

When constructing a tissue-engineered cornea, the choice of scaffold material is vital (Xu et al. 2008, Sachlos, Czernuszka 2003) in order to enable the cells to behave and form the complex arrangement as they would in *in vivo*. Amniotic membrane, collagen, fibrin, cross-linked fibronectin-fibrin gels, gelatine-chitosan, collagen-glycosaminoglcan blended nanofibrous scaffolds, contact lenses and thermoresponsive polymers are amongst the vast assortment of materials investigated as suitable corneal substrates (Mi et al. 2010). The list of requirements for a suitable scaffold is extensive, as they must be biocompatible (Pang et al. 2010), preferably optically transparent, strong as to withstand manipulation in culture, potential suturing, irrigation and handling in surgery. The material also needs to be flexible to take the shape of the eye and lay flat on the surface of the eye. It needs to be able to be produced easily with consistent quality, preferably at high speed and low cost (Levis, Daniels 2009), have controllable biodegradability or bioresorbability enabling cultured or

native tissue to replace the scaffold material (Sachlos, Czernuszka 2003) and have the spatial architecture of the native tissue.

2.6.1.1.1. Collagen based corneas

Many of the current scaffold-materials are type I collagen-based (Alaminos et al. 2006, Vrana et al. 2008). This material is commonly used as the cornea is primarily made up of type I collagen. A popular method is to culture cells in a 3D hydrogel environment as these provide a substrate for the tissue to grow on. Type I collagen hydrogels have been thoroughly investigated (Ahearne 2007, Ahearne et al. 2010a, Mi et al. 2012, Schneider et al. 1999, Minami et al. 1993) and are used to replicate the corneal ECM *in vitro* due to lack of availability of native corneal tissue. The hydrogel is able to act as a temporary matrix in which cells can grow, move and communicate (Ahearne, Wilson et al. 2010) and their viscoeleastic characteristics, biocompatibility and the fact that they can be remodelled by cells (Ahearne 2010b) makes them a suitable material to work with.

Collagen hydrogels are often seeded with human corneal fibroblasts to create a stromal equivalent (Germain et al. 2000, Ahearne 2010a, Schneider et al. 1999, Minami a et al. 1993). This model has currently been used to repair corneal burns (Vasiliev et al. 2005) and to test various ocular drugs (Reichl et al. 2004, Reichl et al. 2005). However the use of fibroblasts can be criticised as they are not found in a natural, healthy cornea. Despite the common use of fibroblasts instead of keratocytes, the (*in vitro*) stromal layer appears to be the most documented layer. This model obviously needs to be built upon to make it up to a full thickness cornea complete with epithelial and endothelial layers. Monolayers of epithelial and endothelial cells can be coated onto collagen hydrogels to create a corneal equivalent (Minami et al. 1993). However, this can present problems as the optimum culture conditions for the different cell types may be different. To compensate for this

when culturing epithelial cells onto a collagen stromal equivalent, an air-liquid interface technique can be used (Minamai et al. 1993) to mimic the conditions that native cells experience. However, care needs to be taken when using this method to ensure that the surface of the epithelial layer does not dry out.

Despite the fact that is has been shown that collagen gels can support epithelial cell migration and differentiation, they have been criticised as they do not promote infiltration of keratocytes and can also exhibit extensive contraction when seeded with fibroblasts prior to polymerisation of the gel (Orwin, Hubel 2000). Therefore transparency can be limited, and wound healing would be reduced should the gels be successfully transplanted (Orwin, Hubel 2000). Collagen hydrogels have also been shown to have significantly lower mechanical strength than the native human cornea (Ahearne et al. 2007). Also the collagen fibril arrangement in hydrogels have been shown to be disorganised and multi-directional.

As an alternative to collagen hydrogels, collagen sponges have also been studied (Orwin, Hubel 2000, Orwin et al. 2003). Collagen sponges are fibrillar matrices that attempt to mimic the 3D architecture to provide a more realistic model of the corneal stroma (Borene et al. 2004). The method of manufacture allows the porosity, strength and composition to be controlled (Orwin, Hubel 2000). Keratocytes grown on collagen sponges have been shown to migrate through the sponge, align with collagen fibrils and show evidence of normal ECM synthesis (Orwin, Hubel 2000). Epithelial and endothelial cells can also be grown on collagen sponges as partial mono-layers. However, reports have suggested that adhesion to the sponge is often weak and that the cells can detach in culture (Orwin, Hubel 2000). Much the same as collagen hydrogels, the direction of the fibrils cannot be controlled to be as organised as a native cornea. Also the diameter of the fibrils is much greater than found in a native cornea. In addition difficulties in acquiring adequate

supplies and ensuring their preservation means that collagen sponges also have their pitfalls as a corneal scaffold.

Collagen has also been used in many other forms including collagen shields, films, membranes, vitrogen (PureCol®) gels and denuded stromas. However, currently there still remains to be a "gold standard" collagen full thickness corneal model available. Although it has been shown to be possible to culture the three different cell types in a collagen-based hydrogel (Vrana et al. 2007) they are currently not as thick as a native cornea and therefore have weaker mechanical properties and so may not be able to withstand the intraocular pressures should they be used as transplant material. Methods of increasing the mechanical properties of collagen-based hydrogels have employed the use of plastic compression (Cauich-Rodriguez et al. 1996, Brown et al. 2005). By pushing fluid out of the hydrogels, this led to an increase in concentration thus an increase in stiffness. It has been reported that the polymer concentration in these hydrogels can increase by a factor of over 100. Problems also occur with transparency when using collagen hydrogels for corneal models. Often the models are transparent enough to observe the different cell types using a phase contrast microscope, but not yet as high as that of an *in vivo* cornea (Minami et al. 1993).

2.6.1.1.2. Some alternative materials to collagen

Although collagen has been extensively used and investigated as a scaffold in tissue engineering it is an expensive material that tends to shrink and lose volume when cells are seeded inside the scaffold (Tegtmeyer et al. 2001, Alaminos et al. 2006). Also stromal substitutes made of collagen are often unstable, mechanically weak and thus degrade quickly (Alaminos et al. 2006, Hui et al. 2005). Thus there have been many materials investigated either in combination or as an alternative to collagen in the development of a TE cornea. **Table 2.2** provides a summary of the more promising materials reported in current literature.

Table 2.2: A summary of currently available scaffold/substrate materials used in current *in vitro* tissue engineered corneal studies.

Scaffold/ substrate type	Description	Advantages	Disadvantages
Acelular corneal matrices	A corneal substrate minus cellular components (usually porcine origin) (Xu et al. 2008, Tegtmeyer et al. 2001).	Good integration. Potentially ideal structure for adhesion and proliferation (Xu et al. 2008). Inexpensive. Easily available.	No standard decelluarisation method. Only been implanted into rabbits.
Fibrin-agarose scaffolds	Combination of fibrin and agarose to form a gel (Alaminos et al. 2006).	Not contracted by stromal cells. Good transparency. Similar structural properties to native cornea.	Reduces growth rate of cells (Alaminos et al. 2006). No long term culture success.
Amniotic membrane (amnion)	The innermost layer of the placenta; has a thick basement membrane and an avascular stromal matrix (Tseng 2001).	Acts as a substrate to culture human keratocytes (Espana et al. 2003) and epithelial cells on (Tseng 2001). Can be successfully transplanted to reconstruct a damaged corneal surface in both rabbits & humans.	Reliant upon host tissue reconstructing ocular surface- not suitable for complete regeneration or transplantation. Not easily available. Variation amongst donors. Expensive screening required. Infection risks.
Silk fibrin	A structural protein obtained from the cocoon of the silkworm *Bombyx Mori.*	No immunogenic response. Transparent. Mechanically strong. Easily handled. Controllable degradation rates (Levis, Daniels 2009). Has successfully been used to support epithelial LSC growth (Levis, Daniels, 2009).	Very expensive. Not readily available.

Scaffold/ substrate type	Description	Advantages	Disadvantages
Polyvinyl alcohol (PVA)	Water soluble polymer that can be used to form gels (Wang et al. 2010).	Transparent. Allows nutrient transfer. Thermally stable. Mechanically strong.	Low cell affinity. Rejection from host. Unknown biocompatibility. PVA corneal substitutes failed in clinical trials (Wang et al. 2010).
Poly-lactic acid (PLA)	A naturally occurring polymer with various synthetic co-polymers that can be tailed to meet the researcher's requirements (Stoop 2008).	Inexpensive. Biodegradable. Biocompatible (Hadlock et al. 1999). Commonly used in TE applications. Food and Drug Administration (FDA) approval for clinical use (Stoop 2008).	Only been investigated in *in vitro* systems or animal models (Stoop 2008). Not well investigated in corneal TE applications. Degradation of scaffold releases acidic by-products (Sachlos, Czernuszka 2003).
Polyglycolic acid (PGA)	A synthetic polymer.	Readily available. Biodegradable. Biocompatible (Hadlock et al. 1999). Mechanically strong.	No long-term viability studies performed. Degradation has been associated with the build-up of acidic by products. Linked to corneal vascularisation when implanted into rabbit corneas (Kobayashi et al. 2004).

There are various arguments as to whether natural or synthetic biomaterials are the most suitable scaffold material choice. In general, the properties of native soft tissues are not easily duplicated by synthetic materials (Vrana et al. 2008). However, problems with natural polymers including poor mechanical strength, lack of availability and cost have meant that researchers have had to look for synthetic solutions or combinations of natural and synthetic polymers.

2.6.1.2. Manipulation of chemical cues

Chemical cues supplied by culture media and supplementation can influence cell phenotype *in vitro*. This is not specific to corneal cells but is true for most cell types. Successful culture of keratocytes is imperative for restoration of corneal transparency in corneal stromal equivalents. Many studies demonstrate that when cultured in serum-free media corneal stromal cells maintain a quiescent cell phenotype associated with keratocytes (Wilson et al. 2012a). However quiescence behaviour alone is not sufficient in determining keratocyte phenotype as it is not unique to the keratocyte phenotype (Berryhill et al. 2002, Beales et al. 1999, Ahearne et al. 2010a). Often, the quiescent behaviour of cells due to removal of serum is followed by apoptosis. Thus supplementation is required in media that can promote cell growth and proliferation of keratocytes without encouraging fibroblastic differentiation (Wilson et al. 2012a).

Studies performed using primary cultures of bovine keratocytes (Berryhill et al. 2002) have shown that the presence of serum causes the cells to turn fibroblastic (Berryhill et al. 2002). The addition of TGF-β without serum can also cause the same result (Jester, Jin 2003, Berryhill et al. 2002). It was hypothesised that the removal of serum would cause the cells to differentiate towards a keratocyte morphology. Following 8 days culture in serum free media the cells did in fact return to a morphology that was keratocyte-like in appearance and it was also suggested that the surrounding ECM was also restored to a keratocyte profile. Unfortunately the levels of aldehyde dehydrogenase ($ALDH_3$,- a cytoplasmic protein vital to corneal transparency) did not return to levels expressed in keratocytes. This promising study suggests that the partial restoration of the keratocyte phenotype following a fibroblastic transition is possible. Unfortunately the addition and removal of serum from media is not enough to fully restore the full phenotypical profile of a keratocytes and more complex biochemical cues still need investigation.

The list of biochemical components included in “keratocyte media” in current literature is extensive and often contradictory. Acetycholine, insulin (Builles et al. 2006), vitamin C (Musselmann 2006, Guo et al. 2007), growth factors (Builles et al. 2006) and cytokines (Jester, Jin 2003) are but a few amongst many supplements that have been investigated when attempting to obtain a “pure” proliferating culture of keratocytes. It should also be noted that often studies that look at the effect of biochemical cues are performed under simplified 2D tissue culture conditions. Interactions between the keratocytes and competing environmental stimuli are not considered (Jester, Jin 2003). Multiple growth factor and ECM signals may be important to keratocyte differentiation. Thus a 3D environment in combination with media supplementation may be required in order to more closely mimic the environmental cues required to successfully culture and between keratocytes and its sub-types.

2.6.1.3. Utilising topographic cues

Naturally, keratocytes grow in an orthogonally arranged architecture, following the organisation of the collagen fibre bundles. Much research has focussed upon mimicking this architecture in both 2D and 3D cultures. Contact guidance techniques have been extensively researched as they are able to affect many cell characteristics including orientation, morphology, differentiation and secretion of ECM proteins (Vrana et al. 2007). It is the material composition and more specifically the 3D nano- and microscale structure (the mesostructure) of bioartificial constructs that are pivotal to their success (Brown et al. 2005). Micro- and nano-patterned surfaces, magnetic alignment and electrospinning techniques are amongst a variety of techniques utilised in order to achieve this.

2.6.1.3.1. Micro- and nano-patterning

Micro- and nano-patterned surfaces have been thoroughly investigated when attempting to mimic the corneal fibrillar arrangement (Vrana et al. 2007). They are often manufactured *via* the use of templates with well defined groove widths and depths into which cells with and without matrix materials are added (Vrana et al. 2007). The patterned surfaces effectively restrict random cell growth *via* the incorporation of either physical or biochemical barriers. Orientated deposition of ECM components is capable of reinforcing the substrate in a given direction, which enhances the global mechanical properties of the original construct (Vrana et al. 2007). Vrana *et. al.* (2007) demonstrated the ability to align both cultured stromal and retinal pigment epithelial cells onto micro-patterned collagen films. The cultured stromal cells showed increased cell and ECM orientation and elongated morphology for up to 7 days culture duration. However, following 3 weeks culture the cell orientation decreased. This was attributed to the fact that the cells were able to adhere to the inclined walls of the micro-patterned surfaces following proliferation and thus filled the space at the base of the aligned channel. The epithelial cultures however, failed to secrete significant ECM proteins and showed reduced proliferation. Fibroblast and epithelial ECM secretions are different, but it has been demonstrated that surface patterning can impede extensive cell-cell contacts characteristic of epithelial cells, which alters proliferation capabilities (Vrana et al. 2007).

2.6.1.3.2. Magnetically aligned collagen

Magnetic fields have been utilised in an attempt to create a stromal like-scaffold made up of multiple intermeshed orthogonal layers of orientated collagen I fibrils (Torbet et al. 2007). The use of magnetic fields to induce collagen orientation is advantageous in that it is non-destructive (Torbet et al. 2007). It has been reported that molecules of collagen can

be assembled into orientated fibrils *via* the application of a magnetic force (Torbet et al. 2007). In brief, this can be achieved by loading an aliquot of collagen into a shallow sample holder and positioning it horizontally in the central region of a split coil superconducting magnet and increasing the temperature from 20 to 30˚C for approximately 30 minutes. The collagen molecules assemble into orientated fibrils perpendicular to the applied field and transform into a viscous gel that is stable and orientated after the magnetic field is removed. The orthogonal arrangement is achieved by adding more collagen and repeating the process at an altered angle, in a layer-by-layer approach. Human keratocytes can then be successfully seeded onto the aligned surface of the gel where they then become uniformly aligned along the collagen fibril direction (Torbet et al. 2007).

Although the author claims that the orthogonal scaffolds produced using this method are structurally similar to a native stroma they are flawed in that they are not highly transparent. Lack of transparency could be due to the fact that the fibril diameter cannot be regulated using this technique and as a result the fibril diameters are much greater than would be found in a native cornea, approximately 100-200 nm, in comparison to 20-30 nm. The addition of proteoglycans has been shown to reduce fibril diameter thus increasing transparency (Torbet et al. 2007), but unfortunately no systematic study has been performed to fully understand and exploit this phenomena.

Despite the claims of this promising technique being used to form the basis of a corneal implant for corneal regeneration, there has been very little literature published since for *in vitro* cornea applications. There is also conflicting evidence suggesting that the application of strong magnetic forces can in fact impair cell function and viability (Torbet et al. 2007, Valiron et al. 2005). It should also be noted that the keratocytes were only added to the collagen construct after the gel had been aligned and set as the technique is non-sterile. So

it is questionable as to whether the cells are able migrate through the full thickness of the construct as they would in a native cornea.

2.6.1.3.3. Electrospinning of nanofibres

Electrospinning is a process that is able to produce continuous fibres from the submicron diameter down to the nanometer diameter (Teo, Ramakrishna 2006). These fibres can then be arranged to recreate the microstructure and arrangement of the collagen fibres in a natural cornea. Typically collagen type I solutions are combined with synthetic polymers such as polyethylene oxide (PEO) or 1,1,1,3,3,3-hexafluro-2-propanol (HFP) as a solvent. However, HFP is difficult to work with and toxic so it could be argued as to whether it would be a suitable or safe material for TE applications (Levis, Daniels 2009). No one as of yet has created aligned type I collagen fibres on a small enough size scale comparable to those in the native cornea (Wray, Orwin 2009). It has been shown in 2D culture conditions that keratocyte populations are able to align in multiple adjacent layers arranged 30-90˚ to each other (Guo et al. 2007, Then et al. 2011). Wray *et. al.* (2009) and Wu *et. al.* (2012) have previously used aligned collagen and poly(ester urethane) urea fibres fabricated by electrospinning, to grow corneal stromal cells. However, these studies were limited to a single dense nanofibre sheet and did build the full organisation similar to that of the native tissue. In order to generate a functional corneal tissue, a 3D environment with defined topographical cues throughout a 3D construct is required (Wilson et al. 2012a).

Wray and Orwin (2009) report that they have managed to recreate smaller collagen fibres without the use of toxic solvents or polymers which support the growth of corneal fibroblasts and encourage the cells to align along the fibres. However, they did not comment on cell morphology, culture duration, or if the fibres induced differentiation of

the cells. Only corneal fibroblasts were reported to grow along the fibres in this study which as previously mentioned are not actually found in the native healthy cornea and are significantly easier to cultivate, expand and manipulate in culture than cells native to the healthy cornea. It has not been yet determined how the fibres affect transparency of the aligned fibrous scaffolds.

It has already been shown that the three main corneal layers can be recreated *in vitro* using collagen-based scaffolds (Griffith et al. 1999). However these models are still lacking the highly organised 3D collagen based architecture that is present in a native stroma (Torbet et al. 2007). Thus the biomechanical and optical properties of the cornea models are compromised as it is the collagen fibrils that reinforce biological materials (Boote et al. 2005). By improving collagen orientation so that it is more organised, as in a native cornea, would result in improvements in both optical and mechanical properties and so is an area that future research needs to pay more attention to. The ability to construct a scaffold that has orthogonal lamellae of aligned collagen fibrils is desirable in the development of TE corneas (Torbet et al. 2007) and has yet to be successfully achieved. It is also interesting to note that the majority of corneal diseases result from disruption of the highly organised collagen fibril arrangement in the stromal layer (Fullwood 2004). Thus if a more accurate corneal model that incorporated the corneal fibril organisation into their design were produced then it could be used by corneal surgeons to more accurately predict the outcome of surgical procedures. Scaffolds able to mimic the native corneal organisation may be beneficial as they create a strong tissue substrate that may accelerate the healing process, aid orientation of the subsequent secreted ECM and increase the tensile strength (Wilson et al. 2012a) that is often lacking in artificial constructs.

The incorporation of electrospun nano-fibres into corneal TE equivalents is a technique that is still in its infancy and evidently needs a lot more research before it can feasibly be

used as a way of mimicking fibril orientation in *in vitro* corneas. It is however a potential avenue for future exploration and improvement.

2.6.1.3.4. The feasibility of achieving native corneal transparency

As previously mentioned, a common "problem" often associated with TE corneal constructs is their lack of optical transparency. Concerted efforts have focussed upon the scaffold or construct manufacture in order to more closely mimic the native corneal tissue architecture as discussed in the previous sections. However, technically speaking, achieving equivalent "native optical transparency" in TE corneal constructs for transplantation use may not be necessary. For instance, Turner *et al.* (2010) recently published a study whereby autologous patch grafts were used to treat corneal preformation injuries in humans. Interestingly, in two cases, tissue transparency was restored to the opaque scleral tissue within two months following surgery. The collagen fibrils within scleral tissue are irregular in their diameter and arrangement in comparison to corneal stromal tissue (Prydal 1996), akin to tissue engineered constructs. Thus, provided that corneal stromal cells are able to successfully infiltrate, remodel and differentiate within their environment it can be hypothesised that they will be able restore the native tissue architecture to engineered constructs. However, it should be stressed that the tissue mentioned in the aforementioned study was autologous in origin and that it was only utilised to replace small areas of damaged cornea and not the whole cornea. However, it does offer promise that provided that engineers can achieve a certain degree of structural homology that corneal constructs may be utilised as an alternative to cadaveric donor tissue.

2.6.1.4. Co-culture approaches

There are numerous cell based approaches that have been reported, all with the similar aim to manipulate the cells to create their own ECM so that they behave the way that they would in a natural cornea. The majority of culture systems for corneal tissue separately culture epithelial cells, keratocytes/fibroblasts and endothelial cells as mono-layer cultures (Minami et al. 1993). However, monolayer culture fails to mimic the *in vivo* physiological environment and lack the 3D physiological environment found *in vivo* tissues and so are often criticised with regards to their limited application to the *in vivo* situation (Dayhaw-Barker 1995a).

Most tissues consist of more than one cell type and it is the organisation of the cells within the tissue that is essential to normal development, homeostasis and in the case of corneal tissue, transparency. *In vivo,* epithelial cells are in close contact with keratocytes (Du et al. 2007, Kawakita et al. 2005) in the stromal layer; they are connected both anatomically and functionally (Wilson et al. 1999). Co-culture studies aim to recapture this cellular anatomy and functionality. It has been suggested that epithelial cells proliferate more actively and are better differentiated in co-culture systems with keratocytes and endothelial cells than when in separate cultures (Minami et al. 1993) and their proteoglycan synthesis is significantly less in monocultures than when cultured as a whole intact cornea or in a co-culture system (Chan, Haschke 1983). It has been suggested that growth factors and cytokines secreted by epithelial cells regulate keratocyte cell function and *vice versa* (Gabison et al. 2009, Nakamura et al. 2002) in a reciprocal bidirectional manner that aid and stimulate normal migration and the secretion of proteoglycans and glycoaminoproteins in a simultaneous, highly coordinated manner which changes dependent upon development, homeostasis and wound healing; although direct cell-cell communications do occur in some situations (Wilson et al. 2003).

Co-culturing of cells is becoming an increasingly popular method to create a full thickness cornea as it has the advantage of cell-cell interactions occurring, thus mimicking normal call behaviour in a natural cornea. In co-culture systems 2 or more cell types are bought together within the same culture environment, enabling them to interact and communicate which can act as a very powerful *in vitro* tool allowing cellular interactions and cell function to be studied (Hendriks et al. 2007). The influence of cellular interactions is of particular interest to tissue engineers because the tissue formation of one or all cell types can be regulated by simulating the natural physiology and differentiation of cells.

When developing co-culture models, it is important to balance the ability to observe, measure and manipulate cell behaviour when constructing *in vitro* 3D environments (Hendriks et al. 2007). For example, *in vitro* corneal tissue has been reconstructed previously (Minami et al. 1993, Nishimura et al. 1998) comprising of epithelial, stromal and endothelial cells in a 3D collagen matrix. Unfortunately the level of complexity involved deemed it unsuitable to accurately monitor and measure proliferation and differentiation in the component cells. Thus, often simplified models are required. These include the use of conditioned media (Hibino et al. 1998), transwell cultures which utilise a semi-permeable membrane (Nakamura et al. 2002, Nakazawa et al. 1997) and direct explant cultures.

Nakamura *et. al.* (2002) demonstrated in a co-culture system that injured epithelial cells secrete soluble factors able to cross a membrane impermeable to cells which stimulate corneal fibroblast proliferation, myodifferentiation and matrix contraction. *In vivo* epithelial-stromal interactions mediate fibrotic or a regenerative response, thus correct manipulation of culture conditions may facilitate the ability to control and initiate the cornea's regenerative capacity on demand in *in vitro* cultures. Nakazawa *et. al.* (1997) have also performed co-culture studies by the use of insert dishes and companion plates to study

epithelial-stromal and endothelial-stromal interactions. Stromal seeded collagen gels were cultured on the insert dish with either epithelial or endothelial cultures on the companion plate. Interestingly, they found that in comparison to mono-cultures, cell growth was not stimulated in any cell type in either epithelial-stromal or endothelial-stromal cultures. However, this is not consistent with the work of others (Chan, Haschke 1983, Wilson et al. 1994, Sotozono et al. 1994). The inconsistency was not determined in the study, although may have been due to the lack of successful adhesion of the epithelial and endothelial cells to the companion plates and/or the fact that the media was changed daily, which could reduce the stimulatory effect of the soluble cytokines released into the media. Additionally, the dispase treatment used to separate the cells from the tissue may have damaged the adhesion sites of the cells. However, it was noted in the previous studies that the proteoglycan content was significantly altered in the co-culture studies; stromal and epithelial cells stimulated proteoglycan synthesis by each other (Chan, Haschke 1983). Analysis *via* proteoglycan radiolabelling demonstrated that epithelial and endothelial cultures had different effects on the stromal cultures, suggesting that *in vivo* proteoglycan synthesis in a normal cornea is defined by a careful balance between the antipodal actions of the epithelial and endothelial layers (Chan, Haschke 1983).

Much of the existing literature regarding corneal co-culture is concerned with epithelial-stromal culture, with the emphasis being on the effect that the additional stromal cells (often fibroblastic in phenotype) will have on the epithelial culture. This may be due to the interest in treating limbal epithelial deficiencies and epithelial wounds. However, often corneal disease and injuries (such as chemical burns and Stevens-Johnson Syndrome (Roujeau et al. 1995)) penetrate deeper into the stromal layer so it is important to also consider the effects that epithelial cultures will have on the corresponding stromal culture.

A greater understanding of stromal-epithelial-endothelial interactions and what mediates them by utilising co-culture approaches offers great pharmacological potential in the regulation of corneal wound healing, with the potential to treat corneal diseases and injury whereby such interactions are vital (Wilson et al. 1999). As the different healing mechanisms, contributing factors and their potency become known, we are able to utilise this information in order to accelerate and enhance the wound healing process (Dayhaw-Barker 1995b).

2.6.1.5. Growth factors

In order to generate transparent corneal constructs *via* TE techniques a feasible strategy to control keratocyte activation and myofibroblast differentiation is to utilise the use of various growth factors. Many studies have been performed using this strategy, however they are often contradictory, and dose dependent or incomplete. For example, it has been shown that FGF may be used to stimulate epithelial coverage (Fredjreygrobellet et al. 1987, Rieck et al. 1992) but few studies have been performed to accurately verify this. FGF has also been shown to reduce the expression of α-SMA in 3D *in vitro* cultured keratocytes (Lakshman, Petroll 2012). However, in 2D cultures FGF has caused fibroblastic differentiation (Bernstein et al. 2007). The contradictory lack of stress fibre formation and change in matrix composition when in 3D cultures compared to 2D cultures suggests the FGF stimulation may be sensitive to the surrounding ECM. Additionally, discrepancies in FGF studies may be due to the use of non purified FGF from bovine brain or human placenta sources which will lead to controversy regarding the appropriate dosage (Hoppenreijs et al. 1994). Discrepancies in the concentrations, combinations of, or the growth factor isoform used can affect the overall cellular response.

There are 3 different isoforms of TGF-β in humans (Agrawal, Tsai 2003, Eraslan, Toker 2009, Imanishi et al. 2000, Klenkler, Sheardown 2004, Karamichos et al. 2011, Petroll et al. 1998, Karamichos et al. 2010) and it becomes strategically obvious that we have to treat the TGF-β isomers differently as the *in vivo* roles of each of the isoforms are distinct and differ from each other (Karamichos et al. 2011). Although their exact roles still eludes us, it has been suggested that optimal treatment may rely upon selective inhibition of more than just one of the isoforms (Carrington et al. 2006). Inhibition of TGF-β1 and -β2 through the use of exogenous agents and antibodies can reduce and eliminate myofibroblast differentiation and fibrosis *in vivo* and *in vitro* (Carrington et al. 2006, Funderburgh et al. 2001). TGF-β neutralising antibody can prevent and block this action and has been used in previous collagen hydrogel co-culture studies to prevent hydrogel contraction caused by the release of soluble factors (Nakamura et al. 2002). Stimulation with TGF-β3 has also been shown to yield corneal stromal models with non-fibroblastic characteristics with ECM properties that more closely mimic the native stromal ECM (Karamichos et al. 2011) and thus has been speculated for use as a therapeutic agent. TGF-β3 is thought to stimulate and activate different signalling molecules to TGF-β1 and –β2 (Karamichos et al. 2011). This results in a differential TGF-β function that inhibits type III collagen synthesis which is usually significantly upregulated and more abundant in wounded, fibrotic corneas (Funderburgh, Funderburgh et al. 2001). Addition of TGF-β3 does not cause the upregulation of α-SMA as occurs with the TGF-β1 and –β2 isoforms (Karamichos et al. 2011).

The effect of using PDGF is frequently associated with the use of serum in media which induces fibroblastic response. However serum contains a vast assortment of undefined factors as well as PDGF that may also contribute to the fibroblastic differentiation. When used in serum-free media, PDGF has been shown to facilitate the elongation and generation

of dendritic procedures of stromal cells (Kim et al. 2012) with little matrix deformation. This allows for keratocyte repopulation of the corneal stroma without disruption to the fibril architecture.

IGF has been used *in vitro* to stimulate keratocyte growth and proliferation and induces the elongation of the keratocyte dendritic processes (Lakshman, Petroll 2012) required for cell migration. Its inclusion in culture media can help to support corneal structure and may facilitate a regenerative wound healing phenotype (Lakshman, Petroll 2012). Like EGF, KGF stimulates epithelial cell growth both *in vivo* and *in vitro* (Agrawal, Tsai 2003). The exogenous *in vivo* addition of KGF to rabbit eyes following epithelial injury has shown to have growth promoting effects to epithelial cells (Sotozono et al. 1995). It is thought to work by stimulating and increasing the mitotic activity of limbal epithelial stem cells in the regenerating cornea. Topical KGF treatment may have clinical potential in the treatment of epithelial disorders, in particular those requiring stem cell differentiation (Imanishi et al. 2000) as, unlike many other growth factors, it does not affect cells of mesoderm origin and thus does not induce neurovascularisation of the cornea as a side effect (Sotozono et al. 1995).

In vivo cytokines and growth factors are involved in complex feedback mechanisms whereby the activation of their receptor in a target cell can stimulate the production of additional growth factors and so on. This cascade affect promotes cross-talk to the original cell in a reciprocal epithelial-stromal interaction (Gabison et al. 2009). Thus when attempting to understand and manipulate the use of growth factors to control cell phenotype in TE constructs and/or a wound healing outcome (i.e. fibrosis or scarring) the use of single growth factors is not enough. We must first unpick and understand the intricate mechanisms and intricate combinations of growth factors needed to provoke the desired response. In order to determine an environment that stimulates organised keratocyte

migration and generation a suitable model system is needed that will allow for stromal cells to be studied in their natural, uninjured state.

2.7. Toxicity testing

Another avenue that is being developed is the use of *in vitro* corneal models for use in toxicity testing and the development of new ocular drugs. The complexity and uniqueness of the cornea often makes the development of ocular drugs particularly challenging. The cornea is sensitive to various irritants and many substances can cause serious irreversible damage to the cornea, including ocular drugs. Before potential new ophthalmic drugs can be routinely used they have to undergo many rigorous toxicity and permeation tests. Pharmaceuticals, cosmetics, toiletries, household, industry, agricultural, and military products are all potential irritants to the eye (Wilhelmus 2001). In order to ensure that they are safe for their intended use all manufactured consumer products and their ingredients must be tested and their eye irritation potential assessed. Eye toxicity tests are therefore required to provide information that can ensure that products are safely manufactured and labelled.

2.7.1. In vivo testing

The current international standard assay for acute ocular toxicity is the rabbit *in vivo* Draize eye test (Jester et al. 2001). Rabbits are often used as they have large eyes with a well described anatomy and physiology, are easy to handle, readily available and relatively inexpensive test subjects (Wilhelmus 2001). The procedure involves the application of 0.1 ml (100 mg solid) test substance onto the eye of a conscious rabbit for 4 hours. The rabbits are observed for up to 14 days for signs of irritation including redness, swelling, discharge, cloudiness, blindness etc. (Wilhelmus 2001). The observed degree of irritancy allows for

chemicals to be classified, ranging from non/mildly irritant to strongly irritant. Draize testing is often criticised due to lack of repeatability and over-prediction of human responses (Jester et al. 2001), primarily due to interspecies differences. Additionally, the test is often disapproved of by animal activist groups due to animal stress.

Low-volume eye-irritation tests are a refinement of Draize testing in that lower volumes of test substances (0.01 ml) (Lambert et al. 1993) are used, so it is less stressful (Jester et al. 2001). Although it has been shown to be more accurate at predicting human responses (Lamber et al. 1993) it is still criticised for its animals use. Also should a negative irritancy result occur at the lower test volumes then the standard procedure to increase the concentration of the drug, effectively resorting back to Draize testing.

2.7.2 Ex-vivo testing

As an alternative to *in vivo* testing enucleated eye tests using isolated rabbit eyes were first introduced in 1981 by Burton *et. al.* (1981). They are ethically advantageous with reduced costs. Corneal thickness, opacity and fluorescein retention (Prinsen 1996) are tested to reveal adverse reactions to test substances. Eye irritation is primarily determined by the extent of initial injury which correlates with the extent of cell death and ultimately the outcome of an irritant on an eye (Jester et al. 2001). Generally, slight irritants damage the superficial epithelium, mild irritants penetrate further to damage the stroma and severe irritants penetrate through the cornea and damage the endothelium (Jester et al. 2001). Although further refinement is required, these observations corroborate with *in vivo* results, providing a potential alternative to reduce and replace live animal use in ocular testing.

Slaughterhouse waste has been investigated as an alternative tissue source (Prinsen 1996). Porcine corneas are often used for corneal testing (Reichl, Muller-Goymann 2001), although chicken enucleated eye tests (CEET) are widely accepted to be the most reliable

and accurate slaughterhouse tissue for assessing the eye irritation potential of test materials (Prinsen 1996). CEET is often used as a pre-screen for Draize testing; although despite promising outcomes the *in vivo* Draize testing results still overrule *ex vivo* results should discrepancies occur.

2.7.3. In vitro testing

Toxicity testing using cultured cells, often on collagen hydrogels are advantageous compared to *in vivo* and *ex vivo* testing in that they are relatively inexpensive and simple and quick to manufacture. Rabbit corneal epithelial (RCE) cells have been cultured onto collagen hydrogels using air-liquid techniques. The RCE model (Matsuda et al. 2009) aims to mimic the native rabbit corneal epithelium. To validate the model 30 chemicals with known degrees of eye irritation (from Draize testing) have been tested. Eye irritation potency can be estimated by using colorimetric MTT assays as a measurement of viability. MTT measures the reduction of yellow 3-(4,5-dimethythiazol-2-yl)-2,5-diphenyl tetrazolium bromide (MTT) to purple formazan by mitochondrial succinate dehydrogenase, measurable *via* spectrophotometry. As MTT reduction only occurs in metabolically active cells the spectrophotometer reading can give an estimate of cell viability that are comparable to Draize test results, although further modification is still required. The RCE model is also somewhat limited in that it only models the epithelial layer and so cannot be used to determine the possible effects of drugs that may penetrate the stroma and endothelium.

Although promising results have been obtained from both enucleated eye testing and RCE models they share the common problem that interspecies differences regarding anatomy and physiology are still present. Such differences produce discrepancies in permeation studies and toxicity tests (Reichl et al. 2004, Reichl, Muller-Goymann 2003).

Pathogens are often species specific and this regularly causes new drugs to fail in clinical trials (Mazzoleni et al. 2009). In response, human cell based culture models are becoming more established, but the main hurdle is the successful manufacture of an *in vitro* cornea with similar barrier functions to the native cornea. Thus there is still a growing need for credible, human-derived *in vitro* models (Mazzoleni et al. 2009).

Griffith *et. al.* (1999) produced the first working equivalent of a human cornea using immortalised human corneal cells. The model was originally developed to help to understand why corneas fail to heal properly after laser eye surgery. A collagen-chondrotin sulphate substrate cross-linked with glutaraldehyde was used as a tissue matrix. Initially a thin layer of endothelial cells were grown in a culture dish. Keratocytes and support proteins were added before finally adding the final epithelial layer. The gross morphology, transparency and histology were reported to be similar to that of a natural cornea. Tests performed using mild detergents determined that the constructed cornea had a similar gene expression and wound-healing response when compared to human eye-bank corneas. Although these TE corneas are a significant advance in the right direction towards replacing animal models as of yet it still has not been accepted as an alternative to Draize testing.

More recently Reichl *et. al.* (2005) claimed to have successfully manufactured a human corneal equivalent for *in vitro* drug permeation studies by culturing all three corneal cell types in a collagen hydrogel matrix. Three reagents commonly used in ophthalmic drugs to treat glaucoma and inflammatory diseases were tested and permeation data obtained was compared with those from excised porcine cornea and a porcine cornea construct (Reichl et al. 2004, Reichl 2003). The porcine cornea was chosen as a comparison as it shares a relatively similar anatomy and physiology to the human cornea- more so than a rabbit cornea. The human cornea construct had similar epithelial barrier properties to a native

cornea with only small untrastructural differences- possibly due to lack of tears and blinking. For all reagents tested there was increased permeability in the TE constructs compared to the exercised porcine cornea, although the differences were relatively small. Unfortunately there was no data available for comparison with an excised human cornea (as in the studies by Griffith *et. al.* (1999).

Similar tests using *in vitro* human corneal models have been performed with the introduction of nerve-target cell interactions (Suuronen et al. 2004). Dorsal root ganglia isolated from chick embryos have been utilised as a neural source, embedded in a collagen hydrogel matrix. Optimal function, maintenance and wound healing of many tissues are dependant to some extent on peripheral sensory innervations (Suuronen et al. 2004) so it would seem a logical justification to include innervation in TE corneas. The innervated corneas were reported to have lower cell death rates when exposed to test chemicals compared to non-innervated cornea equivalents. Thus suggesting that the presence of nerves protects the epithelium from chemical irritation and possibly explaining why previous non-innervated corneal models have been deemed over-sensitive when used in toxicity studies. This model still needs to be further developed though as many of the functional properties of the nerves remain unclear.

The MatTek Corporation has developed a commercially available 3D corneal epitheial model based upon human derived epidermal keratinocytes from human foreskin (McLaughlin et al. 2009, Sheasgreen et al. 2009), marketed as EpiOcular™. Although it is been used by numerous cosmetic companies in place of Draize testing, as of yet EpiOcular™ has not been formally validated (Sheasgreen et al. 2009) as it is unable to predict responses of chemicals that affect the lower layers of the cornea, or that are dependent upon epithelial-stromal cellular interactions (McLaughlin et al. 2009).

Despite numerous screening tests, as of yet there is no validated *in vitro* ocular irritation test to replace the heavily criticised use of animals. This is partly due to a lack of understanding of the underlying mechanisms of eye irritation (Matsuda et al. 2009), a possible the lack of innervation (Suuronen et al. 2004) and an apparent reluctance of regulatory bodies to accept new *in vitro* corneal constructs. However, recent European directives have prohibited the use of laboratory animals in toxicity testing, particularly the use of the Draize eye irritancy test (Vrana et al. 2008), thus the need for alternative testing is crucial, particularly in the development of new ophthalmic drugs.

The general disadvantages of using *in vitro* models is that the composition of the aqueous humour and tear fluid, or the mechanical stress of the eyelids and tear flow (Tegtmeyer et al. 2001) is not accounted for. In a natural cornea all of these factors are important to protection of the eye and are increased when exposed to irritation. The mechanisms that mimic tear production and blinking need to be incorporated into *in vitro* toxicity models.

2.8. Characterising the mechanical properties of the cornea and equivalents

When the stromal layer becomes damaged, whether through disease or surgery the mechanical behaviour of the cornea as a whole is affected (Anderson et al. 2004, El-Sheikh, Anderson 2005). Therefore it is important to have an understanding of the mechanical properties of the cornea in order to develop and improve surgical procedures and ocular treatments. In addition mechanical properties are also important to the development of keratoprostheses and TE corneas (Ahearne et al. 2007).

As the cornea is a load bearing tissue, constantly subjected to forces from intraocular pressure and the movement of the eyelid it can be assumed that these forces will have an effect and are affected by cell and tissue behaviour. Biomimetic materials are frequently

investigated for tissue engineering applications including *in vitro* corneas. The viscoeleastic and mechanical properties of these materials are important to their performance and durability, ultimately dictating whether they are successful or not in their given application (Ahearne et al. 2009). Problems often occur when attempting to mechanically characterise the cornea and TE equivalents as they are often very fragile and have a tendency to rupture easily (Liu, Ju 2001). There have been numerous techniques employed in the testing of the mechanical properties of the cornea. However, many mechanical tests used with corneal tissue are not specific to corneas or TE corneas. They are in fact existing tests that have been adapted for the use of corneal testing. Due to this the various techniques often suffer from pitfalls and may need further optimisation. A summary of some of these methods and their advantages and disadvantages are summarised in **Table 2.3**.

Table 2.3: Commonly used tests to monitor the mechanical properties of corneal tissue and tissue-engineered equivalents; a brief description and common applications; advantages and disadvantages connected with the techniques.

Method/ technique	Description/applications	Advantages	Disadvantages
Bulge/inflation testing	Involves inflation of the whole tissue/membrane/film through a window in the substrate and measuring the displacement as a function of the applied pressure (Tsakalakos 1981, Aheanre et al. 2007). Used to measure mechanical strength of thin films, membranes and corneal tissue.	No gripping problems. Reliable technique. Enables intrinsic properties on a layer-by-layer basis to be determined (Hoeltzel et al. 1992). Whole tissues can be measured.	Complex procedure (Hoeltzel et al. 1992). Difficulties in controlling the applied pressure; i.e. leaking or trapping of dissolved air. Destructive.
Compression testing	Test materials are compressed between two plates and deformed under a known load. Used to determine the mechanical behaviour of materials under crushing loads (Stammen et al. 2001, Krupa et al. 2010).	Regularly used in TE applications (Korhonen et al. 2002). Confined and unconfined tests can be performed. Gives a comprehensive evaluation of a materials load-bearing capacity (Stammen et al. 2001).	Does not account for corneal curvature. Involves flattening of the tissue.
Holographic interferometry	Uses light from a laser to create an image. Can be used to compare pressure changes in healthy and diseased corneas. Measures the elasticity and extensibility of *in vivo* corneas (Maurice 1988).	Very sensitive, precise method. Allows for direct comparison of two adjacent areas in a single sample. Non-destructive.	Rarely used by researchers. Limited to use in linear elastic materials under small deformation (Ahearne et al. 2007).

Method/ technique	Description/applications	Advantages	Disadvantages
Indentation testing	A well-defined indenter is used to deform test materials and measure their force-displacement curves; this can be used to calculate the elastic modulus. Traditionally used to measure the hardness of materials.	Non-destructive. Can be adapted to test for prolonged culture periods under sterile conditions. (Ahearne et al. 2007, Ahearne et al. 2008). Allows for fast, online real-time measurements. Can be performed on a nanometric scale. Suspending the materials eliminated problems associated with backing substrates.	Cannot be used to test high stiffness materials.
***In vivo* mechanical testing**	Pulses of air or poking mechanisms are used to test materials. Used to measure corneal hysteresis by comparing inward and outward pressure values (Sullivan-Mee, et al. 2008).	Can be performed on live patients. Changes in mechanical properties can be directly linked to medical conditions (Abitbol et al. 2010).	*In vivo* tests are difficult to apply to *in vitro* models. Unsuitable for prolonged culture periods. Sample contamination. Creep, stress-relaxation and stress-strain relationships are yet to be assessed.
Optical coherence tomography (OCT)	Functions on the basis of low coherence interferometric backscattering of light (Bagnaninchi et al. 2007). Frequently used by ophthalmologists to examine corneal structures.	Capable of micrometer resolution. Non-invasive, non-destructive technique (Yang et al. 2007). Can be applied both *in vivo* and *in vitro.* Relatively inexpensive.	Limited to 1-2 mm penetration depths. Has to be used in combination with other testing methods in order to determine the mechanical properties of a sample.

Method/ technique	Description/applications	Advantages	Disadvantages
Strip extensiometry (coupon testing)	Involves applying a tensile force to dissected strips of corneal tissue that are gripped and stretched *via* the application of a tensile force. Is used to calculate the Young's modulus, yield strength and ultimate tensile strength of the cornea and equivalents.	A relatively simple technique. Inexpensive. Can be used to compare corneas of different species with each other (Hoeltzel et al. 1992, Zeng et al. 2001).	Unreliable. Does not account for corneal curvature unless complex calculations are employed (Maurice 1988). Stress distribution of corneal tissue is not uniform. Destructive technique (El-Sheikh, Anderson 2005). Cannot be used to study whole tissues. Problems associated with sample gripping. Complex calculations involved (El-Shiek-Anderson, 2005).
Ultrasound	A biomicroscopy technique which utilises high frequency trasducers, creating 2D mages from backscattered ultrasonic waves (Ozdal et al. 2003). Used to visualise numerous ocular structures and to detect *in vivo* foreign bodies.	Allows for detailed surface imaging up to 5mm in depth. Allows for quantitative assessments of the anterior ocular surface to be made (Urbak 1999). Non-invasive technique. Can be applied *in vivo* and *in vitro*.	Expensive. Yields results that are too high when compared to known measurements (Urbak 1999).

With regard to the understanding of the viscoeleastic characteristics of the cornea there still remains a lot to be discovered. The taking of mechanical measurements is usually very challenging. The measurement of mechanical properties under sterile conditions is also highly desirable when monitoring biomechanical processes. Although many mechanical testing techniques are available it is difficult to compare and contrast the information as there are considerable differences in the technological means of carrying out the tests.

Additionally the interpretation of results can also contribute to discrepancies between data acquired by mechanical testing (Ahearne et al. 2009).

2.9. Conclusion

The cornea is an excellent model for studying wound response with regards to cell phenotype due to the unique homogenicity of the cell types that reside in the corneal stroma and the remarkably organised tissue architecture that if disrupted has immediate and obvious effects. Following injury or disease, the cornea is capable of restoring full function *via* a regenerative approach. One of the most demanding challenges in corneal biology is in the assistance of tissue repair *via regeneration* as opposed to *fibrosis*. The interaction between the corneal stroma and the adjacent epithelium is known to have a role in wound healing mechanisms although the exact mechanism is unknown. Derivations in its barrier function render it permeable to cytokines and growth factors which can facilitate an activated fibrotic response and scarring. Scar tissue alters the constituents of the original ground substance of the cornea including the proteoglycans, collagen filaments and various proteins and glycoproteins *via* dynamic feedback mechanisms. The extent of damage or injury is known to have an effect on these mechanisms and may dictate whether the healing response is regenerative or fibrotic. Recognising the diverse epidemiologies of common corneal injuries and diseases is of great significance to corneal research and medicine as it may aid in devising more appropriate treatments and preventative measures. Many of the existing treatments fail to cure the underlying cause, are not cost effective and can only alleviate or treat the secondary symptoms of disease. More knowledge of the underpinning mechanism that leads to scar formation and permanent opacities will aid in treatment.

Currently, the only truly successful treatment available for many corneal diseases is corneal transplant. Presently there are insufficient numbers of corneas or suitable tissue to

meet the demand and technical properties. It is the lack of donor tissue and high graft failure rates that warrant the need for alternative procedures. A clinically viable TE human corneal equivalent has the potential to serve as an alternative source for corneal transplantation and as a substitute for *in vivo* and *in vitro* drug, toxicity and irritant testing. With regard to corneal transplantation, a TE tissue would bypass the problems associated with the availability of donor tissues.

Engineered tissues can potentially be custom made with variable complexity and functionality to suit the patients' needs whether it be to restore solely ocular function or as a device to promote regeneration of the host tissue. It is improbable that one corneal substitute will suit all patient requirements, but taken together, the various TE approaches may soon be able to supplement the supply of human donor corneas for transplantation or permit the restoration of diseased or damaged corneas that currently cannot be treated using existing techniques.

In vitro corneas also have the potential to reduce and replace the use of animal testing for eye irritation, drug and toxicity testing. This is not only advantageous from an ethical standpoint, but also may combat discrepancies and inaccuracies linked to interspecies differences that may cause new drugs to fail during clinical trials.

Currently the main limitations associated with TE corneas are the production of a viable endothelial layer, replication of the stromal architecture and control of the stromal cell phenotype. Efforts have been made to mimic such architecture although still fail to meet the nanoscale arrangement. Both the production of a viable endothelial layer and the control of stromal cell phenotype have important implications linked to tissue transparency and scaring. The impact of scar tissue formation in corneal tissue is significantly greater than all other tissue types as it directly impacts vision. Understanding the *in vivo* mechanisms whereby the cornea is able to regenerate as opposed to repair is fundamental

to clinical and TE engineering approaches as it often determines the difference between a functioning transparent tissue and an opaque scarred tissue.

It is important to have an understanding of the mechanical properties of the cornea in order to develop and improve surgical procedures and occur treatments, and to develop appropriate keratoprostheses and TE corneal equivalents. The mechanical properties are not only important to their performance and durability but can also serve as a means of monitoring biological functionality. However, the taking of corneal mechanical measurements can be very challenging. Many mechanical tests used for corneal tissue and their equivalents are not specific enough and so require further optimisation and validation. Concerted research efforts by multi-disciplinary research groups are ever adding to our knowledge of the complex systems required to monitor, restore and enhance vision in both *in vivo* and *in vivo* models. An accumulation of this knowledge will bring us closer to achieving this goal.

3. Materials and Methods

This chapter details the fundamental techniques commonly used throughout the thesis and will be referred to in the relevant chapters. The development of existing techniques is also detailed. The optimisation of protocols and assembly methods are also described.

3.1. Corneal cell culture

All experiments carried out in this thesis used either human corneal stromal cells or porcine epithelial cells. Cells of porcine origin were used due to the lack of available and suitable human tissue to grow the cells from. The approval had already been granted for the use of human corneal tissue from the Birmingham NHS Health Authority Local Research Committee. Please refer to appendix A2 for ethical approval information.

3.1.1. Isolation of adult human derived corneal stromal (AHDCS) cells

Adult human corneal tissue remaining from corneal transplantation was used for the isolation of adult human derived corneal stromal (AHDCS) cells. The corneal rims were received within 2 weeks post implantation in Dextran storage medium from Birmingham and Midland Eye Centre (UK). Only tissues from donors which had consented for research were used in this study. The mean age of the corneal tissue was 64 years ± 9.6 years. All corneal dissections were performed in a class I laminar flow hood to reduce infection and contamination risk (Bassaire, UK), within 2 days of their arrival and with the aid of a dissection microscope and light box (Leica SD2, L2 light box, Leica Microsystems, Germany). The corneal tissue was first washed in a 1%) The corneal tissue was first washed in a 1% antibiotic/antimitotic (A+A) solution to reduce infection risks (*v/v)* antibiotic/antimitotic (A+A) solution to reduce infection risks. All corneas were dissected

within 24 hr of delivery. The epithelial and endothelial layers were physically stripped from the stromal layer using sharp point forceps. The scleral ring was removed using a sterile blade. The remaining stroma was then cut into smaller sections, approximately 1-2 mm in diameter using a sterile blade and laid flat onto the surface of a T25 cm^2 cell culture flask. The stromal explants were allowed to adhere for approximately 5 minutes before 5 ml of F media was added to the flask. Care was taken to ensure that the tissue had adhered and was not disrupted when adding culture media. The cells migrated and proliferated out from the stromal explants, usually within 2-3 days. The culture media was changed every 2-3 days until the cells reached confluence. When the cells reached confluence they were passaged into T75cm^2 flasks under 10 ml F media. The culture media routinely used for the expansion and culture of corneal stromal cells consisted of Dulbecco's modified eagle medium (DMEM, Biowest, France) supplemented with 10% foetal calf serum (FCS, Biowest, France), 1% antibiotic and antimitotic solution (A+A, prepared in phosphate buffered saline, PBS, Sigma Aldrich, UK) and 1% 200 mM L-glutamine (L-Glut, Sigma-Aldrich, UK). This serum-containing media will be referred to as "fibroblast" or "F" media throughout the thesis. Cultured stromal cells at passage 3 (and no more than passage 4) were used in all experiments.

3.1.2. Isolation of porcine epithelial cells

Due to problems associated with the passaging of epithelial cells and insufficient quantities of suitable human tissue an alternative source of epithelial tissue was sought. Adult porcine eyes were obtained from a local abattoir (Staffordshire Meat Packers, SMP, Bucknall, UK) within 2 hr post mortem and subjected to corneal dissection within 1 hr of acquisition. Porcine eyes were removed and immediately transferred to epithelial culture media supplanted with a high A&A content (5% in solution). The porcine cornea was

dissected from the orbital globe using a sterile blade and dissection scissors. The epithelial layer was mechanically stripped using sharp point forceps. The remaining corneal tissue and orbital structure was discarded. The epithelial tissue was further dissected into sections approximately 2 mm in diameter. 5-6 pieces of epithelial sections were carefully placed anterior side down onto T25 cm^2 culture flasks or fibronectin coated surfaces as appropriate, see **section 3.1.3** and incubated at 37 °C, 5% carbon dioxide (CO_2). A small volume of culture media (approximately 100 µl) was added to each sample to prevent tissue dehydration whilst adhering. The explants were allowed to adhere for at least 2 hr before the media was topped up. Care was taken not to disturb the epithelial explants whilst adding media. Epithelial explants were cultured under CnT20 PCT Corneal Epithelium Medium, defined, supplemented with solution A, B and C (CnT20, CellNTec, Precision Media and Models, Switzerland), and referred to as CnT20 media. The cells migrated out of the tissue usually following 48 hr dissection. Cells were cultured until they reached confluence. Due to difficulties passaging the cells, including reduced cell attachment and outgrowth ensuing passaging, only passage 0 cell were using in all of the experiments.

3.1.3. Fibronectin coating to improve epithelial attachment and outgrowth

Fibronectin coating was utilised to aid epithelial attachment and outgrowth. Human plasma fibronectin (Sigma-Aldrich, UK) was prepared at concentration 10 ng/µl in PBS. Acellular and cell seeded collagen constructs were washed 3 times in PBS before being submerged in 500 µl fibronectin solution per construct. T25 cm^2 tissue culture plastic (TCP) flasks were coated using 3 ml of the solution and 1 ml fibronectin solution was used to coat the permeable membranes of cell culture insert dishes and the surface of individual petri dishes. The constructs, TCP flasks, culture inserts and petri dishes were then

incubated at room temperature for 1 hr. The fibronectin solution was removed prior to corneal epithelial dissection.

3.2. Scaffold manufacture and assembly

In this thesis, two principal scaffolds were manufactured and investigated; collagen type I hydrogel scaffolds (fibre-free) and collagen scaffolds that incorporated portable, aligned electrospun nanofibres (fibre-containing).

3.2.1. Collagen hydrogel preparation

In this thesis semi-3D and 3D collagen scaffolds were prepared. For the majority of the experiments performed commercially available rat tail collagen type-I (BD Bioscience, UK) was used as the source of collagen for the hydrogel scaffolds as type I collagen is the main component of *in vivo* corneal tissue. Sodium hydroxide solution (1M NaOH, Sigma-Aldrich, UK) was prepared by dissolving 2 g of NaOH in 25 ml sterile deionised water. The solution was then sterilised using a filter (pore size 0.25 µm, Millipore, USA). NaOH neutralises the pH of the collagen solutions which is vital for hydrogel formation and cell viability. The gelation procedure as detailed in the manufacturer's protocol was followed except that a concentration of 10 times of DMEM was used in the place of PBS. DMEM at 10X concentration was included to provide cells with a source of nutrients to encourage cell viability during gelation. 10X DMEM was prepared by dissolving DMEM powder and 3.7 g sodium bicarbonate into 100 ml sterile water. The solution was then sterile filtered. Sterile deionised water was also added to the collagen mixture. The volume of reagents required was calculated as follows:

$$\text{Volume 10X DMEM} = \text{Total volume} \times 0.1$$

$$\text{Volume of collagen} = \frac{\text{Required concentration}}{\text{Actual concentration (on bottle)}} \times \text{Total volume}$$

$$\text{Volume 1M NaOH} = \text{Volume of collagen} \times 0.023$$

$$\text{Volume } dH_20 = \text{Total volume} - \text{Volume 10X DMEM} - \text{Volume collagen} - \text{Volume 1M NaOH} - \text{Volume cell suspension}$$

Unless otherwise stated the hydrogels were prepared at a collagen concentration of 3.5 mg/ml. 300 µl of the collagen mixture was used for semi-3D scaffolds and 500 µl was used for the 3D scaffolds. Preparation took place on ice to avoid the hydrogels from setting too quickly. For cellular constructs, AHDCS cells were centrifuged and counted using a haemocytometer (Sigma-Aldrich, UK), mixed with 60 µl F media and added to the gels. This step was omitted for acellular scaffolds. All AHDCS cells used in the experiments were seeded at concentration of 1 x 10^6 cells per ml. The cells were suspended throughout the hydrogel solution prior to setting. The collagen mixture was then immediately used to fabricate the constructs. To fabricate each hydrogel construct, a ring of filter paper with an inner diameter of 20 mm was placed on a polytatrafluoroethylene (PTFE) plate on the bottom of a 6-well plate. The collagen mixture was pipetted into the filter-paper ring to prevent shrinking. A second filter paper ring was added to give added support to the edge of the construct (**Figure 3.1**). The hydrogel constructs were set in an incubator at 37ºC, 5% CO_2. Following 30 minutes gelation time the solution had set to form a hydrogel. The construct was removed from the PTFE using sterile forceps. 3 ml of culture media was added to each hydrogel construct and they were incubated. Media was changed every 3-4 days unless otherwise stated.

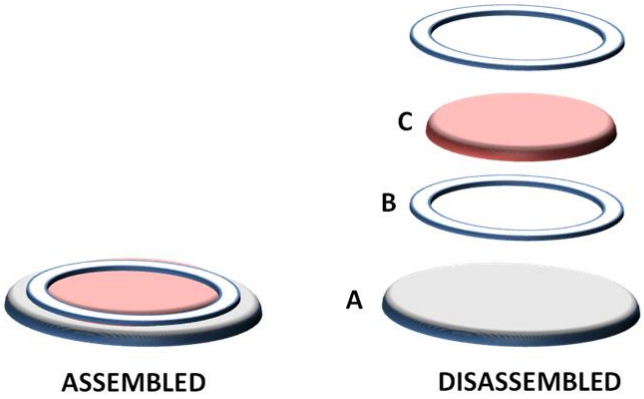

Figure 3.1: A schematic diagram detailing the assembly of collagen hydrogel scaffolds; (A) PTFE disc; (B) filter paper support ring (x2); (C) 500 µl collagen mixture.

3.2.2. Fabrication of fibre-containing scaffolds

Aligned, portable electrospun nanofibres were incorporated into the hydrogel scaffold with the specific aim to increase the cell organisation and the mechanical strength of the resulting cell-seeded constructs.

3.2.2.1. Electrospinning and fabrication of PLDLA aligned nanofibres

Electrospinning was used to fabricate portable poly (L,D lactic acid) (PLDLA, 96% L/4% D; Purac B.V. Netherlands) aligned nanofibres. PLDLA polymer solutions were prepared by adding 0.2 g of polymer to 7 ml chloroform which was thoroughly mixed for a minimum of 4 hr or until all trace of polymer has dissolved using a magnetic stirrer (SB16 Stuart, UK). 3 ml dimethylformamide (DMF) was added to the solution and mixed overnight to ensure a homogenous solution was prepared. This resulted in a 2% (*wt/v*) solution in a 7:3 ratio mixing solvent (chloroform:DMF). The solution was spun the next day and all solutions used within a week of manufacture.

All electrospinning apparatus was set up within a fume cupboard that included interlocks and a voltage dissipater (Allen-Bradey Guardmaster®, Dominican Republic) in

accordance with local health and safety regulations. The elemental components of the electrospinning apparatus were two high voltage power supplies, connected to a master-slave configuration which allowed for voltage adjustments between 0-60 kV, and a current between 0-5 mA; an adjustable height stage, a calibrated syringe pump, a glass syringe attached to a stainless steel needle and a copper collection plate (**Figure 3.2**). The syringe pump (KR Analytical, UK) was used to feed the polymer solution (0.025 ml/min) through a blunt 18G needle (KR Analytical, Sandbach, UK). The needle was connected to the High Voltage Power Supply (HVPS, Spellman HV, UK) which comprised two power supplies, one positive and one negative. The polymer solution was positively charged and the collector negatively charged. Fibres were collected using a custom built portable collector (Manufactured by Mr J Wilson and associates at KMF Precision Sheet Metal, Newcastle-Under-Lyme, UK, **Figure 3.3**) consisting of an adjustable frame (30 x 10 cm) and 2 sheets of thin steel "blades" arranged parallel to each other. The blade distance was set to 4 cm. The frame was then insulated using polyvinyl chloride (PVC) insulating tape (Thorsman, UK), leaving only the blades exposed. The fibres were collected over a width of approximately 10 cm. The collector was electrically connected to a static copper plate. The distance between the needle tip and the portable collector was 20 cm; the distance between the portable collector and the static copper plate was 10 cm. The electrospinning duration was 10 min. A summary of the optimised parameters can be found in **Table 3.1.**

Table 3.1: A summary of the optimised working conditions successfully employed to produce aligned PLDLA electrospun nanofibres.

Parameter/units	
Volume polymer ejected (ml)	0.25
Flow rate (ml/min)	0.025
Needle	18G (ID = 0.84 mm)
Voltage (kV)	6.0
Distance from needle to blades (cm)	20
Distance from blades to ground electrode (cm)	10

3.2.2.2. Collection and quantification of nanofibres

The nanofibres were collected by adhering the aligned fibres to a square cellulose acetate frame (16 cm^2) so that the relatively low density nanofibres mesh could be handled. The frames were removed using forceps and excess fibres were severed from the frames using a scalpel and blade. Once adhered, the frames could be removed with the aligned nanofibres attached to them and arranged as required.

Nanofibre diameter and density was determined using a commonly used method which utilises scanning electron microscopy (SEM) and image processing software (Maroni et al. 2007, Kai et al. 2011, Yang et al. 2012). Briefly, images were taken of the collected nanofibres meshes using a field emission scanning electron microscope (Hitachi S4500, Hitachi, Berkshire, UK). The average density of the fibres was calculated by counting the number of nanofibres per 100 μm length using ImageJ (NIH, USA). Three areas per mesh and a total of 6 meshes were analysed. The average density of fibres in each mesh was calculated to be 45 nanfibres per 100 μm (± 11.65 nanofibres) or 1800 nanofibres per acetate frame (± 329.2 nanofibres. The thickness of the fibres was measured using a line drawing tool in ImageJ. The thickness of the fibres ranged from 0.5- 3.0 μm.

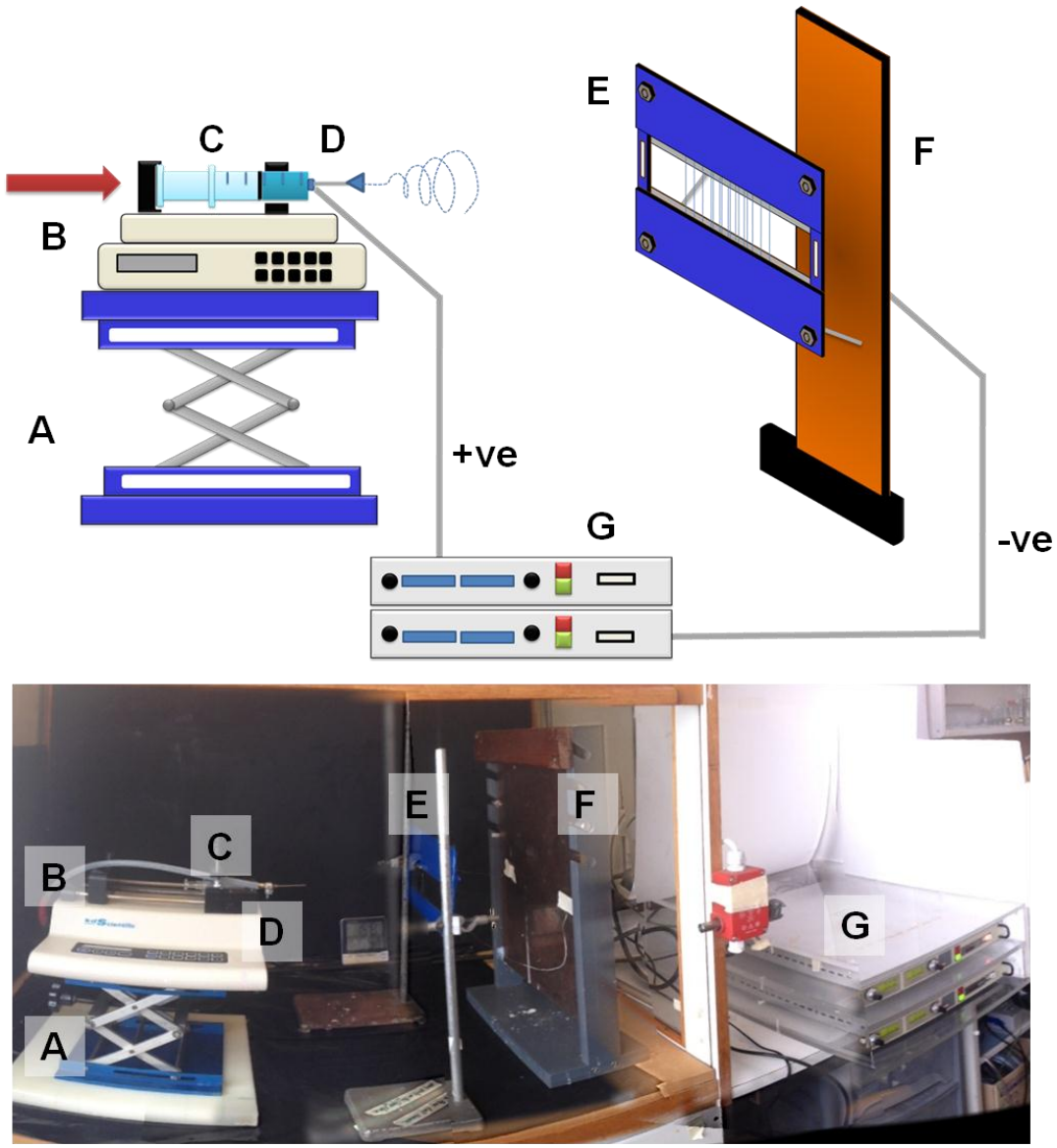

Figure 3.2: A schematic diagram (top) and the actual set up (bottom) of the electrospinning apparatus used for the manufacture of aligned nanofibres; (A) variable height stage, (B) a syringe pump, (C) glass syringe polymer reservoir, (D) stainless steel needle, (E) portable collector, (F) negatively charged copper collection plate, (G) high voltage power supply.

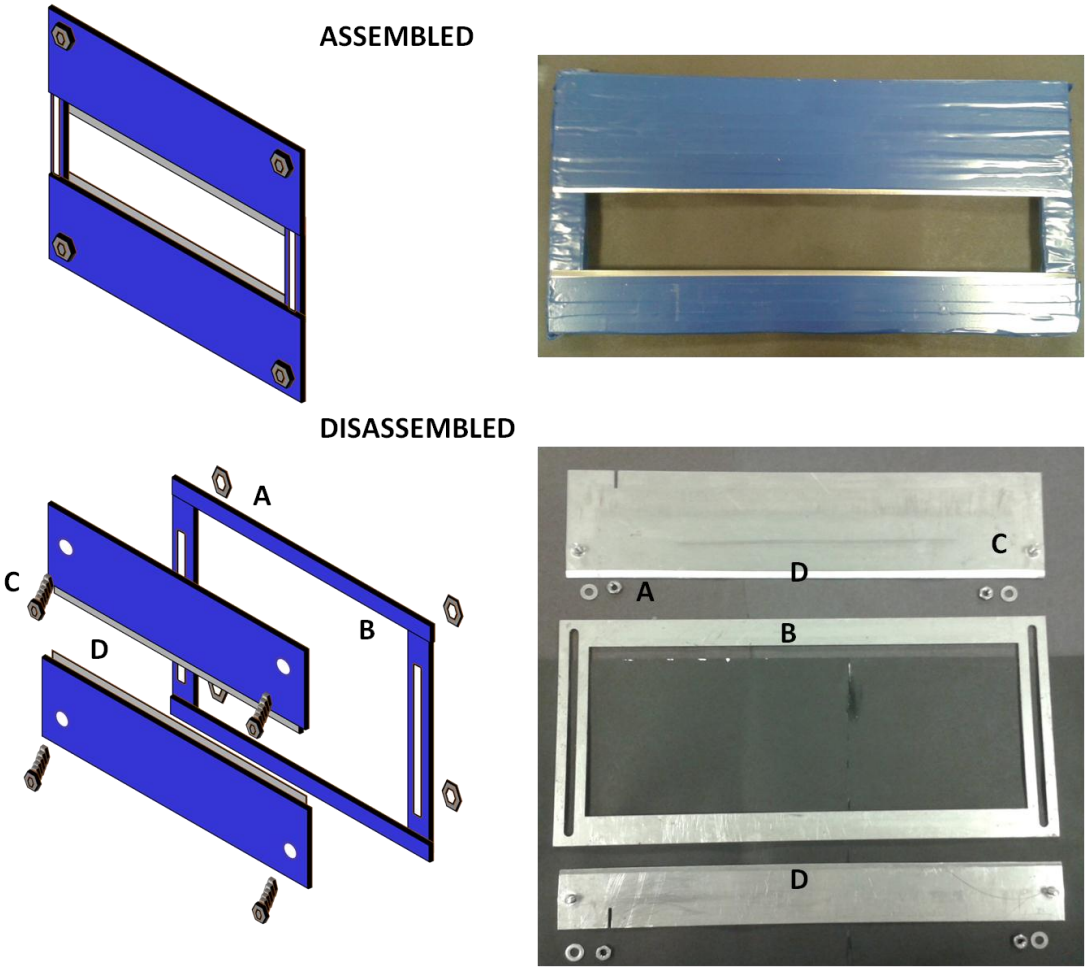

Figure 3.3: Schematic diagrams (left) and the actual apparatus (right) of the custom built portable collector used for the collection of aligned nanofibres; (A) bolts; (B) adjustable frame; (C) screws; (D) stainless steel collecting blades. PVC tape was used to insulate the frame, leaving only the collecting blades exposed.

3.2.3. Acid extraction of collagen

Acid extracted collagen used in this study was kindly supplied by Ms. Marie Guilbert and associates from Université de Reims Champagne-Ardenne, France. Native type I collagen from the rat tail tendons of Sprague Dawley rats (Depre, St. Doulchard, France) was extracted using an acid extraction method. Acid-soluble type I collagen was obtained

from rat tail tendons by 0.5 M acetic acid extraction then purified by dialysis against distilled water and lyophilised. This lyophilised, purified, and non-pepsined collagen was stored at -80°C until further use. For preparing 3D gels, lyophilised collagens were sterilised in ethanol, dried and then dissolved in sterile 18 mM acetic acid at a final concentration of either 3mg/ml or 5 mg/ml.

3.2.3.1. Dissection of rat tails

The rat tails of Sprague-Dawley rats were previously stored at -80 ˚C. The tails were submerged in 70 % alcohol solution for 5 minutes to disinfect them. They were then dried using absorbent paper. Using a scalpel, the skin was removed from the tails. The tail was then gripped using a multi-grip nipper and the vertebra were broken (approximately 12 vertebras per tail). The tendons were extracted by pulling them with the multi-grip nipper from the distal to proximal extremities. An extraction buffer was prepared by dissolving 8.76 g of sodium chloride (NaCl, Sigma-Aldrich, France), 4.16 g ethylendiaminetetraacetic acid disodium salt dehydrate (EDTA, Sigma-Aldrich, France), 1.21 g 10 mM Tris(hydroxymethyl)aminomethane (Tris HCl, Sigma-Aldrich, France), 0.78 g 5 mM Benzamidine (Sigma-Aldrich, France), 0.174 g phenyl-methly-sulfonylfluoride dissolved in 1 ml 99% ethanol (PMSF, Sigma-Aldrich, France), 0.625 g N-ethyl-maleimide dissolved in 1 ml 99% ethanol (NEM, Sigma-Aldrich, France) and 1 g sodium azide (NaN_3, Sigma-Aldrich, France) in 1 litre of sterile, distilled water. After complete dissolution of all of the reagents, the pH was adjusted to 7.4 using NaOH. The tendons were then submerged in the extraction buffer (approximately 600-800 ml buffer for 5 tails) to prevent drying of the tendons. The extracted tendons were incubated at 4 ˚C for 24 hr under low agitation.

3.2.3.2. Precipitation of collagen

Following 24 hr agitation the rat tail tendons were centrifuged for 30 min at 934 rcf. The supernatant was removed and 300 ml 0.5 M acetic acid (Sigma-Aldrich, France) was used to dissolve the tendons. Following 48 hr agitation the dissolved tendons were centrifuged for 30 min at 934 rcf. The supernatant was removed and measured. The same volume of 0.5 M acetic acid and 1.4 M NaCl (the final concentration of NaCl is 0.7 M, Sigma-Aldrich, France) were added progressively to the dissolved collagen under low agitation, allowing for the specific precipitation of type I collagen. The mixture was agitated for a further 24 hr at 4 ˚C.

3.2.3.3. Collagen solubilisation and purification

Following 24 hr agitation, a viscous pellet formed. The mixture was centrifuged for 30 min at 934 rcf. The supernatant was removed and the pellet was placed in 600 ml 18 mM acetic acid. The pellet was incubated at 4 ˚C under low agitation for 24 hr, or until completely solubilised. The collagen was purified using a dialysis step. Dialysis membranes (Medicell, France) 15-20 cm in length was prepared by knotting one end of the tubing. Solubilised collagen was transferred into the tubes and sealed using dialysis clamps. The membranes were placed into distilled water and incubated at 4 ˚C. The distilled water was changed 5 times a day for 5 days. The membranes were then opened and placed into lyophilisation jars. The collagen was then frozen at -20 ˚C and the jars were regularly turned in order to achieve a homogenous deposition. The collagen was then freeze-dried for 12-18 hr using a cryodessicator.

3.3. Development of instrumentation for mechanical and viscoelastic characterisation

The mechanical properties of soft tissues are closely related to their physiological function. For example, following injury or disease, tissue remodelling occurs which will repair the tissue, but may alter the mechanical strength (Yang et al. 2007). When assembling and manufacturing *in vitro* tissues the ability to monitor and measure the mechanical properties of the resulting construct is vital as time, culture and conditioning environments can all influence the structural and biomechanical aspects of the tissue (Yang et al. 2007). A particular challenge to tissue engineering is the ability to monitor 3D cell cultures in a non-destructive manner (Bagnaninchi et al. 2007).

3.3.1. Microindentation and acquisition of lateral deformation images

Many techniques are available that enable the mechanical and viscoeleastic characterisation of biological tissues and their equivalents to be determined, as detailed in **section 2.8**. Indentation techniques are widely used to characterise soft biomaterials including biopolymers and human tissue. They work by measuring the reaction forces by imposing certain indentation depths *via* a rigid indenter (Ahearne 2007, Ahearne et al. 2008). The displacement caused by the indenter versus the applied force (compliance) can be used to deduce the mechanical properties of materials (Ahearne 2007, Ahearne et al. 2008). For example, a stiff, rigid material will deform less than a softer material. Lui and Ju (2001, 2002) developed an experimental technique that allowed for the non-destructive measurement of thin, circular, fragile membrane-like materials including latex and egg membranes. The technique involved the central indentation of a circumferentially clamped construct using a sphere of known weight. The central displacement is then measured. This technique was modified by Ahearne (Ahearne 2007, Ahearne et al. 2008) to allow for the characterisation of cell-seeded hydrogel constructs under sterile cell culture conditions

whilst fully immersed in solution and at elevated temperatures. This allows for on-line, real-time and non-destructive measurements to be taken over prolonged culture periods. The instrumentation developed to measure deformation consisted of a circular sample holder with a spherical indenter and an image acquisition system. Each sample holder allowed for the clamping of one specimen at a time and required the use of four separate screw and bolts to hold the specimen in place (**Figure 3.4**). Assembly of the holder for sample analysis was time consuming and awkward primarily due to the number of screws required. In addition the time required to assemble and disassemble the sample holders meant increased susceptibility to infection and damage to the construct.

A specifically designed sample holder was modified for this project to allow for three gels to be measured at once, (manufactured by Mr J Wilson and associates at KMF Precision Sheet Metal, Newcastle-Under-Lyme, UK; **Figure 3.5**) compared to the holder that only allowed for one gel to be measured in previous studies (Ahearne 2007, Ahearne et al. 2008). The holder was used to clamp the hydrogel constructs around its outer circumference and was advantageous to the previously used holder in that it was more convenient to assemble with reduced infection risk and potential damage to hydrogel constructs due to the reduction in the number of screws and bolts required per construct. The number of bolts required to clamp the apparatus was reduced to 6; so instead of 4 bolts per construct, it was 6 bolts per 3 constructs. Two transparent acetate circular hoops with an inner diameter of 20 mm were used to hold the hydrogel. The design ensured that clamping stress was minimised on the hydrogel constructs. Two 1 mm stainless steel (grade 316L) sheets were positioned above and below the plastic hoops. The steel sheets were then held together by 6 stainless steel screws allowing for up to 3 gels to be viewed at any one time.

All components of the sample holder were autoclaved before use and assembled in a flow hood using autoclaved forceps. The whole assembly was submerged in pre-warmed PBS in a large square petri dish and the hydrogels were viewed laterally. The gels were deformed using a smooth PTFE sphere (Spheric-Trafalgar, London) of weight 0.0711g and diameter 4 mm. The ball was placed at the centre of the hydrogel-cell constructs and caused a central deformation. The diameter-ratio of the hydrogel to the sphere was at 5.0 for these experiments. The petri dish was placed into an incubator at 37˚C, 5% CO_2 for 10 minutes before the images were recorded, thus assuming that time-dependent deformation had reached equilibrium. Within the sample holder, large displacements up to 5 mm could be visualised. The weight of the ball was recalculated to compensate for its submersion in PBS.

The image acquisition system consisted of a long focal distance objective microscope (Edmund Industrial Optics, USA) with a computer linked charged coupled device (CCD) camera (XC-ST50CE, Sony, Japan) that allowed for high magnification (up to 120 times) to visualise the side-view images of the deformation profile of the suspended circular construct under the weight of the ball from outside the incubator through the glass door, see **Figure 3.6. Figure 3.7** demonstrates a typical deformation image of a fibre-free cellular construct, cultured in F media. A multi light emitting diode (LED) ultra-bright torch was used to increase the brightness of the samples (AM-Tech, UK), enabling them to be viewed more clearly. A previously defined theoretical model (Liu, Ju 2001) was employed to allow for a quantitative correlation of viscoelasticity with regards to the deformation profile of the construct.

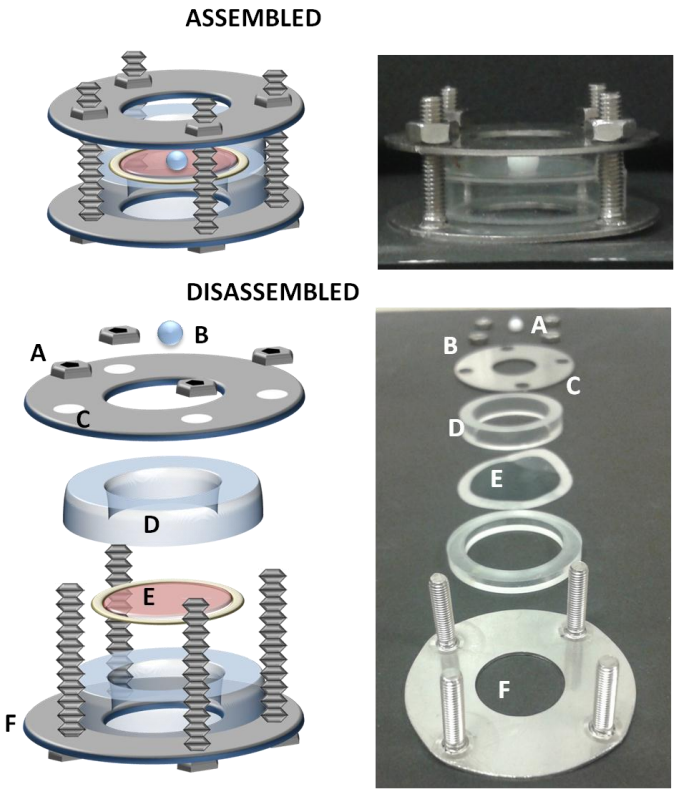

Figure 3.4: Schematic diagrams (left) and the actual set up (right) of the assembled and disassembled previous hydrogel sample holder used for the non-destructive measurement of cell-seeded collagen constructs whereby only one specimen could be measured at any one time; (A) 4 x screws; (B) ball indenter; (C) stainless steel top plate; (D) transparent acetate rings; (E) hydrogel construct; (F) stainless steel base plate and screws.

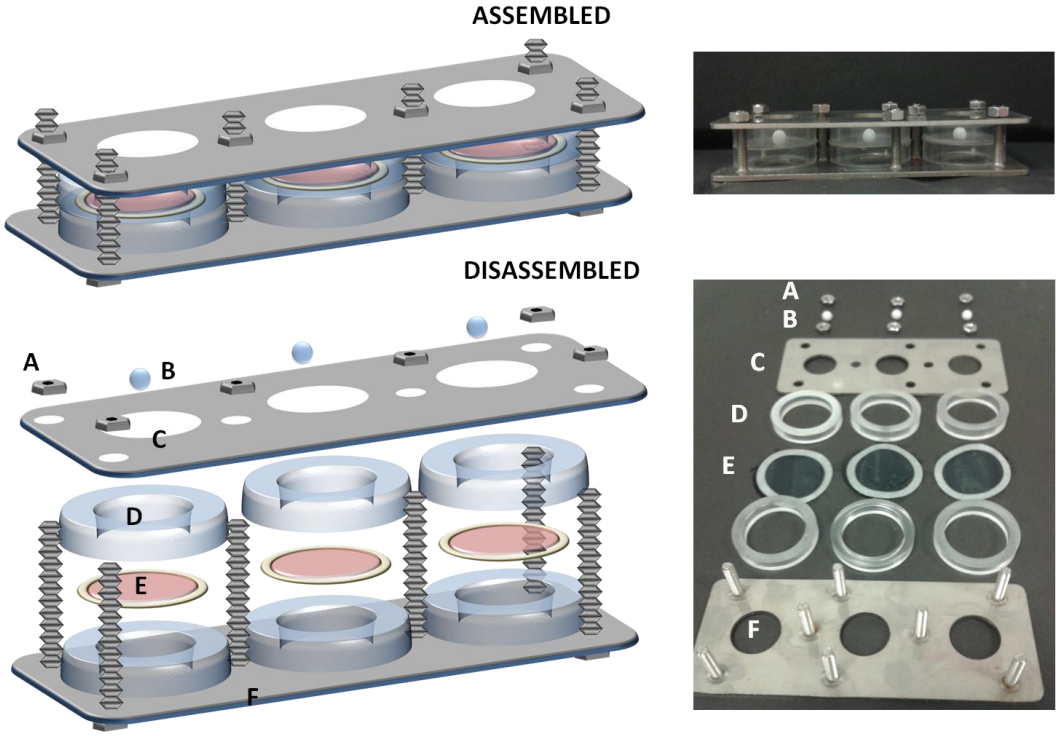

Figure 3.5: Schematic diagrams (left) and the actual set up (right) of the assembled and disassembled modified hydrogel sample holder for the non-destructive measurement of cell-seeded collagen constructs allowing for three specimens to be measured at any one time with reduced contamination and infection risk; (A) 6 x screws; (B) 3 x ball indenters; (C) stainless steel top plate; (D) transparent acetate rings; (E) 3 x hydrogel constructs; (F) stainless steel base plate and screws.

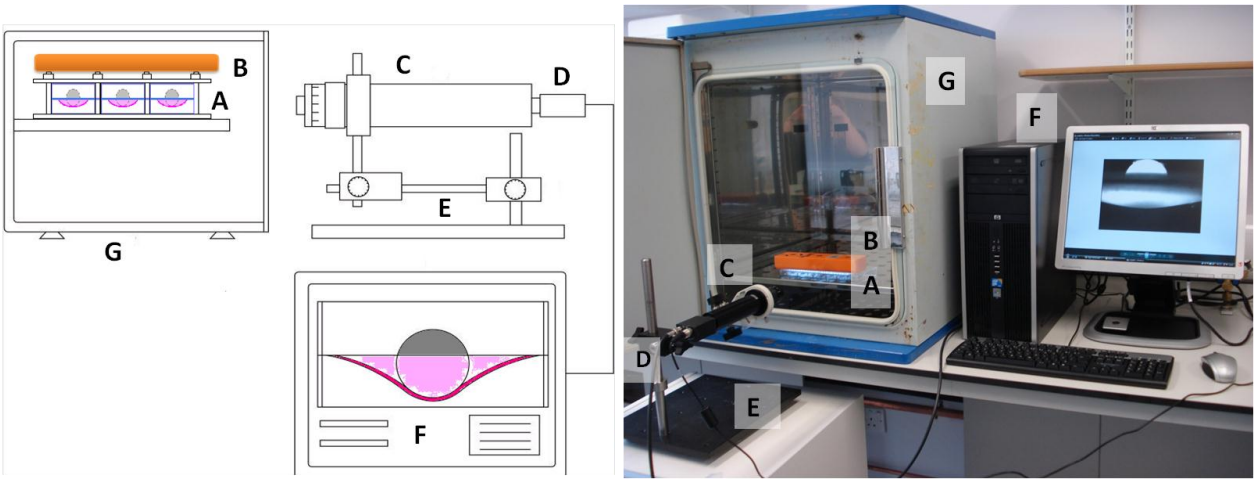

Figure 3.6: A schematic diagram (left) and the actual set up (right) of the instrument system used to measure the deformation behaviour of the collagen constructs; (**A**) sample holders, constructs and balls; (**B**) multi-LED ultra bright torch, (**C**) long working distance microscope; (**D**) CCD camera; (**E**) precision *x-y* translation stage; (**F**) image analysis system (**G**) incubator at 37ºC, 5% CO_2 (Modified from Ahearne et al, 2008, with permission).

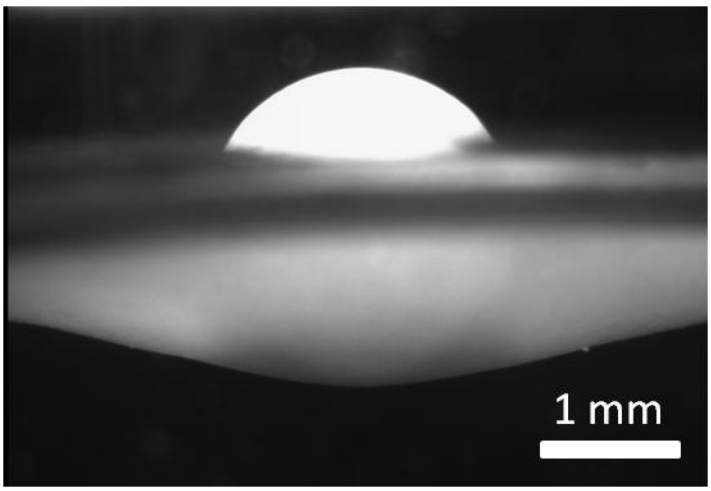

Figure 3.7: A representative image of a collagen construct under ball indentation using the long working distance microscope.

3.3.1.1. Theoretical analysis

Hydrogels can be modelled as viscoeleastic materials that exhibit rubber-like characteristics (Anseth et al. 1996). An applied mechanical stress (or strain) leads to a time dependence on the strain (or stress) when the segments of the polymer chain in the hydrogel move. Such movement causes an internal response that result in a time-dependent recovery when the initial condition is removed. Normally, elastic materials (e.g. metal spring) restore almost instantaneously to its original undeformed status, while visco materials (e.g. water) will never restore back, i.e., recovery time is infinite, when the material is released from the applied forces (Aklonis and MacKnight 1983). However, most biological and biomimetic materials (e.g. hydrogel) which are viscoelastic materials (Anseth et al. 1996) have mechanical behaviours in between. In order words, they will take a certain (finite) time to partially restore after the applied force is removed. Normal rubbers are cross-linked networks with a large free volume allowing them to respond to external stresses with rapid rearrangement of the polymer segments (Anseth et al. 1996), in their swollen state, most hydrogels fulfil this criteria. Throughout the experiments, the gels were immersed in PBS or medium and so sufficiently swollen.

The mechanical behaviour of hydrogels can be characterised using Mooney-Rivlin equations (Rivlin 1948) which characterise isotrophic and incompressible materials-referred to as Mooney materials. The weight of the ball causes deformation. Analysis of the images collected allows the mechanical and viscoeleastic properties to be determined. A mathematical equation (Yang and Hsu 1971) has been developed to determine the Young's modulus of membrane materials (Liu and Ju 2001). **Figure 3.8** is the schematic diagram used to calculate the Young's modulus. The ball caused axisymmetric deformation to occur in the circular membrane as shown in **Figure 3.7**. The microscope system was used to measure the central displacement (δ) and this was used to determine

the Young's modulus (*E*) by applying the following equation:

$$\frac{6w}{EhR} = 0.075 + \left(\frac{\delta}{R}\right)^2 + 0.78\left(\frac{\delta}{R}\right)$$

Equation 3.1.

When a central load *w* is applied to a gel, which has elastic modulus *E*, undeformed radius *a*, and thickness *h* (can be determined by OCT), *via* a sphere of radius *R*, a displacement δ will occur at the centre of the gel. This equation is applicable when the ratio of $a/R = 5$ and $\delta/R < 1.7$, where *a* is the radius of the hydrogel. The model used in this experiment assumes that the ratio of thickness to radius is low and deformation is large; thus stretching of the hydrogel dominates over bending (Ahearne et al. 2008, Begley and Mackin 2004, Wan 1999).

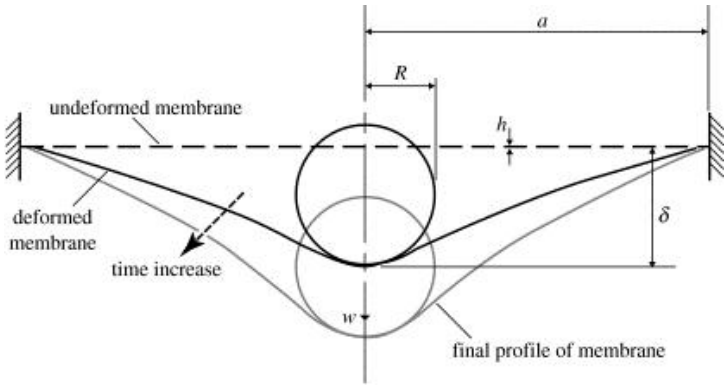

Figure 3.8: Indentation of a viscoelastic membrane by a sphere (Liu, Ju 2001, Ju, Liu 2002).

A limitation of the model is that it assumes that there is no change in thickness of the gel when it is under deformation. Instead the thickness (*h*) is based upon the thickness of the gel when undeformed. In reality, the actual thickness of the hydrogel when under deformation is smaller than what is used in the calculation; which in turn could produce an error in the overall stiffness value. However, since the strain applied to the hydrogel is small (calculated to be approximately 2% for a 2 mm central deformation) then the

"difference" in the gel thickness when under deformation compared to the undeformed thickness value used in the calculation can be presumed to be small. If a Poisson's ratio of 0.5 is assumed (which is the same as rubber materials (Pritz, 2000)) then it can also be assumed that there is 2% strain in the axial direction, which should lead to a 1% strain in the transverse direction. Therefore, there is only a 1% "difference" in thickness value. For example, if an atypical acellular 3.5 mg/ml hydrogel scaffold of thickness (h) 1.1 mm that has been deformed by 2 mm (δ), the calculated elastic modulus (E) would be 1.190 kPa; taking into account the error, the actual modulus value would only differ by ± 0.012 kPa if the thickness of the hydrogel when under deformation was accounted for. This value would bear no significant effect on the overall observed trends, and so the model and *Equation 3.1* was deemed suitable for analysis of the hydrogel constructs.

3.3.2. Characterisation of hydrogel thickness using optical coherence tomography

The thickness of the corneal constructs was recorded using optical coherence tomography (OCT) following deformation as it is a non-invasive imaging technique with micrometer resolution, capable of measuring the structure and thickness of materials up to 2 mm in thickness (**Figure 3.9**). OCT is a technique that is readily used to examine the structure of materials including soft tissues and commercially available OCT systems are often used in medical settings (Yang et al. 2006), frequently by ophthalmologists to examine the ocular structure, in particular the retinal structure. Super bright LEDs generate broadband light sources whereby the beam of light is split into 2 arms, with one beam passing through the experimental construct and the other acts as a reference. The combination of reflected (backscattered) light from the sample and reference arm gives an interference pattern, or a reflectivity profile (Yang et al. 2007). Photodetectors measure the light intensity of the backscattered light and a reconstructed image is produced in the form

of an image detailing the cross-sectional microstructure of the construct. Dense, opaque samples cause greater interference and will reflect back more light than a transparent sample. The resolution of OCT is equivalent to a low-powered microscope. Confocal and multi-photon techniques are also capable of high resonance imaging up to 200 μm depth, however OCT is advantageous in that it does not require fluorescent labelling of samples and it is relatively inexpensive and easily set up with deeper penetration depths (up to 2 mm), thus is the most suitable technique for this purpose. OCT is more clinically relevant (Bagnaninchi et al. 2007) in that it allows for fast, sterile, non-destructive, *in situ*, real-time investigations (Yang et al. 2007) (i.e. the experiment does not have to be terminated or require a fixed sample biopsy (Bagnaninchi et al. 2007)) of soft biomaterial, e.g. collagen hydrogel constructs. A bench top fibre based time-domain OCT system developed by Bagnaninchi *et. al.* (2007) was used in this study which uses a 1300 nm superluminesence diode with bandwidth of 52 nm. The images are scanned at 100 Hz within a frame consisting of 400 x 350 pixels which corresponds to a physical image of 5.8 mm x 2.9 mm. Three dimensional scanning was achieved *via* the use of an *xy*-stage, through the specimen width (*y* direction). The hydrogel construct was placed on the *xy* stage and set in the OCT light path. The scans were performed through the lid of a TCP 6 well plate (Corning, UK). Near infra-red visible light allowed for the accurate focussing of the OCT light source. A mirror controlled by a galvanometer (an instrument that detects and measures small electric currents) focussed the measuring beam. The acquired images were primarily utilised in this research to monitor macroscopic construct changes regarding construct thickness and changes in thickness of the construct due to cellular remodelling for prolonged culture periods. 3-4 images were taken per construct ensuring that the measurements were taken as close to the centre of the hydrogel construct as possible, i.e. where the construct had undergone deformation by the spherical indenter, to ensure that measurements are as

consistent as possible when using this technique. The acquired images were analysed using ImageJ software (NIH, USA) and a mean of the measurements was used to determine the construct thickness.

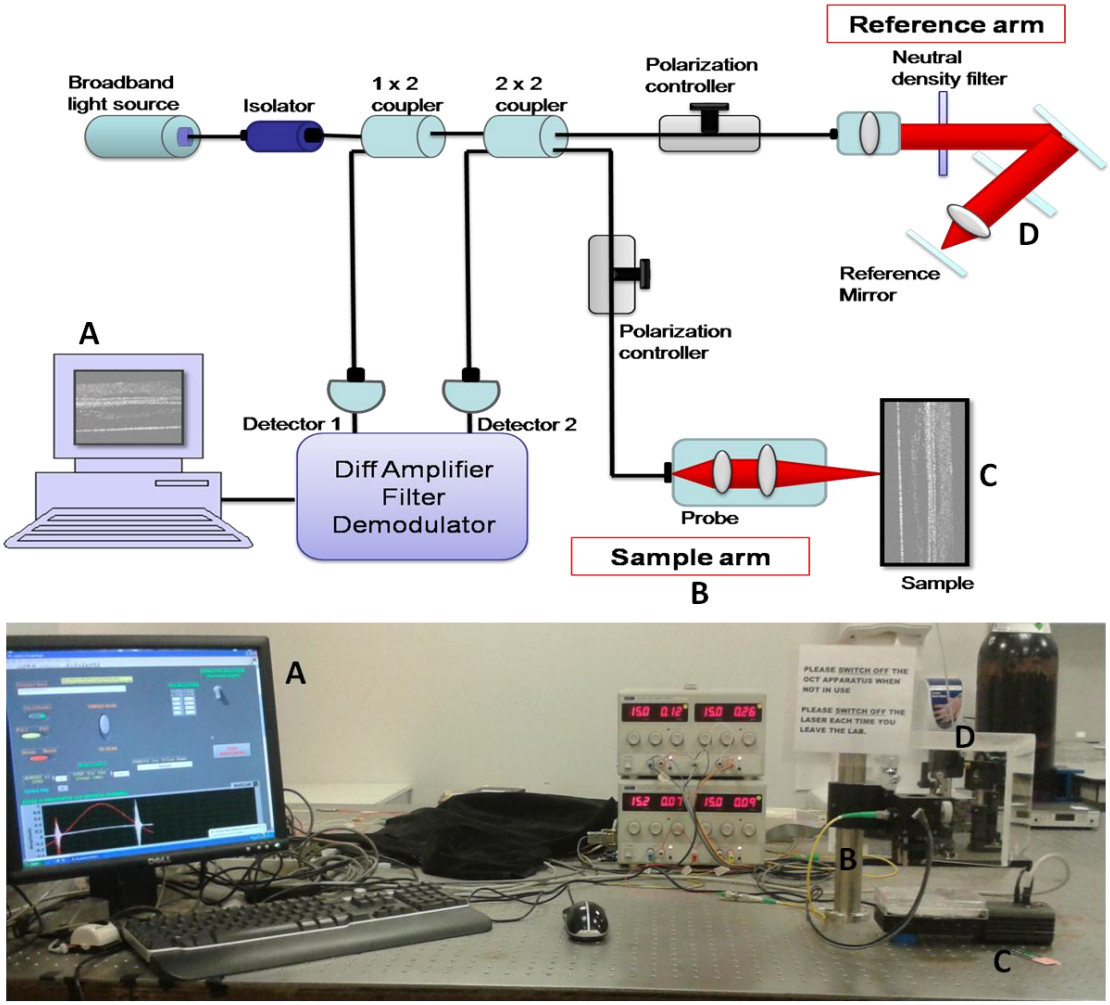

Figure 3.9: A schematic representation (top) and the actual OCT set-up used to non-destructively monitor construct contraction; (A) image analysis system; (B) sample arm; (C) sample on *x-y* stage; (D) reference arm.

3.4. Cellular characterisation

The changes in the mechanical properties of engineered tissues are controlled by cellular activities. The behaviour of cells within hydrogel constructs was examined using either immunohistological or fluorescent staining or gene expression analysis (*via* qPCR) in parallel with the elastic modulus and OCT contraction measurements. This enabled for a relationship between the changes in the macroscopic properties and the change in cell activity and behaviour to be ascertained and established. Immunohistochemical and fluorescent staining techniques were also employed in 2D and semi-3D studies.

3.4.1. Cell viability

The viability of cells in all experiments was assessed using a live-dead double staining kit (Fluka, Japan), able to simultaneously stain both live and dead cells. Calcein-AM ester was used to fluorescently label live cells green, where as Propidium Iodide, which is unable to pass through the membrane of viable cells, labelled the nucleus of dead cells red. Prior to staining, all culture media was removed from the sample and they were washed using PBS. Each sample was immersed in 500 µl staining solution containing 1 µl Calcein-AM and 0.5 µl Propidium Iodide in PBS. Samples were then protected from light by wrapping them in silver foil and incubated at 37 °C, 5% CO_2 for 20 min. Cell staining was observed using fluorescent microscopy (Eclipse T*i*-S, Nikon, Japan).

3.4.2. Cell morphology and aspect ratio

Cell morphology was observed by using phalloidin tetramethylrhodamine-B-isothiocyanate (P1951, Sigma-Aldrich, UK) to fluorescently stain actin filaments in cells. Each sample was fixed in 500 µL 10% neutral buffered formalin solution (Sigma-Aldrich, UK) for 60 min, before washing 3 times in PBS. The samples were then permealised with

500 µL 0.1% Triton® X100 (in PBS, Sigma-Aldrich, UK) for 60 minutes before washing x3 in PBS. The staining solution was prepared by dissolving 1 mg of phalloidin tetramethylrhodamine-B-isothiocyanate in 200 µl dimethyl sulfoxide solvent (DMSO, Sigma-Aldrich, UK), to give a stock solution. The stock solution was protected from light and stored at – 4 °C. 500 µL actin staining solution per sample was prepared by mixing 10 µl of the stock solution with 5 µl DMSO and 485 µl PBS. The samples were protected from light and incubated at room temperature for at least 40 minutes. Cell morphology was examined using fluorescent microscopy (Eclipse T*i*-S, Nikon, Japan).

Following the staining of the cell actin filaments the images were analysed using Image J software and the aspect ratio of the cells was calculated. A line-drawing tool was used to measure the extremities of the cell; the long axis of the cell was measured, followed by the width. The ratio length:width was used to determine and quantify the morphology of the cell; for example, an aspect ratio of 1 indicates that the cells were of equal proportions and demonstrated no elongation; an elevated aspect ratio indicates elongation of the cells.

3.4.3. Cell immunolabelling

Cell phenotype was observed in both epithelial and stromal cell cultures in 2D monoculture, semi-3D and 3D collagen hydrogel environments *via* the use of immunohistochemical staining. Each sample was fixed in 500µL 10% neutral buffered formalin solution as previously described. The samples were then permealised with 500 µL 0.1% Triton® X100 (in PBS) for 60 minutes before washing x3 in PBS. Samples were then blocked to prevent any non-specific binding, with 500 µL 2% bovine serum albumin (BSA, 2% *w/v* in PBS, Sigma-Aldrich, UK) for 2 hr. Samples were then washed x3 in PBS before being stained with the primary antibody at dilution 1:50 (in PBS) overnight at 4 ˚C.

The samples were protected from light by covering the samples in foil. All primary and secondary antibodies were purchased from SanatCruz Biotechnology (UK).

The primary antibodies used to stain the epithelial cultures were cytokeratin-3 goat polyclonal IgG (CK3) and vimentin goat polyclonal IgG. The samples were then washed 5 times in PBS in 5 minute intervals. Donkey anti-goat IgG-fluorecin isothiocyanate (FITC) , donkey anti-mouse IgG FITC, donkey anti-goat IgG-tetramethyl rhodamine isothiocyanate (TRITC) and goat anti-mouse IgG TRITC were used as secondary antibodies to fluorescently label the samples.

The primary antibodies used to stain the stromal cell cultures were split into two panels: Keratocan goat polyclonal IgG, aldehyde dehydrogenase-3 (ALDH3A1) mouse polyclonal IgG and lumican goat polyclonal IgG to act as positive stain for keratocytes. FITC-conjugated Thy-1 goat polyclonal IgG, smooth muscle actin mouse polyclonal IgG and vimentin were used to positively stain for fibroblasts/myofibroblasts. With the exception of Thy-1 staining, the samples were fluorescently labelled with FITC or TRITC secondary antibodies (see **Table 3.2** for details) at dilution 1:100 (in PBS) for 4 hr at 4 ˚C in the dark. The samples were then washed five times with PBS in 5 min intervals. All samples were further counterstained with DAPI (1:500; prepared in PBS (Sigma-Aldrich, UK) in order to visualise nuclei of cells and viewed using fluorescent microscopy (Eclipse Ti-S, Nikon, Japan).

Table 3.2: Summary of the panel of primary and secondary antibodies used for immunohistochemical characterisation of corneal epithelial and stromal cells.

Primary Antibody	Secondary Antibody	Positively expressed in:	References
Cytokeratin-3 goat polyclonal IgG	Donkey anti-goat IgG-FITC	Healthy epithelial cells	Li et al. 2006, Ahmad et al. 2007, Mi et al. 2010, Bayyoud et al. 2012
Keratocan goat polyclonal IgG	Donkey anti-goat IgG-FITC	Healthy keratocytes	Carlson et al. 2003, Espana et al. 2003, Carlson et al. 2005, Kawakita et al. 2005
ALDH3A1 mouse polyclonal IgG	Donky anti-mouse IgG FITC	Healthy keratocytes	Jester et al. 1999, Berryhill et al. 2002, Pappa et al. 2003, Jester et al. 2005, Pei et al. 2006
Lumican goat polyclonal IgG	Donkey anti-goat IgG-TRITC	Fibroblasts	Fundrburgh et al. 2001, Berryhill et al. 2002, Carlson et al. 2003, Carlson et al. 2005, Hayashi et al. 2010
FITC conjugated Thy-1 goat polyclonal IgG	None	Fibroblasts	Pei et al. 2004, Hindman et al. 2010
Smooth muscle actin mouse polyclonal IgG	Goat anti-mouse IgG TRITC	Fibroblasts/ myofibroblasts	Jester et al. 1995, Fundrburgh et al. 2001, Carlson et al. 2003, Espana et al. 2004, Karamichos et al. 2010
Vimentin goat polyclonal IgG	Donkey anti-goat IgG-TRITC	Fibroblasts "Injured" epithelial cells	Espana et al. 2005, Yoshida et al. 2005, Ainscough et al. 2011

3.4.4. Gene expression analysis

Total ribonucleic acid (RNA) was extracted from the hydrogel constructs using a guanidium iso-thiocyanate method that denatures proteins including ribonucleases whilst retaining the integrity of the RNA. The method has been deemed to be a simple and reliable protocol, for the isolation of RNA from both large and small specimens in large numbers of samples which can then be used for downstream processes such as complementary deoxyribonucleic acid (cDNA) synthesis and polymerase chain reaction (PCR) analysis (Chomczynski, Sacchi 1987).

3.4.4.1. Preparation of reagents

The following reagents were prepared for the gene expression analysis: 1M sodium citrate, pH 7.0; denaturing solution "D"; 2M sodium acetate, pH 4.0; and chloroform:isoamyl alcohol, 24:1 (*v/v*). 14.7 g of sodium citrate (Sigma-Aldrich, UK) was dissolved in 50 ml 0.1% (*v/v*) sterile diethyl pyrocarbonate (DEPC, ICN Biomedicals Inc. UK) to prepare the sodium citrate. The pH was adjusted to 7.0 with citric acid (Sigma-Aldrich, UK). A denaturing solution (solution "D") was prepared for the lysis of collagen constructs for qPCR analysis by dissolving 25g guanidine thiocyanate (Sigma-Aldrich, UK), 0.25g n-lauryl sarcosine (Sigma-Aldrich, UK) and 1.25 ml 1M sodium citrate (Sigma-Aldrich, UK) into 0.1% DEPC water. The pH was adjusted to 7.0 and made up to a final volume of 50 ml with DEPC water. 8.2g of sodium acetate (anhydrous, Sigma-Aldrich, UK) was dissolved in 40 ml DEPC water to prepare the sodium acetate solution. The pH was adjusted to 4.0 by adding concentrated hydrochloric acid (HCl, Sigma-Aldrich, UK) accordingly. DEPC water was added to give a final volume of 50 ml. The chloroform:isoamyl alcohol was prepared by simply dissolving 48 ml of chloroform (Sigma-Aldrich, UK) was added to 2 ml isoamly alcohol.

3.4.4.2. Lysis of sample

3D constructs were processed for PCR analysis by removing the filter paper support rings using a sterile scalpel and blade. A denaturing solution (Solution "D") supplemented with 8% β-mercaptoethanol (Sigma-Aldrich, UK) was added was added to the central portion of the hydrogel in a 1.5 ml eppendorf and vortexed for 2-3 minutes (WhirliMixa, FSA laboratory Supplies, UK). The sample was then stored at -80°C for 2-3 days (See **section 3.6.1** for optimised protocol). Whilst still frozen, the sample in solution "D" was vortexed until completely defrosted and dissolved.

3.4.4.3. RNA extraction

RNA was extracted using an acid phenol solution (pH 4.3, Sigma-Aldrich, UK), followed by a solution containing chloroform and isoamyl alcohol. All extractions were performed on ice in pre-chilled eppendorfs to reduce degradation of the samples. The samples were vortexed for 1 minute and then placed on ice for 15 minutes before being centrifuged for 15 minutes (Eppendorf Centrifuge, S41512, Helena BioSciences, Sunderland) at 4 °C, 930 rcf. The RNA aqueous layer that had separated from the cloudy layer containing DNA and proteins was transferred to clean, pre-chilled eppendorfs and a double isoamyl alcohol extraction was performed. Ice-cold isopropanol (Sigma-Aldrich, UK) was then added to the RNA aqueous layer and incubated overnight at -20 °C.

The precipitated RNA was centrifuged for 15 minutes at 4 °C, 930 rcf. The supernatant was removed, taking care not to dislodge the pellet, which was further dried using a heat block (QBT2, Grant, Cambridge, UK) until all residual isopropanol had been removed. The pellet was then washed in 70% ice cold ethanol (Sigma-Aldrich, UK) and centrifuged and dried as before. The pellet was then dissolved in 10-50 µl 0.1% DEPC water (dependent upon pellet size). The RNA samples were stored at -80 °C until use.

3.4.4.4. RNA quantification

Following extraction the RNA was precipitated and the quality and quantity of the nucleic acid isolated from any RNA sample was estimated using spectrophotometric analysis (Nanodrop, ND 2000, ThermoScientific, UK). The Nanodrop measures microvolumes (as small as 0.5 µl) without the use of curvettes or capillaries using patented sample retention technology. Sample RNA was measured at an absorbance wavelength 260 nm. The ratio of the absorbance at 260 nm and 280 nm was used to assess the purity of the RNA. A ratio value of 2 is generally accepted to be pure RNA, lower values signify

residual proteins, phenol or other contaminants are present in the sample (that absorb at 280 nm). The RNA samples were first centrifuged for approximately 10 seconds to ensure that the entire sample had collected at the bottom of the eppendorf. The instrument was initialised by adding 1 µl sterile DEPC to the measuring pedestal, care was taken to ensure no bubbles were present. 1 µl of RNA per sample was pipetted straight onto the measuring pedestal and the optimal path length is automatically adjusted. ND 2000 software (ThermoScientific, UK) was used to quantify the samples. The pedestal was washed with sterile DEPC between readings.

3.4.4.5. Reverse transcription of RNA

0.1 µg of RNA was aliquoted from the stock solution and reverse transcribed to CDNA using a Quantitect Reverse Transcription Kit (Qiagen, Crawley, West Sussex, UK) suitable for 10 pg- 1 µg RNA according to the manufacturer's instructions. Genomic (contaminating) DNA was removed by adding 2 µl gDNA Wipeout buffer and RNase free water to the sample. The sample was incubated at 42 °C for 2 minutes using a thermocycler (PTC-100®, Peltier Thermal Cycler, MJ Reserach, UK) and then immediately placed on ice. A reverse transcription mastermix was prepared on ice by adding Quantiscript Reverse Transcriptase (containing RNase inhibitors) and Quantiscript RT buffer (containing deoxyribonucleotide triphosphates) to a RT primer mix (which contains a blend of random primers and oligodeoxythymidylic acid). The template RNA was then added to the mastermix and incubated at 42 °C for 15 minutes, followed by 3 minutes incubation at 95 °C to inactivate the Quantiscript Reverse Transcriptase enzyme.

3.4.4.6. Quantitative polymerase chain reaction (q-PCR)

Polymerase chain reaction (PCR) refers to an *in vitro* method of DNA synthesis whereby a particular segment of cDNA is copied and amplified. Template DNA is first exposed to high temperature which denatures it; followed by exposure to lower temperatures to amplify the two oligonucleotide primers that flank the DNA. The complementary sequences then anneal to opposite ends of the target sequence. Extension of the primers is achieved by Taq polymerase and the sequence between the primers is synthesised. Specific amplification of the sequence of interest is achieved by multiple rounds of denaturation, annealing and extension using a thermocycler.

CDNA gene expression was amplified using an Applied Biosystems assay on demand kit according to the manufacturer's instructions. TaqMan gene expression incorporating the primer/probe for the gene of interest (**Table 3.3**) was added to 1 µl sample cDNA. The Taqman primers consist of amplification primers (forward and reverse) and intercalating dye SYBR green, which anneal to a specific sequence and fluoresce, which was analysed using an ABI Prism 7000 instrument (Applied Biosystems, UK). 24 µl of the reaction mixture was added to the wells of a 96 well plate (Agilent Technologies, Cheshire, UK) and 1 µl template or no template control (NTC, sterile water) was added.

PCR can be used as a quantitative assay by measuring the levels of amplification in "real time". Values obtained are "relative" in the sense that up- or down-regulation of gene expression is normalised against an endogenous control. The qPCR reaction underwent 40 amplifying cycles. During the amplification cycles, the amount of product generated is directly proportional to the amount of fluorescence; i.e. increased fluorescence occurs as more dye is incorporated into the double stranded DNA with each amplification cycle. The cycle where an increase in fluorescence is detected is called the C_T value. A highly expressed gene will have a low C_T value, and a less expressed gene will have a high C_T

value. Confluent AHDCS cells grown in monolayer (on TCP) in serum-containing F media were used as a cellular control for reference. 18S was used as an endogenous control for normalisation of the expression levels for the gene of interest using the delta-delta C_T ($\Delta\Delta$ C_T) method. Δ C_T was calculated by subtracting the 18S C_T value from the gene of interest C_T value. The cellular control ΔC_T value was then subtracted from the ΔC_T values to calculate $\Delta\Delta$ C_T. Each $\Delta\Delta$ C_T was used in the formula $2^{-\Delta\Delta CT}$ to give a comparative fold change of gene expression level relative to 18S. The "2" refers to the doubling time of the amplified product.

Samples were prepared in triplicate to account for technical variation and three readings per sample were taken. The values were averaged and represented as a mean value ± the calculated standard error.

Table 3.3: The assay on demand primer/probe gene names and assay identification numbers designated by Applied Biosystems.

Primer name	Abbreviation	Assay Identification
Keratocan	KERAT	HS00559942_m1
Thy-1	THY-1	HS00174816_m1
Aldehyde Dehydrogenase 3	ALDH3/$ALDH_3$	HS00964880_m1
α-Smooth Muscle Actin	ACTA2/α-SMA	HS00909449_m1
Eukaryotic 18S	18S	Hs99999901_s1

3.5. Characterisation of collagen

3.5.1. Collagen viscosity

Viscosity can be referred to as fluid friction, a fluids resistance to flow or a fluid's resistance to shear when it is in motion (Sparks et al. 2009). A high viscosity solution equates to a liquid or solution that does not flow easily, where as a low viscosity solution will flow very easily. The viscosity of a solution may have a bearing on its function, for example a collagen solution with a low viscosity will take longer to gelate than a collagen solution with a high viscosity. These differences can have a bearing and act as a measurement as to what is different regarding the molecular structure and resulting collagen network of the final collagen scaffold. Viscosity is frequently denoted as a co-efficient that describes the diffusion of momentum in the fluid. Viscosity measurements have been used to measure a variety of substances ranging from, oil to paint, to blood. In this instance it was used to measure the viscosity of different aged and concentrations of collagen solutions.

The fundamental components of the viscometry apparatus used in this research were a 2 gallon water tank (Clear-Seal Ltd. Birmingham, UK), a heat circulator (Grant Instruments, Cambridge, UK) a vacuum pump (FB70155, Fisherbrand, Loughborough, UK), C-flex tubing (Cole-Palmer Instrument Company, Illinois), a thermometer, a digital timer and a semi micro viscometer (size 75, Cannon-Ubbelohde, Cannon Instruments, USA**, Figure 3.10**).

All collagen samples were diluted using 0.1% acetic acid (*v/v*; Sigma-Aldrich, UK, diluted in PBS) to working concentrations of either 0.3 or 0.5 mg/ml to allow for viscosity measurements to be recorded. 2 ml of each collagen sample was added to the lower reservoir of the viscometer. The viscometer was clamped into holder and inserted into a water tank that remained at a constant temperature of 20 ºC. The viscometer, sample and

the holder were left for approximately 15 minutes to allow for the sample to come up to the bath temperature. A vacuum pump was attached to the viscometer using C-flex tubing and used to apply suction through the capillary tube and collect the sample into a collecting bulb. The efflux time was measured by allowing the collagen solution to flow freely between two measuring marks on the apparatus. The time for the collagen meniscus to pass between two defined measuring markers was measured in seconds. The kinematic viscosity, v, (mm^2/s) of the sample was calculated from a mean measured flow time, t, (seconds) using **Equation 3.2**.

$$v = Ct \qquad \textit{Equation 3.2}$$

The viscometer constant, C, was calibrated to be 0.007813 mm^2/s^2 (Poulten Selfe and Lee, PSL, Essex, UK) for the viscometer used. Three measurements per sample and 6 samples per concentration/age were recorded and a mean value calculated and plotted ± the calculated standard deviation.

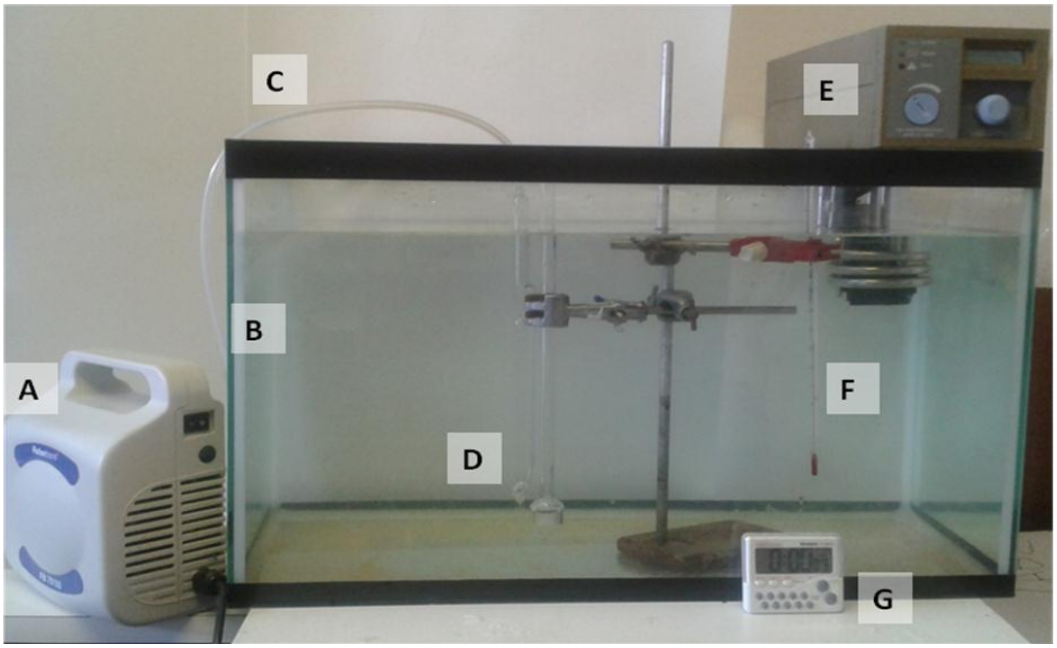

Figure 3.10: Viscosity measurement set-up comprising of a vacuum pump (A), water bath (B), C-flex tubing connecting the pump to a semi-micro viscometer (C). The temperature was kept constant using a heat circulator (E), and monitored using a thermometer (F), efflux time was measured using a digital timer (G).

3.5.2. Magnetic alignment of collagen

Magnetically aligned specimens used in this study were kindly prepared by Dr Ying Yang (Keele University, UK) and Dr James Torbet (The High Magnetic Field Laboratory, Grenoble, France).

Acellular collagen hydrogel samples were prepared at collagen concentration 1.5 mg/ml. 150 µL of gel was pipetted into a precooled (4 ˚C) Millicell EZ 4 well glass slide chamber (Merk Millipore, Oxford, UK) and positioned horizontally to the central region of the magnetic bore at 20 ˚C (room temperature). The split core superconducting magnet used (Thor, Cryogenics, France) had a horizontal (5 cm diameter, 40 cm length) room temperature bore. The collagens were exposed to a 12 Tesla magnetic field (CRETA, Grenoble, France) during fibrillogenesis. Following a few minutes the temperature was progressively raised to 30 ˚C. The temperature of the sample space was controlled by

circulating water from a temperature controlled bath. The passage in the magnet lasted for approximately 30 minutes. During this period the collagen transformed from a solution to a viscous gel.

3.5.3. Collagen hydrogel preparation using extracted collagen

To neutralise the collagen solution as prepared in **section 3.2.3** and to fabricate extracted collagen hydrogel scaffolds, 0.1 M NaOH solution and sodium bicarbonate ($NaHCO_3$) aqueous solution were added to the given collagen solution. 0.1 M NaOH was prepared by dissolving 0.2 g NaOH in 25 ml sterile deionised water. $NaHCO_3$ was prepared by dissolving 2.2 g $NaHCO_3$ (Sigma-Aldrich, UK) in 100 ml deionised water. Minimum essential medium (MEM) at 10X concentration was prepared by dissolving 9.3g of MEM powder (Sigma-Aldrich, UK) into 10 ml sterile water. The inclusion of MEM in the collagen mixtures provides the cells with a source of nutrition during gelation which encourages cell viability. All the solutions were sterile filtered prior to use to remove any impurities. For preparing 1 ml of neutralised collagen gel solution, 100 µl 10X MEM , 100 µl $NaHCO_3$, 90 µl 0.1M NaOH, 10 µl L-Glutamine (100X concentration), 100 µl H_2O, 100 µl FCS and 500 µl collagen at concentrations 5mg/ml and 3 mg/ml were mixed to give constructs of final collagen concentrations of 2.5 mg/ml and 1.5 mg/ml respectively. The collagen mixture was cast into a filter paper ring (internal diameter 20 mm) on non-adherent PTFE plates. Cellular constructs were produced following the same protocols except the stromal cells were suspended throughout the hydrogel solution prior to casting (cell density; 1 x 10^6 cells/ml). Gelation was achieved by incubation at 37˚C, 5% CO_2 for 35-60 min.

3.6. Troubleshooting

3.6.1. Optimisation of RNA extraction

In order to quantify the degree in which AHDCS cells were differentiating towards a keratocyte lineage when exposed to different culture conditions quantitative PCR (q-PCR) was used. However, preliminary experiments highlighted difficulties in extracting sufficient quantities of RNA from the collagen hydrogel constructs for analysis. A reliable, reproducible treatment whereby maximum RNA could be extracted with minimal contamination was required.

3.*6.1.1. Extraction methods*

A series of short extraction experiments were performed in order to determine the optimum technique whereby maximum RNA content could be extracted in a reproducible manner. In order to do this collagen hydrogel constructs were seeded with 0.5 $x10^6$ million cells per construct and cultured for 7 days under F media to allow for cell proliferation. The constructs were then removed from media and the filter paper support rings were removed using a sterile scalpel. The central portion of the construct was then processed. Four different extraction methods were investigated and will be referred to as extraction method 1, 2, 3 and 4 respectively.

Extraction method 1 involved the central portion of the hydrogel construct being snap frozen in liquid nitrogen using a method described by Cheema *et al*. (2008). The construct was then ground into a fine powder using a sterile pestle and mortar. Extraction method 2 uttilised an extraction method described by Chomczynski and Sacchi (1987) which involved simply treating the central portion in denaturing solution "D" before vortexing. Extraction method 3 was a modified version of method 2, with the exception that the central portion was minced and then stored at – 80 °C for 2-3 days. Whilst still frozen, the

sample (in solution "D") was vortexed until completely defrosted and dissolved. Extraction method 4 involved mincing the central portion of the hydrogel construct using a sterile scalpel, before being treated with solution "D" and being vortexed. 3 gels per extraction method were investigated. The mean RNA value was plotted ± the calculated standard deviation (**Figure 3.11**). Data was analysed using one-way analysis of variance (one-way ANOVA) followed by a Tukey post test.

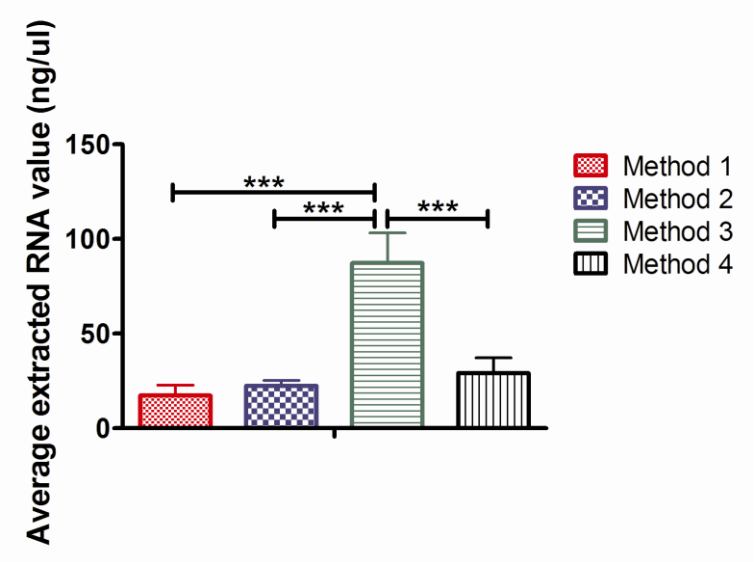

Figure 3.11: Mean volume of RNA extracted from cell-seeded hydrogel constructs following 7 days culture using different extraction methods; n=3, *** $p \leq 0.001$.

3.*6.1.2. Quantification of RNA.*

All constructs were then processed and their RNA extracted as described in **section 3.4.4.3**. Following extraction the RNA was precipitated and then quantified as described in **section 3.4.4.4**. Extraction Method 3 RNA values were significantly greater than all other methods with an mean value of 87 ng/µl RNA per construct extracted ($p \leq 0.001$ inclusive). Extraction method 1 was the least successful with an mean RNA value of 17 ng/µl RNA per construct, although there was no significant difference when comparing the values obtained for extraction methods 1, 2 and 4 respectively.

It was assumed that all constructs would have a similar cell number as all constructs were treated the same during culture. Thus, differences in extracted RNA values were purely due to the extraction method employed. Thus, using the data obtained, extraction method 3, which involved mincing and incubation of the sample at – 80 °C before processing, was deemed the most successful method to be carried forward into future experiments. It is believed than the combination of mincing and freezing of the collagen caused sufficient breakdown of the collagen bonds in order to release the RNA material. The process of freezing itself, made the construct more brittle and so when in combination with extensive vortexing caused the breakdown of the collagen structure.

3.6.2. Determining optimum 3D scaffold assembly of fibre-containing scaffolds

Nanofibres are regularly utilised in tissue engineering and regenerative medicine applications, often to improve the mechanical properties of the scaffold or construct (Lopergolo et al. 2002, Kai et al. 2001), or to more closely mimic the native tissue ECM (Smith et al. 2008, Lim and Mao 2009) to enhance cell adhesion, differentiation and/or orientation (Moroni et al. 2008, Wise et al. 2009, Xie et al. 2009, Baker et al. 2010). However, often the nanofibres are random, not aligned in their orientation (Moroni et al. 2008. The aim of the following sections was to determine the most reliable, reproducible manufacturing technique for the incorporation and assembly of aligned elsctrospun nanofibres into the collagen hydrogel scaffolds.

3.6.2.1. 3D model development of fibre-containing scaffolds

Inconsistencies occurred in preliminary modulus data in fibre-containing constructs and scaffolds. These included inexplicable increases and decreases in elastic modulus, constructs cultured in serum-free keratocyte media having a higher modulus than those cultured under serum-containing fibroblast media, vast differences in the thickness measurements of fibre-containing constructs, cells not aligning on the fibres as expected and constructs becoming damaged and breaking before the termination of the experiment. It was believed that this was due to variations occurring in the manufacture of fibre-containing scaffolds. In order to rectify this, a series of acellular experiments were performed to determine the optimum assembly protocol of fibre containing scaffolds which gave consistent readings, increased the modulus of the constructs and gave homogenous scaffolds.

3.6.2.2. Scaffold manufacture and assembly

Acelular scaffolds were made with the aim of determining the optimum assembly method of fibre-containing constructs. In order to increase the reproducibility of the fibre-containing scaffolds, all electrospinning parameters were kept the same throughout the manufacturing process (as detailed in **Table 3.1**). In addition it was noted that the fibre deposition onto the parallel blades was only homogenous over a width of approximately 15 cm. Although the fibres beyond this range maintained their alignment, their density decreased. Thus, they were discarded and not included in the hydrogel scaffolds. It is hypothesised that the introduction of nanofibres into the acellular collagen scaffold will increase the modulus of the constructs. Three different assembly methods were investigated (**Figure 3.12**) and will be referred to as Method, 1, 2 and 3 respectively. All

collagen constructs were manufactured at concentration 3.5 mg/ml as described in **section 3.2.1**.

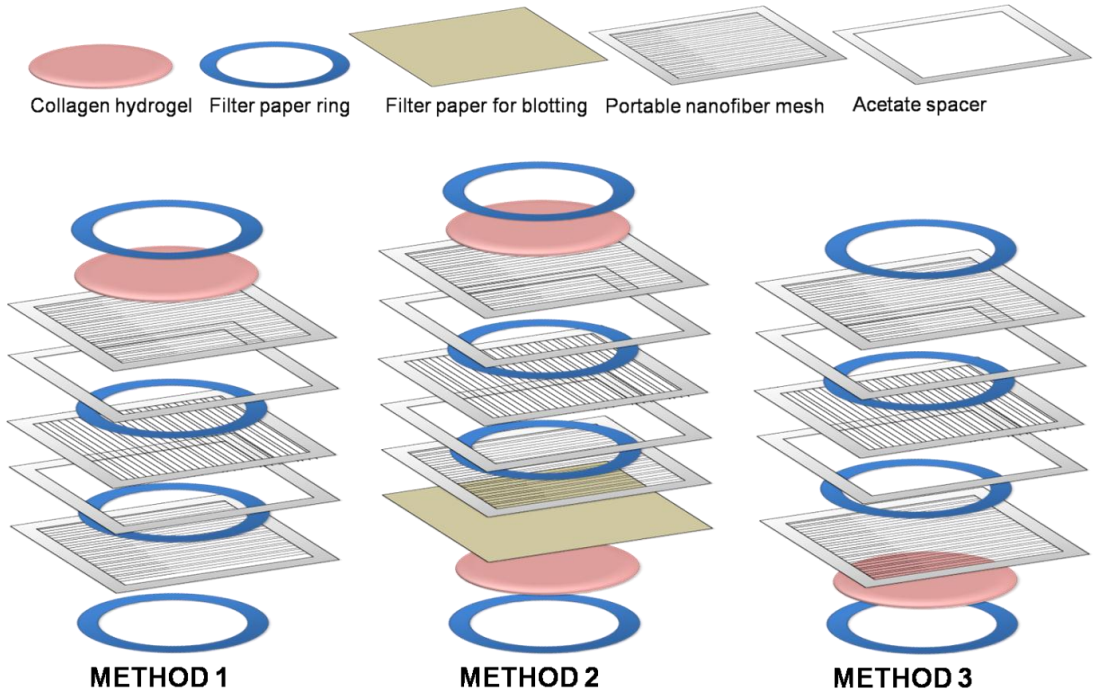

Figure 3.12: Schematic diagram detailing the three different assembly methods used in optimisation of acellular fibre-containing scaffolds.

Method 1 involved a ring of filter paper being placed on a PTFE plate on the bottom of 6-well plate. Three layers of electrospun PLDLA aligned fibres per construct were arranged in an orthogonal arrangement on top of the filter paper ring. Acetate "spacers" and filter papers were used to separate the fibre layers prior to gelation. 500 µL collagen was pipetted on top the fibres and into the filter-paper ring. A final filter paper ring was added to give added support to the edge of the construct and to ensure that the fibres were secure during gelation. Method 2 employed a two-step process where upon a 300 µL "base" gel was allowed to partially set for 20 minutes in the incubator at 37 ˚C, 5% CO_2. Excess liquid which would have caused the gels to run upon the addition of the fibres were removed by using filter paper. Three layers of PLDLA aligned electrospun nanofibres were

added to the construct in an orthogonal arrangement. The hydrogels were allowed to set for an additional 10 minutes in the incubator to allow the fibres to settle into the gels. A 200 µL "top" gel was then added to the construct. This gave a scaffold that had a total volume of 500 µL. Method 3 was very similar to method 1 with the exception that 500 µL of collagen solution was added *before* the PLDLA aligned fibres were arranged on top of the gel. The excess fibres and acetate frames were carefully removed from all scaffolds using an autoclaved scalpel and sterile blade. In addition, fibre-free hydrogels of total volume 500 µL were produced as a comparative control. All hydrogels were kept under F media.

3.6.2.3. Monitoring of fibre containing scaffolds

Due to the manufacturing process of the nanofibres included within the nanofibres containing scaffolds, it is impractical to assume that all fibre containing constructs would be exactly the same on a nanoscale level. This is a limitation of these scaffolds and any other scaffold or technique which utilises nanofibres. Thus, the aim was determine a scaffold that had the most homogenous structure with regards to the spacing of the fibre layers and overall scaffolds thickness, whilst having improved mechanical properties that would remain constant over prolonged culture periods. OCT was used to monitor the structure of the structure of the scaffolds, enabling for scaffold homogeneity to be assessed. The elastic modulus of the scaffolds was measured at 0, 7, 14 and 21 days. Four scaffolds were manufactured using each method. Recorded data was averaged and represented as a mean value ± the calculated standard deviation.

3.6.2.4. Modulus Measurement

The modulus of the scaffolds in all the different test groups remained constant throughout the duration of the experiment (**Figure 3.13A**) thus the data was accumulated

and displayed as a bar graph of the mean modulus for 21 days and represented as a mean value ± the calculated standard deviation (**Figure 3.13B**) for further analysis. One-way ANOVA tests followed by Tukey post-tests revealed that scaffolds manufactured using method 1 had a significantly higher modulus (approximately 2.4 kPa) than all other scaffolds ($p \leq 0.001$). Scaffolds manufactured using method 3 had a significantly greater modulus than scaffolds manufactured using method 2 and the fibre-free control. Scaffolds manufactured using method 2 had the weakest overall modulus of the fibre-containing scaffolds, although it was still significantly higher than the fibre-free control scaffolds ($p \leq 0.001$).

3.6.2.5. OCT analysis

The thickness of the scaffolds in all the different test groups remained constant throughout the duration of the experiment (**Figure 3.13C**) thus the data was accumulated and displayed as a bar graph of the mean thickness for 21 days and represented as a mean value ± the calculated standard deviation (**Figure 3.13D**) for further analysis. The scaffolds manufactured using method 1 were (approximately 1 mm) the closest in thickness to the fibre-free control scaffolds (approximately 1.1 mm). One-way ANOVA tests followed by Tukey post tests revealed that they were significantly thicker than the scaffolds manufactured using methods 2 and 3 ($p \leq 0.001$), but showed no significant difference in thickness when compared to the fibre-free control scaffolds. The thinnest scaffolds were those manufactured using method 2, which were significantly thinner than all other scaffolds ($p \leq 0.001$) with a mean thickness of approximately 0.7 mm. OCT analysis also revealed some interesting results regarding the structure, homogeneity of the constructs and placement of the fibres. In particular scaffolds manufactured using method 2 showed that there were variations in hydrogel thickness, variations in fibre placement and gaps

occurring in the scaffolds (**Figure 3.14**). Scaffolds manufactured using method 3 also displayed some of these characteristics, signifying a lack of reproducibility in the manufacturing method.

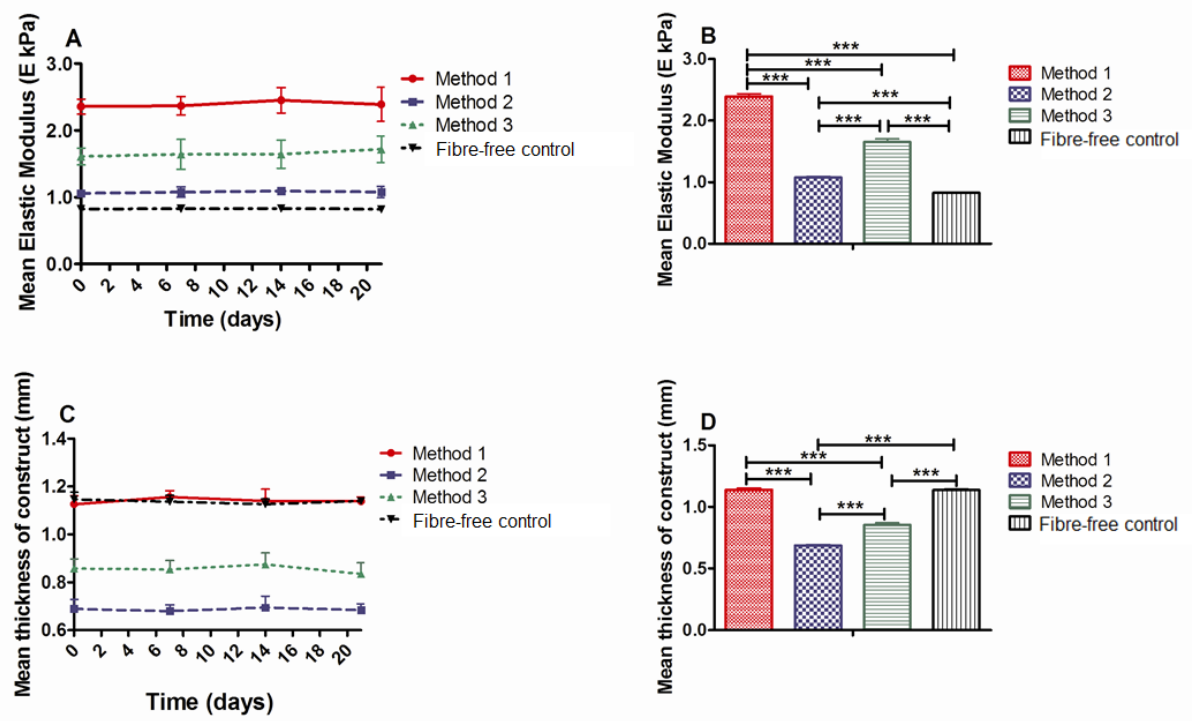

Figure 3.13: The mean elastic modulus of 3.5 mg/ml acellular fibre-containing scaffolds manufactured using different assembly methods compared to a fibre-free control cultured for 21 days in F media, n=4; (B) accumulated elastic modulus values of acellular fibre-containing scaffolds manufactured using different assembly methods compared to a fibre-free control, n=4, *** $p \leq 0.001$; (C) the mean thickness of acellular fibre-containing scaffolds manufactured using different assembly methods compared to a fibre-free control, n=4; (D) accumulated mean thickness values of acellular fibre-containing scaffolds manufactured using different assembly methods compared to a fibre-free control, n=4, *** $p \leq 0.001$.

3.6.2.6. Optimum 3D scaffold assembly

The scaffolds manufactured using method 2 was deemed to be the least successful, with the mean modulus being similar to the fibre-free control scaffold. Problems regarding construct homogeneity were most prevalent in these scaffolds. This was due to the blotting process being inconsistent for each hydrogel scaffold. It would be expected that blotting, would remove excess water from the scaffold, making it more collagen dense and thus causing an increased modulus. However, this was not the case and it can only be assumed that collagen volume (and not just water) was lost during the blotting process.

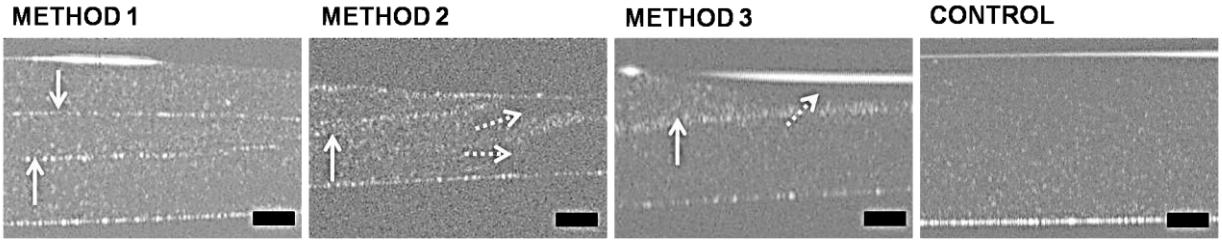

Figure 3.14: Representative OCT images displaying typical scaffold morphology of the acellular scaffolds manufactured using different assembly methods. The solid white line indicates the placement of the fibres, where as the dotted line indicates holes/gaps in the collagen scaffold, all which are linked to reduced homogeneity and modulus results, scale bar = 250 μm.

Additionally, the presence of holes or gaps in the collagen scaffolds would also weaken the overall modulus whilst reducing manufacturing reproducibility. Both method 1 and 3 had a modulus of higher than the control scaffold. However, problems associated with scaffolds manufactured using method 3 were that the fibres did not always penetrate (or sink) into the hydrogel and so detached upon the addition of culture media. This lack of consistency and manufacturing reproducibility meant that it would not be taken forward into the cellular experiments. Scaffolds manufactured using method 1 had the greatest modulus, had a similar thickness to the fibre-free controls and was the most consistently

reproducible manufacturing technique which made it the most desirable technique to employ in future, cellular experiments. Thus this was the optimised assembly technique that was taken forward for the cellular experiments.

3.7.3. Optimisation of epithelial cell culture

In order to investigate the influence of cellular communication on AHDCS cell differentiation, co-culturing with epithelial cells was investigated, see **Chapter 5.** Prior to this, preliminary experiments were performed whereby the most suitable environment for successful epithelial cell culture was investigated. A series of short experiments were devised and carried out as described in the following sections. The use of fibronectin was instigated in 2D, followed by 3D monoculture environments, and finally in 3D epithelial-stromal co-culture environments.

3.7.3.1. The use of fibronectin coating to improve epithelial cell outgrowth

Fibronectin solution was prepared as described in **section 3.1.3** and 1 ml of the solution was used to coat the surface of individual flat-bottomed petri dishes (35 mm diameter, Costar, UK). Non-coated petri dishes were prepared as a control. Porcine epithelial tissue was dissected as detailed in **section 3.1.2.** 3 pieces of explant tissue, approximately 2 mm in diameter were placed anterior side down onto each petri dish and allowed to adhere. 1 ml of CnT20 media was added to each well, media was changed every 2-3 days. Only the wells whereby all the epithelial explants successfully adhered were monitored, although it should be noted that lifting of epithelial explant tissue occurred significantly less on fibronectin surfaces compared to the non-coated surfaces.

3.7.3.2. Monitoring of epithelial outgrowth onto acellular collagen hydrogels versus cell-seeded hydrogel constructs

Collagen hydrogel constructs were prepared as described in **section 3.2.1.** Both AHDCS cell-seeded and acellular constructs were prepared and fibronectin coated prior to the addition of 3 pieces of porcine epithelial explant tissue. Non-coated equivalent constructs were also prepared as a control. 2ml CnT20 media was added to each hydrogel, and media was changed every 2-3 days. As in the previous experiment, only the constructs whereby all the epithelial explants successfully adhered were monitored.

3.7.3.3. Quantification of epithelial outgrowth onto TCP

Cellular outgrowth was monitored using light microscopy (Olympus CKX41, Japan) (**Figure 3.15A-H**) and quantified by simply passaging cells at 3, 5, 7 and 10 days and performing cell counts using a haemocytometer (Simga-Aldrich, UK). Three cells counts were performed per well and three wells per time point were passaged. The mean cell count was plotted ± the calculated standard deviation (**Figure 3.15I**). Two-way ANOVA followed by Bonferroni post tests revealed that cell counts were significantly higher on fibronectin coated TCP compared to non-coated TCP at 7 and 10 days culture ($p \leq 0.05$ and 0.01 respectively). This correlated with the light microscopy images whereby cellular confluence and outgrowth appeared greater on the fibronectin coated TCP (**Figure 3.15E-H**) compared to the non-coated TCP (**Figure 3.15A-D**) at equivalent time points.

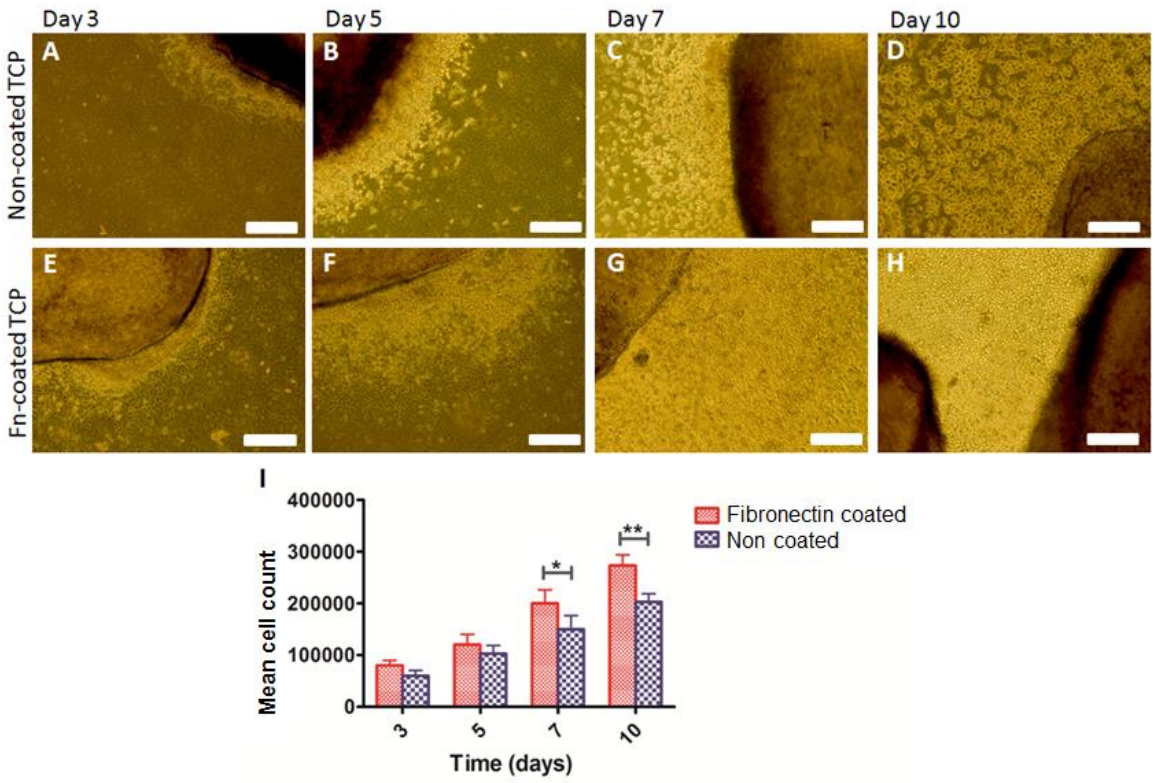

Figure 3.15: Representative light microscopy images of epithelial outgrowth onto non-coated (A-D) and fibronectin (Fn) coated (E-H) TCP, scale bar = 400 μm; (I) mean epithelial cell count of passaged epithelial cells, n=3, * $p \leq 0.05$, ** $p \leq 0.01$.

3.7.3.4. Quantification of epithelial outgrowth onto collagen hydrogels

Cellular outgrowth was monitored using light microscopy as in the prior experiments; however the quantification of epithelial outgrowth employed a slightly different method. Due to the costs involved in the manufacture of the collagen constructs, terminating the experiments in order to perform cell counts was not an option. Thus cellular outgrowth was semi-quantified by calculating epithelial outgrowth as a percentage of the surface area covered by the epithelial cultures. A piece of acetate with a squared pattern was utilised in order to calculate the surface area covered by the epithelial cellular outgrowth. Each petri dish had an acetate sheet affixed to the bottom of the well plate (**Figure 3.16**). The hydrogel constructs were monitored at day 3, 5, 7 and 10 and the cellular outgrowth was

traced onto the acetate sheets. The cellular outgrowth was measured as a mean percentage of the total area of the hydrogel construct that they covered. The semi-quantifiable data was represented as the mean percentage of the hydrogel area covered by epithelial outgrowth ± the calculated standard deviation.

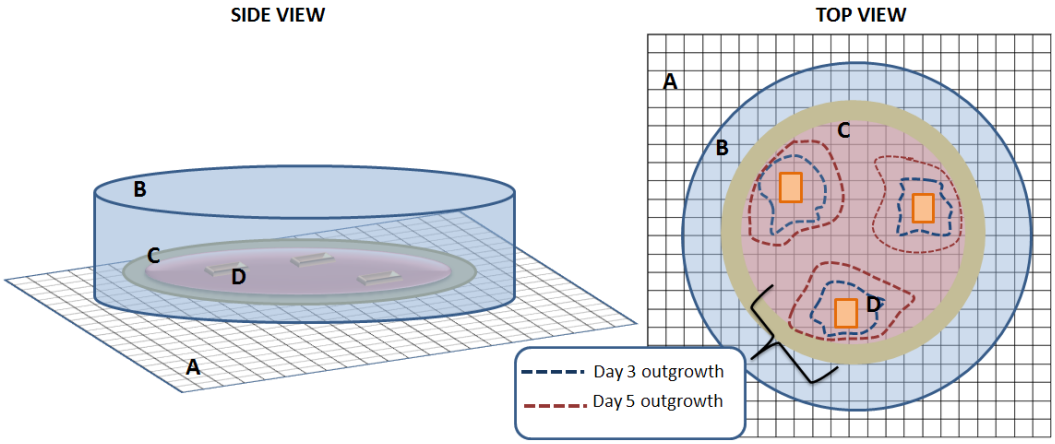

Figure 3.16: A schematic diagram detailing the experimental set-up utilised to quantify epithelial cellular outgrowth from tissue explants when seeded onto 3D collagen hydrogel environments; (A) squared acetate paper; (B) petri dish; (C) hydrogel scaffold; (D) epithelial explanted tissue.

Similar trends to those observed on the 2D TCP coated and non-coated surfaces were observed on the acellular collagen scaffolds. Light microscopy imaging revealed the general trend that epithelial outgrowth was greater on the fibronectin coated hydrogels in comparison to the non-coated hydrogels (**Figure 3.17A-D**). ANOVA tests revealed that the percentage of the collagen scaffold covered by epithelial outgrowth was significantly greater and covered a greater area of the hydrogel at all time points ($p \leq 0.001$ inclusive) on the fibronectin-coated acellular hydrogel scaffolds compared to the non-coated acellular hydrogel scaffolds (**Figure 3.17E**). Although this trend appeared to be replicated in the cellular hydrogel constructs (**Figure 3.17D**), the differences in cell coverage were not as

significant. However, it should be noted that in general epithelial cellular outgrowth was improved on the AHDCS cell-seeded hydrogel constructs in comparison to the acellular hydrogel scaffolds.

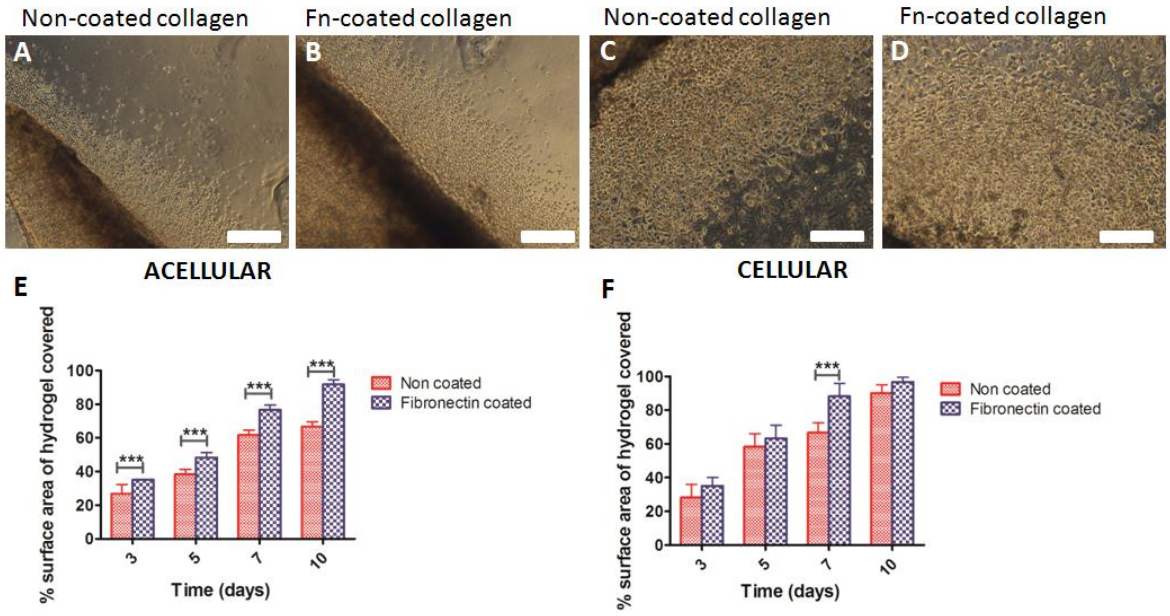

Figure 3.17: Representative light microscope images of non-coated and fibronectin (Fn) coated collagen acellular (A and B) and cellular (C and D) constructs, scale bar = 400 μm; mean % surface area of the hydrogel constructs by epithelial outgrowth in acellular (E) and cellular (F) constructs, n=6, *** $p \leq 0.001$.

3.7.3.5. Optimum epithelial outgrowth

Fibronectin is a multifunctional matrix protein found *in vivo* in the corneal ECM (Dayhaw-Barker 1995a). Its main role is concerned with cell adhesion during migration (Dayhaw-Barker 1995a) *via* its integrin receptor and it has been localised immunohistochemically on the denuded basement membrane *in vivo* during epithelial wounding (Dayhaw-Barker 1995b). By virtue of its structure, fibronectin can bind to fibrin, collagen, herapin and cell surfaces (Dayhaw-Barker 1995b) and due to these properties it is routinely used in cell culture for a variety of cell types as a thin coating that helps promote attachment, spreading and proliferation (Dayhaw-Barker 1995b, Lu et al.

2001). We observed in these short experiments that when compared to non-coated specimens that initial epithelial explant attachment and cell outgrowth was improved on all fibronectin surfaces. Thus, fibronectin coated hydrogel constructs were utilised in the co-culture experiments as described in **Chapter 5**.

4. Chemical and topographical effects on cell differentiation and matrix elasticity in a corneal stromal layer model

4.1. Abstract

Control and maintenance of the keratocyte phenotype is vital to developing *in vitro* tissue engineered strategies for corneal repair. In this study the influence of nanofibre incorporation which has the combined effect of increasing the substrate stiffness whilst providing topographical cues, alongside media supplementation (chemical cues) were investigated with regards to their effects on cultured adult human derived corneal stromal (AHDCS) cell behaviour. Cell proliferation, migration and protein expression were monitored using two dimensional (2D) and semi-three dimensional (semi-3D) culture environments. Mechanical, phenotypical and genotypical behaviour of AHDCS cells in 3D multi-layered organised constructs were then examined. Multiple aligned electrospun nanofibre meshes provided topographical cues, which are capable of aligning individual cells in 2D, semi-3D and 3D cultures; they also altered the stiffness of the substrate. The individual effects of stiffness and topography were not decoupled in this study; they were investigated as a synergistic effect. The influence of chemical cues was examined using different supplements in culture media. An automated cell culture and analysis system was used to monitor the cell behaviour in the 2D and semi-3D environments. A reduction in cell proliferation and migration signified a change from highly proliferative, motile fibroblastic cells towards quiescent keratogenic cells. Cells cultured in serum-containing media on fibre-free constructs were more motile and proliferative than cells cultured in serum-free media on fibre-containing constructs. Additionally cells cultured on aligned nanofibres were more organised and orientated compared to the random orientation of cells grown on fibre-free surfaces. A non-destructive indentation technique and optical coherence tomography (OCT) were used to determine the matrix elasticity (elastic

modulus) and dimensional changes respectively with regards to the 3D cultures. These measurements were indicative of changes in cell phenotype from contractile fibroblasts to quiescent keratocytes over the duration of the experiment and corroborated by quantitative polymerase chain reactions (qPCR). 3D constructs containing nanofibres have a higher initial modulus, reduced contraction and organised cell orientation compared to those without nanofibres. Cell-seeded constructs cultured in serum-containing media increased in modulus throughout the culture period and underwent significantly more contraction than constructs cultured in serum-free and insulin-containing media. This implies that the growth factors present in serum promote a fibroblast-like phenotype; qPCR data further validates these observations. The results from these studies indicate that the synergistic effect of an increase in construct stiffness and increased cell organisation provided *via* the incorporation of electrospun nanofibres in combination with culture in serum-free media plus insulin supplementation in a 3D collagen culture environment provide the most suitable environmental, topographical and chemical niche for reverting cultured AHDCS cells to a native keratocyte lineage. The work detailed in this chapter is based upon the original research paper entitled "**Chemical and Topographical Effects on Cell Differentiation and Matrix Elasticity in a Corneal Stromal Layer Model"** which has been successfully published in Advanced Functional Materials, Volume 22, issue 17, pages 3641-3649, DOI: 10.1002/adfm.201200655.

4.2. Introduction

The cornea is a transparent, avascular (Griffith et al. 1999, McLaughlin et al. 2009), multilaminar structure (Naylor 1953) that forms a barrier to protect the intraocular structure and microenvironment, while refracting light onto the retina (Aurell and Holmgren 1953). The integrity of the cornea is essential for preserving vision (Qu et al. 2009) and is controlled by tissue architecture, cellular morphology and extracellular matrix (ECM) composition and synthesis. In a healthy cornea, quiescent keratocytes inhabit the corneal stromal layer (Jester, Jin 2003, Builles et al. 2006, Pei et al. 2004). They express high levels of aldehyde dehydrogenase ($ALDH_3$) and the proteoglycan keratocan and demonstrate a dendritic phenotype. Their primary function is to metabolise and maintain the stromal ECM (Pei et al. 2004). Injury to the corneal stroma can cause changes in keratocyte behaviour leading to a fibroblastic phenotype, resulting in changes in matrix metabolism and contraction of the tissue (Beales et al. 1999, Funderburgh et al. 2003). A subpopulation of myofibroblasts can form among corneal fibroblasts. These are larger, less mobile and exert greater contractile forces on a tissue in comparison to a fibroblast (Helary et al. 2006). Myofibroblasts are characterised by the presence of actin fibres, including α-smooth muscle actin (α-SMA) (Helary et al. 2006, Jester et al. 1995) which help to convey contractile properties of the cell (Jester et al. 1995, Fini 1999).

Previous experiments have shown that differentiation of corneal myofibroblasts to a fibroblast phenotype is possible (Masur et al. 1996, Maltsever et al. 2001), but it is uncertain if fibroblasts can differentiate into a keratocyte phenotype (Berryhill et al. 2002). Conditioned media has been effective for the differentiation of various cell lines; however, the optimal use of supplements and additives for corneal cell culture is yet to be fully defined. Acetycholine (Builles et al. 2006), ascorbic acid, insulin (Builles et al. 2006, Musselmann et al. 2006), growth factors (Builles et al. 2006) and cytokines (Jester, Jin

2003) are amongst many supplements investigated when attempting to obtain a "pure" proliferating culture of keratocytes. These studies on biochemical cues are often performed under simplified 2D tissue culture conditions. In addition, the role of topographical cues and substrate stiffness on keratocyte differentiation, in particular in a 3D environment, has not been fully established. Naturally, keratocytes grow in an orthogonally arranged architecture, following the organisation of the collagen fibre bundles. Previous *in vitro* 2D studies have demonstrated that stromal cell populations are able to align in multiple adjacent layers arranged 30-90˚ to each other (Then et al. 2011, Guo et al. 2007). Wray *et. al.*(2009) and Wu *et. al.* (2012) have previously used aligned collagen and poly(ester urethane) urea fibres fabricated by electrospinning, to grow corneal stromal cells. However, these studies were limited to a single dense nanofibre sheet and did build the full organisation similar to that of the native tissue. In order to generate a functional corneal tissue, a 3D environment with defined topographical cues throughout a 3D construct is required.

It is hypothesised that the removal of serum from media and the addition of electrospun nanofibres into constructs will influence the cultured stromal cells to become more keratogenic in behaviour in terms of their proliferation, morphology, contractility, organisation and gene expression patterns.

4.3. Aims and objectives

The aim of this study is to investigate the synergistic relationship of increasing substrate stiffness and organisation alongside media supplementation in different *in vitro* cultures and how this effects the differentiation of corneal stromal cells. Preliminary studies were performed under simplified conditions whereby 2D and semi-3D constructs were manufactured in order to determine whether the stromal cells would successfully align, migrate and proliferate onto synthetic aligned eletrospun nanofibre meshes, whilst remaining viable. A serum-free media was investigated to ascertain whether cells would begin to differentiate under these simplified culture conditions. Building on from this, a multiple nanofibre layered 3D approach was then investigated which aspires to further influence cell phenotype from fibroblasts into keratocytes. Our non-destructive monitoring tools developed in recent years (Ahearne et al. 2005, Ahearne et al. 2010b, Yang et al. 2006) were utilised to reveal how biochemical ingredients and the incorporation of aligned nanofibres meshes into scaffolds affect stromal cell differentiation in terms of contraction, migration, organisation and mechanical properties in a 3D environment for prolonged culture periods.

4.4. Materials and Methods

4.4.1. Fabrication of portable nanofibres

Electrospinning was used to fabricate portable aligned nanofibres as previously described see **sections 3.2.2.1** and **3.2.2.2.** The nanofibres were sterilised prior to use using UV light for 90 seconds (Bio-Rad GS Gene Linker UV chamber).

4.4.2. Adult human derived corneal stromal cell culture

Adult human corneal tissue remaining from corneal transplantation was used for the isolation of AHDCS cells; see **section 3.1.1.**

4.4.3. Culture media

Three different types of media, one fibroblast media (F media) and two different serum-free keratocyte media, (K media and K* media), were investigated. F media prepared as detailed in **section 3.1.1.** K media consisted of DMEM-F12 (Biowest, France), supplemented with ascorbic acid (1 mM; Sigma-Aldrich, UK), A+A (1% *v/v*) and insulin (1 µg/ml; Sigma-Aldrich, UK). Advanced keratocyte media (K* media) consisted of Advanced MEM (Gibco, UK) supplemented with ascorbic acid (1 mM) and basic Fibroblast Growth Factor (β-FGF (0.01% *v/v*); BPS BioScience, UK). F and K media were investigated in the 2D and semi-3D studies, F, K and K* were investigated in the 3D studies.

4.4.4. Sample preparation

4.4.4.1. Fabrication of 2D and semi-3D scaffolds

Three different 2D surfaces and two different semi-3D surfaces were prepared. Glass cover slips (24 x 24 mm, Scientific Laboratory Supplies, UK) were prepared with and without the following: aligned electrospun fibres; K or F media; a hydrogel "top". The hydrogel "top" was prepared in order to more closely mimic a 3D culture environment. A full 3D construct could not be monitored using the automated analysis system (Cell-IQ®) as it was impossible to keep the samples completely still during monitoring. Blank coverslips were prepared to act as a comparative control. Aligned electrospun nanofibres on acetate frames were arranged onto coverslips either as a single layer or as two layers, orthogonally arranged. Silicone rubber (Silax Ltd., UK) strips were used to attach the fibres to the coverslip (**Figure 4.1A**). A small volume of silicone glue (RD Scientific, UK) was used to adhere the strips to the coverslips. Sample surfaces were allowed to dry for at least 1 hr to ensure appropriate bonding and drying of the silicone glue. The strips also acted as reinforcement for the delicate coverslip and prevented the coverslips from moving once transferred to 6-well plates and whilst imaging was taking place. Once dry, a scalpel was used to remove the excess fibres and acetate frames from the coverslips (**Figure 4.1C**). The coverslips were then sterilised using UV light for 90 seconds. Once sterilised the samples were transferred to sterile 6-well plates in the flow hood using sterile forceps. To encourage initial cell attachment all 2D and semi-3D surfaces were collagen coated (**Figure 4.1D**). 1000 µL of 0.2 µg rat tail collagen type-1 dissolved in 0.1% acetic acid (diluted in dH_2O, Sigma-Aldrich, UK) was added to each well and incubated for 30 min. The collagen coating was then removed and washed in sterile PBS (x3). The constructs were then seeded with AHDCS cells (**Figure 4.1E)**; see **section 4.4.5**.

Semi-3D environments were prepared by adding a hydrogel "top" to samples that had been prepared as in the 2D studies. 300 µl of collagen mixture at concentration 3.5 mg/ml was used per sample (**Figure 4.1E**), see **section 3.2.1**. The hydrogel "tops" were allowed to gelate at 37ºC, 5% CO_2 for 30 min. 5 ml culture media was added per scaffold prior to loading into the Cell IQ® analysis system (**Figure 4.1G**).

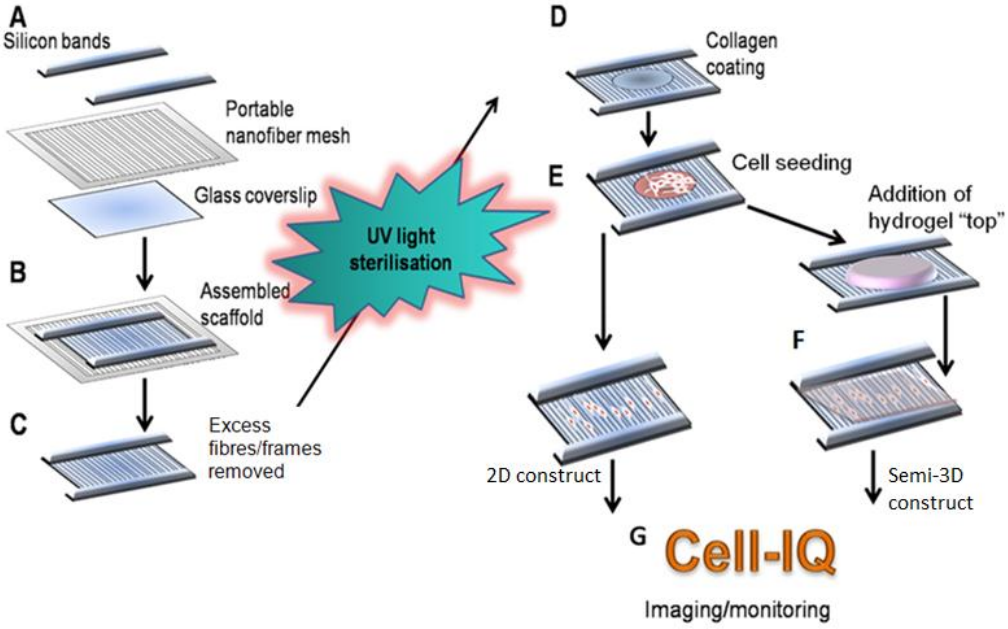

Figure 4.1: Schematic representation of the preparation of 2D and semi-3D scaffolds.

4.4.4.2. Fabrication of 3D constructs

Rat tail collagen type I hydrogels was prepared according to the manufacturer's instructions, using 10X DMEM in place of PBS as detailed in **section 3.2.1**. For construction of hydrogels containing nanofibres a previously optimised method was employed, see **section 3.6.2**; (**Figure 4.2)**. Two different 3D hydrogel constructs were investigated, confined and non-confined. The filter paper "support" rings were removed in the non-confined constructs.

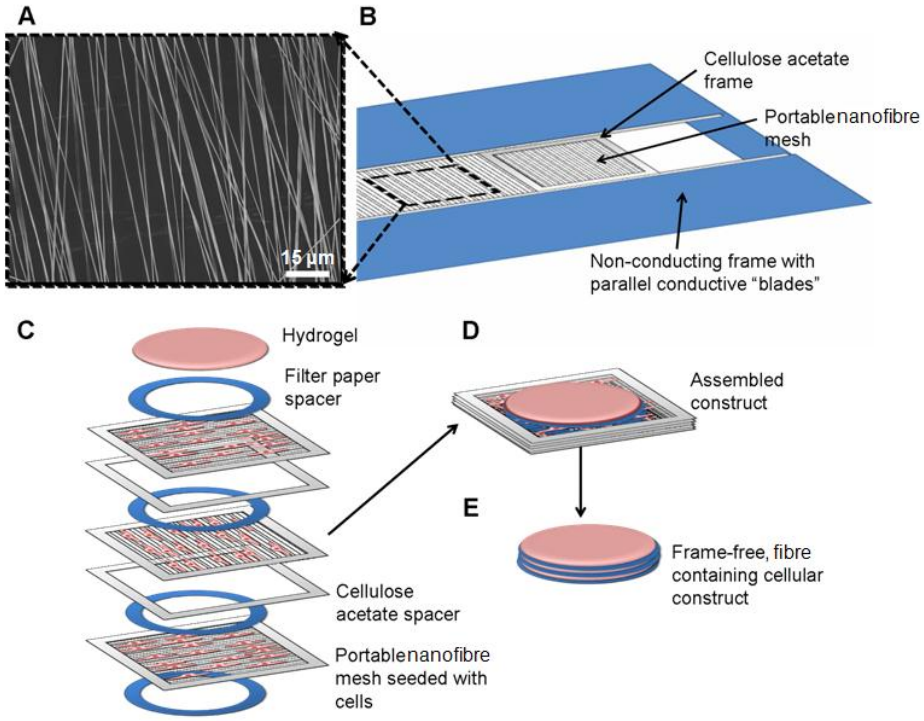

Figure 4.2: Schematic drawing of the fabrication of aligned portable nanofibre meshes and the organised multi-nanofibre mesh cellular 3D constructs.

4.4.5. Cell seeding of scaffolds

4.4.5.1. 2D and semi-3D cultures

0.2 x 10^6 AHDCS cells suspended in 400 µl culture media were seeded directly onto the collagen-coated aligned nanofibres, orthogonally arranged double layers of fibres and blank control cover slips respectively. The cells were incubated for 2 hr at 37 ˚C, 5% CO_2 to allow cell attachment to the nanofibres or cover slips. Excess culture media and non-attached cells were removed from the samples. 5 ml culture media was added to each 2D sample before loading into the Cell-IQ® machine. The additional hydrogel "tops" were added and allowed to gelate before media was added in the semi-3D constructs.

4.4.5.2. 3D hydrogel cultures

AHDCS cells (0.5 x10^6 per construct suspended in 300 µl media) were seeded directly onto the nanofibre layers. The cells were allowed to attach for at least 2 hr. Collagen solution was then added and allowed to infiltrate through the fibres, which stabilised the fibre layers (**Figure 3.2)**. In the fibre-free constructs the cells were suspended throughout the hydrogel solution prior to gelation (cell density 1 x 10^6 cells/ml).

4.4.6 Monitoring cell behaviour

4.4.6.1. Cell proliferation and migration in 2D and semi-3D constructs

All images acquired in the 2D and semi 3D-experiments were obtained by using a demo model of a Cell IQ® Continuous Live Cell Imaging and Analysis System. In brief, Cell IQ is an automated cell culture and analysis system capable of imaging over prolonged culture periods. The system comprises of an incubator and imaging software for data capture and processing. Samples can be monitored continuously using the Imagen™ programme and the Analyser™ software can be used to analyse multiple cellular parameters. Digital images were recorded approximately every 90 min of a defined area of a well plate. Cell counts were taken at regular time intervals of 0, 4.7, 8.9, 17.0, 22.2, 29.3, 35.5, 41.7 and 47.8 hr in the 2D experiments and at time points 0, 2.2, 4.7, 6.6, 8.9, 11.1, 13.3, 15.5, 17.0, 19.95, 22.2, 24.23, 26.4, 29.3, 31.0, 33.2, 35.5, 37.7, 41.7 and 47.8 hr in the semi-3D experiments. The monitoring times were different due to focussing problems.

4.4.6.2. Cellular contraction of 3D constructs

Hydrogels cast into filter paper rings were effectively confined to the dimension of the filter paper ring. Construct contraction was measured with (confined) and without this ring (non-confined). Confined contraction was monitored as a change of thickness of the

hydrogel construct *via* optical coherence tomography (OCT) (Yang et al. 2006), see **section 3.3.2;** constructs were examined every 3 to 4 days over 14 days in culture. Non-confined constructs allowed the constructs to contract in any direction. The central portion of the non-confined constructs was monitored daily for 7 days and images were recorded using digital photography (D5000, Nikon, Japan). Acellular collagen scaffolds, with and without fibres were produced as a control.

4.4.6.3. Cell viability in 2D, semi-3D and 3D constructs

Cell viability was observed following 48 hr culture on the 2D and semi-3D constructs and at 7 and 14 respectively in the 3D constructs, see **section 3.4.1.**

4.4.6.4. Cell morphology and aspect ratio in 3D constructs

Cell morphology was observed at day 14 in the 3D confined constructs using phalloidin tetramethylrhodamine-B-isothiocyanate, see **section 3.4.2** for full details. The relationship of cell morphology, topography and culture environment in 3D confined constructs was investigated by measuring the aspect ratio as described in **section 3.4.2.** Three separate areas per sample were examined and a minimum of 50 cells were measured per sample.

4.4.6.5 Modulus measurement of 3D constructs

The mechanical properties of the 3D confined constructs were measured at different culture times using a non-destructive spherical indentation as described in **section 3.3.1.**

4.4.7. Determining cell lineage

4.4.7.1. Immunostaining of 2D and semi-3D constructs

Cell phenotype was determined *via* immunohistochemical analysis by preparing additional samples, with and without the addition of nanofibres, with and without the addition of a hydrogel "top" and cultured under both serum-containing F media and serum-free K media respectively for 48 hr at 37 ºC, 5% CO_2. Thy-1 was used to positively stain for corneal fibroblasts and keratocan was used to stain for keratocytes, see **section 3.4.3**.

4.4.7.2. Quantitative polymerase chain reaction (qPCR) in 3D constructs

The 3D constructs were processed for PCR analysis as described in **section 3.4.4.** Confluent AHDCS cells grown in monolayer were used as a reference point for comparison, i.e. cellular control.

4.4.8. Statistics

All data was analysed using GraphPad Prism® (CA, USA). The data was subjected to a normality (Kolmogorov-Smirnoff) test. The data was normally distributed, so comparisons were performed using either one-way analysis of variance (ANOVA) followed by Tukey post-tests, or two-way ANOVA followed by Bonferroni post-tests where applicable. Significance was indicated to determine if the effects of time, media and/or nanofibers were statistically significant at three levels: * $p \leq 0.05$, ** $p \leq 0.01$ and *** $p \leq 0.001$.

4.5. Results

For ease of analysis, the results section has been split into two sections. **Section 4.5.1** will discuss the data regarding the 2D and semi-3D constructs; **section 4.5.2** will discuss the 3D construct data.

4.5.1. 2D and semi 3D constructs

4.5.1.1. Cell proliferation and migration

AHDCS cells were cultured onto different 2D and semi-3D surfaces, with and without the inclusion of electrospun nanofibre meshes under serum-containing F media or serum-free K media supplemented with ascorbic acid and insulin. A Cell IQ® Continuous Live Cell Imaging and Analysis System was used to non-destructively record images of cells exposed to the different culture conditions at regular time intervals. Unfortunately the Cell IQ® Analyser™ software was not sensitive enough to accurately perform cell counts when AHDCS cells were seeded onto the aligned nanofibre scaffolds. Thus manual cell counts had to be performed in order to quantify the data. This was done using a cell counting tool using ImageJ software (NIH, USA). Cell proliferation as calculated as a mean percentage change in cell number to account for slight differences in initial cell starting number.

When cultured on either 2D or semi-3D constructs on all surfaces (with or without nanofibres) in serum-free K media, one-way ANOVA revealed that there was no significant change in cell number whether fibres were present or not and cell number remained relatively constant for the duration of the experiments (**Figure 4.3A** and **C)**. In comparison, when cultured in serum-containing F media, on all surfaces, in both 2D and semi-3D conditions, the cells significantly increased in cell number over the duration of the experiments (**Figure 4.3B** and **D**). On 2D constructs when cultured in F media, cell proliferation was greatest on the blank coverslips in comparison to the coverslips with a single layer of aligned fibres ($p \leq 0.001$ from 22 hr onwards) and a double layer of cross fibres ($p \leq 0.01$ from 17 hr and 0.001 from 22 hr onwards). This suggests that the nanofibres were suppressing cell proliferation. Although it appeared that the double cross layer of fibres was further suppressing proliferation in comparison to the single layer of aligned fibres, this difference was not statistically significant. Similar trends were observed

on the semi-3D constructs in that the inclusion of nanofibres appeared to be suppressing cell proliferation when cultured in serum-containing media compared to the cells grown on the blank control coverslips ($p \leq 0.05$ at 22 hr and $p \leq 0.01$ from 29 hr onwards), although proliferation was still significantly greater in the serum-containing media compared to the serum-free media when the collagen top was present.

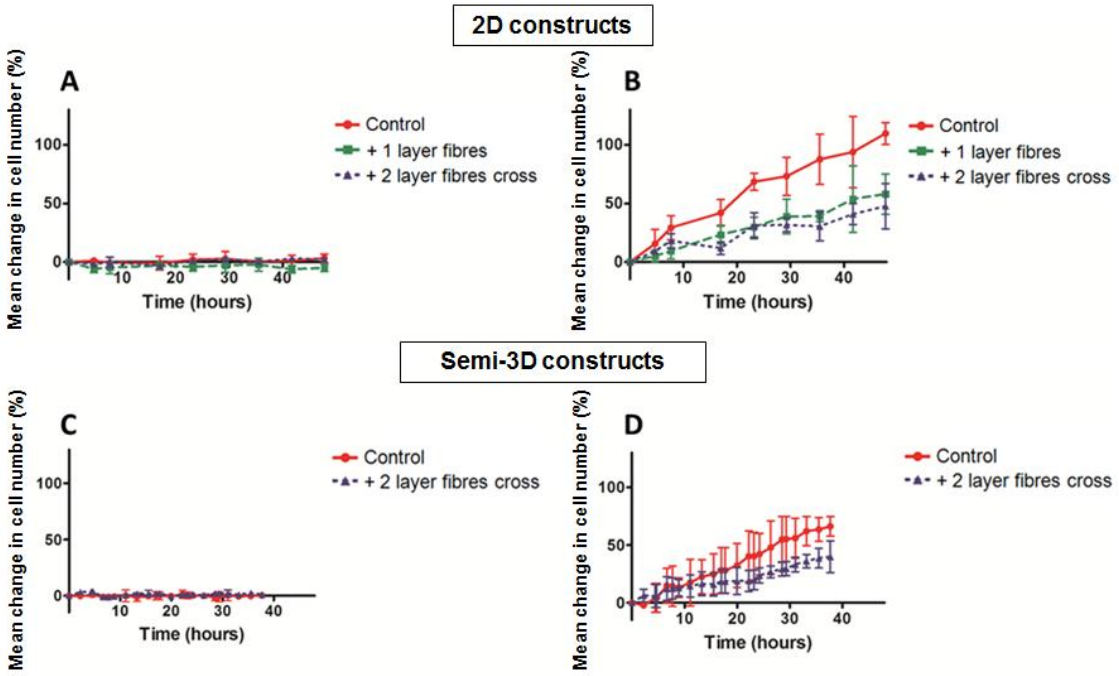

Figure 4.3: Mean % change in cell number of cells seeded onto coverslips in serum-free K media (A and C) and serum-containing F media (B and D) in 2D (A and B) and semi-3D (C and D) constructs, n=3.

The inclusion of the hydrogel "top" did not significantly affect cell proliferation of cells cultured in K media when comparing cell counts from 2D and semi-3D equivalent constructs (i.e. with and without fibres). However, when cultured under F media, the inclusion of the hydrogel top significantly reduced proliferation in both blank control ($p \leq 0.001$ at 23 hr and $p \leq 0.01$ at 35.5 hr) and 2 fibre layer cross arranged samples ($p \leq 0.05$ at 23 hr and $p \leq 0.01$ from 29 hr onwards).

Although not quantified, it was observed on both 2D and semi-3D constructs that the inclusion of the nanofibres scaffolds had an effect on cell migration and morphology. When cultured on blank control surfaces, in all instances, the cells grew in a random orientation (**Figure 4.4A, B, E** and **F**). When nanofibres were present, in all instances, the cells grew in the orientation of the fibres and appeared to be using the nanofibres to migrate along (**Figure 4.4C**). It was also noticed that the cells were thinner and more elongated in morphology (**Figure 4.4C, D, G** and **H**).

4.5.1.2. Determination of cell linage using immunostaining

All samples, whether on 2D (**Figure 4.5A-D**) or semi-3D (**Figure 4.6A-D**) constructs, with and without fibres, in keratocyte and fibroblast media, stained positive for the fibroblastic maker Thy-1, although expression appeared highest in cells cultured under F media in comparison to those cultured K media. Samples stained with keratocyte marker keratocan showed poor immunofluorescence in both 2D (**Figure 4.5E-H**) and semi-3D (**Figure 4.6E-H**) samples, although all the samples cultured in K media had stronger positive staining compared to those cultured F media where staining was minimal or nonexistent. The addition of the hydrogel "top" in the semi-3D constructs appeared to increase keratocan fluorescence in the samples cultured under K media.

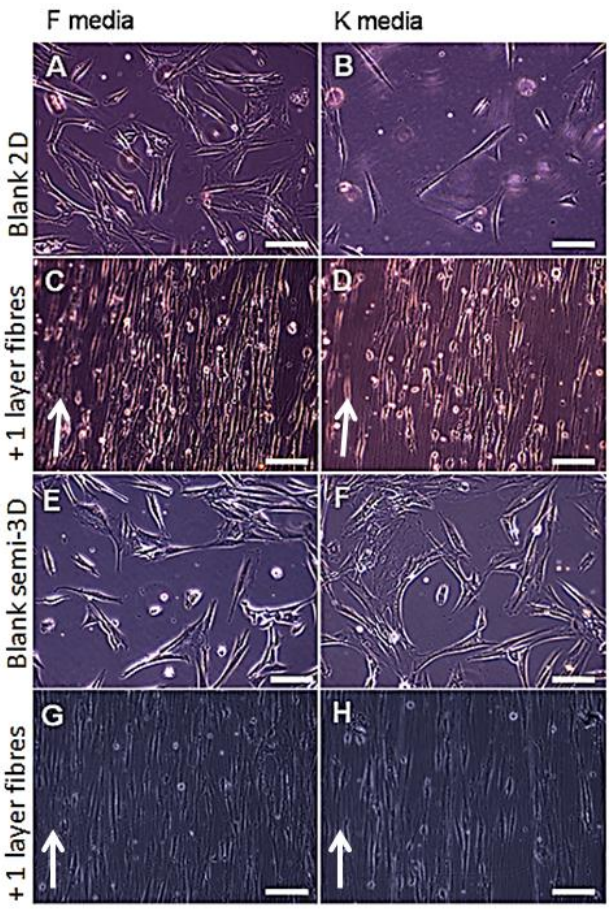

Figure 4.4: Representative stills taken from the Cell IQ® Continuous Live Cell Imaging and Analysis System following approximately 24 hr culture. Cells in both serum-free K and serum-containing F media can be seen aligning along to the fibres compared to the random orientation on the blank coverslips in both 2D (A-D) and semi-3D (E-H) environments; white arrows indicate the direction of the fibres; scale bar = 200 µm.

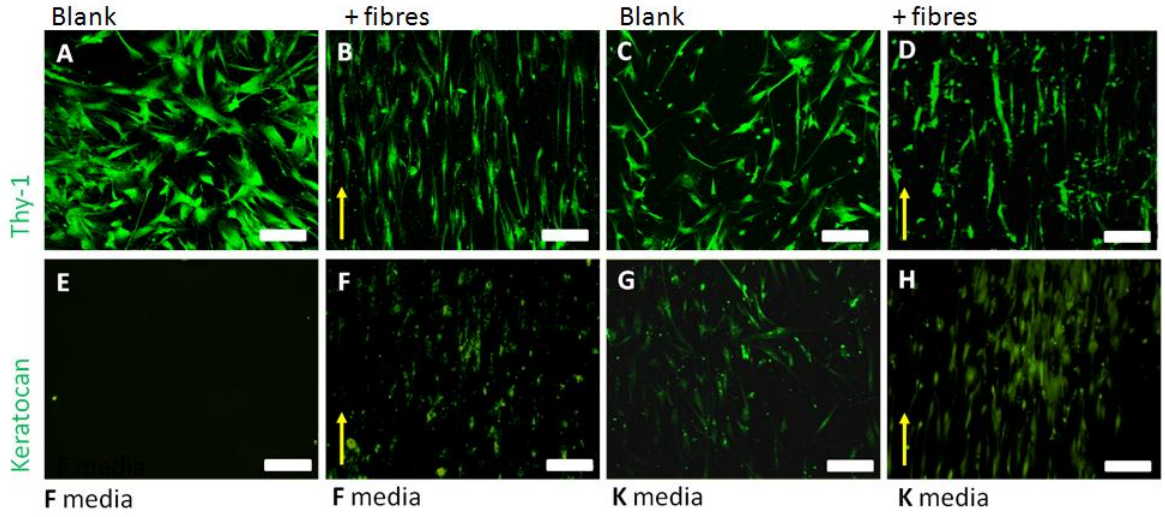

Figure 4.5: Representative immunostaining of cells using Thy-1 (A-D) and keratocan (E-H), imaged using fluorescent microscopy, of fibre-containing (B, D, F and H) and fibre-free (blank, A, C, E and G) 2D constructs following approximately 48 hr culture time under serum-containing F media and serum-free K media, arrows indicate the direction of the fibres in fibre-containing constructs; scale bar= 200 µm.

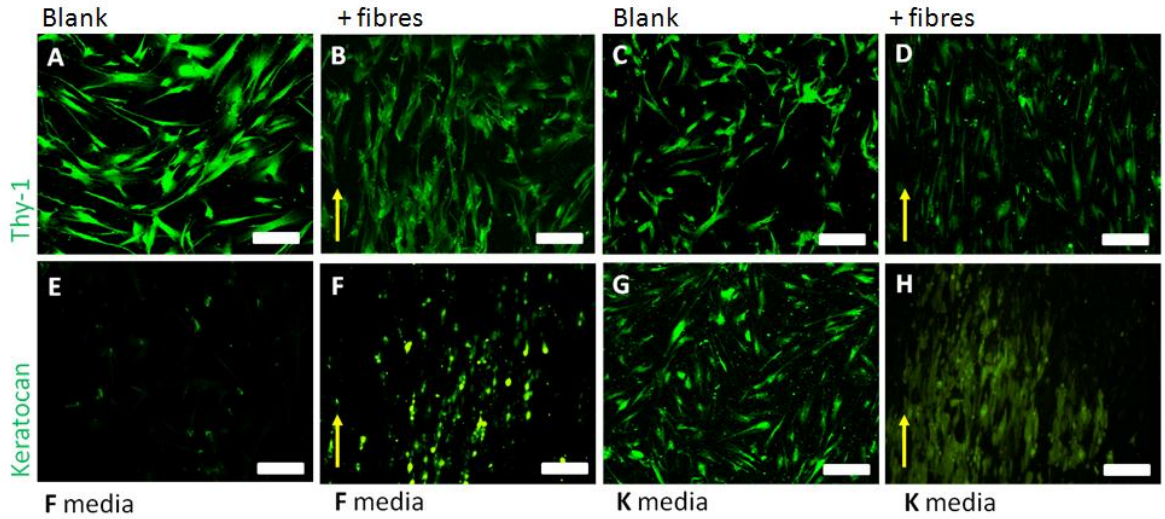

Figure 4.6: Representative immunostaining of cells using Thy-1 (A-D) and keratocan (E-H), imaged using fluorescent microscopy, of fibre-containing (B, D, F and H) and fibre-free (blank, A, C, E and G) semi-3D constructs following approximately 48 hr culture time under serum-containing F media and serum-free K media, arrows indicate the direction of the fibres in fibre-containing constructs; scale bar= 200 µm.

4.5.1.3. Cell viability

In all samples, with and without fibres, in all media, with and without a hydrogel "top" high cell viability was maintained. Organisation of the cells was observed *via* fluorescent microscopy and allowed for the alignment of the cells on the nanofibres to be visualised as opposed to the random orientation of the cells in non-fibre containing constructs (**Figure 4.7**). In all media types, cells were organised in accordance to the nanofibre arrangement in both 2D and semi-3D environments.

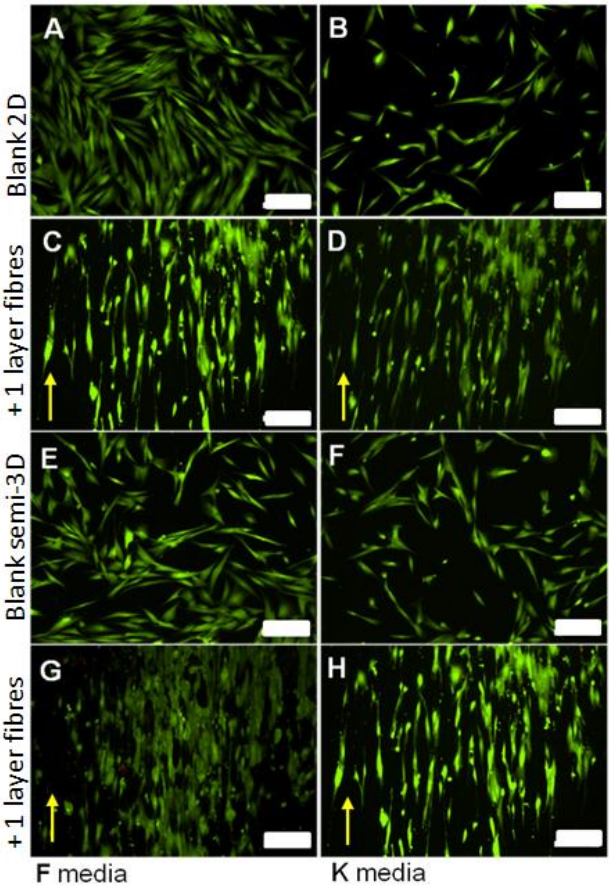

Figure 4.7: Representative live-dead stained cells, imaged using fluorescent microscopy, of 2D (A-D) and semi-3D (E-H) constructs following approximately 48 hr culture time under serum-containing F media (A, C, E and G) and serum-free K media (B, D, F and H); green represents live cells, red represents dead cells. The arrows demonstrate the direction of the nanofibres; scale bar= 200 µm.

4.5.2. 3D constructs

4.5.2.1. Cellular contraction

3D collagen hydrogel constructs were produced with and without aligned nanofibres and then cultured in serum-containing F media supplemented with L-Glutamine, and antibiotic and antimitotic solution; or one of two serum-free keratocyte media supplemented with ascorbic acid and either insulin or basic Fibroblast Growth Factor (β-FGF), respectively (K or K*). Through a layer-by-layer fabrication protocol (**Figure 4.2**), the fragile nanofibre meshes have been successfully incorporated into the collagen constructs and the majority of the AHDCS cells were attached to the nanofibres in an orthogonal arrangement following the nanofibre assembly at the initial stage. The surface area of non-confined constructs seeded with AHDCS cells was monitored every 24 hr for 7 days to determine whether chemical cues and/or in inclusion of nanofibres influence the contraction of the constructs (**Figure 4.8**). The removal of the filter paper ring allowed constructs to contract in all directions, thus altering the surface area and total volume of a construct as a whole.

Digital photography was used to image the constructs and the percentage change in surface area was calculated relative to their initial surface area (**Figure 4.8A** and **B**). A significant amount of contraction was observed in the constructs cultured in F media. The surface area of the constructs was reduced to less than 20% of its original surface area and became opaque in appearance. Although the fibre-containing constructs cultured in F media did contract, the change in surface area was not as prominent and they retained more than 50% of their original surface area. The fibre-containing constructs cultured in both K and K* media maintained 80% of their surface area following 7 days culture. There was no significant difference in contraction of fibre-containing cellular constructs cultured under either serum-free media for the duration of the experiment. The construct surface area

remained constant in all acellular control specimens manufactured with and without the inclusion of fibres and cultured in F, K and K* media respectively.

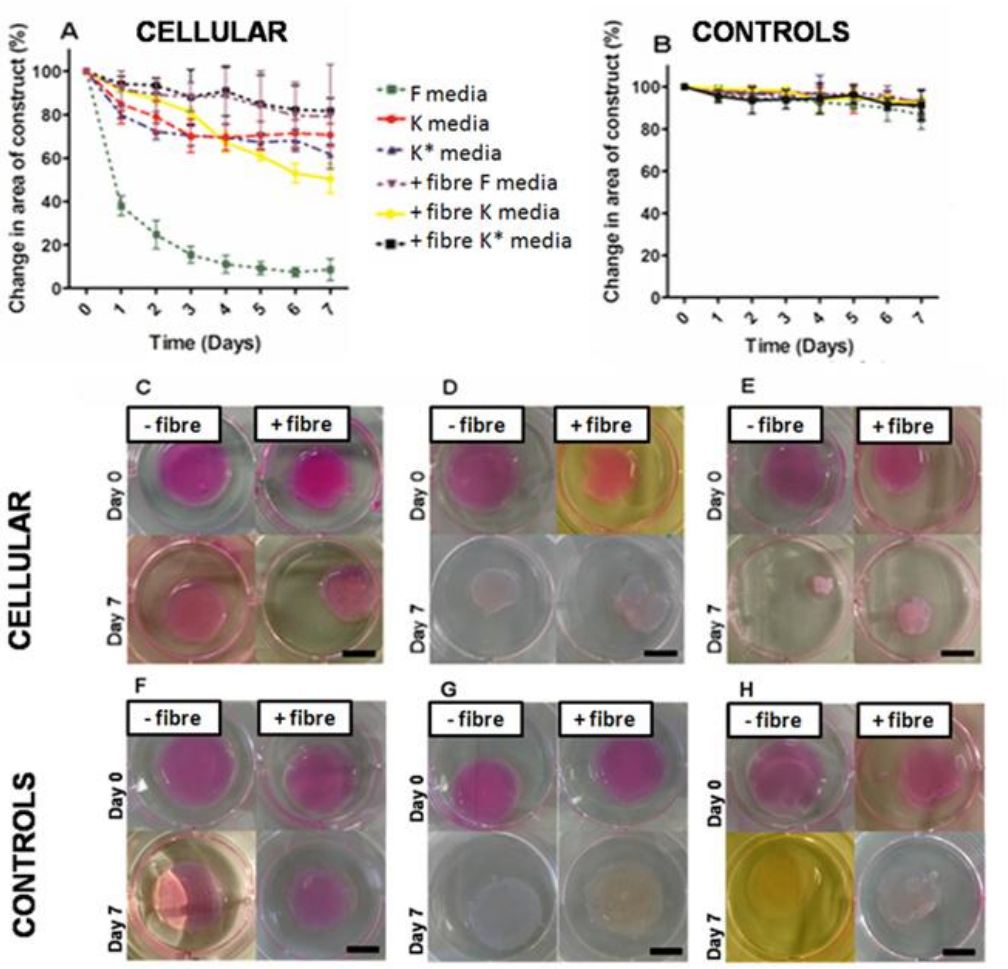

Figure 4.8: Mean change in surface area of non-confined cellular (A) and acellular control (B) constructs cultured with and without nanofibres under F, K and K* media respectively for 7 days; n=6; and representative digital images of non-confined hydrogel constructs with (C-E) and without cells (F-H) cultured under K media (C and F); K* media (D and G); F media (E and H) with and without the inclusion of nanofibres at day 0 and day 7; scale bar = 1000 μm.

The contraction in confined constructs was limited to a change in thickness. The change in thickness of the constructs was measured using optical coherence topography (OCT) (Yang et al. 2006) over 14 days (**Figure 4.9C** and **D**). The thickness of all cellular constructs cultured in either serum-free keratocyte media remained constant throughout the duration of the experiment. The cellular constructs cultured in F media contracted thus making the constructs thinner. Contraction predominantly occurred within the first week. Two-way ANOVA tests revealed that presence of fibres and the supplementation of culture media had a significant effect on the change in thickness of the construct ($p \leq 0.01$). After 3 days in culture, constructs cultured without fibres in F media significantly reduced in thickness compared to all other constructs ($p \leq 0.001$). Fibre containing constructs cultured in F media contracted significantly more compared to other fibre containing constructs but contracted significantly less than the constructs without fibres also in F media. No significant difference in the change of hydrogel thickness was observed between the cellular constructs (with and without fibres) compared to their acellular controls when cultured in K and K* media. The construct thickness of all acellular control specimens remained constant.

4.5.2.2. Modulus measurement

The elastic modulus of 3D confined constructs and scaffolds was measured every 3-4 days for 14 days (**Figure 4.9A and B**). The modulus of constructs cultured in F media without fibres was significantly greater ($p \leq 0.001$) than the constructs without fibres cultured in K and K* media from day 3 onwards and significantly lower ($p \leq 0.001$) than all fibre-containing scaffoldss ($p \leq 0.05$ for acellular gels in F media vs. cellular gels in K* media at day 14. The modulus of fibre-containing constructs cultured in F media was statistically greater ($p \leq 0.01$ at day 3, $p \leq 0.001$ from days 7-14) than fibre containing

constructs cultured in both K and K* media. There was no significant difference observed when comparing the modulus of constructs cultured in K and K* media, with or without fibres throughout the experiment. There was an initial increase in modulus following 3 days culture period in the fibre-containing constructs from approximately 3.6 kPa to 5 kPa and then the modulus remained constant for the remainder of the experiment.

All acellular control hydrogels (**Figure 4.9D**) retained a constant modulus between 0.5 and 1 kPa. All acellular scaffolds cultured with fibres had a significantly higher modulus (2.5-3 kPa) than the corresponding fibre-free scaffolds ($p \leq 0.001$). The modulus of all fibre-containing scaffolds were significantly greater ($p \leq 0.001$) than those without.

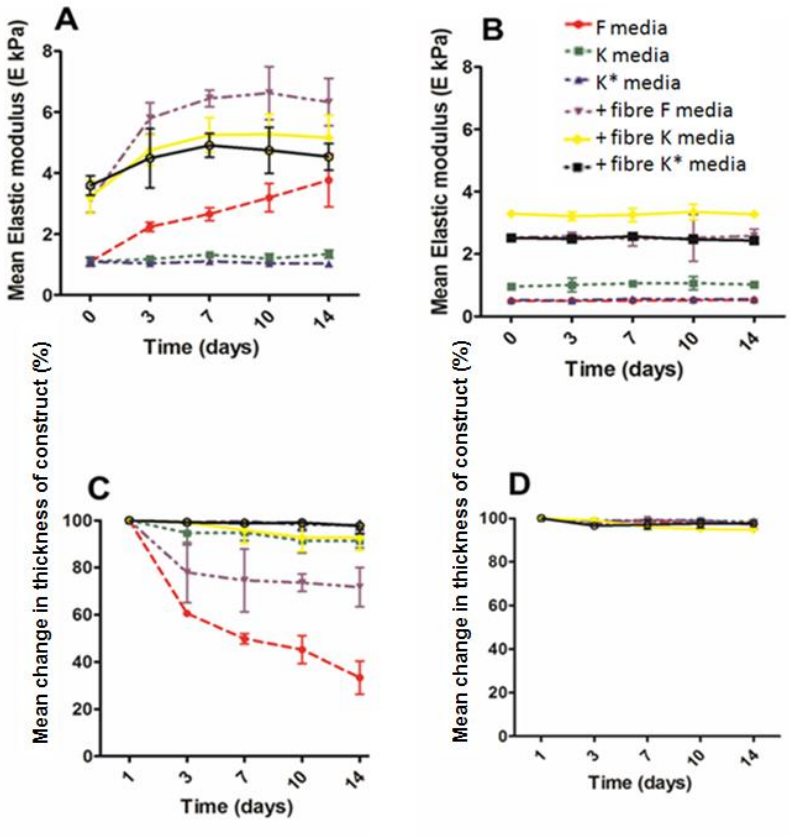

Figure 4.9: Mean elastic modulus of confined cellular (A) and acellular control (B) constructs and mean change in thickness of confined cellular (C) and acellular control (D) constructs cultured with and without nanofibres under F, K and K* media respectively for 14 days; n=6.

4.5.2.3. Cell viability

All constructs, with and without fibres, confined and non-confined, in all media maintained high cell viability at 7 and 14 days (**Figure 4.10**).

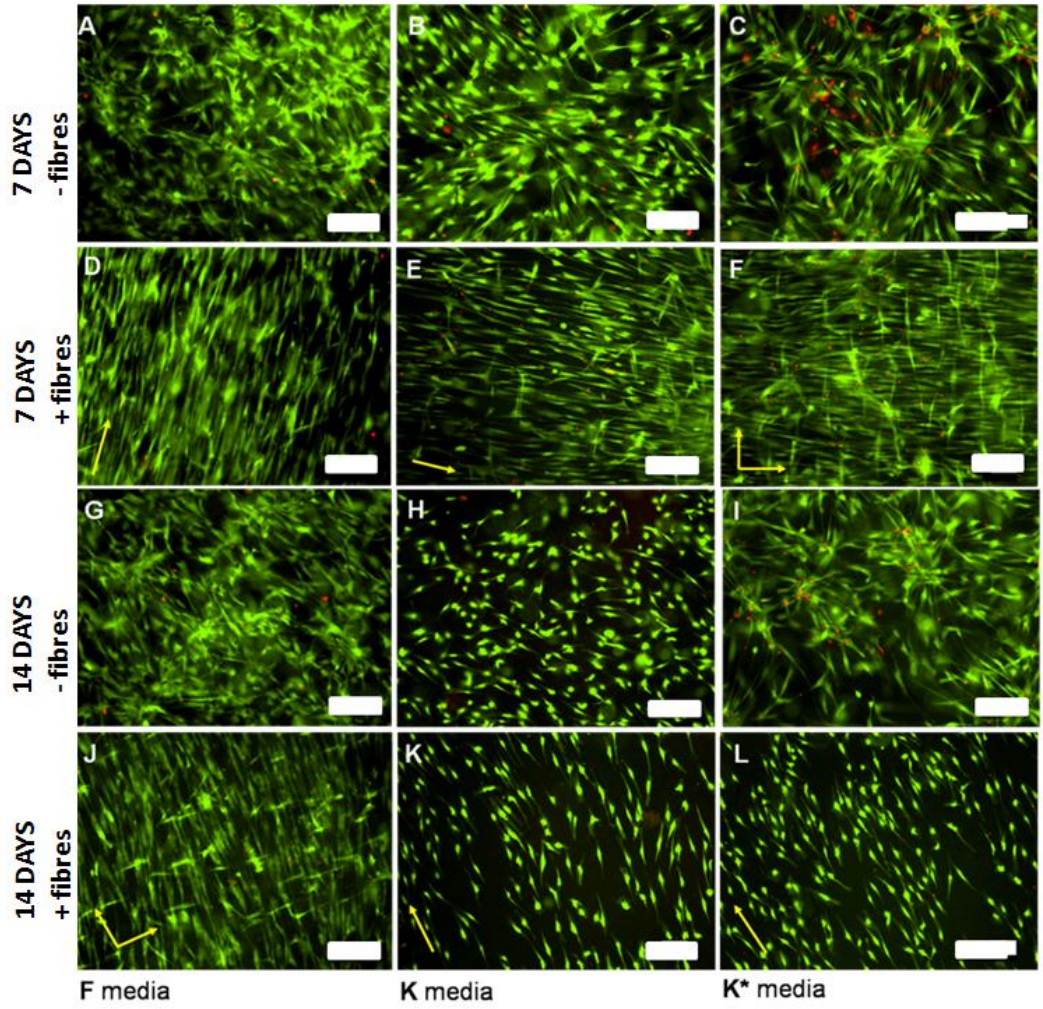

Figure 4.10: Representative live-dead stained cells, imaged using fluorescent microscopy, of collagen hydrogel constructs following 7 (A- F) and 14 (G- L) days culture time under F, K* and K media, respectively; green indicates live cells and red dead cells. Cells in fibre-free constructs (A-C and G-I) have grown in a random orientation whereas in the fibre-containing constructs (D-F and J-L) the cells are mimicking the orientation of the electrospun nanofibres. The arrows demonstrate the direction of the nanofibres and in some images 2 layers of fibres have been captured in the same image (E, F and J); scale bar = 200 µm.

4.5.2.4. Cell morphology and aspect ratio

Phalloidin tetramethylrhodamine-B-isothiocyanate labeling of cells in confined constructs at day 14 revealed that the cells in F media were larger and more fusiform in morphology in comparison to cells cultured in K and K* media which were much thinner and more elongated. Organisation of the cells was observed and allowed for the alignment of the cells on the nanofibres to be visualised (**Figure 4.11D-F**) as opposed to the random orientation of the cells in non-fibre containing constructs (**Figure 4.11A-C**). In all media types, cells were organised orthogonally in a 3D arrangement in accordance with the nanofibres orientation within a particular layer.

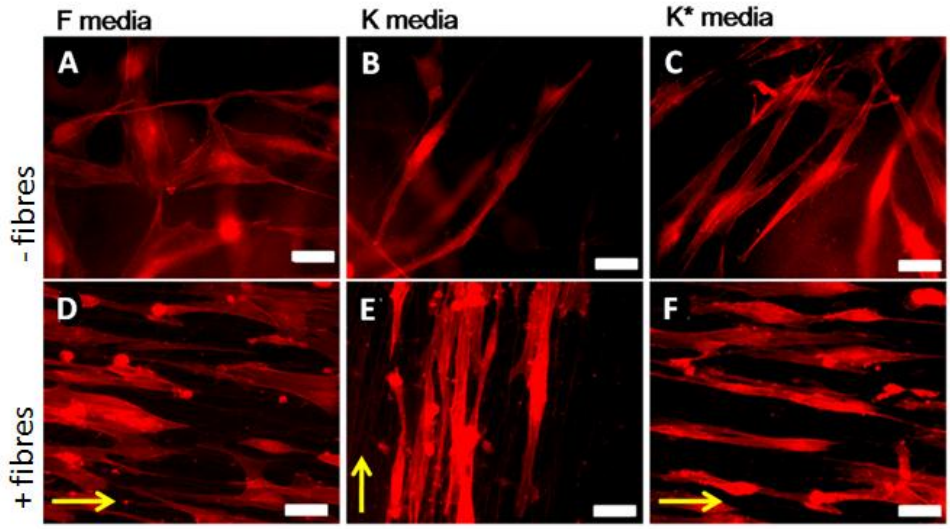

Figure 4.11: Representative phalloidin tetramethylrhodamine-B-isothiocyanate stained cells, imaged using fluorescent microscopy of collagen hydrogel constructs with and without the incorporation of nanofibrous meshes following 14 days culture in F, K and K* media respectively; yellow arrows indicate direction of fibres, scale bar = 50 µm.

The cellular aspect ratios in F media specimens were significantly lower than those in K and K* media with and without nanofibres, both at day 7 and 14 (**Figure 4.12**). Furthermore, the aspect ratios in the specimens with nanofibres were higher than the nanofibre-free counterparts in all culture media and at both day 7 and 14. The enhanced effect of nanofibres on the aspect ratio was greater in keratocyte culture media (K and K*) than in fibroblast culture media (F media). The aspect ratio was highest for cells cultured in fibre-containing constructs in K media for 14 days. Increasing the culture time resulted in an increased aspect ratio for all the specimens.

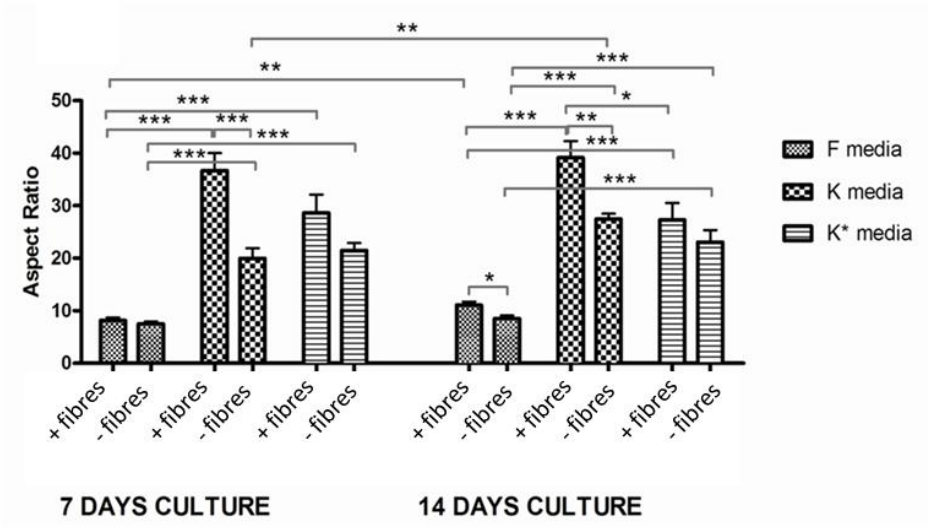

Figure 4.12: Mean aspect ratio for AHDCS cells seeded in the hydrogel constructs with and without the inclusion of nanofibrous meshes cultured under F, K and K* media for 7 and 14 days; * $p \leq 0.05$, ** $p \leq 0.01$, *** $p \leq 0.001$.

4.5.2.5. qPCR gene expression

In order to determine whether the 3D collagen environment and nanofibres had an effect on the expression of genetic markers, AHDCS cells were cultured in 2D monolayer (on Tissue Culture Plastic, TCP) and were compared to the cells cultured in 3D constructs, with and without the inclusion of nanofibres in F culture media (**Figure 4.13**). Following 7 days culture, there was no significant difference in the expression of keratocan and $ALDH_3$

in fibre-free or fibre-containing constructs. However, the fibroblastic marker Thy-1 was significantly down-regulated in both fibre-free and fibre-containing constructs ($p \leq 0.01$ and $p \leq 0.05$, respectively). Additionally, in the fibre-containing constructs, fibroblastic marker α-SMA was also down-regulated significantly ($p \leq 0.05$). Similar trends were observed after 14 days culture in that there was no significant difference in the expression of the keratogenic markers, but Thy-1 was further down-regulated both in fibre-containing and fibre-free constructs ($p \leq 0.01$) and α-SMA was further down-regulated in the fibre containing constructs ($p \leq 0.01$).

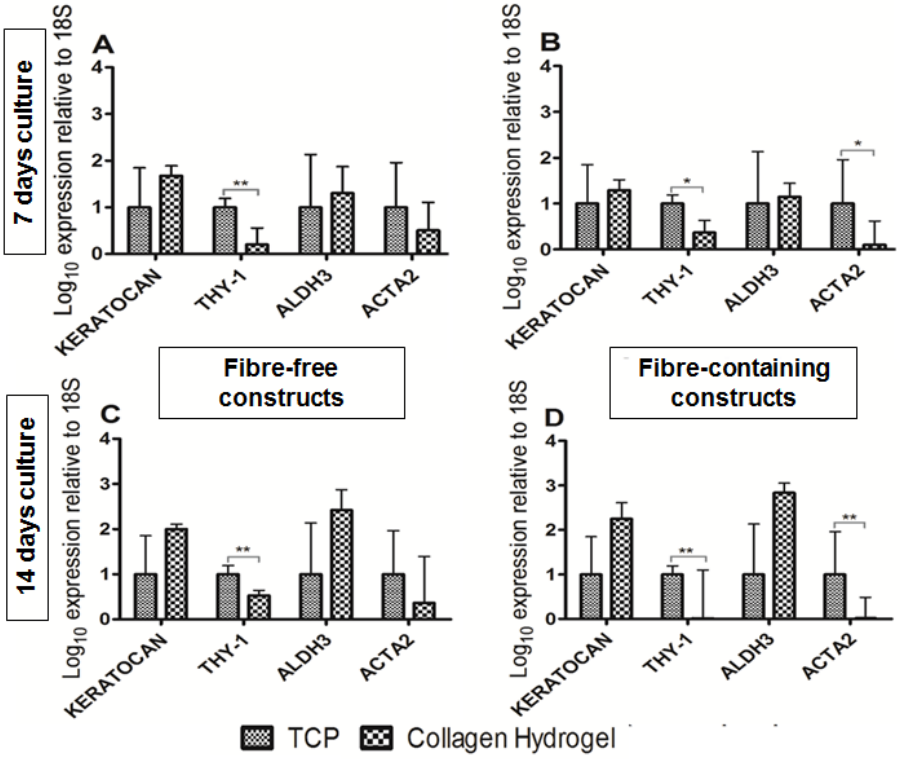

Figure 4.13: qPCR confirmation of the effect of culture conditions of AHDCS cells in 2D monolayer (TCP) culture vs. 3D collagen hydrogel culture under F media for 7 (A and B) and 14 (C and D) days in fibre-free (A and C) and fibre-containing (B and D) constructs; n=6; * $p \leq 0.05$, ** $p \leq 0.01$, *** $p \leq 0.001$.

When cultured in K and K* media for 7 days, there was no significant difference in the expression of keratocan when comparing fibre-free and fibre-containing 3D constructs (**Figure 4.14**). However, when cultured in K media, the expressions of Thy-1 and α-SMA were at significantly lower levels ($p \leq 0.01$ and ≤ 0.05 respectively compared to K*), and $ALDH_3$ at significantly higher levels ($p \leq 0.001$) in the fibre-containing constructs. $ALDH_3$ was also expressed in significantly higher levels ($p \leq 0.05$) in the fibre-containing constructs cultured under K* media.

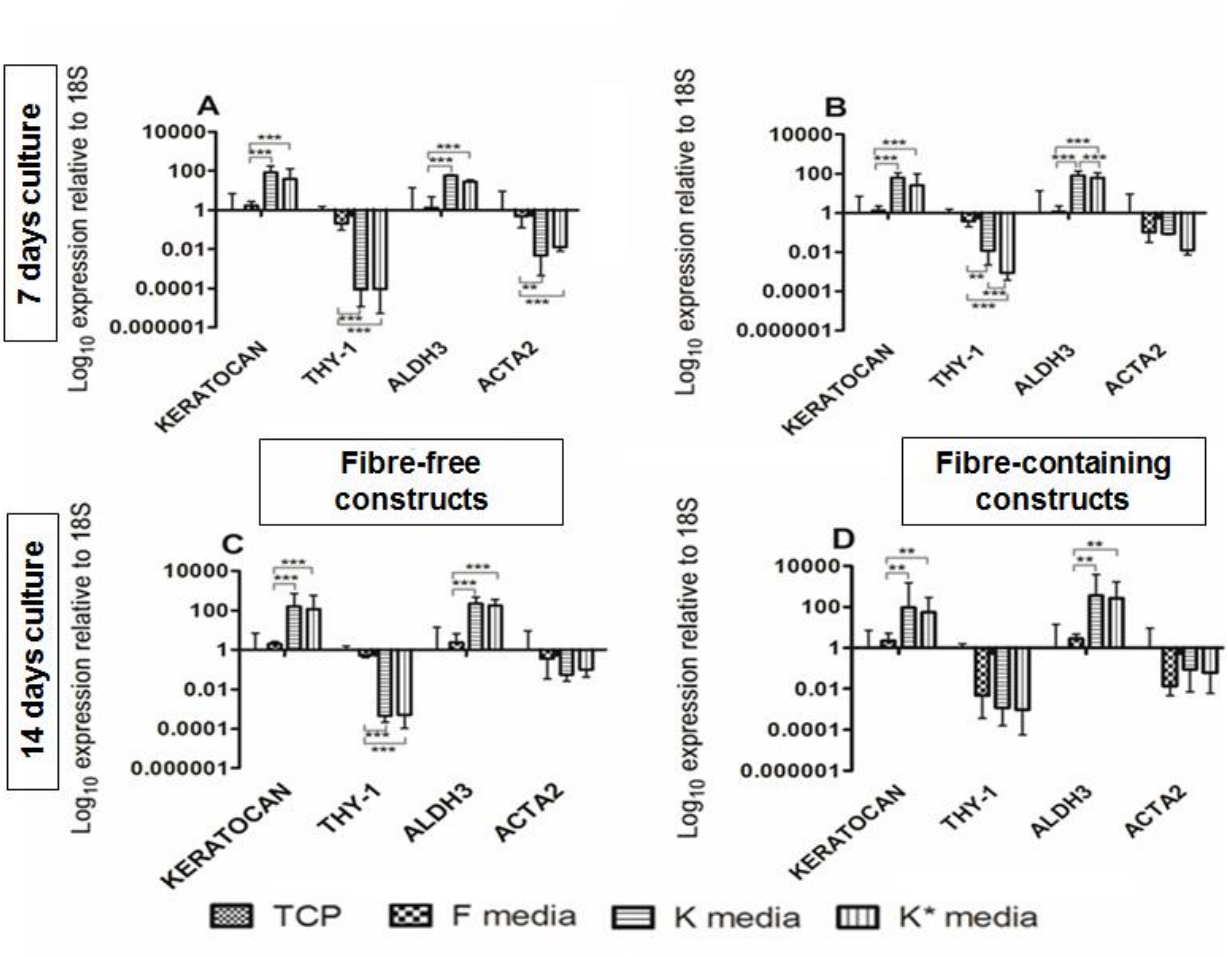

Figure 4.14: qPCR confirmation of the effect of chemical cues (F, K and K* media) and topographical cues (nanofibres) on the expression of keratogenic and fibroblastic markers at 7 (A and B) and 14 (C and D) days in fibre-free (A and C) and fibre-containing (B and D) constructs; n=6; * $p \leq 0.05$, ** $p \leq 0.01$, *** $p \leq 0.001$.

It was apparent that time in culture was having an effect on the reduced expression of fibroblastic markers and increased expression of keratogenic markers in both fibre-free and fibre-containing constructs. When cultured in F media there was only a significant reduction in expression of Thy-1 ($p \leq 0.05$) when comparing day 7 and day 14 fibre-free constructs. However, in the fibre-containing constructs both Thy-1 and α-SMA expression was significantly lower ($p \leq 0.05$ and 0.01, respectively) at 14 days culture. Culture time appeared to have the most significant effect in the fibre-free constructs when cultured under serum-free media (i.e. K and K*). When cultured under K media there was a significant decrease in expression of Thy-1 and α-SMA ($p \leq 0.05$ and ≤ 0.001, respectively) and a significant increase in $ALDH_3$ expression ($p \leq 0.001$). Similar trends were also observed in K* media. Culture time appeared to have an exclusively significant effect on $ALDH_3$ expression in fibre-containing constructs ($p \leq 0.001$). Other genes did not show this trend.

4.6. Discussion

Obtaining sufficient numbers of stromal cells with a keratocyte phenotype is a central challenge in the *in vitro* regeneration of a corneal stroma. By nature, keratocytes are quiescent, i.e. not proliferative, hence it is difficult to obtain a high population while maintaining the keratocyte phenotype. Sufficient numbers of stromal cells can be obtained from dissected corneal rims, by allowing the cells to adopt a fibroblastic phenotype. In this study, we demonstrated that corneal fibroblasts can partially differentiate back towards a keratocyte phenotype in 2D, semi-3D and 3D culture environments by careful manipulation of the chemical and topographic environment.

The purpose of the 2D and semi-3D studies was to establish if the cells were behaving as hypothesised (i) in the chosen media; and (ii) on the nanofibres structures. When

engineering a transparent cornea *in vitro* the ability of corneal fibroblasts to return back to a keratocyte phenotype is important (Berryhill et al. 2002). The ability to visually monitor the way the cells are migrating and proliferating is a relatively straightforward means to initially determine whether the cells are behaving as a native keratocyte or as a wound subtype. For example, native keratocytes are quiescent in behaviour (Fini 1999, Jester, Jin 2003, Builles et al. 2006, Berryhill et al. 2002, Pei et al. 2004) in that they are relatively dormant with respect to migration and proliferation. Conversly, activated keratocytes (fibroblasts) are highly motile and proliferative in thier behaviour; thus if the cells in both topographical and chemical environments were proliferating and migrating rapidly then it could be safely assumed that the cells were fibroblastic, in phenotype as opposed to keratogenic.

In this study it was examined how/if the culture conditions and/or the inclusion of nanofibres affected cell behaviour regarding proliferation and migration. This was achieved by using the Cell IQ® technology which enabled cell behaviour to be monitored in a favourable cell culture environment over relatively short culture periods of up to 48 hr continuous monitoring. The positive outcomes of these studies were used to build complexity into the culture environment *via* the use of a 3D collagen scaffolds. The elastic modulus measurements in the 3D constructs enabled us to reveal the effect of the differentiation process over a prolonged culture and the corresponding phenotype of the AHDCS cells have been defined by qPCR at 7 and 14 days.

4.6.1. The chemical cue effect

The addition of serum to culture media results in the differentiation of keratocytes to fibroblasts (Beales et al. 1999, Berryhill et al. 2002, Barry et al. 1994). Platelet derived growth factor (PDGF) in combination with a vast assortment of undefined factors found in

serum, is believed to cause the differentiation towards a fibroblastic-like lineage, resulting in cells that have increased migration, proliferation and collagen contraction (Jester, Jin 2003, Musselmann et al. 2005). These results were observed in all the culture conditions investigated. Thus, the removal of serum from culture media is an essential component in the restoration of a keratocyte phenotype. To promote a keratogenic phenotype, the use of a serum-free media supplemented with ascorbic acid and insulin (K media) was investigated on 2D and semi-3D constructs. An additional serum free-media (K*) was examined in the 3D cultures.

Previous studies (Beales et al. 1999, Berryhill et al. 2002, Barry et al. 1994) have shown that when cultured in serum-free media, stromal cells maintain a quiescent phenotype. However, quiescence alone is not sufficient in determining a keratocyte phenotype. Often, the removal of serum from media results in cell quiescence followed by apoptosis. Thus supplementation is required in media that can promote cell growth and proliferation without encouraging fibroblastic differentiation.

Insulin was used as a supplement in the K culture media as it has been suggested that it is useful in maintaining keratocyte phenotype and cell viability in *in vitro* cultures (Jester, Jin 2003, Musselmann et al. 2005). The addition of insulin to *in vitro* cultures resulted in elongated cell morphology, maintained keratocan expression and quiescence. Our results are consistent with these studies, as when cultured on either 2D or semi-3D constructs under K media, the mean cell number remained relatively constant for the duration of the experiment, whether nanofibres were present or not. In the 3D constructs the increased aspect ratio measurements, reduced construct contractibility and keratocyte gene marker expression further confirmed that the inclusion of insulin and ascorbate in keratocyte media is valid for the control of stromal cell phenotype.

In contrast, β-FGF was the main supplement in K* culture media, which has previously been used to differentiate and expand human corneal stromal stem cells (hCSSC) in monolayers (Du et al. 2007, Funderburgh et al. 2005). It has been reported that when cultured in this media, hCSSCs expressed the genetic markers unique to the keratocyte genotype (keratocan and keratan sulphate) (Du et al. 2007, Funderburgh et al. 2005), but they lacked the degree of organisation required to mimic the ECM of the corneal stromal layer. The addition of β-FGF to keratocyte culture media has also been shown to reduce the expression of α-SMA and increase keratan sulphate expression (Jester, Jin 2003). The reduced expression of α-SMA suggests that β-FGF is capable of blocking differentiation towards a myofibroblast phenotype. Our study confirmed that in β-FGF-containing media, AHDCS cells retained a keratocyte-like phenotype in a 3D structured environment.

When comparing the use of K and K* media in the 3D constructs, it was apparent that K media was preferable for restoring characteristic markers of keratocytes, manifested by the cell aspect ratio and qPCR data. The combination of ascorbate and insulin in culture media has been shown to stimulate collagen synthesis and increase keratocan and lumican accumulation (Musselmann et al. 2005). The insulin-containing K media encouraged cells to become significantly more elongated than the cells cultured in K* media, facilitating the cells to become closer to the desired elongated morphology of a native keratocyte. Our study suggests that through the suppression of proliferation rate of fibroblasts and using appropriate supplements in culture media, the partial restoration of the keratocyte phenotype following a fibroblastic transition, is possible.

4.6.2. The topographical effect

It was evident from the images recorded using the Cell-IQ® system that when cells cultured under both F and K media on coverslips coated with nanofibres in both 2D and

semi-3D environments that they successfully aligned and migrated in response to the surface topography provided by the fibres. In comparison the cells cultured on the blank coverslips migrated with random orientation and no alignment was observed.

The inclusion of nanofibre scaffolds also appeared to suppress the degree to which the cells were able to proliferate, indicated by a lesser increase in cell number compared to the cells cultured on the control blank surfaces when cultured in serum-containing F media. It appeared that the double crossed layered of fibres further emphasised this affect. Thus this double-layered cross arrangement was carried over to the semi-3D experiments as this set-up more closely mimicked the orthogonal fibril topography the cells would experience *in vivo.* It should be noted that the inclusion of nanofibres had no apparent affect on the stromal cell viability whether in 2D, semi-3D or 3D cultures.

The addition of the hydrogel "top" to the coverslip slowed down the rate of proliferation in both fibre-containing and fibre-free constructs when cultured in F media compared to the 2D equivalent samples. This suggests that simply changing the surrounding niche from 2D to a semi-3D collagen environment alone has an effect on cell phenotype, even when cultured in serum-containing F media. This phenomenon was also correlates with trends observed in the gene analysis studies whereby the switch from 2D monolayer stromal cell culture (on TCP) to a 3D (collagen hydrogel) environment saw alterations in gene expression patterns.

Native corneal tissue primarily consists of collagen type I. Collagen type I hydrogels formed by conventional thermal gelation often have poor mechanical strength and lack organisation, which is contrary to the characteristics of native stroma (Kotecha 2007). In order to rectify this problem we implemented a facile new technique in this study to align AHDCS cells through the incorporation of polymeric aligned nanofibres. The addition of the nanofibres in the 2D and semi-3D constructs acted as a contact guidance platform, on

which, cells could orientate and elongate, whilst they also improved the mechanical properties of the hydrogel (i.e. increased stiffness). Our 3D protocols enabled us to more closely mimic the native extracellular environment *via* the manufacture of multiple lamellae which increased the organisation of the cells through the whole construct thickness, with a tuneable distance between the layers. The novelty of our protocol is using portable meshes fabricated by a smart parallel electrode collector. These meshes have high fibre alignment and relative low fibre density (mean line density of 45 nanofibre/100 μm and a thickness ranging between 0.5 and 3.0 μm) whilst remaining transportable (Yang et al. 2011). The nanofibre meshes enabled us to align individual cells in the desired orientation and also permitted the cells to penetrate between layers when multiple nanofibrous meshes, were used in the 3D constructs. High density aligned nanofibre meshes have been produced previously by other groups using a rotary mandrel device (Wu et al. 2012). However, the density of the nanofibres was so high that the cells were essentially immobilised within the mesh because cells could not migrate through sub-micron pore sizes within the mesh.

The incorporation of orientated nanofibre layers clearly influenced cell proliferation on the 2D and semi-3D constructs, whilst increasing organisation and altering cell morphology in all constructs. Observations of the 3D constructs *via* fluorescent microscopy demonstrated that the orthogonal arrangement of cells was not confined to one plane, rather, that the cells were on three different planes. It was considered that the altered cell morphology of the AHDCS cells (higher aspect ratio), had induced the changes in the gene and protein expression within the cells. Two mechanisms may be used to explain the effect of the inclusion of nanofibres with regards to the alteration of the construct modulus, cell morphology and gene expression of the stromal cells in comparison to collagen only constructs. Firstly, the incorporation of the nanofibres increased the stiffness of the 3D

constructs as shown in the acellular constructs, which could potentially induce the AHDCS cells towards a more keratogenic lineage, as it has been previously described that substrate stiffness can affect differentiation of stem cells (Engler et al. 2006). Secondly, the attachment of cells to the nanofibres reduced the cells ability to contract the surrounding collagen. As the nanofibres were stiffer than the collagen, once attached the stromal cells either stopped cellular contraction due to sensing the stiffer substrate or were physically unable to deform the substrate. Reducing the contraction of the construct could be associated with promoting a keratogenic lineage.

A limitation of incorporating aligned nanofibres meshes within the collagen hydrogel constructs is that it is an onerous task to decouple the synergistic effect of increasing the substrate thickness from the effect of increased cellular organisation with regards to the observations made. For instance, it is extremely difficult to induce topographic guidance without altering the overall stiffness; equally it is difficult to alter the stiffness of the construct without altering other properties of the construct. For example, cross-linking of hydrogels is known to increase the stiffness of hydrogel constructs (Cauich-Rodriguez et al. 1996, Ahearne et al. 2007, Sunyer et al. 2012), but the reagents or techniques used may also have a chemical effect.

4.6.3. Interactions between the effect of chemical and topographical cues in 3D constructs

Both the use of F media and the incorporation of nanofibres produced constructs with a higher modulus. However, the cells cultured in K and K* media did not appear to have much of an effect on the elastic modulus of the construct. The hydrogel constructs that contained cells had a modulus that was very similar to the acellular scaffolds containing fibres in keratocyte media. This supports the hypothesis that the cells were behaving in a

quiescent manner and were not exerting a contractile force on the hydrogel construct. In serum-containing media, the presence of nanofibres in constructs reduced the cell contraction to a certain extent when compared to the fibre-free counterpart. The most significant reduction in cell contraction occurred in the specimens cultured in K and K* media, implying nanofibres acted as a topographical cue in combination with chemical cues.

4.6.4. The effect of chemical and topographical cues on the protein expression of AHDCS cells

In vivo, healthy keratocytes express the proteoglycan keratocan which is a major contributer to the stromal ground substances and is a key mediator of fibrillar organisation. Following corneal injury keratocan expression is lost, although it can return during and following the healing process (Carlsson et al. 2003). Therefore keratocan was determined to be a suitable positive marker for restoration of the keratocyte phenotype.

Conversely, Thy-1 is a cell surface glycoprotein belonging to the immunoglobulin superfamily (Pei et al. 2004) and its expression is usually associated with inflammation and wound healing. Its expression is not visible by immuno-labelling of uninjured corneal tissue or isolated keratocytes (Pei et al. 2004). Thus Thy-1 was determined to be a suitable positive marker for corneal fibroblast phenotype.

Determination of cell phenotype using the immunofluorescent stains Thy-1 and keratocan proved to be inconclusive in that they could not give a definitive answer regarding whether cells were fibroblastic or keratogenic in lineage. The fact that the stromal cells were capable of expressing both markers for keratocytes and fibroblasts appears to be contradictory to previous studies (Pei et al. 2004, Musselmann et al. 2005). An explanation for this may be that the stains used may not have been specific enough to

distinguish between the two cell types. Another hypothesis is that the cells are not fully differentiated into either keratocytes or fibroblasts and were displaying characteristics of both cell types. In studies performed on bovine keratocytes the addition of serum to isolated keratocytes caused the cells to become fibroblastic, but changing the media to serum-free media caused the cells to return to morphology similar to that of a keratocyte, suggesting that the removal of serum in media causes partial restoration of cell morphology (Berryhill et al. 2002). Therefore longer culture periods in serum-free media and the optimisation of topographical cues may be required for the cell to fully revert to the keratocyte lineage. In order to test this hypothesis, q-PCR was adopted as a quantitative method to more accurately detect levels of keratocyte and fibroblastic markers in the 3D construct experiments for prolonged culture periods.

4.6.5. The effect of chemical and topographical cues on the gene expression of AHDCS cells

As quiescence or cell morphology alterations are not unique to the keratocyte phenotype (Jester, Jin 2003), we corroborated our 3D mechanical findings with traditional qPCR, to examine the gene expression of characteristic markers, specific to a keratocytic genotype. In previous studies lumican (Musselmann et al. 2005, Karamichos et al. 2007), keratocan (Musselmann et al. 2005, Kao, Liu 2003), $ALDH_3$ (Musselmann et al. 2005, Funderburgh et al. 2005, Kao, Liu 2003), Thy-1 (Pei et al. 2004, Pei et al. 2006, Hindman et al. 2010), α-SMA (Jester, Jin 2003, Builles et al. 2006, Pei et al. 2004, Jester et al. 1995, Berryhill et al. 2002), fibronectin (Jester, Jin 2003), CD34 (Espana et al. 2004) and vimentin (Espana et al. 2005) have all been examined to help to determine and distinguish the differences in gene and protein expression between corneal keratocytes, fibroblasts and myofibroblast phenotypes in *in vitro* cultures. In this study, we chose to monitor the gene expression

profiles of four markers, keratocan, $ALDH_3$, Thy-1 and α-SMA in response to the chemical and topographical cues. We observed two interesting phenomena. Firstly, AHDCS cells did not entirely lose their keratocyte gene expression, even after being cultured in serum-containing media for two weeks. Secondly, the relative expression of keratocyte and fibroblast marker genes could be affected by chemical and topographical factors. Three cues were investigated alone, and in combination in this current study. Simply changing from 2D (TCP) to 3D (collagen hydrogel) culture conditions in F media increased the gene expression of keratocyte markers. This alteration of the gene expression pattern was more obvious in the fibre-containing collagen constructs cultured in F medium. Both keratocan and $ALDH_3$ gene expression were significantly up-regulated, whilst Thy-1 and α-SMA were significantly down-regulated. Furthermore, the alteration of supplements in culture media encouraged gene expression toward a keratogenic phenotype. Fibroblast gene expression was suppressed in both K and K*, serum-free medium. The presence of nanofibres in the constructs made the effect of the chemical supplements more prominent.

In vivo healthy keratocytes characteristically express high levels of keratan sulphate associated molecules lumican (glycoprotein) and keratocan (proteoglycan) (Musselmann et al. 2005). Whilst lumican is found in many tissues (Musselmann et al. 2005), keratocan is exclusive to the cornea (Musselmann et al. 2005). During wound healing, keratocan expression decreases, which is the phase associated with fibroblastic activity and contraction of the wound. $ALDH_3$ is expressed in high levels in a healthy keratocyte (Musselmann et al. 2005). When cultured in the presence of serum, which is associated with differentiation of keratocytes towards fibroblastic lineage, the expression of $ALDH_3$ is reduced or lost. Therefore, this gene served as a marker for keratocyte phenotype.

Both myofibroblasts and fibroblasts express Thy-1 (Pei et al. 2004) and it is regularly used in corneal tissue engineering applications to help distinguish corneal fibroblasts from

keratocytes (Pei et al. 2004, Pei et al. 2006, Hindman et al. 2010). In addition, corneal wound fibroblasts and myofibroblasts express α-SMA, which is linked to wound contraction (Builles et al. 2006, Jester et al. 1995, Berryhill et al. 2002). Therefore, expression of α-SMA is associated with keratocytes differentiating towards fibro/myofibroblastic lineages. The qPCR results in our study demonstrate that the four genes selected were effective at determining the effect of culture conditions (chemical cues) and nanofibres (topographical cues) on the phenotype of AHDCS cells.

The gene data corresponded well with elastic modulus data in that the stromal cells in the fibre-containing constructs had reduced fibroblastic tendencies, even in the presence of serum-containing media; while serum-free media were capable of altering the keratocyte gene expression. The differences in gene expression correlated with the contractile nature of the cells, with high levels of fibroblastic markers being expressed with increased contraction. Previous studies (Wray, Orwin 2009, Wu et al. 2012, Musselmann et al. 2005) in 2D culture conditions have shown that media conditions and topographical cues can stimulate the up-regulation of genetic markers associated with a keratocytic phenotype and switch off fibroblastic gene expression. Another possible explanation in the the inclusion of nanofibres into the hydrogel constructs is having a mechanical as well as a topographical effect. Previous studies have demonstrated that cells respond to the resistance of their surrounding environment (Griffin et al., 2004), which in turn affects their behaviour and differentiation as the cells adapt their adhesions, cytoskeletal configurations and general morphology in response to substrate resistance or stiffness (Discher et al., 2005).

Our studies demonstrated a cumulative, combined effect of media and topographical stimulation towards maintaining a keratocytic phenotype and gene expression. Switching from 2D monolayer culture to a 3D collagen environment and then to an organised 3D

environment has an observable effect on the AHDCS cell lineage, which can be manipulated to improve current corneal tissue engineering models.

4.7. Conclusion

It has been demonstrated that both chemical and topographical cues can be used to manipulate the phenotype of AHDCS cells *in vitro* in 2D, semi-3D and 3D collagen hydrogel environments. The use of simplified 2D and semi-3D environments confirmed that the addition of serum to culture media resulted in fibroblastic cells that were more motile and proliferative than cells cultured on equivalent constructs in serum-free media. The introduction of stiff, aligned nanofibres caused the cells to become more organised and elongated in morphology as they used the surface topography to align and migrate. Additionally, even in the presence of serum, cells cultured onto fibre-containing 2D and semi-3D surfaces exhibited a reduced motility and cell proliferation and became more elongated in morphology compared to cells grown on fibre-free surfaces. The removal of serum appeared to further emphasise this effect. Indeed, immunohistochemical staining demonstrated that despite only relatively short culture periods that changes in protein expression that correlated with cell behaviour were occurring. However, the de-differentiation of the AHDCS cells to a keratocyte lineage was incomplete in these simplified 2D and semi-3D models. Increasing the culture time may have caused more significant changes to the cell phenotype; however the complexity of the native corneal extracellular environment was still missing.

Introducing complexity into the culture environment *via* the introduction of a 3D collagen hydrogel aimed to more closely mimic the *in vivo* situation and as a result, the cellular differentiation was more complete. Even in the presence of serum-containing media, the change from a 2D to a fully 3D culture environment caused a down-regulation

of fibroblastic gene markers. This demonstrates that despite *in vitro* culturing, AHDCS cells are still able to retain their capacity to differentiate upon the (partial) restoration of the surrounding environment.

The combined effect of a 3D collagen environment, chemical and topographical cues caused a significant alteration in cell behaviour. The cells in serum-free fibre containing 3D collagen constructs in particular were organised, quiescent, non-contractile and elongated in their morphology, characteristics all reminiscent of the native keratocyte phenotype. The most significant changes were concerned with the change in gene marker expression. There was a significant up-regulation of keratocyte markers and a down-regulation of fibroblastic markers, demonstrating that the phenotype and genotype of cultured corneal stromal cells remains interchangeable, dependent upon careful tailoring of the culture environment. Utilising chemical and topographical cues, particularly in a 3D culture environment for prolonged culture periods could represent an opportunity for developing new regenerative strategies for corneal repair and regeneration. The combination of non-destructive monitoring technique and analysis of protein and gene expression provide important feedback for optimising culture conditions, which has not previously been shown in 3D corneal models.

5. Corneal stromal cell plasticity: regulation of stromal cell phenotype using epithelial-stromal co-culture

5.1. Abstract

In vivo, epithelial cells are in close contact with keratocytes (Du et al. 2007, Kawakita et al. 2005) in the stromal layer; they are connected both anatomically and functionally (Wilson et al. 1999), and it is these interactions that are vital to the maintenance of tissue homeostasis and transparency. Co-culture studies aim to recapture this cellular anatomy and functionality by bringing together two or more cell types within the same culture environment, enabling them to interact and communicate which can act as a very powerful *in vitro* tool (Hendriks et al. 2007). The influence of cellular interactions is of particular interest to tissue engineers because the tissue formation of one or all cell types can be regulated by simulating and stimulating the natural physiology and differentiation of cells.

In order to more closely mimic the native niche environment three different co-culture methods have been examined; epithelial explant; transwell; the use of epithelial conditioned media and their effects on stromal cell function were studied. The different co-culture models help us to determine as to whether cell-cell interactions are due to direct cell contact or not, and as to whether the cells themselves have to be present to elicit a response. By more closely mimicking the *in vivo* cellular niche environment we are able to aid our understanding of corneal wound healing mechanisms and the importance of cell mediated interactions; thus enabling us to engineer corneal tissue with stromal cells that are in a healthy, native, uninjured (non-activated) state. The effects of the addition of transforming growth factor β-1 (TGF-β1) and wortmannin to the culture media was also investigated to examine cell plasticity within the corneal model and whether this can be blocked. The work detailed in this chapter is based upon the original research paper entitled "**Corneal stromal cell plasticity: in vitro regulation of cell phenotype through**

cell-cell interactions in a 3D model" which has recently been accepted for publication in the journal Tissue Engineering: Part A, submitted in revised format, manuscript ID: TEA-2013-0167.R1 (accepted 17th July 2013).

5.2. Introduction

Tissue engineering *ex vivo* involves an understanding of the relationship between cell communities in regulating cell behaviour and function. Most tissues consist of more than one cell type and it is the organisation of the cells within the tissue that is essential to normal development, homeostasis and in the case of corneal tissue, transparency. *In vivo*, epithelial cells are in close contact, anatomically and functionally (Wilson et al. 1999) with keratocytes (Du et al. 2007, Espana et al. 2005) in the stromal layer. *In vivo* studies have demonstrated that epithelial cells coordinate with the keratocytes in the adjoining stromal layer *via* bidirectional soluble cytokine, growth factor and chemokine release mechanisms, although direct cell-cell communications do occur in some situations (Wilson et al. 2003). Such communications aid and stimulate normal migration and the secretion of proteoglycans and glycoaminoproteins by the keratocytes. The process occurs simultaneously, in a highly coordinated manner which changes dependent upon development, homeostasis and wound healing. Proteoglycan biosynthesis readily changes under varying conditions both *in vivo* and *in vitro* (Chan, Hasche 1983), which is pivotal to collagen structure, spatial distribution and overall organisation. This also demonstrates the remarkable cell plasticity of stromal keratocytes with regard to their ability to differentiate in response to subtle chemical, topographical and environmental cues *in vivo*. Less is known how stromal cell behaviour is affected *in vitro.*

In vivo, a fibroblastic wound healing response is augmented by epithelial destruction (Tuft et al. 1993) or loss of contact between the epithelial cells with the stromal layer (Nakamura et al. 2002) which can result in detrimental effects on the tissue architecture,

resulting in loss of tissue transparency due to an "activation" of the stromal keratocytes to a fibroblastic or myofibroblastic cell type (Fini 1999). *In vitro* when cultured onto TCP or as monocultures, corneal stromal cell behaviour is significantly altered, for example, the proteoglycan synthesis of cultured stromal cells in monoculture is significantly less compared to when cultured as whole intact cornea (Chan, Haschke 1983), reinforcing the concept the corneal constituent layers interact with each other during normal tissue homeostasis. In a healthy, uninjured cornea cell generation and loss, and the quantities of growth factors that stimulate and inhibit, are balanced (Wilson et al. 2012c) *via* an ongoing communication between corneal epithelial, keratocytes and nerve cells; and the maintenance of the Bowman's layer also requires ongoing cytokine-controlled stromal-epithelial interactions, with this layer showing evidence of the incessant attractive and repulsive cellular communications (Wilson et al. 2003). It is also likely that the endothelial cells communicate with the keratocytes during homeostasis (Wilson et al. 2003), although there is currently little *in vitro* research in this field.

Co-culture systems act as very powerful *in vitro* tools which allow for tissue cellular interactions and cellular function(s) to be investigated. The influence of cellular interactions is of particular interest to tissue engineers because the tissue formation of one or all cell types can be regulated by simulating and stimulating the natural physiology and differentiation of cells. Two-dimensional (2D) monolayer cultures are often used to investigate the way that various exogenous growth factors can be used to regulate growth, differentiation and function of corneal cells (Nishimura et al. 1998). However, 2D monolayer cultures often lack the three-dimensional (3D) physiological environment found *in vivo* and so are often criticised with regards to their limited application to the *in vivo* situation (Dayhaw-Barker 1995a). In the cornea, a 3D environment may be more applicable to mimic the extrinsic environmental as well as the intrinsic cellular cues

necessary to successfully culture and differentiate stromal cells and their subtypes. Previous co-culture studies have displayed that a collagen gel matrix is essential for epithelial cell growth and maintenance of structural differentiation (Nishimura et al. 1998) and that additional stromal cell cultures can influence the differentiation of epithelial cultures.

Much of the existing literature regarding corneal co-culture is concerned with epithelial-stromal culture, with the emphasis being on the effect that the additional stromal cells (often activated/fibroblastic in phenotype) will have on the epithelial culture. This may be due to the interest in treating limbal epithelial deficiencies and epithelial wounds. However, often corneal disease and injuries (such as chemical burns and Stevens-Johnson Syndrome, SJS (Roujeau et al. 1995)) penetrate deeper into the stromal layer so it is important to also consider the effects that epithelial cultures will have on the corresponding stromal culture.

When developing co-culture models, it is important to balance the ability to observe, measure and manipulate cell behaviour when constructing *in vitro* 3D environments. **Chapter 4** demonstrated that careful manipulation of both media and topography can influence stromal cell phenotype and genotype towards a keratocyte phenotype when in a 3D organised collagen construct in the absence of an epithelium or epithelial culture. However, the differentiation is not complete and some fibroblastic tendencies still remain.

5.3. Aims and Objectives

The aim of this study is to investigate the nature of stromal cell plasticity and to understand the role of cell-cell signalling for the control of stromal cell phenotype *in vitro*. In this study, we investigate the nature of cell-cell contact, cell signalling molecules and the inhibition of critical pathways in controlling stromal cell phenotype. Using our non-destructive monitoring tools it has been revealed how the introduction of an epithelial culture affects stromal cell differentiation in terms of construct contraction and elastic modulus measurements in a 3D collagen hydrogel environment for prolonged culture periods. Cell viability, phenotype, morphology and protein expression was also investigated to corroborate our mechanical findings with regards to stromal cell differentiation and biological function.

5.4. Materials and Methods

5.4.1. Experimental design

A series of experiments were devised in order to investigate a number of factors which may influence stromal cell plasticity. Initially the influence of different co-culture systems was studied to understand the nature of cell-cell contact with regard to restoration of the native keratocyte phenotype in cultured (fibroblastic) stromal cells. Cell-seeded collagen hydrogel constructs were cultured with and without the presence of an additional epithelial co-culture. Samples cultured without the presence of epithelial cells were cultured under serum-containing F media and serum-free CnT20 media to (i) provide a negative control where upon cells are behaving as fibroblastic-like cells; and to (ii) determine if the switch in media from serum-containing F media to serum-free CnT20 media alone was sufficient to promote differentiation towards a keratocyte lineage. These specimens were referred to

as “monocultured” constructs. Co-cultured specimens were split into 3 groups, explant; transwell and conditioned media co-cultures (**Figure 5.1**).

Acellular collagen scaffolds were produced as a control. All cell-seeded collagen constructs were initially cultured for 24 hr under serum-containing (fibroblast) media as used in the 2D expansion of AHDCS cells. This encouraged the cells to maintain an activated, fibroblastic phenotype causing the constructs to contract, reduce in thickness and become more collagen dense. Increasing the collagen density of the constructs was aimed at improving epithelial cellular outgrowth and stratification (Mi et al. 2010; Brown et al, 2005). Following 24 hr the media was then swapped for serum-free CnT20 media accordingly.

Epithelial explants were transferred and cultured onto the fibronectin coated insert dishes, thus allowing us to investigate as to whether the epithelial cultures had to be in direct contact with the stromal cell-seeded constructs (as in the explant cultures) in order to initiate a response, or whether the presence of the cells themselves was enough to provoke a response as the membrane was impermeable to the cells, but not to soluble factors. Epithelial conditioned media was used to determine whether a response could be provoked without the cells being present by using the soluble factors released into the spent media.

Cell signalling molecules were then investigated *via* the introduction of a well-documented chemotactic and mitogen, TGF-β1 (Imanish et al. 2000, Nakamura et al. 2000) to culture media to determine if cell plasticity remained following culture in our 3D collagen models. Media was supplemented with TGF-β1 at two different time points to see if (i) it could initiate a fibroblastic/myofibroblastic cellular response once the stromal cells had undergone differentiation towards a keratogenic lineage; (ii) if the epithelial cultures could overcome the mitogenic effect of this growth factor.

Finally, it was investigated as to whether it was possible to block the epithelial-stromal molecular pathways responsible for stromal cell differentiation by supplementing media with a known phosphoinositide-3-kinase (PI3K) inhibitor, wortmannin (Chandrasekher and Bazan, 1999, Zhang et al. 1999, Islam and Akhtar, 2001, Kakazu et al. 2004). Separate rounds of experiments were performed where the reagent was added to culture media to see if it could block/prevent the affect that the epithelial cultures were having on stromal cell differentiation at two different time points.

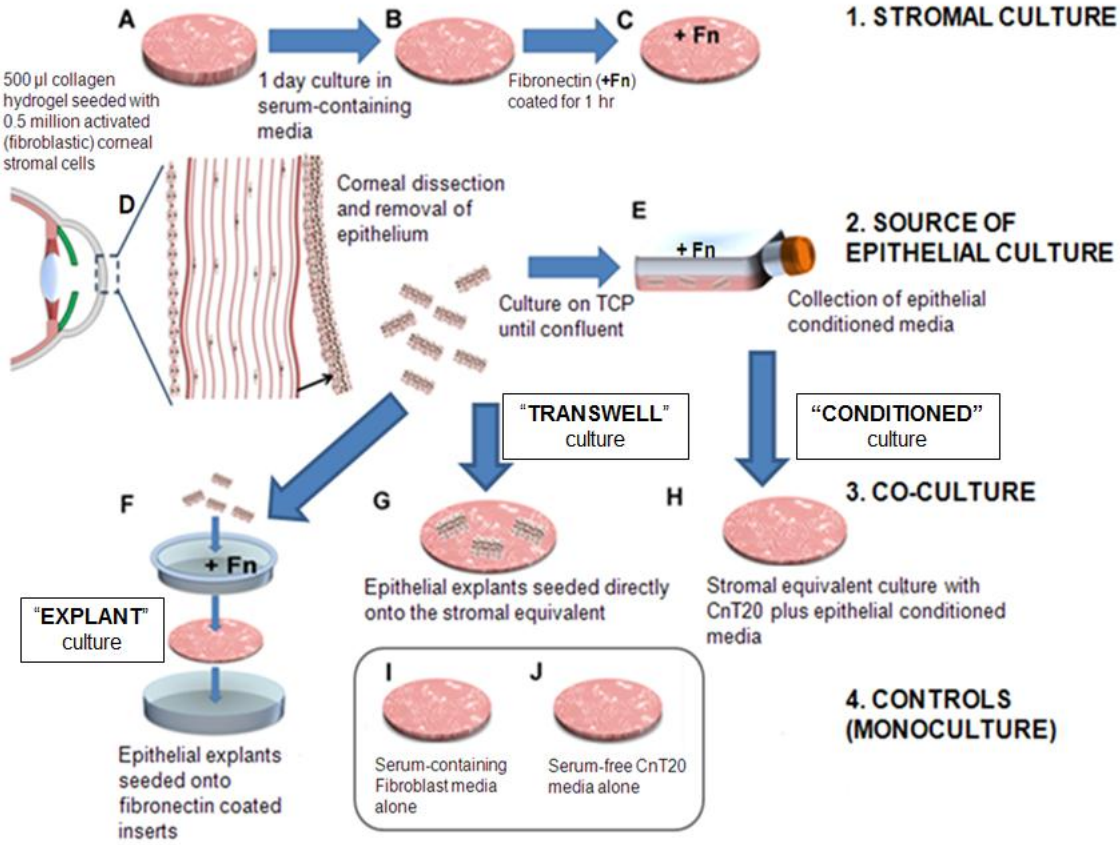

Figure 5.1: Schematic drawing of the experimental design and set-up of different co-culture environments.

5.4.2. Adult human derived corneal stromal (AHDCS) cell culture

Adult human corneal tissue remaining from corneal transplantation was used for the isolation of AHDCS cells; see **section 3.1.1.**

5.4.3. Epithelial cell culture

Adult porcine eyes were obtained from a local abattoir (Staffordshire Meat Packers, SMP, Bucknall, UK) were used as a source of epithelial tissue explants; see **section 3.1.2.**

5.4.4. Stromal cell monoculture

Cell-seeded hydrogels were prepared as detailed in **section 3.2.1** and cultured in monoculture under two different media; serum-containing F media, see **section 3.1.1** and serum-free CnT20 media, see **section 3.1.2.**

5.4.5. Epithelial-stromal co-culture

The stromal co-culture experiments were split into 3 separate groups: explant; transwell and conditioned media cultures (**Figure 5.1F, G** and **H**). Explant cultures referred to dissected epithelial tissue explants that were transferred directly to fibronectin coated acellular scaffolds or stromal cell-seeded hydrogel constructs (**Figure 5.1G**) cultured under 3 ml CnT20 media. Transwell cultures referred to stromal cell-seeded collagen constructs that were placed into sterile 6-well companion plates (BD Falcon, USA) below a permeable cell culture insert dish (pore size 0.4 μm; BD, Falcon, USA) onto which epithelial explant were cultured (**Figure 5.1F**) and were cultured under 3 ml CnT20 media. Conditioned media was obtained by seeding epithelial explants onto fibronectin coated T25 cm^2 tissue culture plastic (TCP) flasks and allowing them to reach confluence (**Figure 5.1E**). The spent media (5 ml per flask) was collected. It was sterile filtered and pH

balanced using HEPES buffered saline solution (Fluka, Sigma-Aldrich, UK) before being mixed with CnT20 media at 10% (*v/v*) concentration. 3ml of conditioned media was added to each stromal cell seeded collagen construct

5.4.6. Treatment with TGF-β1

In order to determine as to whether the corneal stroma cells retained their plasticity, TGF-β1 (Sigma-Aldrich, UK) was used to supplement all culture media at a concentration of 10 ng/ml, following 14 days mono- or co-culturing respectively as described in **section 5.4.4** and **5.4.5**. All constructs were cultured for a further 7 days in TGF-β1 supplemented media before the experiment was terminated at day 21. In a separate round of experiments, TGF-β1 was used to supplement all culture media at day 2, to coincide with the addition of the epithelial cultures. All constructs were cultured for 14 days under the TGF-β1 supplemented media.

5.4.7. Inhibition of cell-cell signalling with wortmannin

Wortmannin (Sigma-Aldrich, UK) was used to supplement all media (100 nM, as previously used by Chandrasekher and Bazan (1999) and Kakazu et al. 2004)) at 2 different time points. Initially, all constructs were mono- or co-cultured for 14 days, following the supplementation with wortmannin at day 2 in the experiment. In a separate round of experiments stromal cells were cultured for 14 days in either mono- or co-culture conditions as described in **section 5.4.4** and **5.4.5**. Wortmannin supplementation occurred on the 14^{th} day and all constructs were cultured for a further 7 days in the wortmannin supplemented media before the experiment was terminated at day 21.

5.4.8. Cell viability

Cell viability was observed at using a live-dead fluorescent double staining kit, it was used according to the manufacturer's instructions; see **section 3.4.1**.

5.4.9. Construct contraction

Hydrogel constructs cast into filter paper rings were effectively confined to the dimension of the filter paper ring. This permitted analysis of confined contraction in terms of a change of thickness of the hydrogel construct *via* optical coherence tomography (OCT) see **section 3.3.2.** Constructs were examined every 1-2 days over 14-21 days in culture, dependent upon when/if exogenous factors were used to supplement the media.

5.4.10. Modulus measurement

The mechanical properties of the constructs were measured at different culture times using a non-destructive spherical indentation technique as described in **section 3.3.1**. Modulus measurements were performed on all samples apart from the explant co-cultured constructs. It was not possible to perform the spherical indentation technique on these specimens as the surface of the construct was non homogeneous due to the presence of the tissue explants. Thus the spherical indenter was unable to spontaneously centre (Liu, Ju 2001) and axisymmetrical deformation did not occur. The elastic modulus was measured every 1-2 days for 14 or 21 days dependent upon the experimental group being investigated.

5.4.11. Immunolabelling of epithelial and stromal cell cultures

Cell phenotype was observed in both epithelial and stromal cell cultures. Each sample was fixed, permealised, blocked and stained as detailed in **section 3.4.3**. The primary

antibodies used to stain the epithelial cultures were cytokeratin-3 (CK3) and vimentin. The primary antibodies used to stain the stromal cell cultures were split into two panels: keratocan, $ALDH_3$ and lumican to act as positive stain for keratocytes and Thy-1, α-SMA and vimentin were used to positively stain for fibroblasts/myofibroblasts.

5.4.12. Statistics

All data was analysed using GraphPad Prism® (CA, USA). The data was subjected to a normality (Kolmogorov-Smirnoff) test. The data was normally distributed, so comparisons were performed using two-way analysis of variance (two-way ANOVA) followed by Bonferroni post-tests. Significance was indicated to determine if the effects of time, media and epithelial culture method were statistically significant at three levels: * $p \leq 0.05$, ** $p \leq 0.01$ and *** $p \leq 0.001$. All results are expressed as a mean value ± the calculated standard deviation.

5.5. Results

Due to the large quantities of data generated in this chapter, the analysis of results has been split into three separate sections regarding the effect of co-culturing, the addition of TGF-β1 and wortmannin to cultures. Any analogous findings are drawn together and commented on in the discussion section.

5.5.1. The role of epithelial cultures on AHDCS cell differentiation

5.5.1.1. Cell viability

Cell viability of epithelial and stromal cultures was monitored at day 7 and 14 in the co-culture studies. Cell viability in all epithelial populations remained high at both 7 and 14 days (**Figure 5.2**) and all cells displayed the characteristic cobblestone morphology. In

stromal cell monocultures, cell viability was high in constructs cultured in serum-containing F media at both 7 and 14 days (**Figure 5.3E** and **J**). However, the constructs monocultured in CnT20 media alone had a higher proportion of dead cells following 7 days culture (**Figure 5.3D**) compared to all other samples and following 14 days culture most of the cells within the constructs were dead (**Figure 5.3I**). In co-cultured samples, high stromal cell viability was maintained in explant, transwell and conditioned media cultures following 7 days culture (**Figure 5.3A, B** and **C**). This high viability was maintained in the explant co-cultures for the 14 day duration of the experiment (**Figure 5.3F**). However, in the transwell co-cultured constructs, although overall stromal cell viability was good there were a higher number of dead cells observed (**Figure 5.3G**) when compared to explant culture. A significant drop in stromal cell viability was observed in the conditioned cultured constructs following 14 days (**Figure 5.3H**), although overall stromal cell viability was still higher than observed in CnT20 mono cultures.

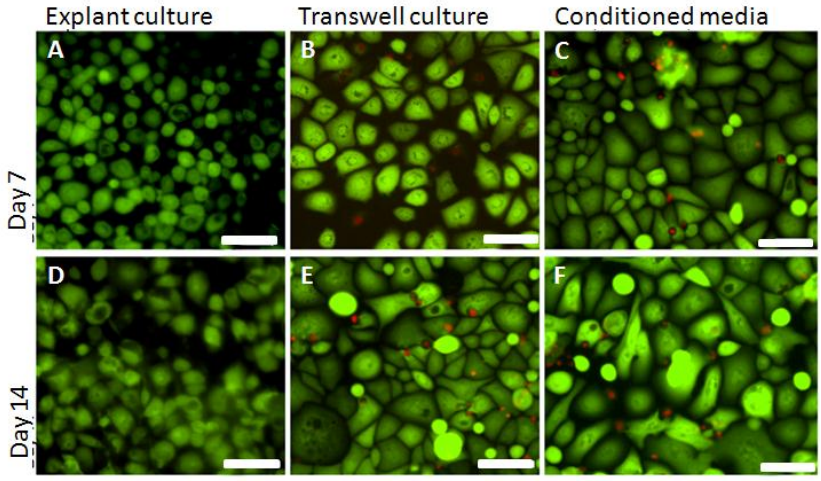

Figure 5.2: The effect of co-culturing on epithelial cell viability; representative live-dead fluorescent images of epithelial cells cultured using different co-culture methods at 7 (A-C) and 14 days (D-F); green indicates live cells, red indicates dead cells; scale bar = 100 µm.

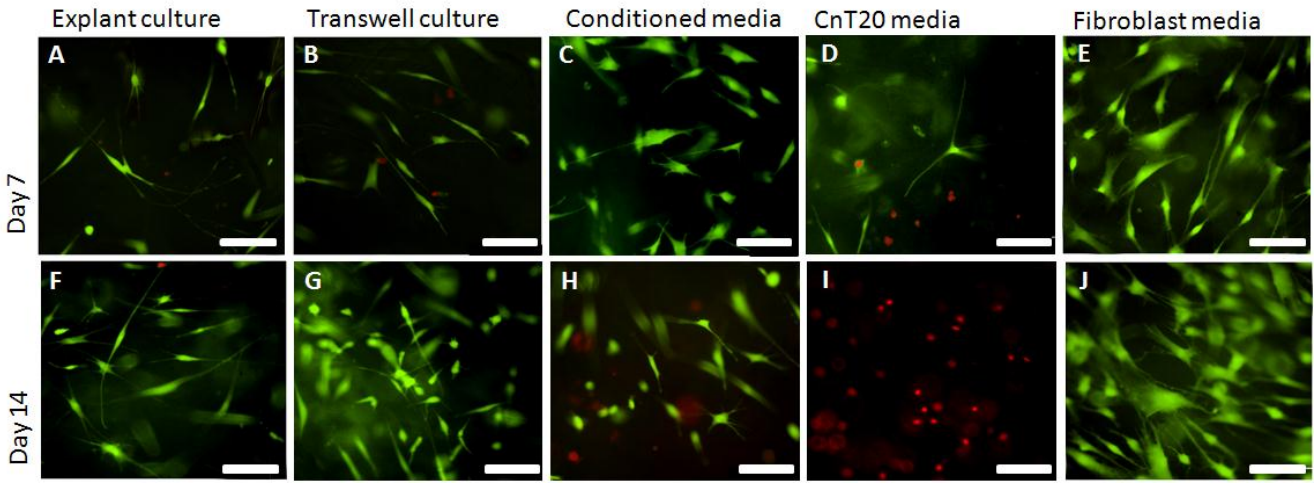

Figure 5.3: The effect of different co-culturing methods (A-C and F-H) versus monoculture (D,E, I and J) on stromal cell viability; representative live-dead fluorescent images of stromal cells cultured using different mono and co-culture environments at 7 (A-E) and 14 (F-J) days; green indicates live cells, red indicates dead cells; scale bar = 100 µm.

5.5.1.2. Construct contraction

All cellular constructs were cultured in serum-containing F media for the first 24 hr. This resulted in an initial contraction of all cellular constructs, manifesting as a reduction in the thickness of the constructs. The thickness of all cellular constructs thus reduced by approximately 15% (**Figure 5.4A**), which was significantly thinner than the acellular control scaffolds (**Figure 5.4B**). The thickness of all subsequent constructs switched to the CnT20 culture media, irrespective of the culture method employed, remained constant for the duration of the experiment. The constructs that remained in serum-containing F media continued to contract for the duration of the experiment, with most contraction occurring in the first week. The resulting constructs were approximately 30% of their original thickness at day 14**.** ANOVA tests revealed that change to CnT20 media had a significant effect on the change in thickness of the construct. Following 2 days in culture, constructs cultured in F media contracted and reduced significantly more in thickness compared to all other constructs ($p \leq 0.001$). No significant difference in construct thickness was observed

between any of the constructs cultured in CnT20 media irrespective of the culture method employed. The construct thickness of all acellular control specimens remained constant for the duration of the experiment.

5.5.1.3. Modulus measurement

The modulus of the constructs cultured in serum-containing F media continually increased over the duration of the experiment and were significantly greater ($p \leq 0.001$) than all other constructs from day 2 onwards (**Figure 5.4C**). The modulus of the constructs cultured in transwell co-culture were significantly greater ($p \leq 0.001$ at day 9 and 14; $p \leq 0.05$ at day 10 and 11) than monocultured specimens in CnT20 media and co-cultured conditioned media constructs ($p \leq 0.05$ at day 9 and 10; $p \leq 0.001$ at day 14). The modulus of the transwell cultured constructs remained relatively constant for the 14-day duration of the experiment, whereas the modulus reduced in both CnT20 and conditioned media cultures following 9 days culture. There was no significant difference in the modulus of constructs cultured in CnT20 media compared to conditioned media specimens. The modulus of all acellular control scaffolds remained constant at approximately 0.9 kPa for the duration of the experiment (**Figure 5.4D**).

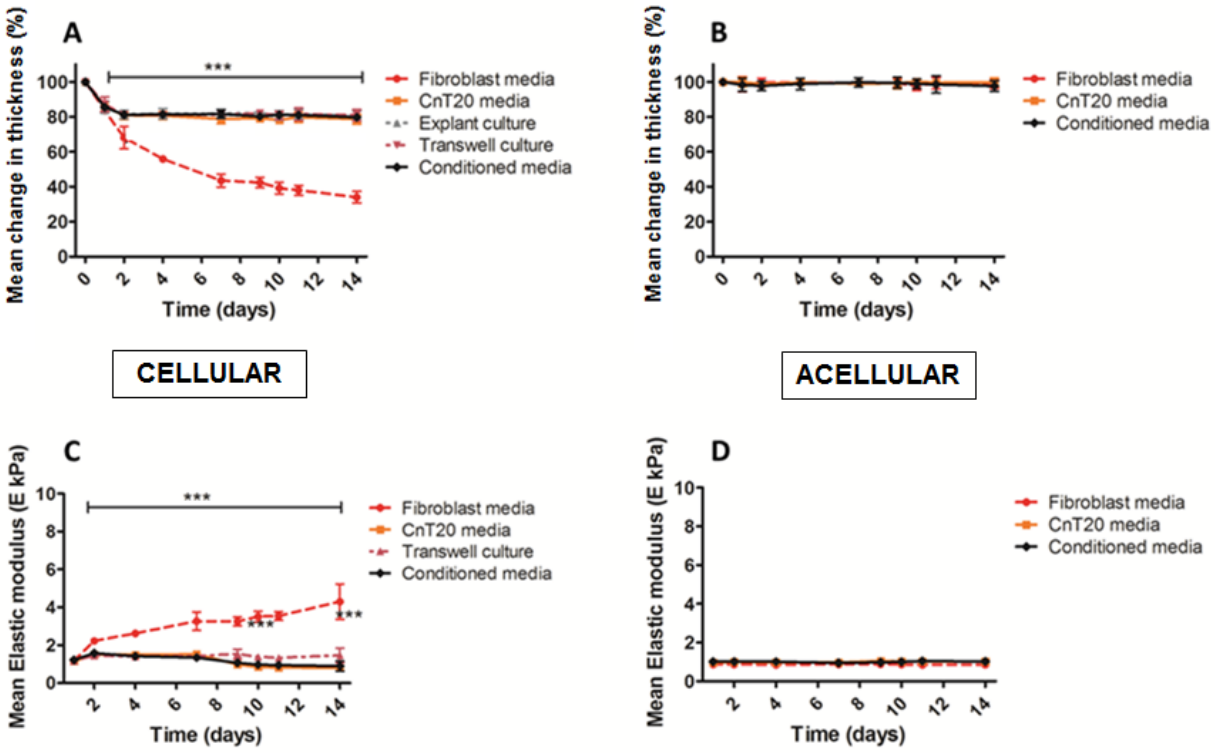

Figure 5.4: The effect of different mono- and co-culturing methods on the mean thickness change of cellular (A) and acellular control (B) scaffolds and the mean elastic modulus of cellular (C) and acellular (D) scaffolds cultured for 14 days; n=6.

5.5.1.4. Protein marker expression

All epithelial cultures were characterised using primary antibodies cytokeratin-3 (CK3) and vimentin. All epithelial samples stained positive for CK3 (**Figure 5.5A-C**) and negative for vimentin (**Figure 5.5D-F**). There was no apparent difference in CK3 expression detected in the samples.

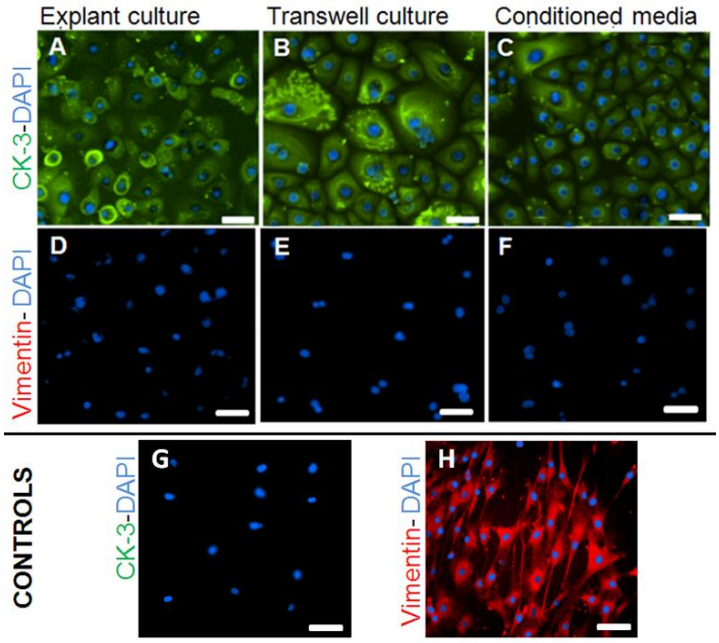

Figure 5.5: The effect of different co-culturing methods on CK3 (A-C) and vimentin (D-F) protein marker expression in epithelial cells. Representative fluorescently stained cells, imaged using fluorescent microscopy following 14 days culture; All epithelial cells stained positive for CK3 (A-C) and negative for vimentin (D-E), irrespective of the culture conditions used. Activated stromal cells control staining showed negative expression of CK3 (G) and positive expression of vimentin (H). Scale bar = 50 μm.

Immunohistochemistry was performed on all samples (except stromal cells cultured in CnT20 monoculture) following 14 days culture. The cell viability of the CnT20 monocultured constructs was so poor at day 14 that they were deemed unsuitable for further characterisation. The markers keratocan, aldehyde dehydrogenase-3 ($ALDH_3$) and

lumican were used to positively stain for keratocyte differentiation of the AHDCS cells. All three markers were positively expressed in explant, transwell and conditioned media co-cultured constructs (**Figure 5.6A-C**; **E-G**, **I-K**), however the level of fluoresce for all the keratocyte markers appeared lower in the cells cultured in conditioned media (**Figure 5.6C**, **G** and **K**) in comparison to explant and transwell co-cultured stromal cells. None of the keratocyte markers were detected in the serum-containing fibroblastic monocultured cells (**Figure 5.6D**, **H** and **L**).

The markers Thy-1, vimentin and α-SMA were used to positively stain for fibroblastic/myofibroblastic cell types. None of these markers were expressed in either the explant or transwell co-cultured cells (**Figure 5.6M**, **N**, **Q**, **R**, **U** and **V**). All markers were positively detected in the fibroblastic monocultures (**Figure 5P**, **T** and **X**). Interestingly, low levels of both Thy-1 and vimentin were detected in the conditioned media co-cultured cells (**Figure 5.6O** and **S**). α-SMA was exclusively detected in the fibroblast monocultured cells (**Figure 5.6T**).

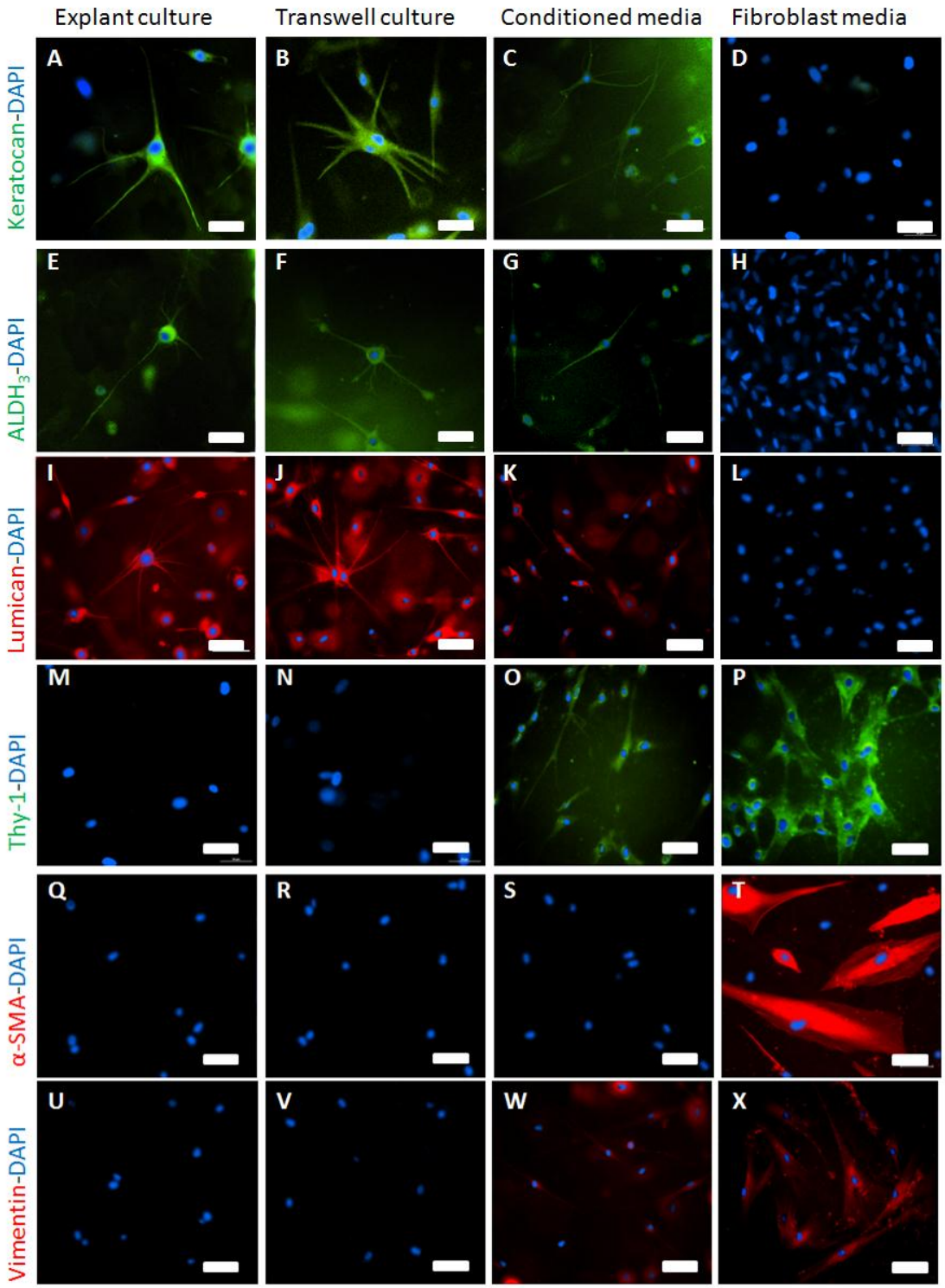

Figure 5.6: The effect of different co-culturing methods versus monoculture on keratocyte (A-L) and fibroblast (M-X) marker expression in AHDCS cells; representative fluorescently stained cells, imaged using fluorescent microscopy of collagen hydrogel constructs following 14 days culture; scale bar = 50 µm.

The morphology of the stromal cells cultured in fibroblastic monolcultures (**Figure 5.6P, T** and **X**) was significantly different to the cells cultured in co-culture. The cells co-cultured in explant and transwell cultures in particular were much smaller, with multiple dendritic processes (**Figure 5.6 A, B, E. F, I** and **J**) compared to the larger, spindle-shaped cells observed in the fibroblast monocultures. Although the stromal cells were smaller and more elongated in the conditioned co-cultured constructs (**Figure C, G, K** and **O**), they lacked the dendritic processes associated with the keratocyte morphology.

5.5.2. TGF-β1 regulation of AHDCS cell plasticity

5.5.2.1. Cell viability

AHDCS cell viability following TGF-β1 media supplementation following 14 days culture was monitored at day 21 (**Figure 5.7A-E**). The cell viability was high in all constructs with the exception of those cultured in CnT20 monoculture (**Figure 5.7D**). It was assumed that all these cells had died prior to supplementation with TGF-β1, as in the previous experiments.

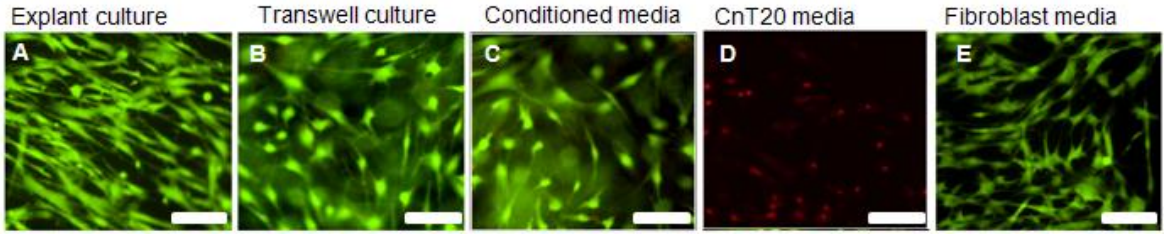

Figure 5.7: The effect of the addition of TGF-β1 following 14 days mono- and co-culturing on stromal cell viability at day 21; green indicates live cells, red indicates dead cells; scale bar = 100 μm.

AHDCS cell viability following TGF-β1 media supplementation at day 2 of the experiment was also measured at day 14 (**Figure 5.8A-E**). The cell viability was high in all constructs, including those cultured in CnT20 monoculture, suggesting that the supplementation aided cell viability.

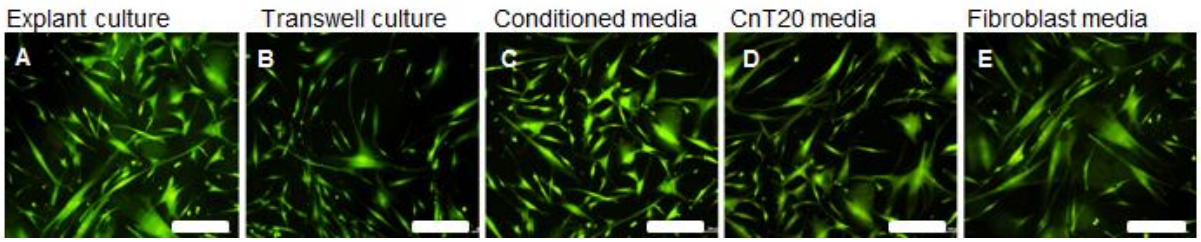

Figure 5.8: The effect of the addition of TGF-β1 to different mono- and co-cultures at day 2, stained at day 14; green indicates live cells, red indicates dead cells; scale bar = 100 μm.

5.5.2.2. Construct contraction

The effect of TGF-β1 media supplementation was investigated at two different time points. The addition of TGF-β1 to culture media at day 14 caused a significant decrease in the thickness of all constructs, with the exception of those cultured in CnT20 monoculture by day 15 (**Figure 5.9A**). Constructs co-cultured in explant, transwell and conditioned media conditions all showed a significant decrease in construct thickness compared to the constructs cultured in CnT20 monoculture from day 15-21 ($p \leq 0.001$ day 15-21 compared to explant and transwell cultures; $p \leq 0.01$ at day 15, $p \leq 0.05$ day 15, $p \leq 0.001$ days 17-21 compared to conditioned media constructs). Both the explant and transwell co-cultured constructs contracted significantly more than the co-cultured conditioned media constructs ($p \leq 0.001$ day 15-21). There was no significant difference in the contraction profiles of the explant and transwell co-cultured constructs. As in the initial co-culture experiments, the constructs cultured in serum-containing F media monoculture contracted significantly more than all other constructs ($p \leq 0.001$ days 2-21 inclusive). However, the addition of TGF-β1 did promote a sharp decrease in construct thickness at day 15.

The addition of TGF-β1 to the culture media at day 2 of culture caused all constructs in all experimental groups to contract significantly more (**Figure 5.9B**) than they did in the previous co-culture experiments whereby only the effect of culture conditions was investigated ($p \leq 0.01$ inclusive). Within the experimental group, the constructs cultured

under serum-containing F media still contracted significantly more than the CnT20 monoculture, explant, transwell and conditioned co-cultured constructs ($p \leq 0.001$ inclusive). There was no significant difference in the contractile behaviour of any of the co-cultured constructs.

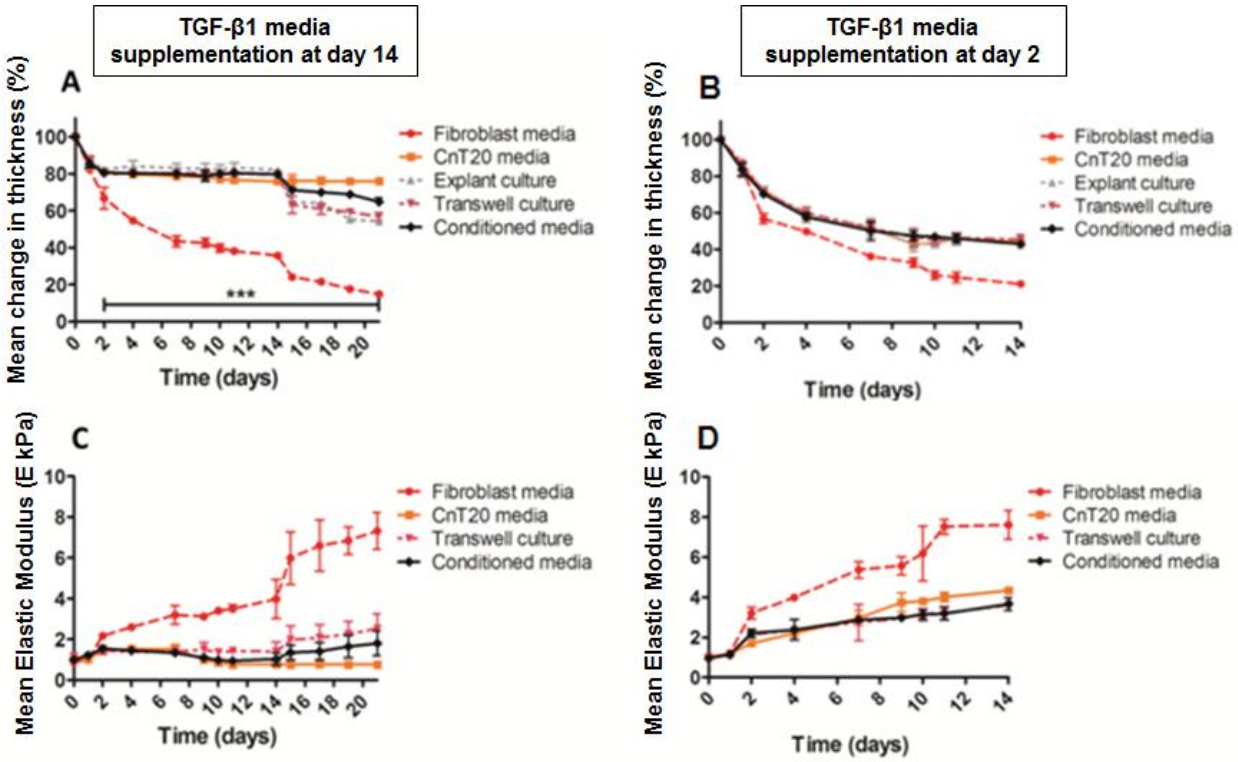

Figure 5.9: The effect of TGF-β1 supplementation following 14 (A and C) and 2 (B and D) days culture on the mean thickness change (A and B) of cellular constructs and the mean elastic modulus (C and D) of cellular constructs after culturing for 21 and 14 days respectively; n=6.

5.5.2.3. Modulus measurement

The addition of TGF-β1 to the culture media at day 14 promoted an increase in the modulus of all constructs in all culture conditions with the exception of those monocultured under CnT20 media (**Figure 5.9C**). The trend for all constructs cultured in monoculture under serum-containing F media to have significantly higher modulus compared to all the other constructs was repeated up to day 14. However, the addition of TGF-β1 at day 14 manifested as a sharp increase in the elastic modulus of the constructs at day 15. The addition of TGF-β1 at day 14 also caused an increase in the previously constant modulus of the co-cultured constructs in transwell and conditioned media. The modulus of the transwell co-cultured constructs was significantly higher than that of the CnT20 monocultured constructs ($p \leq 0.01$ days 15 and 17; $p \leq 0.001$ days 19 and 20). Constructs co-cultured under conditioned media were also significantly greater in modulus than those cultured in CnT20 monoculture by day 21 of the experiment ($p \leq 0.05$). Although the modulus of the co-cultured transwell constructs appeared higher than that of the conditioned media constructs from days 15-21, the difference was not significant.

The addition of TGF-β1 at day 2 caused an increase in the modulus of all constructs, including those cultured in CnT20 monoculture (**Figure 5.9D**). As seen in all previous experiments, the constructs cultured in fibroblast monoculture had a significantly higher modulus than all other cultured constructs in the experimental group ($p \leq 0.001$ day 4-14). However, there was no significant difference in the final modulus value of the fibroblast monocultured constructs following treatment with TGF-β1 at day 2, compared to those treated at day 14, as both had a peak modulus of approximately 7.5 kPa. There was no significant difference in the modulus of the remaining groups. However, the peak elastic modulus values were higher in all groups (CnT20 monoculture, transwell and conditioned co-cultures) when compared to the equivalent constructs in both the prior experiments

investigating the effect of different co-culturing methods and the investigation of TGF-β1 added at day 14 respectively.

5.5.2.4. Protein marker expression

Following 14 days culture using different culture methods and a further 7 days culture following TGF-β1 media supplementation to the culture media, all constructs were stained with a panel of keratocyte and fibroblastic markers (**Figure 5.10**). The constructs monocultured using CnT20 media alone were omitted from further analysis as they were deemed unsuitable for characterisation due to poor cell viability. The addition of TGF-β1 to the culture media at day 14 had a significant effect on the protein expression of all the co-cultured constructs and resulted in none of the keratocyte markers being expressed (**Figure 5.10A-C, E-G, I-K**). Conversely, all of the fibroblastic markers, including α-SMA were expressed in all constructs irrespective of the culturing conditions (**Figure 8M-X**).

The addition of TGF-β1 to the culture media at day 2 (**Figure 5.11)** mimicked these results. All constructs stained negative for the presence of any of the keratocyte markers (**Figure 5.11A-O**) and positive for all fibroblastic markers (**Figure 5.11P-δ)**. Additionally the constructs cultured in CnT20 media alone were able to be characterised in this instance. They too stained positive for all fibroblast markers (**Figure 5.11T, Y** and **δ)** and negative for all keratocyte markers (**Figure 5.1E, J** and **O)**.

TGF-β1 supplementation resulted in cells that were all large and fusiform in morphology, characteristic of fibroblastic/myofibroblastic cell types.

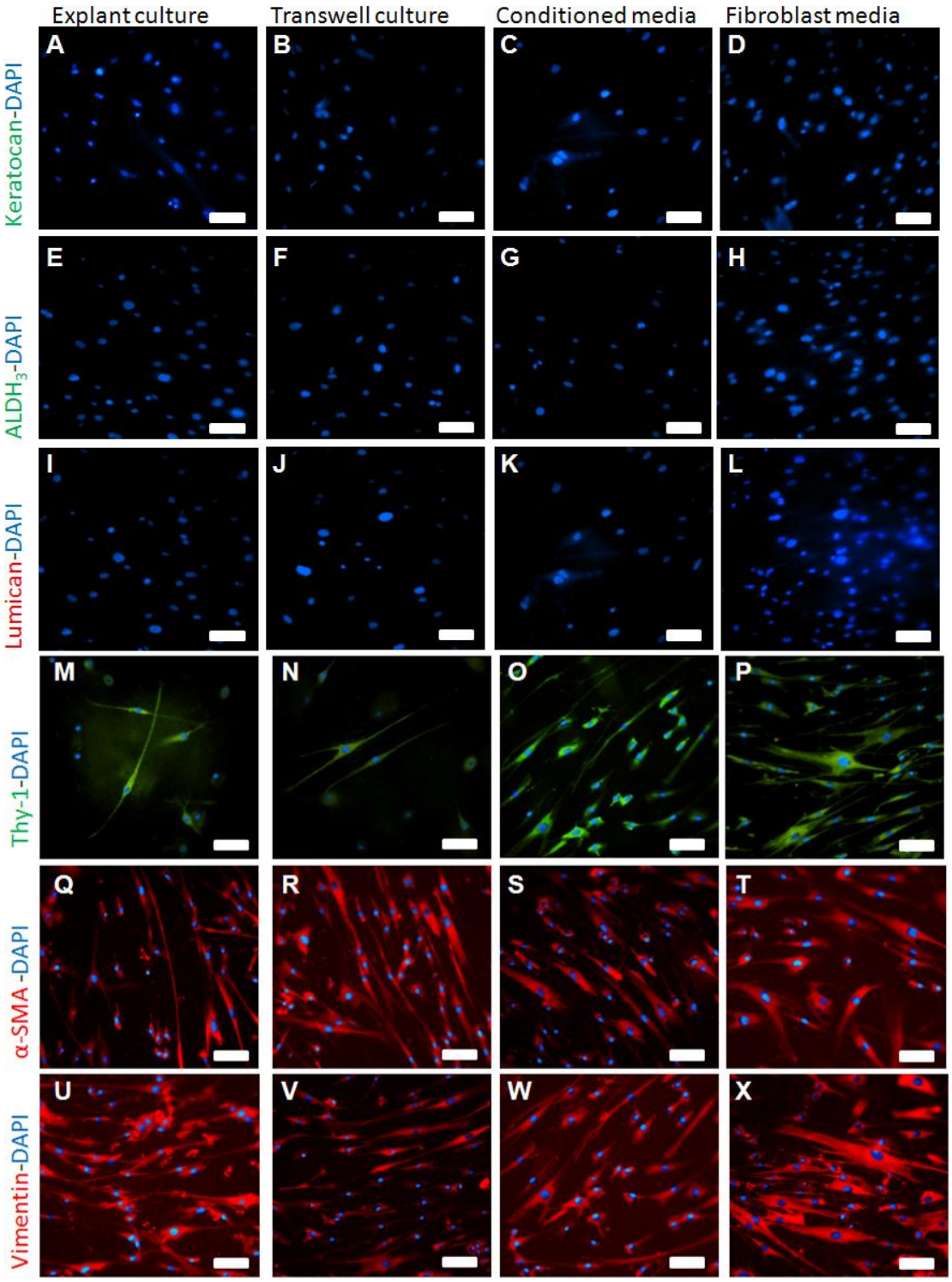

Figure 5.10: The effect of TGF-β1 addedd at day 14 to keratocyte and fibroblast marker expression in AHDCS cells; representative fluorescently stromal stained cells, imaged at 21 days; scale bar = 50 µm.

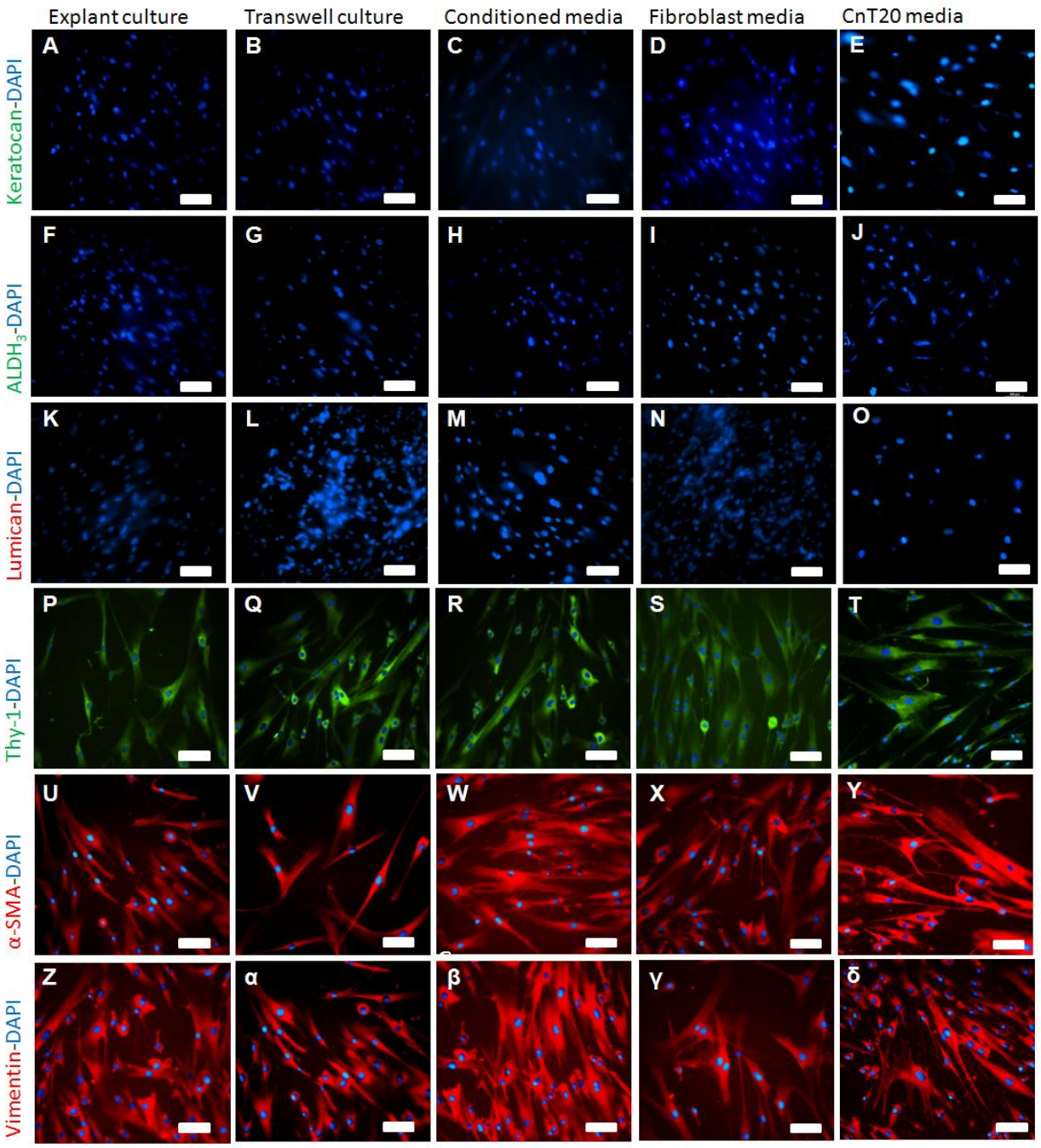

Figure 5.11: The effect of TGF-β1 added at day 2 to keratocyte and fibroblast marker expression in AHDCS cells; Representative fluorescently stained stromal cells, imaged at 14 days; scale bar = 50 µm.

5.5.3. Blocking of cellular interactions using wortmannin

5.5.3.1. Cell viability

AHDCS cell viability in response to the addition of wortmannin following 2 days culture was monitored at day 14 (**Figure 5.12**). The viability of all cells, with the exception of those monocultured in serum-containing F media (**Figure 5.12E**), following treatment with wortmannin was poor and all the cells stained dead.

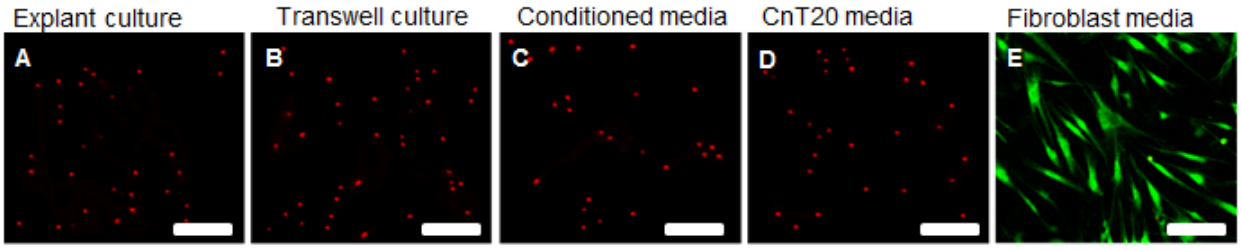

Figure 5.12: The effect of the addition of wortmannin to different mono- and co-cultures at day 2, stained at day 14; green indicates live cells, red indicates dead cells; scale bar = 100 µm.

Stromal cell viability in response to the addition of wortmannin to the culture media following 14 days mono- or co-culturing was also monitored at day 21. Cell viability remained high in all samples except for those cultured in CnT20 monoculture and conditioned media co-cultured cells, where all cells were dead.

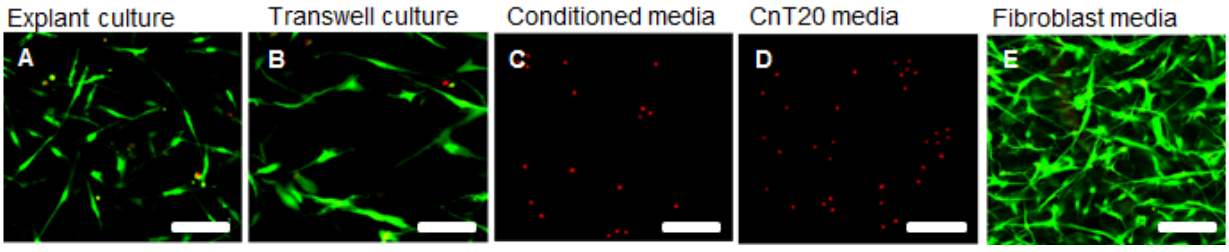

Figure 5.13: The effect of the addition of wortmannin following 14 days mono- and co-culturing on stromal cell viability at day 21; green indicates live cells, red indicates dead cells; scale bar = 100 µm.

5.5.3.2. Construct contraction

The addition of wortmannin at day 2 culture had no apparent effect on the contractile behaviour of any of the constructs when compared to the previous experiments investigating the effects of co-culturing alone. No significant differences were observed in the contraction profiles of any of the experimental groups for the duration of the experiment with the exception of constructs monocultured in serum-containing F media (**Figure 5.14A**); they contracted significantly more from day 2 onwards ($p \leq 0.001$ inclusive). The addition of wortmainnin to the culture media at day 14 had no apparent effect on the contraction profiles of any of the constructs (**Figure 5.14B**).

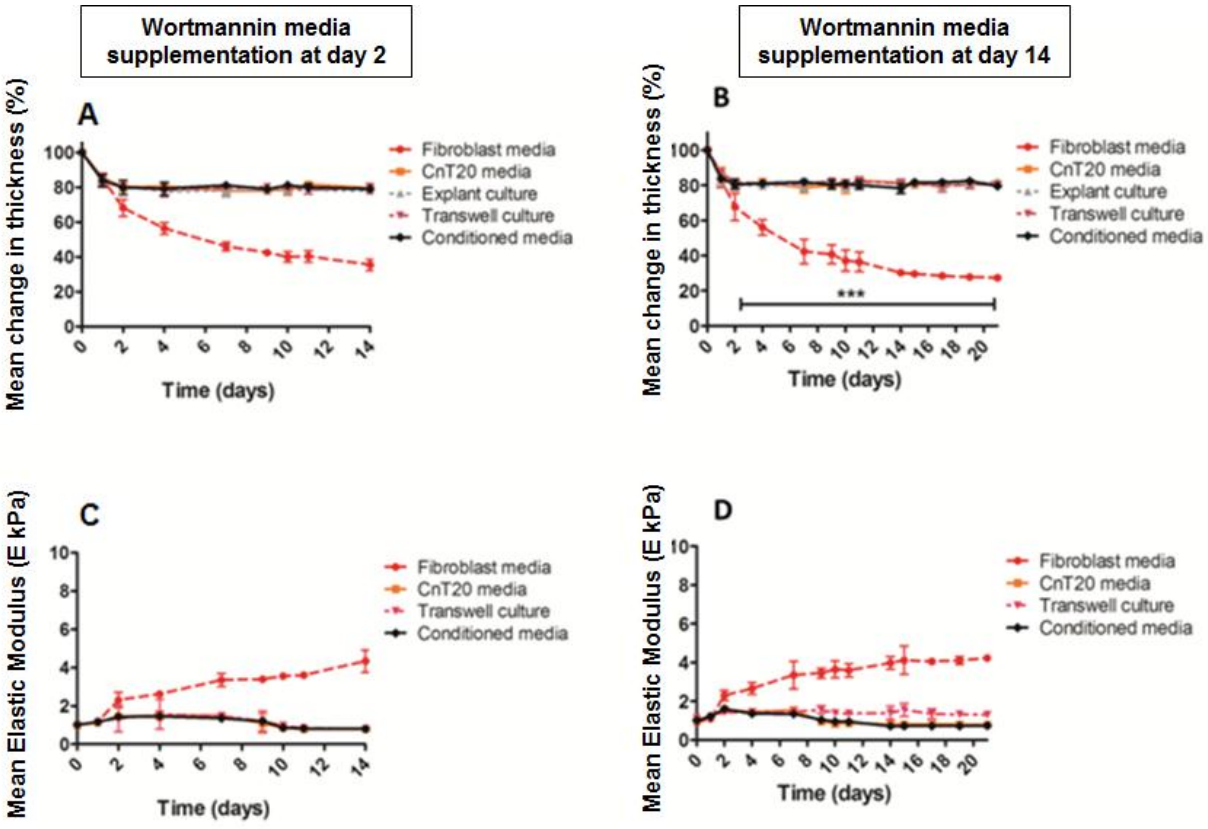

Figure 5.14: The effect of wortmannin supplementation following 2 (A and C) and 14 (B and D) days culture on the mean thickness change (A and B) of cellular constructs and the mean elastic modulus (C and D) of cellular constructs cultured for 14 and 21 days respectively; n=6.

5.5.3.3. Modulus measurement

The addition of wortmannin at either day 2 (**Figure 5.14C**) or day 14 (**Figure 5.14D**) did not have an obvious effect on the modulus of any of the constructs and the modulus measurements mimicked that described in the co-culture experiments.

5.5.3.4. Protein marker expression

Cell viability was so poor in all samples treated with wortmannin at day 2 that further characterisation was not possible. The only exception to this were the constructs cultured in serum-containing F media which stained positive for all fibroblastic markers as observed in all previous experiments (data not shown). The addition of wortmannin at day 14 did not appear to have any effect on the expression patterns of either explant (**Figure 5.14A, E, I, M, Q** and **U**) or transwell (**Figure 5.14B, J, N, R** and **V)** co-cultured cells or monocultured (**Figure 5.14D, H, L, P, T** and **X**) fibroblastic cells. All keratocyte markers showed positive expression; and all fibroblast markers showed negative expression in the explant and transwell cultures respectively; all keratocyte markers showed negative expression and all fibroblast markers showed positive expression in the fibroblast monocultures. The only culture that appeared to be influenced by the addition of wortmannin at day 14 was the conditioned media co-cultured cells in that the cultures lost their keratocyte marker expression (**Figure 5.14C, G** and **K)**. Fibroblastic marker expression was not affected and the results mimicked what had previously been observed in the co-culture studies (**Figure 5.14O, S** and **W**).

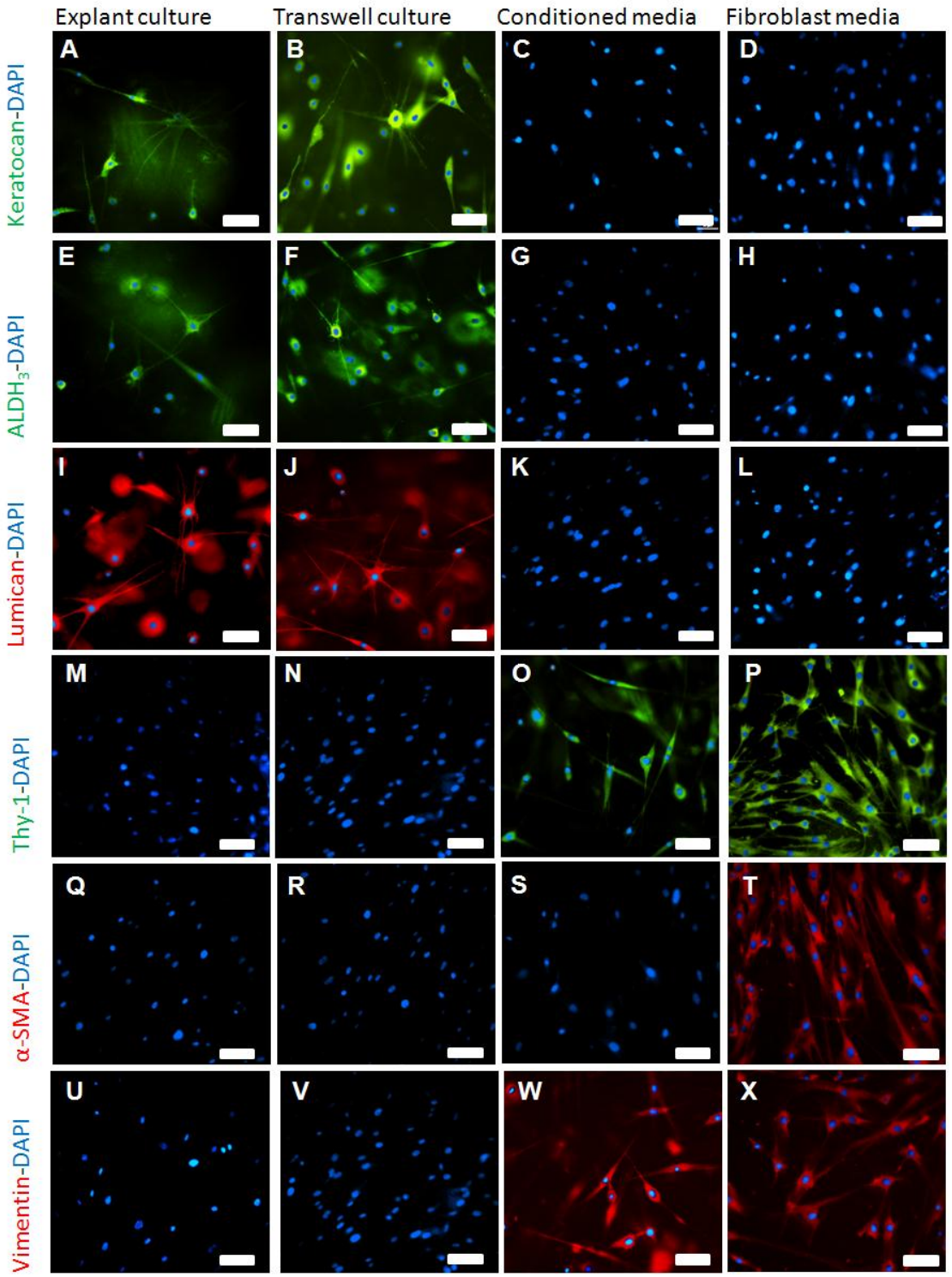

Figure 5.15: The effect of wortmannin added at day 14 to keratocyte and fibroblast marker expression in AHDCS cells; representative fluorescently stained cells, imaged at 21 days; scale bar = 50 µm.

5.6. Discussion

In the previous chapter, it has been demonstrated that cultured stromal cells can be partially restored to a keratocyte phenotype in a 3D collagen hydrogel structure by controlling the chemical and topographical environment. The work has been added to work by showing that the addition of an epithelial culture can further emphasise this effect *via* cell-cell interactions leading to a more complete de-differentiation of cells towards a keratocyte lineage. It has then then been demonstrated that media supplementation with TGF-β1 can supersede the epithelial-stromal crosstalk causing co-cultured stromal cells that are keratogenic in lineage to become re-activated and revert to an injury sub-type. Finally, it was shown that it is possible to inhibit the cell-cell interactions responsible for keratocyte differentiation *via* the use of wortmannin.

5.6.1. Co-culturing aids the restoration of the keratocyte phenotype to cultured stromal cells

Assessment of construct contraction in combination with elastic modulus measurements enabled us to non-destructively reveal the effects of stromal-epithelial interactions on the stromal cell differentiation process over prolonged culture periods. The ability to measure matrix contraction in 3D hydrogel constructs can inform us of the phenotype of cultured stromal cells in response to different culture conditions (Lakshman et al. 2010). Keratocytes are non-contractile, fibroblasts are moderately contractile and myofibroblasts are highly contractile (Jester, Jin 2003). When used in combination with modulus data the mechanical findings provided a more descriptive insight into what was happening at a cellular level within the constructs. For example, the lack of contraction and simultaneous reduction in modulus measurement that occurred in both the conditioned and CnT20 monocultured specimens can be linked to the drop in cell viability that occurred in both

samples, although to a lesser extent in the conditioned media co-cultured specimens. To discern whether contraction was due to cell viability or cell-cell interactions we assessed cell viability in all constructs, we have demonstrated that the lack of contraction and constant modulus measurement in the transwell co-cultured constructs coincided with quiescent, but viable cell types. However, such global assessments may be limited as they do not supply information on the change in cell morphology, cytoskeletal organisation (Lakshman et al. 2010) and biological function such as protein expression. Thus we have corroborated our mechanical data with protein phenotypical analysis in order to determine morphological and protein expression changes.

CK3 is often used as a specific marker for corneal epithelial cells (Mi et al. 2010, Pang et al. 2010, Lu et al. 2001) and immunofluorescent staining demonstrated that CK3 was expressed in all epithelial cultures (TCP, transwell and in direct explant cultures) and additionally that all epithelial cultures displayed the typical characteristic cobblestone morphology. Direct epithelial-stromal interactions are known to trigger epithelial cell differentiation, which can lead to higher expression. However, there was no apparent significant difference in CK3 expression observed in any of the epithelial cultures to confirm that this is the case in our investigation. More sensitive testing methods such as quantitative-PCR may be required to detect subtle differences in expression.

Vimentin has previously been used as a marker for injured epithelial cells (Nakamura et al. 2002). Injured epithelial cells express vimentin and secrete soluble factors that promote myodifferentiation of fibroblasts (Nakamura et al. 2002). As vimentin was not detected in any of the epithelial cultures it was assumed that none of the epithelial cultured were “injured” and that they were expressing the cytokines to the adjacent stromal cells to initiate differentiation towards a keratogenic, not myofibroblastic lineage. However, a limitation of this study was that epithelial cell expression was only monitored at day 14. As

vimentin expression has been shown to alter, dependent upon the stage of wound healing the cornea is in (Chaurasia et al. 2009); a quantitative investigation of epithelial protein analysis at multiple time points, i.e. not just at day 14 would be required to more definitely determine epithelial cell behaviour and response.

Keratocan and lumican are key keratan sulphate proteoglycans expressed in abundance by healthy keratocytes (Jester, Jin 2003, Musselmann et al. 2005). Both are fundamental to mediating corneal structure and transparency and were utilised in this study along with $ALDH_3$ as positive markers for keratocyte phenotype. The lack of keratocan, lumican and $ALDH_3$ expression in all constructs cultured in serum-containing F media confirm previous studies (Pei et al. 2006) findings whereby their expression is not detected in human fibroblasts, myofibroblasts, nor in keratocyte repair subtypes *in situ* or during culture in serum.

Thy-1 is a cell-surface antigen whose function has yet to be fully determined. It is thought to participate in cell-cell and cell-matrix interactions, during inflammation and fibrotic responses. Expression of the cell surface proteins Thy-1 and vimentin have both previously been used to demonstrate that corneal keratocytes have transformed into a repair phenotype (Pang et al. 2010). This was confirmed in our results by the fact that the cells cultured in serum-containing F media were Thy-1 and vimentin positive. The absence of Thy-1 and vimentin staining in the explant and transwell cultures implies that we were successfully able to induce the cultured stromal cells to de-differentiate towards the phenotype of a healthy, uninjured keratocyte. Interestingly, the conditioned media studies expressed both Thy-1 and vimentin as well as all the keratocyte markers.

α-SMA was not detected in any of the serum-free co-cultured samples, however it was detected in the serum-containing fibroblastic monocultured samples which is in agreement with previous studies performed by Jester *et. al*. (1999). However, not all of the cells

stained positive for α-SMA, suggesting that there was a mixed population of the cells within the samples that had both fibroblastic and myofibroblastic lineages.

Vimentin is an intermediate filament protein (Lazarides, 1980) that supports and anchors the position of organelles in the cytosol. Vimentin has previously been used as a marker to help distinguish between corneal stromal cell phenotypes in normal and wounded corneas *in vitro* (Ishizaki et al. 1993, Espana et al. 2005, Chauraisa et al. 2009, Pang et al. 2010). Vimentin expression was highest in fibroblastic monocultured constructs and often appeared alongside α-SMA, which is in agreement with previous studies, where it has been shown that vimentin expression is highest in wounded corneas when compared to non-wounded controls (Chauraisa et al. 2009); and had been suggested to be a precursor to the myofibroblast cell phenotype (Ishizaki et al. 1993).

The immunofluorescent imaging also highlighted significant changes to the morphology of corneal stromal cells when exposed to different culture conditions. The cells cultured under serum-containing F media or in the presence of TGF-β1 were distinctly lager and fusiform in morphology compared to all other specimens. Although the cells cultured in conditioned media co-cultures were clearly different to these cells in that they were smaller and more elongated; it was the cells cultured in explant and transwell co-cultures that that displayed the greatest change in cell morphology. The cells in these constructs were not only smaller, but also had multiple dendritic processes, characteristic of *in vivo* or freshly isolated keratocytes.

Explant and transwell co-culturing of stromal cells were deemed to be the most successful methods of initiating stromal cell differentiation in comparison to the use of conditioned media or the use of serum-free CnT20 media alone. The use of transwell co-cultures is well documented and has been previously used to determine whether injured epithelial cells are capable of stimulating stromal cell myodifferentiation (Nakamura et al.

2002). The study demonstrated that injured corneal epithelial cells secrete soluble factors capable of instigating collagen gel contraction, proliferation and myodifferentiation of corneal stromal cells, thus the injured differentiating epithelial cells are able to influence fibroblast behaviour. It can be surmised that uninjured epithelial cells can likewise secrete soluble factors which can potentially influence fibroblasts to revert to their pre-injury phenotype, i.e. a keratocyte.

Epithelial conditioned culture media has also been previously investigated with regards to stromal cell differentiation (Hibino et al. 1998). These results demonstrated that the addition of epithelial conditioned media accelerated construct contraction, which is contradictory to the findings in this study. However, it should be noted that the rabbit "keratocytes" used in the study were of high passage number (P8) and were cultured in up to 12.5% foetal calf serum (FCS) and that the epithelial cells used were also cultured in the presence of 15% FCS. Thus the stromal cells were likely to be of a fibroblast/myofibroblast phenotype. This was confirmed by the fact that the constructs cultured in serum-free media did not contract. The use of serum in these studies may have been causing the stromal cells to initiate a reparative/fibrotic healing approach as opposed to a regenerative approach that we were aiming for in our studies.

5.6.2. Epithelial cells mediate through soluble factors

Under normal, disease and injury free conditions, cellular tissue maintenance and growth is reliant upon the timely interactions of many factors including hormonal, pancrine, vascular and cellular interactions (Dayhaw-Barker 1995a) with epithelial-stromal interactions being pivotal determinants of corneal function *via* highly coordinated mechanisms which maintain normal development, homeostasis and wound healing response (Wilson et al. 1999). Specifically, the cellular communication aids in the

restoration of activated keratocytes (fibroblasts) back to a quiescent keratocyte phenotype following injury, thus restoring tissue transparency which avoids excessive scarring that is detrimental to vision. It is believed that the cells communicate *via* the release of soluble factors such as proteoglycans, glycoaminoproteins and growth factors in a bidirectional manner. Using this principal, we aimed to more closely mimic the *in vivo* conditions *via* the inclusion of different epithelial culture conditions to a previously described collagen hydrogel stromal layer model (Wilson et al. 2012a, Ahearne et al. 2010a) *via* the use of explant, transwell and conditioned media co-cultures respectively.

The restoration of the inactivated keratocyte phenotype, as determined by protein marker expression and cell morphology, was greater in the transwell and explant co-cultured stromal cells when compared to the conditioned media constructs. The use of a low concentration of conditioned media suggests that although the soluble factors collected and included in the conditioned media have the ability to partially inactivate or de-differentiate the activated stromal cells to a keratocyte phenotype, the differentiation/inactivation is incomplete. Furthermore, the fact those stromal cells in conditioned media cultures expressed both keratocyte and fibroblastic markers suggests that the stromal cells may undergo a transient "transitional state" whereby the stromal cells have characteristics of both the activated and non-activated cell phenotypes. Although this would require further characterisation, it is not impractical to assume that there are more than three stromal cell phenotypes. Jester *et al.* (2003) have previously suggested that they may be more than one type of fibroblastic stromal cell phenotype that participate in wound healing type I and type II. Type I enhance keratan sulphate proteoglycan expression and down regulate α-SMA expression, and may be involved in non-fibroblastic wound healing responses, so no loss of tissue transparency occurs. Type II (also known as protomyofibroblasts) decrease keratan sulphate expression and participate in autocrine

TGF-β induced myofibroblastic differentiation that cause fibrotic healing responses associated with tissue scarring and opacity (Jester, Jin 2003). Likewise, a similar phenomenon was demonstrated in the previous chapter where it was demonstrated that it is possible to partially de-differentiate, or inactivate serum-activated stromal cells towards a quiescent keratocyte phenotype, whilst still retaining some of their fibroblastic tendencies.

In the explant cultures the different cell types grew and existed in two distinct layers on and within the construct; with the stromal cells encapsulated throughout the construct, and the epithelial cells forming a separate cell sheet on top of the hydrogel surface. This, along with the corresponding data from the transwell cultures whereby the insert dishes comprised of a membrane that was permeable to soluble factors, but not to the cells, demonstrated that change in cell behaviour and protein expression in both explant and transwell cultures was due to stromal cell differentiation occurring, and not cell migration from the epithelial culture down into the stromal culture.

5.6.3. Epithelial-stromal cytokine mediated responses may be dose dependent

The differentiation of the AHDCS cells in conditioned media co-culture was not as complete as seen in the explant and transwell co-cultured constructs. A possible explanation for this is that the growth factors and cytokines secreted by the epithelial cells regulate the function of keratocytes and *vice versa* (Nakamura et al. 2002, Suzuki et al. 2003) and that the signalling is not mutually exclusive, i.e. the action of one may depend or mediate the expression of the other (Agrawal, Tsai 2003) *via* dynamic feedback loops. Thus in order for keratocyte differentiation to be successful (or more complete) both cell types need to present in the culture system, although not necessarily in direct contact.

Another possible explanation was that the "dose" or concentration of soluble factors within the conditioned media used in our experiments was too low to initiate a more

complete restoration of the keratocyte phenotype. We calculated that the stromal cells in the explant and transwell cultures were potentially subject to twice as many soluble factors compared to the stromal cells in the conditioned media co-cultures. To do this we took into account the ratios of confluent epithelial cells, to the surface area that they were grown on, in comparison to the volume of media used. For example, the conditioned media was collected from confluent epithelial cells grown on the surface on a T25 cm^2 culture flask. Cell counts revealed that this equates to approximately 1 million cells or 400,000 cells per cm^2. 5 ml of media was collected per confluent flask, which equates 200,000 cells worth of soluble factors per ml. However, the collected media was diluted and only 10% of the collected media was used in the conditioned media, so the amount of soluble factors present in the media was further diluted to approximately 20,000 cells worth of soluble factors per ml. In comparison, the surface area of the culture insert dishes was 4.2 cm^2 and cell counts revealed that approximately 160,000 epithelial cells were on a confluent insert dish. 3 ml of media was used to culture the transwell cultures, which would have diluted the soluble factors to approximately 50,000 cells worth of soluble factors per ml. The surface area of the hydrogel constructs was approximately 3.1 cm^2 and epithelial cell counts revealed that approximately 125,000 cells grew on the surface of a confluent hydrogel construct. As in the transwell cultures, 3 ml of culture media was used which would have diluted the epithelial soluble factors to approximately 40,000 cells worth of soluble factors per ml.

The same volume of media was used in all samples and the same numbers of stromal cells were seeded into all hydrogel constructs, thus in order to initiate the same differentiation response, the total volume of soluble factors should be equivalent. This helps not only to explain why the differentiation of the stromal cells in the conditioned media samples was not as complete but also may explain why the blocking efficiency of

wortmannin was different in the conditioned media specimens when supplementation was introduced at day 14. Increasing the concentration of the conditioned media could therefore increase and improve the differentiation of the stromal cells and restoration of the keratocyte phenotype as more of soluble factors responsible for the differentiation would be present. In order to determine this for sure, a thorough proteomic assay using spectroscopic techniques capable of analysing specific cytokine, growth factor and protein release profiles would have to be performed.

5.6.4. Stromal cells retain their plasticity

Since native keratocytes originate from a population of cranial neural crest cells (West-Mays, Dwivedi 2006) and are capable of regenerative healing it has been hypothesised that they retain stem cell-like properties. We have shown that despite prolonged culture periods *in vitro* that corneal stromal cells are capable of retaining their plasticity. In fact they are capable of numerous differentiation cycles. By adopting different cell-based co-culture approaches we have established that it is possible to revert cultured corneal stromal cells that are fibroblastic in phenotype towards a native uninjured (keratocyte) cell type in terms of cell behaviour and biological properties. We have then demonstrated that the cells can differentiate again following exposure to exogenous TGF-β1.

TGF-β1 is a known chemotactic agent and mitogen for fibroblasts secreted by almost all nucleated cells (Imanish et al. 2000) which initiates wound contraction *in vivo* (Nakamura et al. 2002, Kim et al. 2012). TGF-β1 induces fibroblastic and myofibroblastic differentiation by stimulating cell stratification and matrix component production (Karamichos et al. 2011), whilst increasing fibrotic protein marker expression (Karamichos et al. 2011) such as α-SMA, which was confirmed by immunohistochemical data. The action of TGF-β1 in this study was very potent in that it blocked epithelial cell

proliferation whilst stimulating the proliferation and differentiation of the stromal cells irrespective as to whether it was added at day 14 or day 2 to the culture media. When added at day 14 of culture TGF-β1 stimulation superseded the effect that co-culturing had on the stromal cell differentiation and almost immediately caused the quiescent, non-contractile cells which had previously shown positive expression for keratocan, $ALDH_3$ and lumican to become highly contractile and fibroblastic in their behaviour and genotype. In fact, all keratocyte marker expression was lost and replaced by positive expression of Thy-1, α-SMA and vimentin. When TGF-β1 was used to supplement the media at day 2, the stromal cells never differentiated towards a keratogenic lineage; the growth factor prevented epithelial proliferation from occurring in the first place, thus thwarting epithelial-stromal interactions from occurring.

Our findings suggest that corneal stromal cells are able to differentiate numerous times whilst in culture and that their transition and response is heavily dependent upon the niche environment. Since the corneal is avascular, it is the overlying epithelium that is pivotal to stromal cell differentiation. It is therefore assumed that it is possible for keratocyte differentiation to occur once TGF-β1 supplementation is removed and the "epithelium" has been restored.

5.6.5. Epithelial-stromal interactions can be inhibited

Having demonstrated that it is possible to differentiate cultured stromal cells that are fibroblastic in phenotype towards a keratogenic lineage *via* the introduction of epithelial co-cultures, we then investigated as to whether we could block these interactions and if it was possible to detect a difference in the mechanical properties of the resulting constructs. Using wortmannin, a known inhibitor of epithelial-stromal interactions, we have demonstrated that epithelial restoration of the keratocyte cell phenotype can be blocked. Although blocking agents such as wortmannin may have multiple effects on cell signalling

pathways, the inhibitory effect of wortmannin with regards to epithelial activities has been demonstrated in numerous studies (Zhang et al. 1999, Chandrasekher, Bazan 1999, Lyu et al. 2006, Islam, Akhtar 2001, Kakazu et al. 2004). Wortmannin works by inhibiting phosphoinositide 3 kinases (PI3Ks). PI3Ks are a family of enzymes that are involved in immune response mechanisms (Zhang, Liou et al. 1999) including epithelial growth, proliferation and differentiation by mediating the interactions between growth factors with tyrosin kinase receptors including PI3K (Chandrasekher, Bazan 1999, Islam, Akhtar 2001). *In vivo* this manifests as delayed corneal wound repair and reduced epithelial proliferation and increased epithelial cell apoptosis *in vitro* (Islam, Akhtar 2001, Kakazu et al. 2004). Wortmannin effectively blocks epithelial proliferation and the release of important growth factors including HGF and EGF (Islam, Akhtar 2001, Kakazu et al. 2004) and cytokines which ultimately effects keratocyte growth and behaviour, dependent upon what stage of wound healing the cells are in. In agreement with these studies, it was observed (data not shown) that epithelial outgrowth and proliferation following treatment with wortmannin at day 2 was significantly less in comparison to untreated specimens. It may also be possible that wortmannin exposure alone has an effect on keratocyte differentiation of *in vitro* cultured stromal cells. However, to our knowledge, no-one has investigated this yet.

Following supplementation with wortmannin at day 2, all constructs, with the exception of those cultured in serum-containing F media retained a constant construct thickness, a phenomena which was previously linked to quiescent cell behaviour, either caused by a keratogenic differentiation or cell death. In this instance the quiescence was linked to stromal cell death, confirmed by live-dead staining. *In vivo*, when such a loss of communication occurs between the epithelial cells and keratocytes, whether the cause be injury, surgery or disease a “re-expression” of usually dormant genes, proteins and growth factors is initiated (Dayhaw-Barker 1995a). This leads to an activation and differentiation

of the stromal cells, causing them to become fibroblastic, with histological changes to the keratocytes occurring within 30 min of the original loss (Dayhaw-Barker 1995b). This activation would also cause changes to the surrounding ECM, due to cellular contraction and remodelling. However, this was not the case in this particular study, as no changes to the construct thickness due to cellular contraction occurred. A possible explanation for this is that in blocking the release of cellular communication and soluble cytokines, the stromal cells were effectively in an environment comparable to CnT20 monoculture. As deduced from the co-culture experiments CnT20 media alone was not sufficient in sustaining stromal cell growth for prolonged culture periods. CnT20 media alone can only sustain stromal cell growth for short time periods of up to 7 days. Thus cell death occurred in all constructs except those in serum-containing F media.

Another possible explanation is that the dose (100 nM) of wortmannin used was having a toxic effect on the stromal cell cultures. The dose was chosen based upon previous work by Chandrasekher and Bazan (1999) and Kakazu et al. (2004), which predominantly investigated the effects of *in vivo* re-epithelisation following injury and the involvement of growth factors that prevent apoptosis following injury respectively. However, it should be noted that neither study was focussed upon the stromal cell activity and both studies were based on the investigation of rabbit corneas, where it was found that epithelisation was reduced by approximately 50% in the presence of wortmannin (Chandrasekher and Bazan, 1999). A limitation of the work carried out in this chapter is that only a single dose of wortmannin was investigated. In order to determine if the wortmannin was in fact having a toxic effect on the stromal cells a more thorough examination whereby different (reduced) doses were investigated would have to be carried out.

Interestingly, when wortmannin was used to supplement the culture media following 14 days prior co-culturing, the results were slightly different. The transwell and explant co-

cultures and CnT20 and fibroblast media monocultures did not appear to be affected, but the conditioned media co-cultured samples were. Immunohistochemical analysis revealed that the addition of wortmannin caused a loss in expression of all keratocyte markers. It is believed that wortmannin did not have any effect on the explant and transwell co-cultured constructs as they had already effectively epithelialised and differentiated; perhaps if the culture period had been extended then a fibroblastic differentiation would have been observed. The monocultured constructs were not affected as there was no cellular interaction(s) occurring. As previously mentioned, the cell differentiation in conditioned media co-cultures was not as complete as when epithelial cells themselves were present in the cultures. Bi-directional, reciprocal interactions were not occurring as there was effectively only one cell type present in the culture; thus these cells were more "vulnerable" to exogenous factors. The "dose" of growth factors present in the conditioned media was not high enough to cause complete keratogenic differentiation; nor was it high enough to overcome the effect of wortmannin.

5.7. Conclusion

Differentiation of myofibroblasts and fibroblasts back to the keratocyte has yet to be clearly established and still remains an important question that we have attempted to address in this investigation. Using different co-culturing techniques we have demonstrated that it is possible to revert cultured corneal stromal cells that are fibroblastic in lineage towards the native uninjured cell type in terms of cell behaviour and biological properties. Although the two cell types to not have to be in direct contact, they do have to be present in the culture system to have an optimal effect. This method of activating corneal keratocytes into their fibroblastic lineage and then being able to differentiate them back to the keratocyte lineage is vital to corneal tissue engineering with its benefits being

threefold; firstly, it allows for sufficient numbers of corneal stromal cells to be grown up quickly and easily in serum-containing media; secondly the ability to differentiate the expanded activated cells back to a keratocyte linage is important in aiding our understanding of corneal wound healing mechanisms and the importance of the cell interactions during these processes; and finally it allows us to engineer corneal tissues that more closely mimic the native cornea, with cells that are in a healthy uninjured state which may have the potential to act as an important tool in with regards to toxicity testing of drugs and irritants which could in turn improve the development of new and improved ocular drugs to treat corneal disease and/or injury.

It was also shown that cultured stromal cells retain their plasticity *in vitro*. AHDCS cells that were fibroblastic in phenotype were successfully reverted to a keratocyte lineage and then back again *via* TGF-β1 media supplementation. This manifested as an initial reduction in thickness of the constructs, followed by a period of constant thickness, followed by a decrease in construct thickness. These macroscopic changes coincided with the removal of serum and the addition of TGF-β1 to the culture media respectively.

It was then revealed that the epithelial-stromal interactions can be blocked *via* the use of wortmannin inhibition. However, our findings suggested that the blocking of the soluble factors that are so crucial to keratocyte restoration may be time dependent. For example, wortmannin had no apparent effect on explant and transwell cultures when added at day 14, whereby epithelialisation and keratocyte differentiation was complete. A greater understanding of stromal-epithelial interactions and what mediates them offers great pharmacological potential in the regulation of corneal wound healing, with the potential to treat corneal diseases and injury whereby such interactions are vital (Wilson et al. 1999). As the different healing mechanisms, contributing factors and their potency become

known, we are able to utilise this information in order to accelerate and enhance the wound healing process (Dayhaw-Barker 1995b).

6. A microscopic and macroscopic study of ageing collagen on its molecular structure, mechanical properties, and cellular response

6.1. Abstract

Collagen is an important component of the extracellular matrix (ECM) and plays a pivotal role in individual tissue function in mammals. Collagen type I has been used as a scaffold in this project intensively. During ageing, the structure of collagen changes, often detrimentally affecting the tissues' biophysical and biomechanical properties due to an accumulation of advanced glycation end-products (AGEs). To date, how the microstructural changes in collagen influence the macroscopic properties has not been reported. In this chapter we conducted a parallel study of microscopic and macroscopic properties of reconstituted hydrogel constructs manufactured using different aged collagens extracted from the rat tail tendons ranging in age from 2 days to 2 years. We examined the effect on the biomenchanical properties of the reconstituted hydrogel constructs in terms of the construct gelation rates, viscosity measurements, contraction capacity, modulus measurement, AGEs content and cellular behaviour when constructs were seeded with corneal stromal cells. In addition, hydrogel constructs were also manufactured under a 12 Telsa magnetic field and the fibril formation was investigated. A non-destructive indentation technique and optical coherence tomography (OCT) were used to determine the elastic modulus and dimensional changes respectively under prolonged culture periods with and without cell presence. It has been revealed that in comparison to the younger specimens, the older collagens exhibit higher viscosity, faster gelation rates and higher AGEs fluorescence. Young collagens were able to form highly aligned fibrils when exposed to high external magnetic fields, while older collagens did not. The collagen constructs from the youngest animals demonstrated a higher elastic modulus and increased contraction in comparison to the older collagen. From these results we concluded that

ageing changes the collagen monomer structure, which affects the fibrillogenesis process, the architecture of the collagen fibres, the global network and the macroscopic properties of the resulting reconstituted hydrogel constructs, which we believe is linked to AGEs accumulation.

The work carried out in this chapter was done in collaboration with Université de Reims Champagne, France and The High Magnetic Field Laboratory, Grenoble, France with the assistance of Marie Guilbert, James Torbet, Pierre Jeansson and Ganesh D. Sockalingum and is based upon the proceedings article entitled "**The effect of collagen ageing on its structure and cellular behaviour**" which has been successfully published in Proc. SPIE 8222, Dynamics and Fluctuations in Biomedical Photonics IX, 822210, doi: 10.117/12.908749. This work has also been successfully published as an original research article entitled "**A microscopic and macroscopic study of aging collagen on its molecular structure, mechanical properties, and cellular response**" in FASEB J, doi: 10.1096/fj.13-227579.

6.2. Introduction

Collagen is a key life-long structural protein that is the most prevalent protein in the body (Isobe et al. 2012, Guo, Kaufman 2007, Newman et al. 1997, Mays et al. 1991, Mocan et al. 2011) constituting to approximately one-third of the total body mass (Jiang, Liao et al. 2000). Collagens are made up of 3 polypeptide subunits referred to as α-chains that assemble into a triple helix structure (Guo, Kaufman 2007), with cross-links between and within the triple helices (Willems et al. 2011) (**Figure 6.1**). There are more than 20 types of collagen in animal tissues which vary in the length (Guo, Kaufman 2007), with collagen type-I being the most abundant form. The collagens are capable of self-assembly into large-scale structures under physiological conditions. Networks of type I collagen can

also be formed *in vitro* (Newman et al. 1997). Such structures are often highly tensile in strength (Guo, Kaufman 2007, Bailey, Paul 1999) although have little strength in flexion or torsion (Bailey, Paul 1999). Tissue specific architecture is often pivotal to tissue function and the ability of a tissue to sustain an applied load (Bailey, Paul 1999). The primary role of the collagen networks is to provide a supportive extracellular framework for cells, allowing for adhesion, aggregation, cell attachment, morphogenesis and development (Mays et al. 1991). Detrimental changes to biochemical and biomechanical interactions are all a result, amongst other causes, of the ageing process (Schulze et al. 2012) and consequently collagen loses flexibility, enzymatic digestibility (Mikulikova et al. 2007) and becomes less deformable (Bruel, Oxlund 1996, Singh et al. 2002). *In vivo* this manifests as a decline in anatomical integrity and function often affecting multiple organ systems resulting in increased pathology and a higher risk of death (Semba et al. 2010); or *in vitro* as a decline in biomechanical properties (Wilson et al. 2012b). Tissues that are most vulnerable to such changes include the kidney, capillary basement membranes, cardiovascular and pulmonary systems (Bailey 2002). Alterations to collagen biosynthesis have been implicated in a number of disease states including atherosclerosis, pulmonary fibrosis, rheumatoid arthritis and Ehlers-Donlas syndrome (Mays et al. 1991). Collagen molecules have active reactive groups on their side chains and any chemical alterations with these amino groups will have an effect on the triple helix properties and so on tissue and organ function (Mikulikova et al. 2007, Bruel, Oxlund 1996, Lingelbach et al. 2000). Such changes are often associated with inter- and intra-molecular cross-linking of the peptides. Cross-linking can occur enzymatically (lysyloxidase mediated (Bruel, Oxlund 1996)) or non-enzymatically. Enzymatic processes usually occur during developmental and maturation stages of the collagen; whereas non-enzymatic changes occur due to the ageing process and are damaging to the protein and associated biomolecules (Mikulikova et al.

2007). Frequently non-enzymatic changes are a result of the glycation process caused by the accumulation of advanced glycation end-products (AGEs) (Reiser 1991).

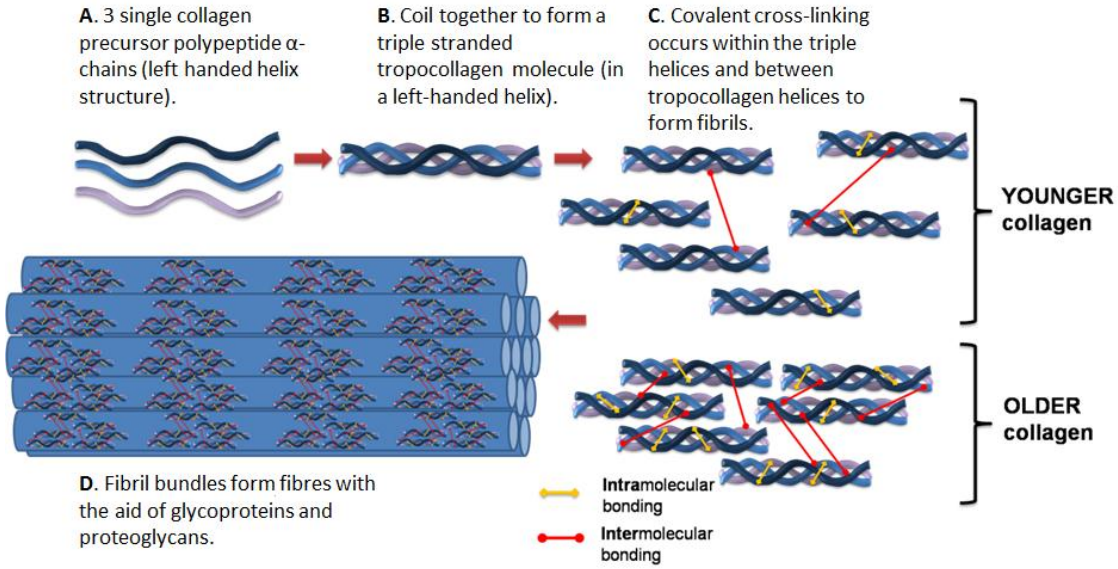

Figure 6.1: A schematic diagram of collagen structure and assembly; accumulation of AGEs with ageing causes an increase in intra- and intermolecular collagen cross-linking which results in an increase in collagen density.

AGEs are a complex and heterogeneous group of compounds whose presence have been shown to increase in tissues with chronological and physiological ageing (Singh et al. 2002, Semba et al. 2010). AGEs formation causes proteins to cross-link which is the underlying process by which they cause damage. AGEs accumulation in collagen is the result of a reaction of the reducing oxo-group of sugars with a free ε-amino group of the protein (amino group of lysine or arginine) (Bruel, Oxlund 1996) through a series of reactions to form a Schiff base (Semba et al. 2010). The initial Schiff base (a compound with a functional group containing a carbon-nitrogen double bond, with nitrogen connected to an aryl or alkyl group and resulting Amadori products undergo an irreversible series of reactions resulting in cross-linked structures (Mikulikova et al. 2007). The phenomenon was first described by Lois Camille Maillard in 1912 in relation to food studies (Semba et

al. 2010). However, it was much later that these Maillard reactions were shown to occur slowly *in vivo* during glycation and that they controlled tissue modifications that occur during ageing (Semba et al. 2010). Advanced glycation occurs over a period of weeks (Singh et al. 2002) thus affecting long-life proteins such as collagen, disrupting collagen fibril arrangement and spatial architecture during cross-linking. Cross-linking interferes in cell-matrix interactions affecting adhesion and cell spreading, impeding function and decreasing tissue remodelling capabilities (Singh, Barden et al. 2002). AGEs are known to increase oxidative stress and inflammation in tissues *via* binding with the receptor for advanced glycation end-products (RAGE). RAGE is a multi-ligand member of the immunoglobulin superfamily widely expressed in tissues (Semba et al. 2010). Sustained RAGE formation results in chronic inflammation and tissue damage. The binding of AGEs with RAGEs induces the expression of transforming growth factor beta-1 (TGF-β1). TGF-β1 is a known mediator of fibrogenesis (Nakamura et al. 2002), associated with inflammatory response, fibroblast/myofibroblast cell activation and differentiation and scarring (Jester 2003, Jester et al. 1995, Imanishi et al. 2000, Funderburgh et al. 2001). AGEs are formed continually in the human body (Semba et al. 2010) although they are accelerated by some physiological situations such as ageing and pathophysiological conditions such as diabetes (Singh et al. 2002, Haar, Ackerman 1971). The process of advanced glycation itself is not harmful, only the products of it (Singh et al. 2002). The assessment of non-enzymatic changes are difficult (Mikulikova et al. 2007) and unfortunately AGEs measurement varies widely between studies. Many different methods exist for measuring AGEs and as of yet there is no “gold standard” method for detecting AGEs. However, the methods most commonly used include high-performance liquid chromatography (HPLC), enzyme-linked immunosorbent assay (ELISA) and immunohistochemistry (Singh et al. 2002).

6.3. Aims and Objectives

The aim of this study is to reveal the change in molecular structure of collagen due to ageing. A simple magnetic alignment technique was used to reveal the effects of ageing on fibril formation. Changes to the mechanical properties and cellular capacity of matrix remodelling due to age-related collagen structural changes in reconstituted hydrogel constructs was monitored using our non-destructive imaging techniques. We hypothesise that age-related inter- and intra-molecular cross-linking of collagen due to ageing interferes greatly with the fibrillogenesis process. Consequently, the mechanical properties of the reconstituted hydrogel construct are affected, which in turn influences the cell's ability to contract and remodel the collagen constructs.

6.4. Materials and Methods

6.4.1. Corneal stromal cell culture

Adult human corneal tissue remaining from corneal transplantation was used for the isolation of AHDCS cells; see **section 3.1.1.** All cells were cultured in the presence of serum-containing F media and so were fibroblastic in phenotype.

6.4.2. Collagen extraction

Acid extracted collagen used in this study was kindly supplied by Ms. Marie uilbert and associates from Université de Reims Champagne-Ardenne, France. Native type I collagen was obtained by acetic acid extraction from rat tail tendons of different-age animals, 2 days (newborns), 2 months, 6 months, 18 months and 2 years, as previously described (Garnotel et al. 2000), **see section 3.2.3**. In order to ensure the best homogeneity between age groups, the ratio of extracted collagen (mg) per weight of animal (g) was calculated (**Table 6.1**). Consequently, in order to collect 1g of lyophilized collagen for each age group the number

(n) of animals for each age group was determined as follows: n was 105 for newborn; 8 for 2 month; 7 for 6 month; 5 for 2 year old). For preparing 3D gels, lyophilised collagens were sterilised in ethanol, dried and then dissolved in sterile 18 mM acetic acid at concentrations of 3 mg/ml and 5 mg/ml respectively.

Table 6.1: Extraction yield of different aged collagen

Age-group / Parameter	Newborn	2 month	6 month	2 years
Average weight of one animal (g)	35	380	450	650
Average amount of type I collagen extracted from one animal (mg)	9	120	140	190
Extracted collagen (mg) / g of animal	0.257	0.316	0.311	0.292
Number of animals sacrificed to obtain 1g of collagen	105	8	7	5

6.4.3. Biochemical analysis of collagen

The biochemical properties of the different aged collagens were evaluated after solubilising the collagens at 2 mg/ml in 18nM acetic acid. Their electrophoretic properties were estimated using 5% sodium dodececyl sulphate-polyacrylamide gels (SDS-PAGE) following denaturation by heating to 90 °C for 2 min. The gels were stained with Coomassie Brilliant Blue R250 to reveal the two characteristic bands of type I collagen (α1 and α2 chains). AGEs-specific fluorescence in different aged collagen specimens was measured using a Shimadzu RF-5000 fluorescence spectrophotometer (Shimadzu, Mane l Vallée, France) at 380 nm excitation and 440 nm emission. A solution of AGE-modified bovine serum albumin (BSA) was used to create a standard curve.

6.4.4. Collagen viscosity

All ages of 3 mg/ml and 5 mg/ml collagen samples were further diluted using 0.1% acetic acid (*v/v*; Sigma-Aldrich, UK, diluted in distilled water) to working concentrations of 0.3 mg/ml and 0.5 mg/ml respectively to allow for viscosity measurements to be recorded. Commercially available rat tail collagen (BD Biosciences Mountain Science, CA, referred to as "BD") was also diluted using the same method. A semi-micro viscometer (size 75, Cannon-Ubbelohde, Cannon Instruments, USA) was used according to the manufacturer's instructions; see **section 3.5.1**, to determine the kinematic viscosity of the different collagen solutions.

6.4.5. Fabrication of acellular and cell-containing hydrogels

Cellular and acellular collagen hydrogels of two different concentrations from both extracted and BD rat tail collagen were investigated; initial gels were made at a final collagen concentration of 1.5 mg/ml; followed by 2.5 mg/ml concentration gels following the protocols as described in **sections 3.2.1** and **3.5.3** respectively.

6.4.6. Construct contraction

Hydrogels cast into filter paper rings were effectively confined to the dimension of the ring. This permitted analysis of confined contraction in terms of a change of thickness of the hydrogel construct *via* OCT. Acellular collagen hydrogels were produced as a control. OCT was used to measure the change in thickness of constructs daily. The detailed description of the instrument can be found in **section 3.3.2**. Acellular control data was relatively constant for the duration of the experiment so the data was accumulated and displayed as the mean of 7 days and represented as a mean value ± the calculated standard deviation.

6.4.7. Modulus measurement

The mechanical properties of the constructs were measured daily using a non-destructive spherical indentation technique as described in **section 3.3.1**.

6.4.8. Cell proliferation

Methylthiazolyldiphenyl-tetrazolium bromide (MTT) was used to monitor cell proliferation within the different aged hydrogel constructs. MTT was dissolved in PBS at a concentration of 5 mg/ml and sterile filtered. Each construct examined was placed into a cell culture well containing 10% (*v/v*) MTT solution in culture media. The wells were placed into an incubator at 37 °C, 5% CO_2 for 3 hr under gentle agitation. The MTT/culture media was removed and each construct was washed twice in PBS. DMSO solution was then added to each well for 1 hr. The DMSO solution was transferred into a 96 well plate and the absorbance of light was measured using a microplate reader (Synergy 2, BioTek,USA). Readings were obtained at two wavelengths of 570 nm and 690 nm which were subtracted from each other to give single values for each well. A standard curve was created by suspending a known numbers of cells in a hydrogel. From the standard curve, the number of viable cells was calculated.

6.4.9. Cell viability and morphology

Cell viability was observed at day 7 using a live-dead fluorescent double staining kit used according to the manufacturer's instructions, see **section 3.4.1**. Cell morphology was observed at day 7 in the hydrogel constructs and day 3 in the magnetically aligned samples using phalloidin tetramethylrhodamine-B-isothiocyanate to fluorescently stain actin filaments of the cells which effectively displays directionality see **section 3.4.2.**

6.4.10. Magnetic alignment of collagen

Acellular collagen hydrogel samples of different aged collagens were prepared at concentration 2.5 mg/ml and magnetically aligned as described in **section 3.5.2**. The magnetically aligned hydrogels were viewed using polarised light microscopy (SP-60P, Brunel, UK) and the collagen fibre organisation images were captured using digital photography (D5000, Nikon, Japan). AHDCS cells were seeded at density 20,000 cells per well in 100 μl media. The cells were allowed 2 hr to adhere before the media was topped up to 500 μl per well. The cells were cultured for 3 days before their orientation was viewed using fluorescent microscopy (Eclipse T*i*-S, Nikon, Japan).

The cell alignment was then quantitatively evaluated as previously described (Charest et al. 2007, Nichol et al. 2010). Briefly, the cell/nuclear alignment angle as defined by the orientation of the major elliptic axis of individual nuclei, with respect to the horizontal axis was measured using ImageJ (NIH, USA). All nuclear/cellular alignment angles were normalized to the "preferred" nuclear/cellular orientation as defined by the mean orientation of all nuclei/cells per sample. Six images per collagen age group containing a minimum of 25 cells per image were analyzed. For analysis, alignment angles were grouped in 10˚ increments with respect to the preferred nuclear/cellular orientation.

6.4.11. Statistics

All data was analysed using GraphPad Prism® (CA, USA). The data was subjected to a normality (Kolmogorov-Smirnoff) test. The data was normally distributed, so comparisons were performed using either T-tests for pairs of data, or one-way analysis of variance (one-way ANOVA) followed by Tukey post-tests or two-way ANOVA followed by Bonfferoni post-tests where applicable. Significance was indicated to determine if the effects of time, collagen age and collagen concentration were statistically significant at three levels: * $p \leq$

0.05, ** $p \leq 0.01$ and *** $p \leq 0.001$. Three specimens per group have been tested. Recorded data was averaged and represented as a mean value ± the calculated standard deviation.

6.5. Results

6.5.1. Biochemical analysis of collagen

Collagens of all ages were obtained in a homogenous solution in acetic acid which were colorless in appearance. As shown on the electrophoretic profile (**Figure 6.2A**), all extracted different-age type-I collagens exhibited the two characteristic α_1 and α_2 chains of native type-I collagen. With increasing age, the electrophoretic mobility decreased, indicating that the collagen was decreasing in solubility with increasing age due to post-translational modifications. The fluorescent-AGEs quantification (**Figure 6.2B**) showed a significant increase of fluorescence intensity for the oldest specimen (2-years).

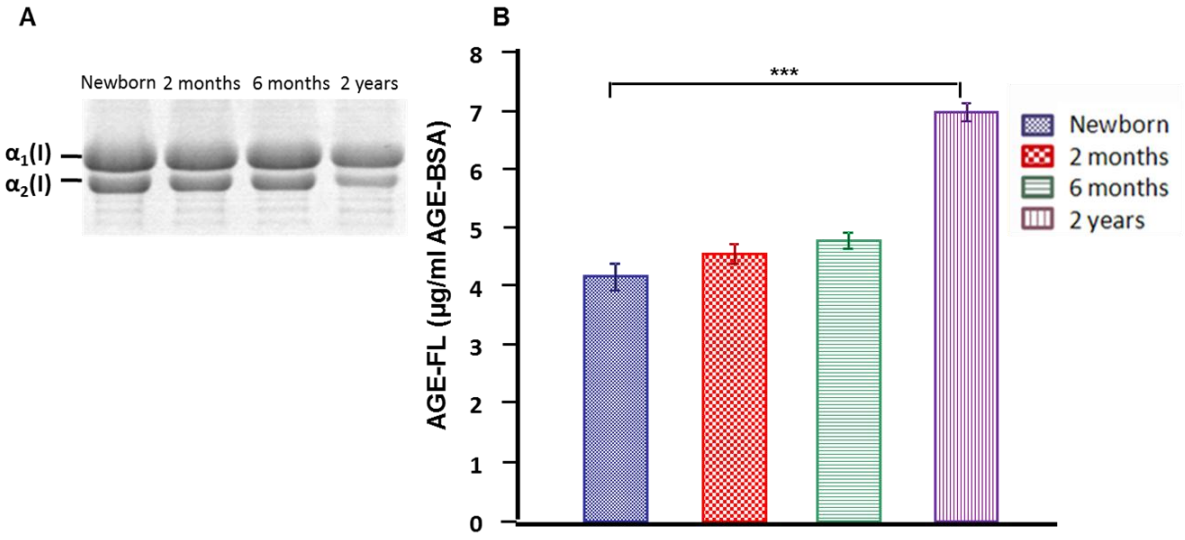

Figure 6.2: Electrophoretic profile (A) and fluorescent-AGEs content (B) of different-age type I collagens extracted from different aged rats, ***: $p<0.001$; n= 3.

6.5.2. Collagen viscosity

Differences in viscosity were observed between the collagen groups. The older collagen solutions (6 month, 18 month and 2 years) were visibly more viscous than the younger collagens (newborn and 2 month) at the same concentration. Although all collagens formed homogenous hydrogels, the gelation time for the younger collagen was longer compared to the older collagen. For example, the newborn collagen took up to an hour to gelate while the 2-year old collagen formed a gel within 10 min. Viscosity studies were performed using a semi-micro viscometer and the kinematic viscosity was calculated (**Figure 6.3**). ANOVA tests revealed that the age of the collagen had a statistically significant effect on the viscosity of the collagen solution when prepared at both 0.3 mg/ml and 0.5 mg/ml concentration. In the collagens diluted to 0.3 mg/ml, the youngest collagen, 2 month, was significantly less viscous than all other samples ($p \leq 0.001$ vs. 6 month, 18 month and 2 years; $p \leq 0.01$ vs. BD). The viscosity of the 0.3 mg/ml 6 month collagen was significantly less than both the 18 month and 2 year old collagens ($p \leq 0.001$) although there was no significant difference when compared to the 0.3 mg/ml BD sample. The viscosity of the 0.3 mg/ml 18 month collagen was significantly lower than the 2 year collagen ($p \leq 0.05$); although it was significantly higher than the BD 0.3 mg/ml sample ($p \leq 0.001$). The viscosity of the 2 year collagen was significantly greater ($p \leq 0.001$) than the 0.3 mg/ml BD sample.

Similar trends were observed in the samples prepared at 0.5 mg/ml. The youngest collagen, newborn, has a significantly lower viscosity than all other samples ($p \leq 0.001$ inclusive). The 2 month collagen has a significantly lower viscosity than the 6 month, 2 year and BD 0.5 mg/ml samples. The 6 month collagen had a significantly lower viscosity than both the 2 year and the BD 0.5 mg/ml samples. The viscosity of the 2 year collagen was significantly greater ($p \leq 0.001$) than the 0.5 mg/ml BD sample. T-tests revealed that

the concentration of the collagen had a significantly significant effect on the viscosity of the construct at all ages. The viscosity of equivalent groups, 2 month, 6 month, 2 years and the BD collagens were compared. The 0.3 mg/ml collagen samples all had a significantly lower viscosity when compared to the 0.5 mg/ml equivalents (**Figure 6.3**).

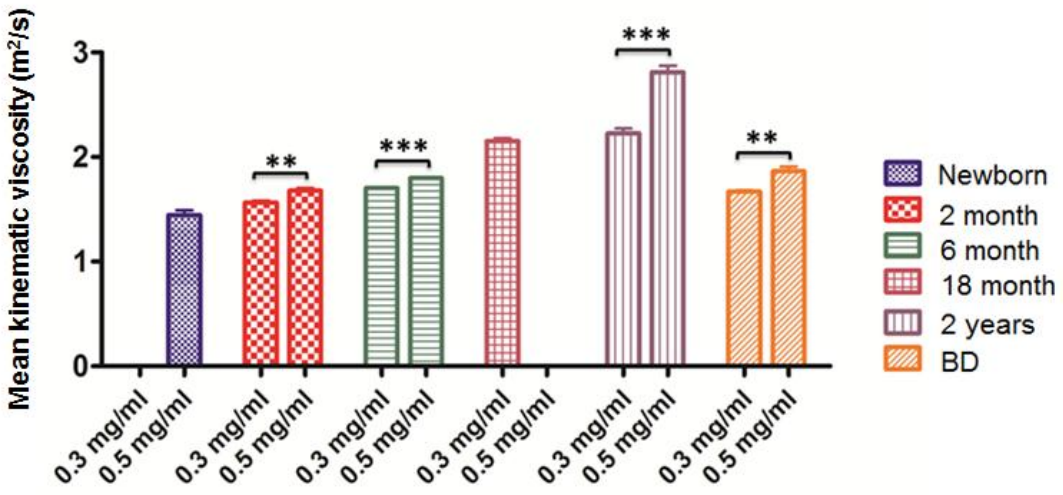

Figure 6.3: The mean kinematic viscosity of 0.3 mg/ml and 0.5 mg/ml collagen from different aged rats and commercially available (BD) collagen; n=3, ** $p \leq 0.01$ and *** $p \leq 0.001$.

6.5.3. Cell contraction

The AHDCS cells in the hydrogel constructs caused contraction during the culture. However, the contraction of the constructs was limited to a change in thickness since the presence of the filter paper rings prevented the hydrogels from contracting horizontally. The change in thickness of all constructs was measured using OCT daily for 7 days. The thickness of all acellular scaffolds in both 1.5 mg/ml (**Figure 6.4D**) and 2.5 mg/ml (**Figure 6.5D**) collagen concentration samples remained constant and showed no significant differences between groups throughout the duration of the experiment and so could be accumulated into bar graphs for easier comparisons to be drawn (**Figure 6.6**). All cellular constructs contracted thus making the constructs thinner. Most contraction occurred within

the first 3 days. ANOVA tests revealed that the age of the collagen had a statistically significant effect on the change in thickness of the construct when at both collagen concentrations. The initial experiments were performed using collagen gels at concentration 1.5 mg/ml. This group did not include the newborn collagen samples. It did include an additional sample of 18 month old collagen. However, there was no significant difference in contraction data when comparing 18 month to the 2 year old specimens in both cellular and acellular results; thus it was not forwarded into the later experiments.

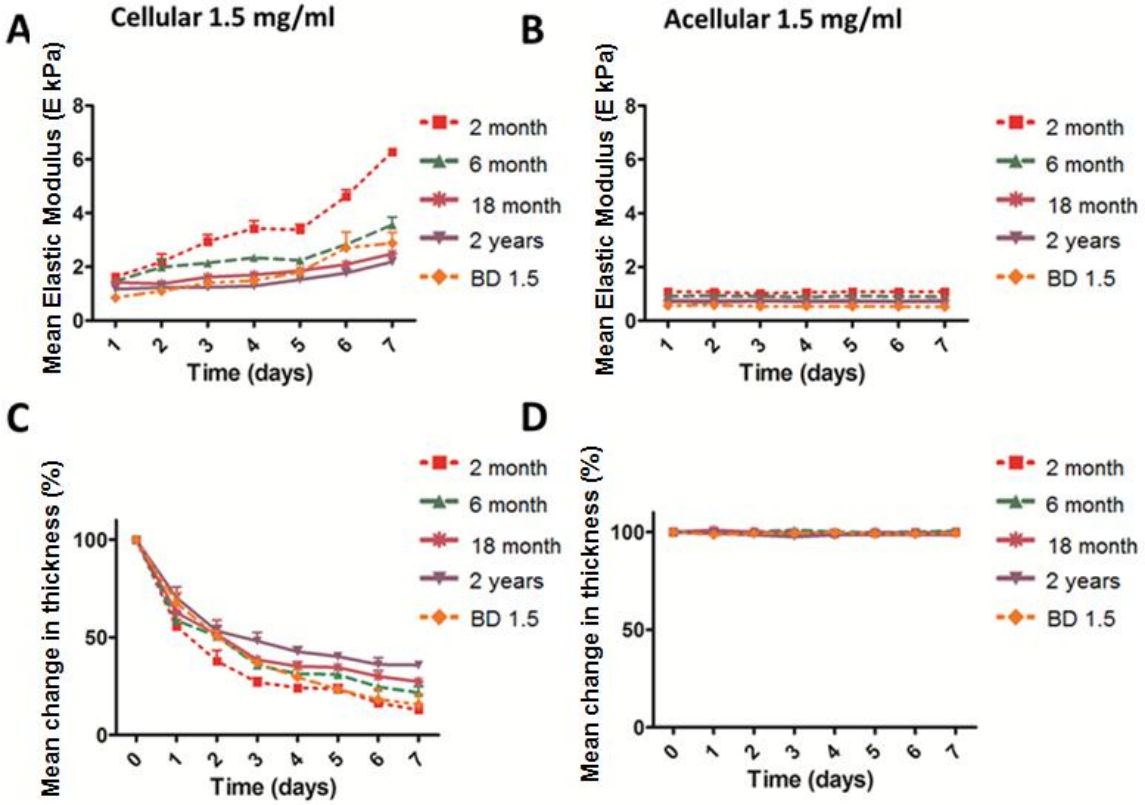

Figure 6.4: The mean elastic modulus of 1.5 mg/ml collagen concentration cellular constructs (A) and acellular scaffolds (B) using collagen extracted from different aged rats cultured for 7 days; is directly linked to the mean change in thickness of the cellular constructs (C) and acellular scaffolds (D); n=3.

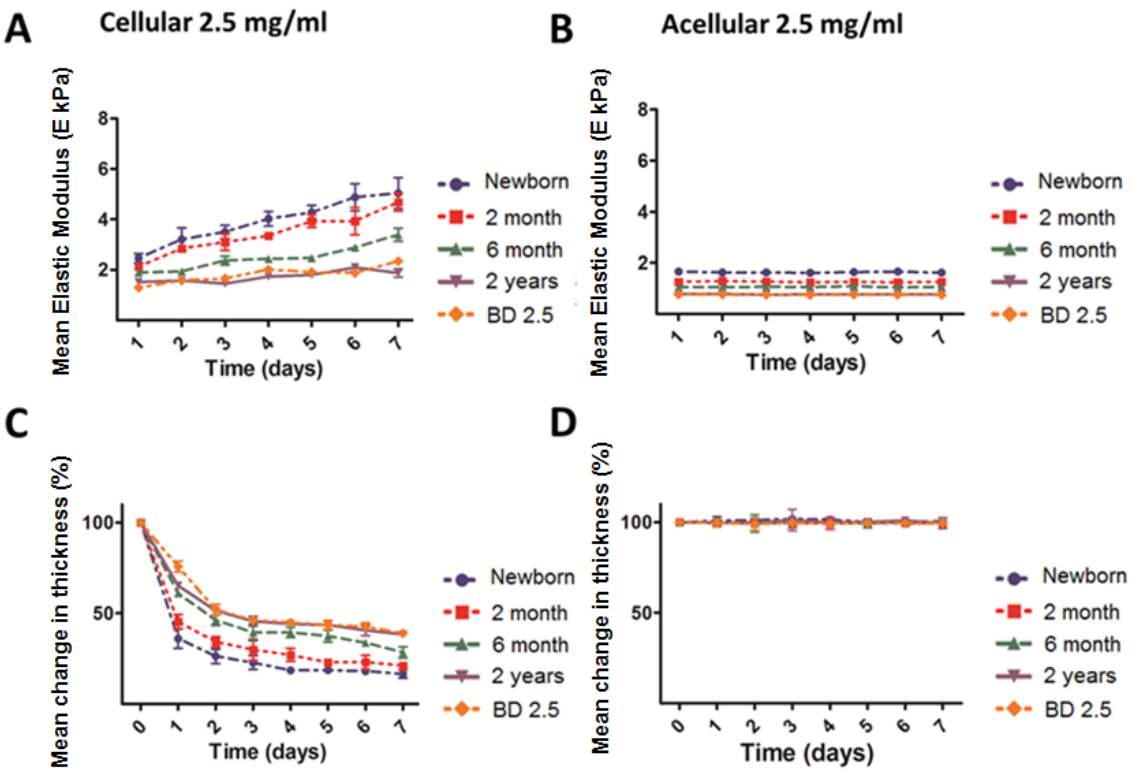

Figure 6.5: The mean elastic modulus of 2.5 mg/ml collagen concentration cellular constructs (A) and acellular scaffolds (B) using collagen extracted from different aged rats cultured for 7 days; is directly linked to the mean change in thickness of the cellular constructs (C) and acellular scaffolds (D); n=3.

In the cellular constructs prepared at 1.5mg/ml the 2 month collagen contracted significantly more following 2 days culture ($p \leq 0.001$) than all other constructs with the exception of the BD constructs. Initially the 2 month collagen contracted at a greater rate than the BD collagen for the first 3 days ($p \leq 0.001$); but following 4 days culture there was no significant difference observed. There was no significant difference in the contraction of the 6 month constructs compared to the 18 month constructs for the duration of the experiment. However, the 6 month constructs contracted significantly more than the 2 year collagen constructs ($p \leq 0.001$) from day 1 onwards. As previously mentioned, there was no significant difference in construct contraction observed between the 18 month and

2 year collagen constructs, however 18 month collagen contracted significantly less than the BD constructs from day 4 onwards ($p \leq 0.001$). The BD collagen gels also contracted significantly more than the 2 year constructs ($p \leq 0.001$) following 3 days culture.

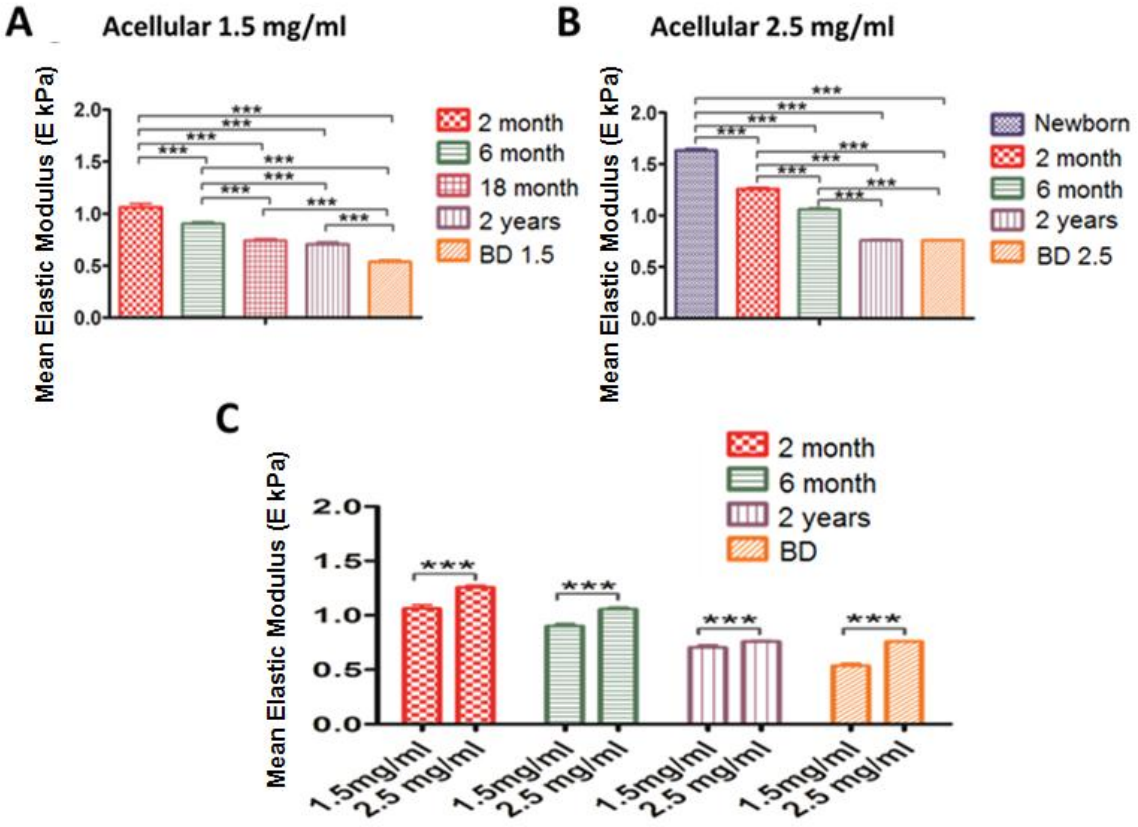

Figure 6.6: Mean elastic modulus of acellular collagen extracted from different aged rats compared to commercially available (BD) collagen at collagen concentration 1.5 mg/ml (A) and 2.5 mg/ml (B) following 7 days culture; direct comparison of the different collagen concentrations of equivalent aged collagens (C); n =3, *** = $p \leq 0.001$.

In the constructs prepared at 2.5 mg/ml the youngest collagen, 2 days (newborn) showed the greatest degree of contraction and by the end of the experiment was less than 20% of its original thickness (**Figure 6.5C**). The newborn collagen decreased significantly more in thickness than all other collagen used ($p \leq 0.001$ days 1-7 inclusive vs. 2 month, 6 month, 2 years and BD) with the exception of the 2 month collagen (where $p \leq 0.001$ days

1-4, $p \leq 0.05$ days 2 and 4 and $p \leq 0.05$ on day 3). Similar trends were observed when comparing 2 month collagen to 6 month, 2 year and BD collagen ($p \leq 0.001$ days 1-7 inclusive). 6 month collagen also decreased in thickness significantly more than 2 year and BD collagen ($p \leq 0.05$ day 2-4; $p \leq 0.01$ day 3-5; $p \leq 0.001$ day 6-7). The 2 year old collagen decreased significantly more than the 2.5 mg/ml BD collagen on day 1 only ($p \leq 0.001$).

The constructs which showed the greatest contraction by the end of the experiment were the 2 month 1.5 mg/ml constructs, which were less than 15% of their original thickness. When comparing the equivalent cellular groups (2 month, 6 month, 2 years and BD) at 1.5 mg/ml and 2.5 mg/ml the 2 month 1.5 mg/ml constructs contracted significantly more than the 2 month 2.5 mg/ml constructs at day 6 and 7 ($p \leq 0.01$ and $p \leq 0.05$ respectively). The 6 month 1.5 mg/ml constructs contracted significantly more than the 6 month 2.5 mg/ml constructs following 4 days culture ($p \leq 0.01$ day 4; $p \leq 0.05$ days 5 and 6; $p \leq 0.001$ day 7). No significant difference was observed when comparing the 2 year constructs at 1.5 mg/ml and 2.5 mg/ml collagen concentrations. The BD 1.5 mg/ml collagen constructs contracted significantly more than the BD 2.5 mg/ml constructs from day 4 onwards ($p \leq 0.001$).

6.5.4. Modulus measurement

6.5.4.1. Acellular scaffolds

The elastic modulus of the different aged collagen constructs in both acellular scaffolds and cellular constructs at collagen concentrations 1.5 mg/ml and 2.5 mg/ml respectively was measured daily for 7 days. All acellular control hydrogels retained a constant modulus with a visible trend for the younger the collagen, the higher the modulus (**Figure 6.4A** and **B**; **Figure 6.5A** and **B**). This was true for all specimens, irrespective of the collagen

concentration. In the 1.5 mg/ml acellular scaffolds the modulus of the 2 month constructs was significantly greater than all other constructs for the duration of the experiment ($p \leq 0.001$). No significant difference was observed in modulus between the 18 month and 2 year old groups. Thus the 18 month collagen was removed from further experiments performed at the higher concentration and replaced with a younger (2 days, newborn) collagen. The BD constructs had a significantly lower modulus than all other samples ($p \leq 0.001$).

Similar trends were observed in the acellular 2.5 mg/ml collagen concentration scaffolds with the modulus of the acellular newborn scaffolds being significantly greater than 2 month, 6 month, 2 year and BD scaffolds for the duration of the experiment ($p \leq 0.001$ inclusive). 2 month scaffolds were significantly greater in modulus than the 6 month, 2 year and BD ($p \leq 0.001$) scaffolds; 6 month constructs were significantly higher in modulus than the 2 year and BD scaffolds. However, in the 2.5 mg/ml samples, there was no significant difference between the 2 year and BD scaffolds.

When comparing the equivalent acellular 2 month, 6 month, 2 year and BD collagen scaffolds at collagen concentration 1.5 and 2.5 mg/ml respectively it is clearly demonstrated that the higher concentration gels are consistently significantly higher in modulus ($p \leq 0.001$) in all instances (**Figure 6.6C)**, which is to be expected and is in agreement with previous studies (Ahearne, Liu et al. 2010).

6.5.4.2. Cellular constructs

The elastic modulus of the 2 month cellular constructs at collagen concentration 1.5mg/ml were significantly higher ($p \leq 0.001$) than all other constructs following 3 days culture and remained higher for the duration of the experiment. The 6 month collagen constructs was significantly greater than the 18 month, 2 year and BD collagens following

3 days culture ($p \leq 0.05$ day 4, $p \leq 0.01$ day 6, $p \leq 0.001$ day 7, vs. 18 month; $p \leq 0.001$ days 3-7 vs. 2 year; $p \leq 0.01$ day 1, ≤ 0.001 day 2-4 and day 7 vs. BD). There was no significant difference in the 18 month and 2 year constructs; and no significant difference in the modulus of either 18 month or 2 year collagen constructs compared to the BD constructs.

The modulus of the newborn constructs in the 2.5 mg/ml collagen constructs was significantly greater than the 6 month, 2 year and BD collagen constructs for the duration of the experiment ($p \leq 0.001$ inclusive). However, the newborn collagen only showed a significantly greater modulus when compared to the 2 month collagen at day 5 ($p \leq 0.05$) and day 6 ($p \leq 0.05$). Similar trends were observed when comparing the modulus of the 2 month collagen to the 6 month and 2 year collagen ($p \leq 0.001$ day 2-7, with the exception of 6 month collagen at day 5 where $p \leq 0.05$). 6 month collagen also had a significantly higher modulus when compared to 2 year old collagen ($p \leq 0.05$ day 2 and 4, $p \leq 0.01$ day 3 and 5, $p \leq 0.001$ day 6-7). There was no significant difference in the modulus of the 2 year old collagen when compared to the BD collagen.

The constructs which had the highest modulus by the end of the experiment was the 2 month 1.5 mg/ml collagen concentration constructs with a final modulus of above 6 kPa. The modulus value was significantly greater than all other specimens in both the 1.5 mg/ml and 2.5 mg/ml groups following 7 days culture ($p \leq 0.001$ inclusive). When comparing the modulus of equivalent cellular groups (2 month, 6 month, 2 years and BD) at collagen concentration 1.5 mg/ml and 2.5 mg/ml, the 2 month 1.5 mg/ml constructs had a significantly higher modulus than the 2.5 mg/ml constructs ($p \leq 0.05$ days 1 and 5. $p \leq 0.01$ days 2 and 6; $p \leq 0.001$ day 7). There was no significant difference in the modulus of the 6 month and 2 year constructs at the different collagen concentrations. However, the 1.5

mg/ml BD constructs had a significantly higher modulus than the 2.5 mg/ml BD constructs ($p \leq 0.05$ days 2, 4 and 7; $p \leq 0.001$ day 6).

6.5.4. Cell proliferation

Cell proliferation of the different aged constructs was measured following 7 days culture, all constructs were initially seeded with 0.5 million cells. Cell proliferation was observed in all constructs, with a visible trend for the younger the collagen the higher the rate of proliferation (**Figure 6.7**). ANOVA tests revealed that the newborn collagen promoted significantly more proliferation compared to all other constructs ($p \leq 0.001$). There was no significant difference when comparing cell proliferation within the 2-month and 6-month collagen constructs. However cells in the 2-month collagen proliferated significantly more than the cells in both the 2-year old and BD collagens ($p \leq 0.001$). Similarly, the cells in the 6-month collagen proliferated significantly more than the cells in the 2-year old and BD collagens ($p \leq 0.001$ and ≤ 0.01 respectively). However, the cells in the 2-year old collagen proliferated significantly less than the cells in the BD collagen (≤ 0.05).

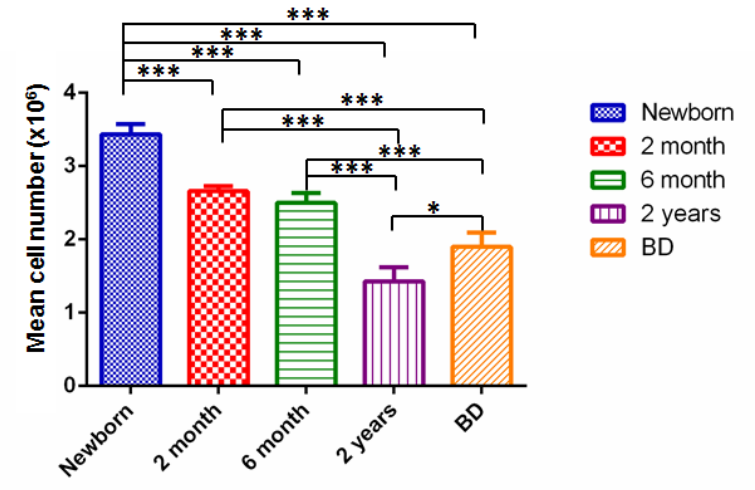

Figure 6.7: Cell proliferation, measured using MTT of 2.5 mg/ml collagen concentration constructs using collagen extracted from different aged rats cultured for 7 days; n=3, * $p \leq 0.01$,*** $p \leq 0.001$.

6.5.6. Cell viability and morphology

All constructs had good cell viability following 7 days culture (**Figure. 6.8**) with no obvious differences in cell viability when comparing the different collagen concentrations, ages or commercially available (BD) to extracted collagen. The morphology of all the cells were characteristically fibroblastic in appearance. However, it was observed that in the specimens manufactured using the younger collagen (2 months) in both 1.5 and 2.5 mg/ml samples (**Figure 6.9A** and **G**) and in the 2 day (newborn) collagen (**Figure 6.9F**) that the cells appeared to be denser and more organised, appearing to spontaneously align, compared to the other samples. This denser appearance is likely to be due to the fact that they were more closely packed as these specimens contracted the greatest, thus causing the surrounding collagen matrix to be denser. All other, older samples appeared to have disorganised actin arrangements that were less dense in appearance.

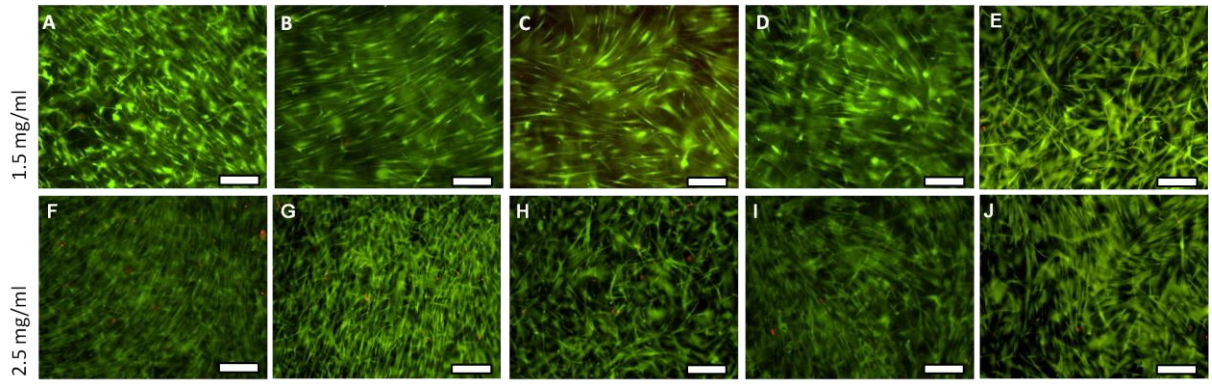

Figure 6.8: Representative live-dead fluorescent images of collagen constructs following 7 days culture at collagen concentration 1.5 mg/ml (A-E) and 2.5 mg/ml (F-J); of rats aged 2 months (A and G); 6 months (B and H); 18 months (C); 2 years (D and I); 2 days (newborn, F) and the commercially available BD collagen (E and J); green represents live cell, red represents dead cells, scale bar = 200 µm.

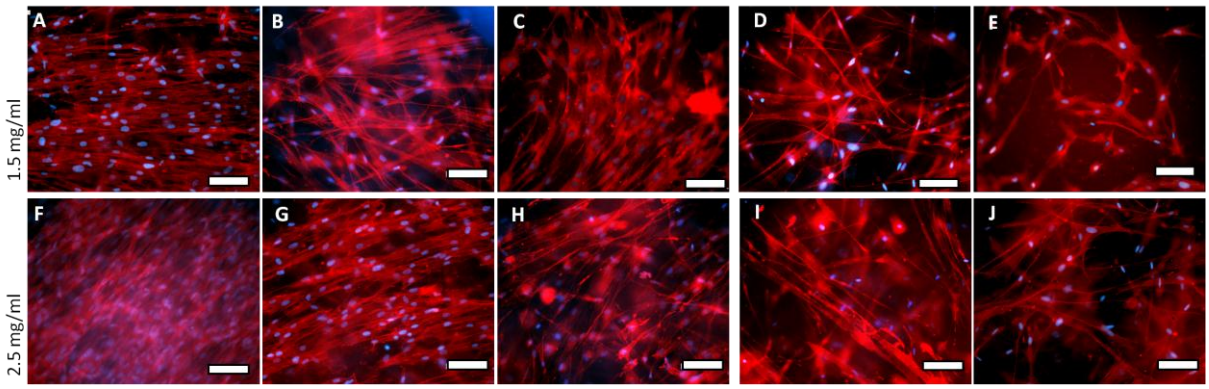

Figure 6.9: Representative fluorescent phalloidin tetramethylrhodamine-B-isothiocyanate (red) and DAPI (blue) stained cells in collagen constructs following 7 days culture at collagen concentration 1.5 mg/ml (A-E) and 2.5 mg/ml (F-J); of rats aged 2 months (A and G); 6 months (B and H); 18 months (C); 2 years (D and I); 2 days (newborn, F) and the commercially available BD collagen (E and J), scale bar = 100 µm.

6.*5.7. Magnetic alignment of collagen*

Following exposure to a 12 Tesla magnetic field during fibrillogenesis with a step heating programme, collagen fibres in 2.5 mg/ml collagen concentration newborn and 2 month samples aligned perpendicular to the applied magnetic field, whereas fibres in the older (6 month and 2 year) specimens remained random in orientation (**Figure 6.10E-H**). Following cell seeding and culture for 3 days it was observed that the cell growth mimicked the surface topography of the aligned or disorganised collagen surface. The newborn and 2 month collagen surfaces caused the cells to align and grow in the defined direction (**Figure 6.10A** and **B**) whereas the cells on the 6 month and 2 year collagen surfaces failed to align and continued to grow in a random orientation (**Figure. 6.10C** and **D**). When quantified, it was revealed that over 80% of the cells on the newborn and 2-month old collagen surfaces were aligned (i.e. cells arranged in the same direction and only experiencing up to 10˚ variation from the mean value (**Figure 6.10I** and **J**); whereas the cells seeded onto the older, 6-month (**Figure 6.10K**) and 2-year old (**Figure 6.10L**) collagens had only approximately 40% of the cells that were in the same orientation.

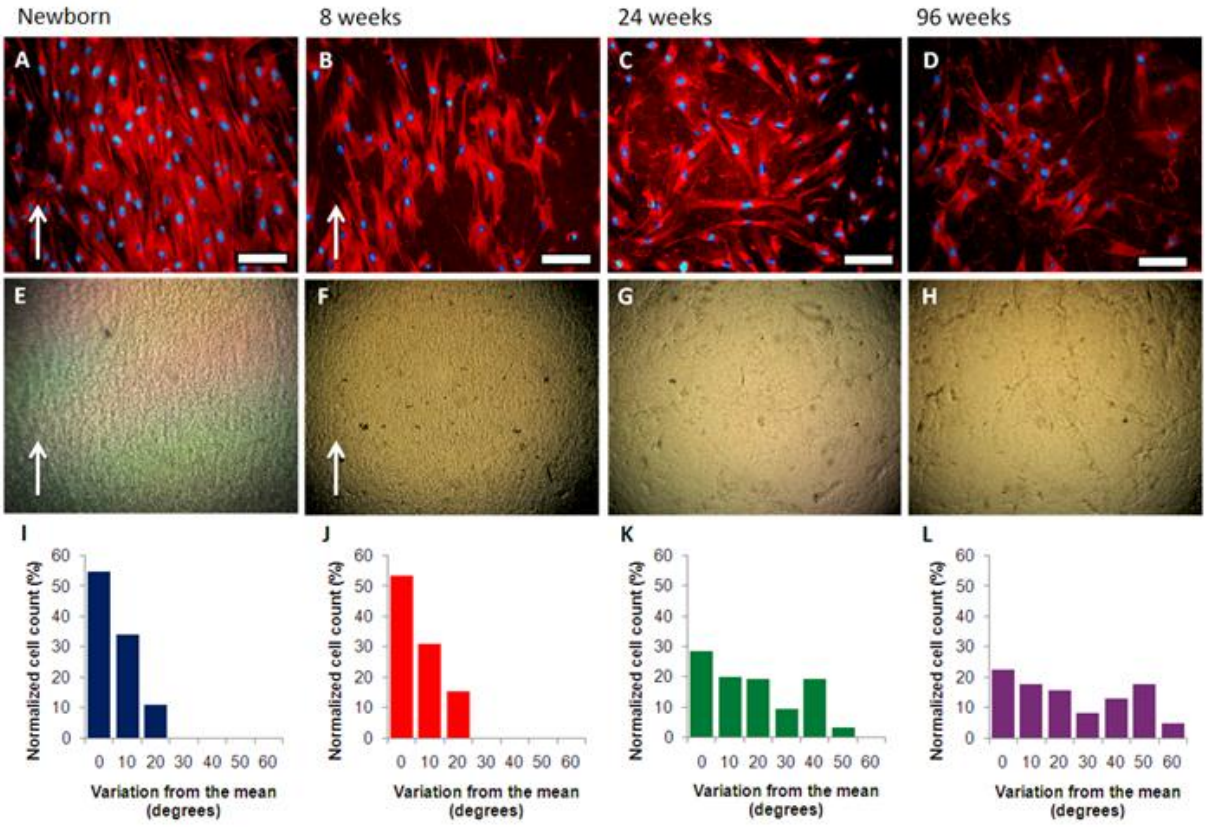

Figure 6.10: Representative fluorescent phalloidin tetramethylrhodamine-B-isothiocyanate (red) and DAPI (blue) stained cells (A-D) cultured for 3 days on different aged collagens fibrillogenesis under a 12 T magnetic field at concentration 2.5 mg/ml, scale bar = 100 μm; the corresponding polarised light microscope images (E-H) of different aged collagen samples under 12 T magnetic field, the newborn (E) and 2 month (F) collagen solutions aligned, whereas the 6 month (G) and 2 year (H) specimens did not. The white arrows indicate the directionality of the collagen fibres. The subsequent histograms (I-L) of the cell and nuclear alignment in 10˚ increments relative to the preferred nuclear orientation quantifiably demonstrate that the cells on the newborn (I) and 2-month (J) collagens were more aligned than the 6-month (K) and 2-year old (L) collagens.

6.6. Discussion

It is well known from clinical pathology and normal daily life that ageing affects connective tissues considerably, such as wrinkle formation and reduced skin elasticity as humans become older. However, to date, there is no systematic report of the molecular changes of ageing collagen and its influence on the mechanical properties of reconstructed collagen hydrogels and the cellular response when fibroblast-like cells are seeded into the construct. In this chapter, the molecular and functional changes of ageing collagen have been investigated in parallel using microscopic and macroscopic modalities. The macroscopic parameters including kinematic viscosity, fibril alignment, elastic modulus and the contraction capability (thickness change), demonstrated that there was an age-dependent variation in the reconstituted collagen hydrogel constructs. This suggested that through the measurement of macroscopic parameters, we may obtain insights of age-induced changes at the monomer level and of the global network of the reconstituted hydrogel constructs.

6.6.1. Changes to collagen quality with ageing

Type I collagen is a fibre-forming protein and is an important scaffold component of both *in vivo* and *in vitro* tissues. The source, age, extraction method and post-processing all result in a collagen structure with a defined structure, regarding the absence or presence of telopeptides, the nature of the fibrils and the extent of cross-linking. All the different collagens (excluding the BD samples) used in this chapter were sourced, extracted and processed using the same protocols and so it was be assumed that the age of the collagen would be the only contributing factor to the observed differences in collagen structure and behaviour.

Collagen is intrinsically autofluorescent, which is mainly due to tyrosine and phenylalanine amino acids and pyridinoline cross-links (enzymatic cross-links catalysed by lysyl-oxydase during fibril assembly) (Mikulikova et al. 2008). In addition, most AGEs, such as pentosidine and crossline, have been found to be fluorescent and cross-linking compounds (Mikulikova et al. 2008). These fluorescence properties of collagen and AGEs are largely used to quantify collagen content and modifications due to the ageing process or physical alterations such as photo-damage in tissues (especially skin) (Kollias et al, 1998). Furthermore, in pathophysiology, spectrofluorimetric analysis is often used to detect AGEs (in tissues as well as in serum/plasma/urine) and in clinics, this methodology is well accepted to screen age-associated pathologies such as diabetes (De la Maza et al. 2012). This technique is less destructive, more direct, and easier than conventional mass spectrometric and chromatographic techniques, thus was deemed to be a suitable, convenient method for detecting AGEs content. The higher content of AGEs products was believed to be the cause of the poor fibril alignment capacity in the older collagen specimens and provided evidence that aged collagen has additional intra- and inter-cross-linking in comparison to the younger collagens. This suggested that AGEs accumulation may be the predominant mechanism for additional collagen cross-linking as the decrease of electrophoretic mobility of collagen with post-translational modifications is largely described in the literature (Jaisson et al. 2006, Said et al. 2012). Also, it is well-known that the solubility and flexibility of collagen decreases during aging (Bartling et al. 2009). Furthermore, the quantification of fluorescent AGEs (resulting from non-enzymatic glycation, the most post-translational modification observed for collagen and other matrix proteins) confirms that electrophoresis changes are due to glycation reactions with increasing collagen age. Addition of AGEs to the collagen molecule is responsible for a

molecular weight increase; the resulting cross-links are responsible for the solubility decrease, both which lead to a decrease in electrophoresis mobility.

Previously, both enzymatic and acid extraction methods have been used to obtain solubilized collagen for studies on collagen aging (Bellmunt et al. 1995, Jiang et al. 2000,). A number of studies have demonstrated that enzymatic extraction gives rise to subtle changes in the subsequent collagen products, although the gross physical characteristics of the molecules were not altered (Rubin et al. 1963, Steven and Jackson 1967). In this study, we used an acid extraction protocol. Unlike enzymatic extraction methods, the acid-extracted products consist primarily of monomeric tropocollagen with intact telopeptides (Pauling 1979). It has been shown that telopeptides are essential for the end-to-end aggregation of tropocollagen molecules, a crucial step in fibrillogenesis (Torbet and Ronziere 1984). Thus, we hypothesise that the quality and quantity of the acid-extracted collagen monomers (tropocollagen) from rat tail tendon will bear a mark of aging and the subsequent alteration to the fibrillogenesis process among the aging collagen specimens would reflect the monomeric alteration.

Our results suggested that the older tissues (even at 2 years) still contained a substantial portion of acid-soluble tropocollagen. However, the viscosity of the older collagens was higher than the younger collagen counterparts, this implies that the older solubilised tropocollagen solution contained a substantial number of trimeric, polymeric triple-helices, or AGEs aggregates. The variation in alignment capacity during fibrillogenesis of the different aged collagens when exposed to a high magnetic field provided further evidence that structural alterations to the telopeptide region had occurred in the older samples with reduced end-to-end cross-linking of tropocollagen which prevented the formation of homogenous and densely packed fibres.

6.6.2. Collagen anisotropy and fibrillogenesis

Biological polymers such as collagen and fibrin are diamagnetically anisotropic. The diamagnetic anisotropy of such proteins largely depends on the relative orientations of the peptide bonds and aromatic residues present in their structure (Worcester 1978). As collagen contains few aromatic groups its diamagnetic anisotropy is entirely due to the regular arrangement of the peptide bonds that form the collagen triple helix. Worcester (1978) has shown that the diamagnetic anisotropy of a single peptide bond in the collagen triple helix conformation is $-0.25|\Delta\chi_p|$, where $\Delta\chi_p$ is the diamagnetic anisotropy of a single peptide bond. The diamagnetic anisotropy of collagen is negative and consequently molecules tend to orient perpendicular to an applied field. As diamagnetic anisotropy is approximately additive, the anisotropy of a single collagen molecule consisting of about 2730 peptide bonds is $-680|\Delta\chi_p|$. When N molecules are aligned parallel, the diamagnetic anisotropy of the ensemble, $\Delta\chi$, is N times greater following **Equation 6.1**:

$$\Delta\chi = -680 \times N \times |\Delta\chi_p|$$

Equation 6.1

The orienting effect of the magnetic torque is countered by randomising Brownian motion so the degree of alignment in a magnetic field, H, depends on the ration in **Equation 6.2**.

$$|\Delta\chi|H^2/kT$$

Equation 6.2

where k is Boltzmann's constant and T the absolute temperature. In order to reach a high degree of orientation, the condition, $|\Delta\chi|H^2 > 20kT$, has to be satisfied (Worcester 1978). For collagen fibres this means that $680 \times N \times |\Delta\chi_p|H^2 > 20kT$. The experiments reported here were carried out at room temperature in a field of 12 Tesla (i.e. 1.2×10^5 G (Gauss)). By using

the lowest value, $|\Delta\chi_p|=8.9\times10^{-30}$ $ergG^{-2}$ (Torbet 1984), we calculate that a high degree of magnetic orientation requires a freely rotating group of approximately 10,000 near mutually parallel collagen molecules. The number of collagen molecules within fibrils easily exceeds this number.

When acid solubilised collagen is neutralised the solution becomes viscous and gelates as self-assembly into fibrils and fibres occurs. In the presence of a strong magnetic field a gel of highly aligned fibres results, provided assembly is not so fast that gelation occurs before orientation has maximised. For orientation to work, the initial solution must be largely composed of intact single molecules, or small parallel aggregates thereof, which come together in a parallel fashion giving rise to a high magnetic anisotropy. However, if the solution contains a significant proportion of disorganised aggregates, in which the constituent molecules are not parallel, or the molecules are not freely rotated, the effective diamagnetic anisotropy of these groups is strongly reduced or eliminated making magnetic orientation virtually impossible.

Our experiments demonstrate that when exposed to high magnetic fields, solutions of collagen extracted from young rats readily formed aligned gels, whilst gels produced from older animals showed a random morphology. This suggests that the collagen solutions derived from young rats consist largely of monomeric tropocollagen molecules, which come together in parallel fashion and rotate as a group to attain high orientation before gelation takes place. In contrast, the collagen solutions extracted from older rats oriented poorly probably because they contained a high proportion of weakly anisotropic aggregates, for example, AGEs aggregates and polymeric tropocollagnes as schematically shown in **Figure 6.11**. Hence, the fibrillogenesis under a magnetic field provided a simple technique to reveal molecular alterations of collagen due to ageing.

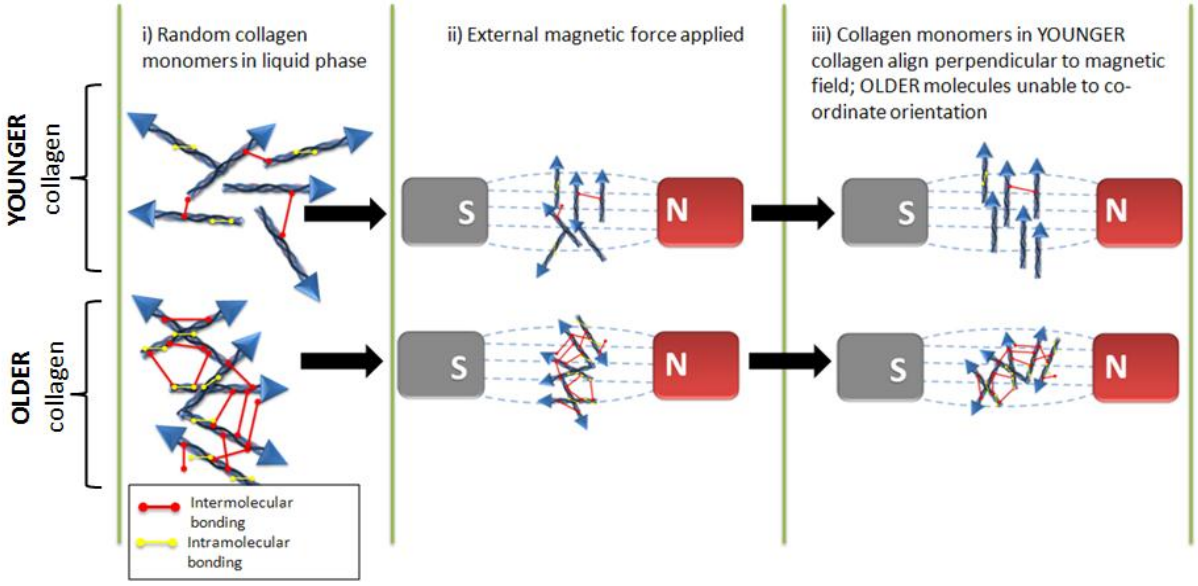

Figure 6.11: Schematic representation of the mechanisms of collagen alignment in young and aged collagen. The younger collagen monomers have less cross-linking and diamagnetic anisotropy and so can overcome thermo randomisation and align; older collagen monomers are unable to overcome thermo randomisation and thus remain random in their orientation.

6.6.2.1. Cellular alignment

When AHDCS cells were seeded onto the aligned and non-aligned 2D collagen surfaces that had been exposed to a high magnetic field, the orientation of the cell populations simply replicated the alignment architecture underneath, manifesting as parallel densely packed, aligned cell cytoskeletons in the younger collagen samples, whilst the cells on the older collagen specimens were randomly orientated in morphology and less densely packed. In fact, the aligned collagen fibers acted as contact guidance for the cells.

A similar phenomenon was also observed in the 3D collagen environments (which were not exposed to an external magnetic field) whereby the expression pattern of the actin filaments mirrored the mechanical properties of the hydrogels. The actin filaments in the younger collagen samples (newborn and 2 month) appeared denser and more organised, appearing to spontaneously align together without any external force; at both collagen

concentrations; whereas the older and subsequently more viscous constructs appeared disorganised and less dense in appearance, providing further evidence of collagen structural differences occurring.

6.6.3. The effect of ageing on the mechanical properties of collagen hydrogels

6.6.3.1. Modulus measurement

The different molecular structure of extracted collagens due to ageing can be used to explain the variation in the modulus of the acellular collagen samples. The formation of the collagen network and the alteration of the composition of the fibres with increasing age (Bailey, Paul 1999) has a bearing on its morphogenesis (Newman et al. 1997). The nature of the collagen cross-links alters with age, from reducible cross-links to a stable non-reducible form, which occurs through the formation of polyvalent cross links (Bishop, Laurent 1995). The more viscous, less movable monomers (due to aggregation or light cross-linking) or high molecular weight molecules in the older collagens resulted in lower density and less organised fibrils, fibres and fibre bundles. The presence of trimeric or polymeric tropocollagen or AGEs accumulation in the older collagen specimens caused difficulties regarding molecular rotation and movement during fibrillogenesis. As a result, the formed hydrogel had a poor quantity and quality of fibre packing resulting in a hydrogel construct with an amorphous-like ultrastructure in comparison to densely packaged fibrous structure in the younger specimens. Hence, at both 1.5 and 2.5 mg/ml collagen concentration, the younger collagen hydrogels (newborn and 2 month) with highly organised fibrous structures resulted in a higher scaffold modulus compared to the randomly and loosely packaged (older) specimens (6 month, 18 month and 2 years). This is consistent with mechanical properties appearing in both biological and non-biological engineering materials as organised (orientated) scaffolds increase the mechanical strength

of a scaffold when compared to disorganised (non-orientated) equivalents (Isobe et al. 2012). These observations are also in agreement with previous studies by Damodarasamy et al. (2010) whereby transmission electron microscopy analysis revealed that collagen fibrils formed from older collagens (approximately 2 years old) had thinner fibre diameters, reduced homogeneity and displayed less dense collagen networks in reconstituted collagen hydrogels when compared to younger specimens (4-5 month old).

6.6.3.2. Cellular contraction

The variation of elastic moduli in cell-containing constructs from different aged collagens involved slightly different mechanisms, which included the cellular contraction capability and cellular proliferation. In the present study, the corneal stromal cells used have a proven contraction capacity (as demonstrated in the previous chapters) when cultured in collagen hydrogels of rat-tail tendon origin under serum-containing medium. We and other groups have already observed that fibroblasts can "sense" the mechanical strength of their surrounding environment. They contract soft substrates through actin-myosin attachment mechanisms that are controlled by complex intracellular signalling pathways (Discher et al. 2005, Wang et al. 2012) and the contraction ceases once they have reached a harder environment. It has been proven that under the given fibrous collagen hydrogel, higher seeding cell numbers and lower collagen concentrations trigger the largest contraction rates (Ahearne et al. 2010b).

Although identical cell seeding densities and collagen concentrations were used for the different aged reconstituted collagen hydrogel constructs, the microstructures of the formed collagen hydrogels were quite different. The younger collagen hydrogel specimens consisted of a more organised, fibrous ultra-structure, with less AGEs accumulation, suggesting less inter-molecular cross-linking; whilst the older collagens consisted of more

randomly packed fibrous structures with higher AGEs accumulation, suggesting a highly cross-linked network. In our study, the cells contracted the soft, well organised and dispersed collagen fibre bundles in the younger, less viscous lower concentration collagen constructs more, displaying fibroblastic/myofibroblastic tendencies in both their behaviour and morphology. Thus, high contraction rates have been observed. The higher collagen concentration constructs (2.5 mg/ml) resulted in a higher initial stiffness of the constructs and a higher elastic modulus, which is in agreement with previous studies (Ahearne et al. 2010b). However, the concentration and viscosity of the construct affected the rate at which hydrogel contraction occurred as the individual AHDCS cells encountered different local mechanical environments in younger and older collagen hydrogel environments respectively as shown in **Figure 6.12**. Thus the lower concentration (1.5 mg.ml, lower viscosity, newborn and 2 month) specimens were able to contract at a faster rate which gave a higher overall collagen dense construct by the end of the culture period which manifested as a higher overall elastic modulus. The molecular organisation of ECM polymers controls the material properties and function of the ECM (Marenzana et al. 2006). In the older collagen specimens, the AHDCS cells were in contact with a highly cross-linked network. Intermolecular spacing of collagen molecules within fibrils increases with glycation, which alters the aggregation of collagen monomers into fibres, which subsequently alters collagen interactions with matrix components and cells (Bailey, Paul 1999). Despite the global hydrogel properties of older constructs being mechanically inferior to the younger counterparts, locally, the stiffness or hardness of the older collagen environment was much higher compared to the younger counterparts, hence resulting in lower contraction. The lower collagen concentration and younger less viscous specimens had less mechanical resistance for the AHDCS cells to contract and hence the contraction

was faster and easier. In addition, the increased cell proliferation rates in the younger collagens further emphasised this effect.

Irrespective of collagen concentration, the younger collagen hydrogel specimens consisted of more organised fibrous ultra-structures with less inter crosslinking and AGEs accumulation; whilst the older collagen hydrogels consisted of randomly packed fibrous structures with increased AGEs, suggesting a highly cross-linked network. Although the modulus of acellular collagen in the younger hydrogels was higher than in the older collagen, the cells applied strain that pulled and contracted the fibres and fibre bundles, not the entire construct, thus remodelling it. The cells in older collagens experienced a cross-linked aggregated collagen network. It is difficult for a single cell to contract this local network environment even though the older acellular collagen hydrogels had the lowest modulus. The local environment was already too great for an individual cell to overcome the strain of the matrix. A possible explanation why the modulus in youngest collagen specimens was highest is due to the additive effect of cell contraction, proliferation and high acellular modulus. Furthermore, the well packed acellular fibrous structure in the younger cellular collagen specimen guided cells' organisation. Upon contraction, the younger, denser collagen hydrogel constructs adopted a highly organised 3D structure, which has been confirmed by our actin staining images (**Figure 6.9A, F** and **G**). These experiments imply that we can predict hydrogel microstructure by fibroblast contractibility. We note that the cell contractibility in this study differs from previous previous studies, in which older collagens have a higher contraction capacity compared to younger collagens (Damodarasamy et al. 2010). The discrepany in these results may be due to the cell density, cell type and culture times investigated. We utilised collagen samples wherby all rats in the group were of the same age (as opposed to mixed groups in

the aforementaioned study), used youger age groups for comparison and made daily observations for 7 days (as opposed to a single 18 hr observation).

The acellular and cellular contraction experiments suggest that aged collagen is not really “stiffer” or “stronger” than the younger collagens. Instead, it is weak and less deformable. Our multiple measurements can be used to predict the microstructural changes in collagen during the ageing process through macroscopic parameter differences. Fibroblasts seeded into collagen hydrogels have previously been shown to influence the structural characteristics of the matrix (Ahearne et al. 2010b, Bell et al. 1979). Guidry and Grinnel (1985) have previously investigated the contraction of collagen gels using human skin fibroblasts seeded on the top of collagen constructs that were attached to an underlying solid support. They determined that gel reorganisation was not due to collagen degradation and that the protein content within the collagen gels was not destroyed. Thus the reorganisation and contraction of the gels occurred *via* a physical rearrangement of pre-existing collagen fibrils, rather than a replacement of the pre-existing fibrils *via* newly synthesised matrix (Guidry, Grinnell 1985). We expect that a similar scenario is occurring in our 3D experiments. In addition, the regular media changes in our investigation would have prevented the potential accumulation of matrix metalloproteinases (MMPs) that may degrade the collagen matrix.

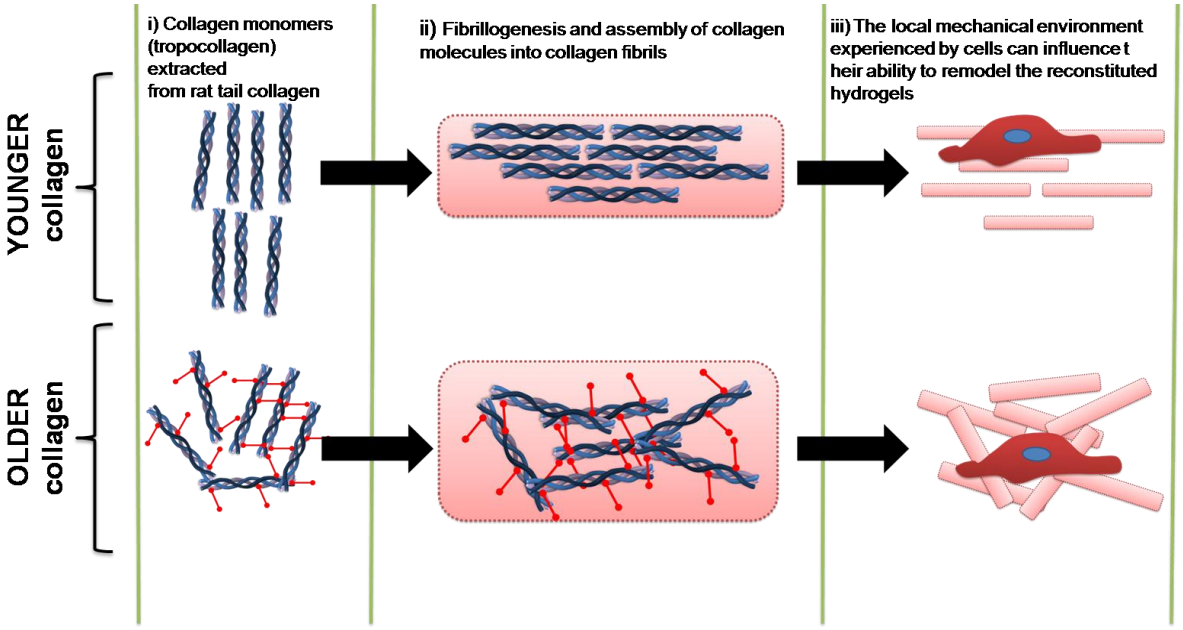

Figure 6.12: Schematic representation of the mechanisms of cellular collagen contraction in young and aged collagen. The cells in the younger collagens experienced densely packed collagen fibres or fibre bundles and were able to contract them; whilst cells encounter highly cross-linked collagen constructs in older collagen specimens and were unable to contract the specimens.

A potential limitation of the work presented in this chapter is that the different aged collagens have been quantified as equivalent collagen weights (i.e. mass per unit volume) as described in previous studies (Bartling et al, 2009, Jiang et al. 2000, Damodarasmay et al. 2009). As collagen ages its structure becomes more branched, therefore when the collagen backbone is broken down into its monomers, i.e. *via* enzymatic digestion, each monomer in the younger collagen is in its linear form, with a lower molecular mass compared to the older, more branched collagens. Thus the molecular weights and number of collagen monomers within each different aged reconstituted hydrogel construct was not taken into account, and so would be different, i.e. the constructs were not equivalent at a monomeric level (**Figure 6.13A**) resulting in more collagen monomer units in the younger collagens compared to the older collagens. However, once the collagens undergo

fibrillogenesis into reconstituted hydrogel constructs of the same mass/volume (i.e. 1.5 mg/ml and 2.5 mg/ml respectively), the comparisons that have been made are between the different aged hydrogel constructs of the same collagen density. It was at the reconstituted hydrogel stage that the hydrogels were being compared and utilised in this chapter. If the formula weight was used and normalised, i.e. the same number of collagen monomers included in the different aged constructs, then the resulting reconstituted hydrogel constructs would have been at different collagen densities (**Figure 6.13B**).

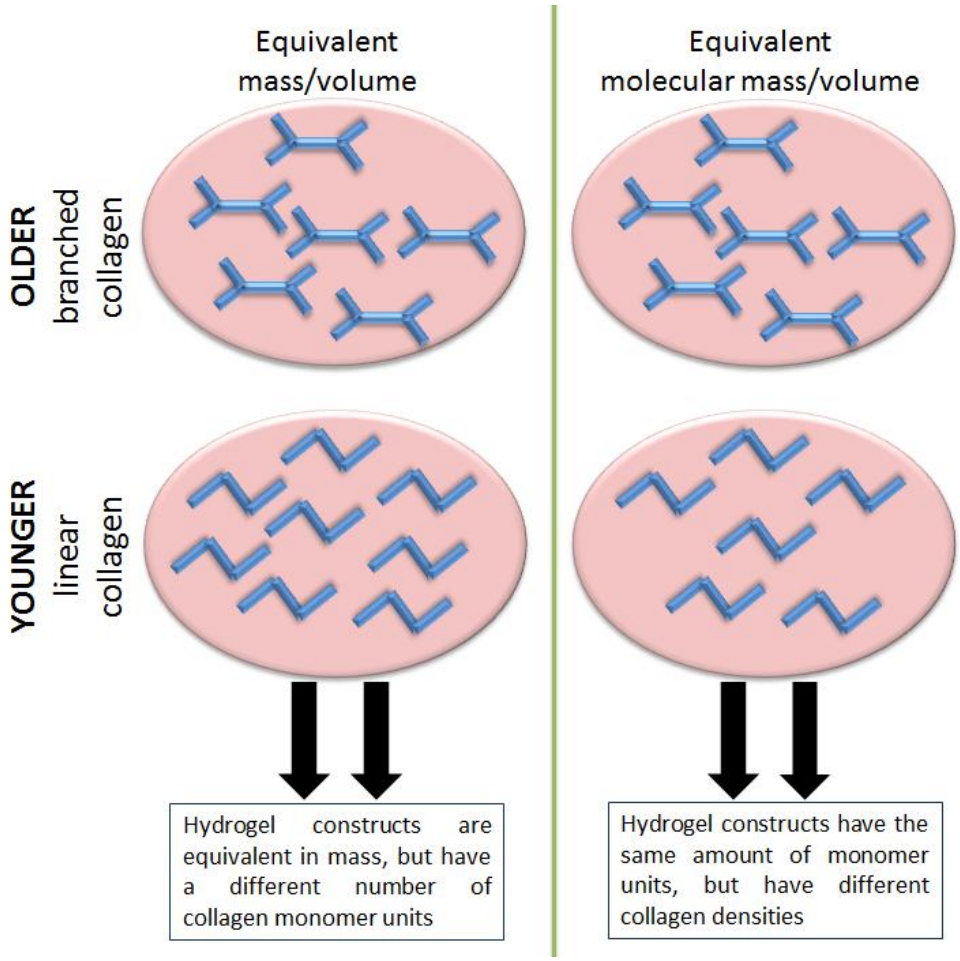

Figure 6.13: Schematic representation of hydrogel construct formation using either (A) equivalent mass per volume or (B) equivalent molecular mass of young, linear collagen versus aged, branched collagen.

6.7. Conclusion

It has been frequently documented that age-dependent intra- and inter-molecular cross-linking results in changes in the biophysical characteristics of purified soluble collagen (Jiang et al. 2000). Formation of AGEs might be the main process for the cross-linked structure. AGEs affect virtually every tissue in the human body (Semba et al. 2010) and accumulation of AGEs in collagenous tissue negatively affects tissue function (Haus et al. 2007) as it affects cellular signalling and activation of gene expression. ECM composition, matrix modelling proteinases and integrins are all important factors modulating cell behaviour, in terms of migration, proliferation, spatial organisation and differentiation *in vitro* and *in vivo* (Jiang et al. 2000). Our findings are in agreement with previous studies (Jiang et al. 2000, Bruel, Oxlund 1996) in that increasing age causes structural changes in collagen, which triggers downstream reactions. In studies on intramuscular connective tissue (Haus et al. 2007) it was suggested that differences in AGEs concentration in young and old tissues *in vivo* was related to the chronological component of ageing in that the longer the protein residues are exposed to glucose, the greater is the risk of AGEs formation (Haus et al. 2007). The rate by which glycation occurs may be influenced by the location of glycation sites (Lingelbach et al. 2000) which differ with age, thus causing increased differences in the collagen structure. Age-related differences in the degree of collagen cross-linking certainly lead to changes in rigidity of 3D structure of the reconstructed collagen hydrogels (Jiang et al. 2000).

It has been demonstrated that increasing age of collagen has a direct impact on the biomechanical properties of reconstituted 3D collagen constructs. A combination of non-destructive monitoring techniques has been utilised to demonstrate the effect the collagen matrix has on the cells' ability to manipulate and remodel their surrounding environment.

It has been shown that younger collagen constructs are mechanically stronger and are more easily remodelled by cells. In addition the younger collagens are less viscous and are able to form more organised tissues with regards to the collagen fibril arrangement. This has important connotations for tissue engineered tissues as it is the 3D nano-structure and microstructure (the mesostructure) that are pivotal to their success. This research has revealed that we are able to predict microscopic differences in the collagen monomer and hydrogel constructs by measuring macroscopic parameters, which provides a good platform to further investigate the mechanisms of ageing and the screening of new agents for slowing the ageing process.

7. Conclusions and future recommendations

7.1. Concluding remarks

One of the most demanding challenges in corneal biology and tissue engineering is to replicate corneal regenerative mechanisms as opposed to reparative processes associated with tissue fibrosis. Literature suggests that differentiation of myofibroblasts to fibroblasts in achievable. However, it is the differentiation of myofibroblastic and fibroblastic cells back to the keratocyte lineage that has yet to be clearly established and still remains an important question that we have attempted to address in this body of work.

A number of techniques and methods have been explored in order to mimic and exploit the regenerative capacity of corneal stromal cells. Non-destructive characterisation techniques have been developed and an existing mechanical testing rig was improved and used to characterise the mechanical properties of cell-seeded collagen hydrogel corneal equivalents under sterile culture conditions without risk of damage or infection to the cells or constructs. Environmental, chemical, topographical and biological interactions have all been considered and investigated and their influence on the macroscopic properties of the construct (elastic modulus and thickness change) have been monitored for prolonged culture periods. The mechanical property change served as a biomarker of cell behaviour which was corroborated using more "traditional" techniques such as immunohistochemical, morphological and genetic characterisation.

It has been demonstrated that chemical and topographical cues can be used to manipulate the phenotype of cultured AHDCS cells. Tailoring of the culture niche has been shown to encourage stromal cells towards keratocyte, fibroblast or myofibroblast lineages in 2D, semi-3D and 3D collagen environments. This is important in highlighting that the stromal cell phenotype is interchangeable *ex vivo*. The removal of serum from media and

the introduction of stiff, orthogonally arranged nanofibre layers caused cultured stromal cells that were fibroblastic in phenotype to revert to a quiescent, non proliferative, elongated keratocyte-like phenotype with increased cell organisation. The combination of chemical and topographical manipulation in a 3D hydrogel environment caused the most significant alteration to the stromal cell phenotype and genotype. Following two weeks culture the once fibroblastic cells were not only quiescent and non-proliferative, but also showed a significant up-regulation of gene markers specific to the keratocyte phenotype and a significant down-regulation of fibroblastic markers. These results provide valuable new insights of the significance of chemical and topographical cues in mimicking the native environment for the development of new regenerative strategies for corneal repair and regeneration. However as highlighted in this research, the transformation remains incomplete and some fibroblastic tendencies remained. This could have been due to the fact that fundamental biological cues were absent from our niche environment.

In vivo it is the interactions between the keratocytes and adjacent epithelial cells that are vital to maintaining tissue homeostasis and transparency. Often a wound healing response or cell activation is instigated *via* the loss or disruption of the corneal epithelium; which disrupts the complex cellular communication that is usually so pivotal to maintaining organ function. It is the restoration of the epithelium which often determines as to whether the wound healing response is regenerative or fibrotic. Since *in vivo* keratocyte activity does not manifest until the corneal surface has been re-epithelialised it is unsurprising that corneal regeneration and full keratocyte differentiation was not achieved by chemical and topographical manipulation alone. Thus in order to rectify this, the use of epithelial-stromal co-culturing was investigated. It was demonstrated that the restoration of biological interactions are potentially more pivotal to the niche environment in the restoration of the keratocyte phenotype than chemical and topographical cues. It has been established that

through the use of co-culturing techniques it is possible to revert cultured corneal stromal cells that are fibroblastic in lineage to a native keratocyte phenotype *in vitro.* The addition of an epithelial culture caused contractile, fibroblastic cells to significantly alter in morphology and behaviour. The fusiform, larger fibroblastic cells changed in morphology into smaller cells with multiple dendritic processes. Immunohistochemical analysis using an extensive panel of known keratocyte/fibroblastic markers revealed significant changes regarding protein expression; co-cultured stromal cells stained positive for all keratocyte markers and negative for all fibroblastic markers. It also revealed that there may be a period whereby the stromal cells undergo a transitional stage in their differentiation whereby they have both keratocyte and fibroblastic characteristics. This study was important in highlighting that the mechanical properties of the cornea may be defined by epithelial-stromal interactions and that the corneal stroma requires the presence of the epithelium for stromal cells to reach a mature keratocyte phenotype. Most importantly, it demonstrates that despite *in vitro* culturing, corneal stromal cells retain their plasticity. This was further confirmed by the fact that following fibroblast-keratocyte differentiation, the cells could differentiate again following TGF-β1 media supplementation.

The method of activating corneal keratocytes into their fibroblastic lineage and then being able to differentiate them back to the keratocyte lineage is vital to corneal tissue engineering with its benefits being threefold; firstly, it allows for sufficient numbers of corneal stromal cells to be grown up quickly and easily in serum containing media; secondly the ability to differentiate the expanded activated cells back to a keratocyte linage is important in aiding our understanding of corneal wound healing mechanisms and the importance of the cell interactions during these processes; and finally it allows us to engineer corneal tissues that more closely mimic the native cornea, with stromal cells that are in a healthy uninjured state which may have the potential to act as an important tool in

with regards to toxicity testing of drugs and irritants which could in turn improve the development of new and improved ocular drugs to treat corneal disease and/or injury.

Collagen was used as a scaffold intensively and exclusively throughout this work. It has been verified that the natural alteration of collagen structure caused by the ageing process has a direct impact on the biomechanical properties of the resulting hydrogel constructs. Older collagens gave rise to constructs that were mechanically inferior compared to their younger counterparts. The highly-crossed linked amorphous structures were unable to successfully align during fibrillogenesis, despite the application of an external magnetic force. When collagen constructs were seeded with corneal stromal cells, they were able to easily remodel and contract the younger collagen specimens, which resulted in constructs with a higher elastic modulus. In addition the cellular interaction resulted in constructs that were more organised and collagen dense. The macroscopic changes enable us to predict microscopic difference regarding the collagen monomer structure and arrangement. This has important connotations for tissue engineered tissues, in particular corneal tissue engineering as it is the 3D nanostructure and microstructure that are pivotal to their success.

7.2. Future Recommendations

There are several recommendations for future research resulting from this thesis. One of the most important findings from this work was that cultured corneal stromal cells retained their plasticity and demonstrated the capability to differentiate multiple times whilst cultured in a 3D collagen hydrogel environment. Control of the stromal cell phenotype is vital to tissue engineering corneal equivalents as it allows for models to be engineered that more closely mimic a healthy native tissue. This has important connotations for both the refinement and replacement of *in vivo* toxicity testing models and as a potential alternative

to corneal allografts. However, the epithelial cells utilised in these studies to achieve keratocyte differentiation were porcine in origin. Although tissues and matrices of porcine origin are well used in many tissue engineering applications and porcine corneas are anatomically similar and have been shown to be tolerated following heterogeneous implantation (onto rhesus monkeys), a prevailing problem linked to their usage is disease transmission and graft failure due to discrete interspecies and structural differences. Also poor public perceptions of the use of xeno-materials mean that the use of such materials is unlikely to progress further than pre-clinical research. In order to alleviate such a problem human epithelial tissue needs to be sought, sourced and used in place of porcine cells.

It has been demonstrated that biological interactions and the use of co-culture was the most suitable niche environment for restoration of the keratocyte phenotype; however the differentiated stromal cells within these constructs still lacked the *in vivo* tissue organisation. Future experimentation could combine both biological and topographical cues into the stromal layer model; in doing so both organisation and keratocyte phenotype would be incorporated into the *in vitro* stroma.

Furthermore, although the choice of nanofibre material (PLDLA) used to increase cellular organisation has been FDA approved, no investigation into the degradation properties of the nanofibres was performed in this body of work. Degradation of synthetic polymers occurs *via* hydrolysis reactions, causing the release of acidic by-products. As the polymer degrades the local environment becomes more acidic, causing an auto-catalytic reaction. The incurring pH changes could affect cell behaviour and response, i.e. causing a fibrotic activation of the cells or cell apoptosis. Extensive studies investigating the nanofibre degradation are required before this could be definitively determined. The degradation rate of the fibres in terms of mechanical stability would also need to be

characterised to determine how/if the constructs changed in mechanical stiffness over time. It is hypothesised that the ECM deposited by the cells would increase the stiffness of the construct, thus compensating for the degradation of the nanofibrous support and that regular media changes may prevent the potentially harmful (to cells) build up of acidic products.

Another potential avenue for exploration would be the inclusion of electrospun collagen type-I nanofibres. Literature suggests that currently, although problematic, it is possible to electrospin collagen or collagen polymer solutions. A current drawback is that the solvent solutions used to achieve release by-products which are toxic to the cells. Extensive studies would have to first be performed to ascertain the optimum conditions and electrospinning solutions whereby a suitable solvent that is non-toxic to cells is identified. Also, a reduction in the nanofibre diameter so that they more closely mimic the native collagen fibrils is desirable. The current fibril diameter of the electrospun nanofibers used in the hydrogel constructs is currently approximately 500 nm. The diameters of the collagen fibrils in an *in vivo* human cornea are 25-35 nm. In order to achieve diameters so small, various parameters would need to be investigated and adjusted accordingly, primarily the concentration of the polymer used in the electrospinning solution.

It should also be noted that the stromal layer equivalents produced in this body of work are considerably lower in modulus that the native tissue that they are attempting to mimic. The inclusion of an increased number of nanofibre meshes (i.e. more than three) and increasing the overall collagen concentration of the constructs would be a sensible starting point. It was also demonstrated in the final experimental chapter that the source and processing of collagen has an impact on not only its mechanical properties but also the cell's ability to interact with and remodel the surrounding matrix. A scale-up process whereby collagen at high concentration from young-age animals could be achieved could

provide an optimal collagen starting material which could negate the need for the inclusion of nanofibre meshes; thus making production and assembly time faster and potentially more cost effective.

Due to time and monetary constraints the corneal stromal cells differentiated in the co-culture studies were characterised using immunohistochemical techniques. Although a positive outcome was achieved, immunohistochemical techniques are subject to criticism as they are not a quantifiable technique. Although the cells were distinctly different in morphology to the cells that were partially differentiated in the media and topography studies it was still only assumed that the differentiation had been more complete in these studies. Thus complementary q-PCR analysis would validate our assumptions. This would confirm as to whether expression of the keratocyte markers was further up-regulated due to the presence of an epithelial cell culture or not. Also, it would be beneficial to know the gene expression profiles of the native stromal cells. Despite our best efforts we were unable to successfully isolate and purify adequate volumes of RNA information from native corneal tissue. Although we demonstrated that the cultured stromal cells were distinctly different from the fibroblastic stromal cells cultured in the presence of serum, we were unable to definitely say how close we were to a naive healthy keratocyte genotype. The use of a homogeniser or sonocation techniques in combination with the use of digestion enzymes such as collagenase could be investigated and optimised in order to ascertain a more complete analysis.

Although the use of epithelial-stromal co-cultures was proven to be hugely advantageous we were unable to produce a complete epithelial-stromal equivalent whereby both cell types were included in a homogenous construct that could be characterised both mechanically and immunohistochemically. This was due to problems associated with adhesion and viability of epithelial cells following passaging. Explant co-culturing was the

closest that we came to achieving an epithelial-stromal *in vitro* equivalent. However, due to fact that there were pieces of tissue attached to the collagen construct, mechanical testing with regards to elastic modulus measurement using the spherical indentation technique was not possible. Removal of the explanted tissue once confluence had been achieved still resulted in a non-homogenous surface. A potential avenue for exploration could be the use of thermo-responsive tissue culture plastic. This technique could potentially be used to produce intact sheets of epithelial cells, complete with matrix which could then be transferred to the collagen stromal layer thus producing a homogenous epithelial-stromal corneal construct.

Optical transparency is another factor that needs to be considered when developing *in vitro* corneal equivalents. Although transparency was not measured as a parameter in the body of this work, a future recommendation would be the use of an optical system capable of providing objective measurements of corneal equivalent tissues in comparison to freshly isolated corneas. Spectrophotometry techniques could be investigated as a means of measuring light scattering and absorbance to accurately ascertain and quantify light transmission through corneal tissues and tissue engineered equivalents.

Finally, the corneal equivalents could be further developed *via* the inclusion of an endothelial culture. This would provide a full thickness corneal equivalent, whereby epithelial-stromal-endothelial interactions could be monitored. It can be hypothesised that the inclusion of the three fundamental cellular layers would further improve the restoration of the keratocyte phenotype to cultured stromal cells within the 3D collagen hydrogel environment.

References

ABITBOL, O., BOUDEN, J., DOAN, S., HOANG-XUAN, T. and GATINEL, D., 2010. Corneal hysteresis measured with the Ocular Response Analyzer (R) in normal and glaucomatous eyes. *Acta Ophthalmologica,* **88**(1), pp. 116-119.

AGRAWAL, V.B. and TSAI, R.J.F., 2003. Corneal epithelial wound healing. *Indian journal of ophthalmology,* **51**(1), pp. 5-15.

AHEARNE, M., 2007. Mechanical characterisation of cornea and corneal stromal equivalents, *PhD Thesis,* Keele University.

AHEARNE, M., LIU, K., EL HAJ, A.J., THEN, K.Y., RAUZ, S. and YANG, Y., 2010a. Online Monitoring of the Mechanical Behavior of Collagen Hydrogels: Influence of Corneal Fibroblasts on Elastic Modulus. *Tissue Engineering Part C-Methods,* **16**(2), pp. 319-327.

AHEARNE, M., SIAMANTOURAS, E., YANG, Y. and LIU, K.K., 2009. Mechanical characterization of biomimetic membranes by micro-shaft poking. *Journal of the Royal Society Interface,* **6**(34), pp. 471-478.

AHEARNE, M., WILSON, S.L., LIU, K., RAUZ, S., EL HAJ, A.J. and YANG, Y., 2010b. Influence of cell and collagen concentration on the cell-matrix mechanical relationship in a corneal stroma wound healing model. *Experimental eye research,* **91**(5), pp. 584-591.

AHEARNE, M., YANG, Y., EL HAJ, A.J., THEN, K.Y. and LIU, K.K., 2005. Characterizing the viscoelastic properties of thin hydrogel-based constructs for tissue engineering applications. *Journal of the Royal Society Interface,* **2**(5), pp. 455-463.

AHEARNE, M., YANG, Y., THEN, K.Y. and LIU, K.K., 2007. An indentation technique to characterize the mechanical and viscoelastic properties of human and porcine corneas. *Annals of Biomedical Engineering,* **35**(9), pp. 1608-1616.

AHEARNE, M., YANG, Y., THEN, K.Y. and LIU, K., 2008. Non-destructive mechanical characterisation of UVA/riboflavin crosslinked collagen hydrogels. *British Journal of Ophthalmology,* **92**(2), pp. 268-271.

AINSCOUGH, S.L., LINN, M.L., BARNARD, Z., SCHWAB, I.R. and HARKIN, D.G., 2011. Effects of fibroblast origin and phenotype on the proliferative potential of limbal epithelial progenitor cells. *Experimental eye research,* **92**(1), pp. 10-19.

ALAMINOS, M., SANCHEZ-QUEVDO, M.D., MUNOZ-AVILA, J.I., SERRANO, D., MEDIALDEA, S., CARRERAS, I. and CAMPOS, A., 2006. Construction of a complete rabbit cornea substitute using a fibrin-agarose scaffold. *Investigative ophthalmology & visual science,* **47**(8), pp. 3311-3317.

ALLAN, B., 1999. Artificial corneas - Risks of complications are high now, but better materials are on the way. *British medical journal,* **318**(7187), pp. 821-822.

ANDERSON, K., EL-SHEIKH, A. and NEWSON, T., 2004. Application of structural analysis to the mechanical behaviour of the cornea. *Journal of the Royal Society Interface,* **1**(1), pp. 3-15.

ANSETH, K.S., BOWMAN, C.N. and BRANNONPEPPAS, L., 1996. Mechanical properties of hydrogels and their experimental determination. *Biomaterials,* **17**(17), pp. 1647-1657.

AURELL, G. & HOLMGREN, H. 1953. On the metachromatic staining of the corneal tissue and some observations on its transparency. *Acta Ophthalmologica,* 31**,** 1-27.

AZAR, D. T., ANG, R. T., LEE, J. B., KATO, T., CHEN, C. C., JAIN, S., GABISON, E. & ABAD, J. C. 2001. Laser subepithelial keratomileusis: electron microscopy and visual outcomes of flap photorefractive keratectomy. *Current opinion in ophthalmology,* 12**,** 323-8.

BAGNANINCHI, P.O., YANG, Y., ZGHOUL, N., MAFFULLI, N., WANG, R.K. and EL HAJ, A.J., 2007. Chitosan microchannel scaffolds for tendon tissue engineering characterized using optical coherence tomography. *Tissue engineering,* **13**(2), pp. 323-331.

BAILEY, A.J., 2002. Changes in bone collagen with age and disease. *Journal of Musculoskeletal & Neuronal Interactions,* **2**(6), pp. 529-531.

BAILEY, A. and PAUL, R., 1999. The mechanisms and consequences of the maturation and ageing of collagen. *Proceedings of the Indian Academy of Sciences-Chemical Sciences,* **111**(1), pp. 57-69.

BAKER, B. M., NATHAN, A. S., GEE, A. O. & MAUCK, R. L. 2010. The influence of an aligned nanofibrous topography on human mesenchymal stem cell fibrochondrogenesis. *Biomaterials,* 31**,** 6190-6200.

BALDWIN, H. and MARSHALL, J., 2002. Growth factors in corneal wound healing following refractive surgery: A review. *Acta Ophthalmologica Scandinavica,* **80**(3), pp. 238-247.

BARADARAN-RAFII, A., KARIMIAN, F., JAVADI, M.A., JAFARINASAB, M.R., NOWROOZPOUR, K., HOSSEINI, M. and ANISIAN, A., 2007. Corneal Graft Rejection: Incidence and Risk Factors. *Iranian Journal of Opthalimis Research,* **2**(1), pp. 7-14.

BARRY, P.A., CAVANAGH, H.D. and JESTER, J.V., 1994. Effect of Serum, Bfgf, Tgf(beta-1) and Heparin on In-Vitro Myofibroblast Transformation in Rabbit Corneal Keratocytes. *Investigative ophthalmology & visual science,* **35**(4), pp. 1356-1356.

BARTLING, B., DESOLE, M., ROHRBACH, S., SILBER, R. E. & SIMM, A. 2009. Age-associated changes of extracellular matrix collagen impair lung cancer cell migration. *FASEB J,* 23**,** 1510-20.

BEALES, M.P., FUNDERBURGH, J.L., JESTER, J.V. and HASSELL, J.R., 1999. Proteoglycan synthesis by bovine keratocytes and corneal fibroblasts: Maintenance of the

keratocyte phenotype in culture. *Investigative ophthalmology & visual science,* **40**(8), pp. 1658-1663.

BEGLEY, M.R. and MACKIN, T.J., 2004. Spherical indentation of freestanding circular thin films in the membrane regime. *Journal of the Mechanics and Physics of Solids,* **52**(9), pp. 2005-2023.

BELL, E., IVARSSON, B. and MERRILL, C., 1979. Production of a Tissue-Like Structure by Contraction of Collagen Lattices by Human-Fibroblasts of Different Proliferative Potential Invitro. *Proceedings of the National Academy of Sciences of the United States of America,* **76**(3), pp. 1274-1278.

BELLMUNT, M. J., PORTERO, M., PAMPLONA, R., COSSO, L., ODETTI, P. & PRAT, J. 1995. Evidence for the Maillard reaction in rat lung collagen and its relationship with solubility and age. *Biochimica et Biophysica Acta,* 1272**,** 53-60.

BERNSTEIN, A.M., TWINING, S.S., WAREJCKA, D.J., TALL, E. and MASUR, S.K., 2007. Urokinase receptor cleavage: A crucial step in 14 fibroblast-to-myofibroblast differentiation. *Molecular biology of the cell,* **18**(7), pp. 2716-2727.

BERRYHILL, B.L., KADER, R., KANE, B., BIRK, D.E., TENG, J. and HASSELL, A.R., 2002. Partial restoration of the keratocyte phenotype to bovine keratocytes made fibroblastic by serum. *Investigative ophthalmology & visual science,* **43**(11), pp. 3416-3421.

BISHOP, J. and LAURENT, G., 1995. Collagen Turnover and its Regulation in the Normal and Hypertrophying Heart. *European heart journal,* **16**(3), pp. 38-44.

BONEVA, R.S. and FOLKS, T.M., 2004. Xenotransplantation and risks of zoonotic infections. *Annals of Medicine,* **36**(7), pp. 504-517.

BOOTE, C., DENNIS, S., HUANG, Y.F., QUANTOCK, A.J. and MEEK, K.M., 2005. Lamellar orientation in human cornea in relation to mechanical properties. *Journal of structural biology,* **149**(1), pp. 1-6.

BORENE, M.L., BAROCAS, V.H. and HUBEL, A., 2004. Mechanical and cellular changes during compaction of a collagen-sponge-based corneal stromal equivalent. *Annals of Biomedical Engineering,* **32**(2), pp. 274-283.

BRON, A., 2001. The architecture of the corneal stroma. *British Journal of Ophthalmology,* **85**(4), pp. 379-381.

BROWN, R.A., 2006. Cytomechanics in connective tissue repair and engineering. In: Tissue repair, Contraction and the Myofibroblast. Edited by, CHAPONNIER C. and DEMOULIERE, A., *Biotechnology Intelligence Unit,* 233 SPRING STREET, New York, NY 10013, UNITED STATES:, pp. 7-24.

BROWN, R., WISEMAN, M., CHUO, C., CHEEMA, U. and NAZHAT, S., 2005. Ultrarapid engineering of biomimetic materials and tissues: Fabrication of nano- and

microstructures by plastic compression. *Advanced Functional Materials,* **15**(11), pp. 1762-1770.

BRUEL, A. and OXLUND, H., 1996. Changes in biomechanical properties, composition of collagen and elastin, and advanced glycation endproducts of the rat aorta in relation to age. *Atherosclerosis,* **127**(2), pp. 155-165.

BUILLES, N., BECHETOILLE, N., JUSTIN, V., DUCERF, A., AUXENFANS, C., BURILLON, C., SERGENT, M. and DAMOUR, O., 2006. Development of an optimised culture medium for keratocytes in monolayer. *Bio-medical materials and engineering,* **16**(4), pp. 95-104.

BURTON, A.B.G., YORK, M. and LAWRENCE, R.S., 1981. The Invitro Assessment of Severe Eye Irritants. *Food and cosmetics toxicology,* **19**(4), pp. 471-480.

BUSSOLINO, F., DIRENZO, M., ZICHE, M., BOCCHIETTO, E., OLIVERO, M., NALDINI, L., GAUDINO, G., TAMAGNONE, L., COFFER, A. and COMOGLIO, P., 1992. Hepatocyte Growth-Factor is a Potent Angiogenic Factor which Stimulates Endothelial-Cell Motility and Growth. *Journal of Cell Biology,* **119**(3), pp. 629-641.

CAMELLIN, M. 2003. Laser epithelial keratomileusis for myopia. *Journal of Refractive Surgery,* 19**,** 666-670.

CARLSSON, D.J., LI, F., SHIMMURA, S. and GRIFFITH, M., 2003a. Bioengineered corneas: how close are we? *Curr Opin Ophthalmol,* **14**(4), pp. 192-7.

CARLSON, E., WANG, I., LIU, C., BRANNAN, P., KAO, C. and KAO, W., 2003b. Altered KSPG expression by keratocytes following corneal injury. *Molecular Vision,* **9**(75), pp. 615-623.

CARRINGTON, L., ALBON, J., ANDERSON, I., KAMMA, C. and BOULTON, M., 2006. Differential regulation of key stages in early corneal wound healing by TGF-beta Isoforms and their inhibitors. *Investigative ophthalmology & visual science,* **47**(5), pp. 1886-1894.

CAUICH-RODRIGUEZ, J. V., DEB, S. & SMITH, R. 1996. Effect of cross-linking agents on the dynamic mechanical properties of hydrogel blends of poly(acrylic acid)-poly(vinyl alcohol-vinyl acetate). *Biomaterials,* 17**,** 2259-2264.

CHAN, K. and HASCHKE, R., 1983. Epithelial-Stromal Interactions - Specific Stimulation of Corneal Epithelial-Cell Growth-Invitro by a Factor(s) from Cultured Stromal Fibroblasts. *Experimental eye research,* **36**(2), pp. 231-246.

CHANDRASEKHER, G. & BAZAN, H. E. P. 1999. Corneal epithelial wound healing increases the expression but not long lasting activation of the p85 alpha subunit of phosphatidylinositol-3 kinase. *Current eye research,* 18**,** 168-176.

CHAREST, J. L., GARCÍA, A. J. & KING, W. P. 2007. Myoblast alignment and differentiation on cell culture substrates with microscale topography and model chemistries. *Biomaterials,* 28**,** 2202-2210.

CHAURASIA, S. S., KAUR, H., DE MEDEIROS, F. W., SMITH, S. D. & WILSON, S. E. 2009. Reprint of "Dynamics of the expression of intermediate filaments vimentin and desmin during myofibroblast differentiation after corneal injury". *Experimental eye research,* 89**,** 590-596.

CHEEMA, C., BROWN, R.A., ALP, B. and MACROBERT, A.J., 2008. Spatially defined oxygen gradients and vascular endothelial growth factor expression in an engineered 3D cell model. *Cellular and Molecular Life Sciences,* **65**(1), pp. 177-186.

CHIRILA, T.V., 2001. An overview of the development of artificial corneas with porous skirts and the use of PHEMA for such an application. *Biomaterials,* **22**(24), pp. 3311-3317.

CHOMCZYNSKI, P. and SACCHI, N., 1987. Single-Step Method of Rna Isolation by Acid Guanidinium Thiocyanate Phenol Chloroform Extraction. *Analytical Biochemistry,* **162**(1), pp. 156-159.

COSTER, D.J., JESSUP, C.F. and WILLIAMS, K.A., 2009. Mechanisms of corneal allograft rejection and regional immunosuppression. *Eye,* **23**(10), pp. 1894-1897.

DAYHAW-BARKER, P., 1995a. Corneal wound healing: I. The players. *International Contact Lens Clinic,* **22**(5), pp. 105-109.

DAYHAW-BARKER, P., 1995b. Corneal wound healing: II. The process. *International Contact Lens Clinic,* **22**(5), pp. 110-116.

DISCHER, D. E., JANMEY, P. & WANG, Y.-L. 2005. Tissue Cells Feel and Respond to the Stiffness of Their Substrate. *Science,* 310**,** 1139-1143.

DU, Y., SUNDARRAJ, N., FUNDERBURGH, M.L., HARVEY, S.A., BIRK, D.E. and FUNDERBURGH, J.L., 2007. Secretion and organization of a cornea-like tissue in vitro by stem cells from human corneal stroma. *Investigative ophthalmology & visual science,* **48**(11), pp. 5038-5045.

DUPPS, W.J. and WILSON, S.E., 2006. Biomechanics and wound healing in the cornea. *Experimental eye research,* **83**(4), pp. 709-720.

EGUCHI, H., HICKS, C.R., CRAWFORD, G.J., TAN, D.T. and SUTTON, G.R., 2004. Cataract surgery with the AlphaCor artificial cornea. *Journal of cataract and refractive surgery,* **30**(7), pp. 1486-1491.

EKSER, B., EZZELARAB, M., HARA, H., VAN DER WINDT, D. J., WIJKSTROM, M., BOTTINO, R., TRUCCO, M. & COOPER, D. K. C. 2012. Clinical xenotransplantation: the next medical revolution? *Lancet,* 379**,** 672-683.

ELSHEIKH, A. and ANDERSON, K., 2005. Comparative study of corneal strip extensometry and inflation tests. *Journal of the Royal Society Interface,* **2**(3), pp. 177-185.

ENGLER, A.J., SEN, S., SWEENEY, H.L. and DISCHER, D.E., 2006. Matrix elasticity directs stem cell lineage specification. *Cell,* **126**(4), pp. 677-689

ESPANA, E.M., HE, H., KAWAKITA, T., DI PASCUALE, M.A., RAJU, V.K., LIU, C.Y. and TSENG, S.C.G., 2003. Human keratocytes cultured on amniotic membrane stroma preserve morphology and express keratocan. *Investigative ophthalmology & visual science,* **44**(12), pp. 5136-5141.

ESPANA, E.M., KAWAKITA, T., LIU, C.Y. and TSENG, S.C.G., 2004. CD-34 expression by cultured human keratocytes is downregulated during myofibroblast differentiation induced by TGF-beta 1. *Investigative ophthalmology & visual science,* **45**(9), pp. 2985-2991.

ESPANA, E., KAWAKITA, T., LIU, C.Y. and TSENG, S.C.G,, 2005. The Heterogeneous Murine Corneal Stromal Cell Populations in Vitro. *Investigative Ophthalmology & Visual Science,* **46**(12), pp. 4528-4535.

ETHEREDGE, L., KANE, B.P. and HASSELL, J.R., 2009. The Effect of Growth Factor Signaling on Keratocytes In Vitro and Its Relationship to the Phases of Stromal Wound Repair. *Investigative ophthalmology & visual science,* **50**(7), pp. 3128-3136.

FAGERHOLM, P., LAGALI, N. S., MERRETT, K., JACKSON, W. B., MUNGER, R., LIU, Y., POLAREK, J. W., SÖDERQVIST, M. & GRIFFITH, M. 2010. A Biosynthetic Alternative to Human Donor Tissue for Inducing Corneal Regeneration: 24-Month Follow-Up of a Phase 1 Clinical Study. *Science and Translational Medicine,* 2**,** 46-61.

FINI, M.E., 1999. Keratocyte and fibroblast phenotypes in the repairing cornea. *Progress in retinal and eye research,* **18**(4), pp. 529-551.

FREDJREYGROBELLET, D., PLOUET, J., DELAYRE, T., BAUDOUIN, C., BOURRET, F. & LAPALUS, P. 1987. Effects of αFGF and βFGF on wound-healing in rabbit corneas. *Current Eye Research,* 6**,** 1205-1209.

FULLWOOD, N.J., 2004. Collagen fibril orientation and corneal curvature. *Structure,* **12**(2), pp. 169-170.

FUNDERBURGH, J., FUNDERBURGH, M., MANN, M., CORPUZ, L. and ROTH, M., 2001. Proteoglycan expression during transforming growth factor beta-induced keratocyte-myofibroblast transdifferentiation. *Journal of Biological Chemistry,* **276**(47), pp. 44173-44178.

FUNDERBURGH, J., HEVELONE, N., ROTH, M., FUNDERBURGH, M., RODRIGUES, M., NIRANKARI, V. and CONRAD, G., 1998. Decorin and biglycan of

normal and pathologic human corneas. *Investigative ophthalmology & visual science,* **39**(10), pp. 1957-1964.

FUNDERBURGH, J.L., MANN, M.M. and FUNDERBURGH, M.L., 2003. Keratocyte phenotype mediates proteoglycan structure - A role for fibroblasts in corneal fibrosis. *Journal of Biological Chemistry,* **278**(46), pp. 45629-45637.

FUNDERBURGH, M., DU, Y., MANN, M., SUNDARRAJ, N. and FUNDERBURGH, J., 2005. PAX6 expression identifies progenitor cells for corneal keratocytes. *Faseb Journal,* **19**(7), pp. 1371-1373.

GABISON, E.E., HUET, E., BAUDOUIN, C. and MENASHI, S., 2009. Direct epithelial-stromal interaction in corneal wound healing: Role of EMMPRIN/CD147 in MMPs induction and beyond. *Progress in retinal and eye research,* **28**(1), pp. 19-33.

GARANA, R., PETROLL, W., CHEN, W., HERMAN, I., BARRY, P., ANDREWS, P., CAVANAGH, H. and JESTER, J., 1992. Radial Keratotomy .2. Role of the Myofibroblast in Corneal Wound Contraction. *Investigative ophthalmology & visual science,* **33**(12), pp. 3271-3282.

GERMAIN, L., CARRIER, P., AUGER, F.A., SALESSE, C. and GUERIN, S.L., 2000. Can we produce a human corneal equivalent by tissue engineering? *Progress in retinal and eye research,* **19**(5), pp. 497-527.

GLASS, D.H., ROBERTS, C.J., LITSKY, A.S. and WEBER, P.A., 2008. A viscoelastic biomechanical model of the cornea describing the effect of viscosity and elasticity on hysteresis. *Investigative ophthalmology & visual science,* **49**(9), pp. 3919-3926.

GONZALEZ-ANDRADES, M., DE LA CRUZ CARDONA, J., MARIA IONESCU, A., CAMPOS, A., DEL MAR PEREZ, M. and ALAMINOS, M., 2011. Generation of Bioengineered Corneas with Decellularized Xenografts and Human Keratocytes. *Investigative ophthalmology & visual science,* **52**(1), pp. 215-222.

GOTTSCH, J.D., BOWERS, A.L., MARGULIES, E.H., SEITZMAN, G.D., KIM, S.W., SAHA, S., JUN, A.S., STARK, W.J. and LIU, S.H., 2003. Serial analysis of gene expression in the corneal endothelium of Fuchs' dystrophy. *Investigative ophthalmology & visual science,* **44**(2), pp. 594-599.

GRIFFIN, M. A., SEN, S., SWEENEY, H. L. & DISCHER, D. E. 2004. Adhesion-contractile balance in myocyte differentiation. *Journal of cell science,* 117**,** 5855-5863.

GRIFFITH, M., OSBORNE, R., MUNGER, R., XIONG, X.J., DOILLON, C.J., LAYCOCK, N.L.C., HAKIM, M., SONG, Y. and WATSKY, M.A., 1999. Functional human corneal equivalents constructed from cell lines. *Science,* **286**(5447), pp. 2169-2172.

GRINNELL, F., 2008. Fibroblast mechanics in three-dimensional collagen matrices. *Journal of Bodywork and Movement Therapies,* **12**(3), pp. 191-193.

GUIDRY, C. and GRINNELL, F., 1985. Studies on the Mechanism of Hydrated Collagen Gel Reorganisation by Human-Skin Fibroblasts. *Journal of cell science,* **79**(1), pp. 67-81.

GUO, C. and KAUFMAN, L.J., 2007. Flow and magnetic field induced collagen alignment. *Biomaterials,* **28**(6), pp. 1105-1114.

GUO, X.Q., HUTCHEON, A.E.K., MELOTTI, S.A., ZIESKE, J.D., TRINKAUS-RANDALL, V. and RUBERTI, J.W., 2007. Morphologic characterization of organized extracellular matrix deposition by ascorbic acid-stimulated human corneal fibroblasts. *Investigative ophthalmology & visual science,* **48**(9), pp. 4050-4060.

HAAR, J.L. and ACKERMAN, G.A., 1971. Phase and Electron Microscopic Study of Vasculogenesis and Erythropoiesis in Yolk Sac of Mouse. *Anatomical Record,* **170**(2), pp. 199-223.

HADLOCK, T., SINGH, S., VACANTI, J.P., MCLAUGHLIN, B.J., 1999. Ocular cell monolayers cultured on biodegradable substrates. *Tissue Engineering,* **5**(3), pp. 187-196.

HARA, H. & COOPER, D. K. 2011. Xenotransplantation-the future of corneal transplantation? *Cornea,* 30**,** 371-8.

HAUS, J.M., CARRITHERS, J.A., TRAPPE, S.W. and TRAPPE, T.A., 2007. Collagen, cross-linking, and advanced glycation end products in ageing human skeletal muscle. *Journal of applied physiology,* **103**(6), pp. 2068-2076.

HAYASHI, Y., CALL, M.K., CHIKAMA, T., LIU, H., CARLSON, E.C., SUN, Y., PEARLMAN, E., FUNDERBURGH, J.L., BABCOCK, G., LIU, C., OHASHI, Y. and KAO, W.W., 2010. Lumican is required for neutrophil extravasation following corneal injury and wound healing. *Journal of cell science,* **123**(17), pp. 2987-2995.

HELARY, C., OVTRACHT, L., COULOMB, B., GODEAU, G. and GIRAUD-GUILLE, M.M., 2006. Dense fibrillar collagen matrices: A model to study myofibroblast behaviour during wound healing. *Biomaterials,* **27**(25), pp. 4443-4452.

HENDRIKS, J., RIESLE, J. and VAN BLITTERSWIJK, C.A., 2007. Co-culture in cartilage tissue engineering. *Journal of Tissue Engineering and Regenerative Medicine,* **1**(3), pp. 170-178.

HIBINO, T., WADA, Y., MISHIMA, H. and OTORI, T., 1998. The effect of corneal epithelial cells on the collagen gel contraction by keratocytes. *Japanese journal of ophthalmology,* **42**(3), pp. 174-179.

HICKS, C.R., FITTON, J.H., CHIRILA, T.V., CRAWFORD, G.J. and CONSTABLE, I.J., 1997. Keratoprostheses: Advancing toward a true artificial cornea. *Survey of ophthalmology,* **42**(2), pp. 175-189.

HINDMAN, H.B., SWANTON, J.N., PHIPPS, R.P., SIME, P.J. and HUXLIN, K.R., 2010. Differences in the TGF-beta 1-Induced Profibrotic Response of Anterior and Posterior

Corneal Keratocytes In Vitro. *Investigative ophthalmology & visual science,* **51**(4), pp. 1935-1942.

HOELTZEL, D.A., ALTMAN, P., BUZARD, K. and CHOE, K.I., 1992. Strip Extensiometry for Comparison of the Mechanical Response of Bovine, Rabbit, and Human Corneas. *Journal of Biomechanical Engineering-Transactions of the Asme,* **114**(2), pp. 202-215.

HOPPENREIJS, V., PELS, E., VRENSEN, G. and TREFFERS, W., 1994. Basic Fibroblast Growth-Factor Stimulates Corneal Endothelial-Cell Growth and Endothelial Wound-Healing of Human Corneas. *Investigative ophthalmology & visual science,* **35**(3), pp. 931-944.

HU, X.J., LUI, W., CUI, L., WANG, M. and CAO, Y.L., 2005. Tissue engineering of nearly transparent corneal stroma. *Tissue engineering,* **11**(11-12), pp. 1710-1717.

HUANG, Y. and LI, Q., 2007. An active artificial cornea with the function of inducing new corneal tissue generation in vivo - a new approach to corneal tissue engineering. *Biomedical Materials,* **2**(3), pp. 121-125.

HUANG, D., SWANSON, E. A., LIN, C. P., SCHUMAN, J. S., STINSON, W. G., CHANG, W., HEE, M. R., FLOTTE, T., GREGORY, K., PULIAFITO, C. A. & FUJIMOTO, J. G. 1991. Optical coherence tomography. *Science,* 254**,** 1178-1181.

IMANISHI, J., KAMIYAMA, K., IGUCHI, I., KITA, M., SOTOZONO, C. and KINOSHITA, S., 2000. Growth factors: Importance in wound healing and maintenance of transparency of the cornea. *Progress in retinal and eye research,* **19**(1), pp. 113-129.

ISHIZAKI, M., ZHU, G., HASEBA, T., SHAFER, S. S. & KAO, W. W. Y. 1993. Expression of collagen-I, smooth-muscle alpha-actin, and vimentin during the healing of alkali-burned and acerated corneas. *Investigative ophthalmology & visual science,* 34**,** 3320-3328.

ISOBE, Y., KOSAKA, T., KUWAHARA, G., MIKAMI, H., SAKU, T. and KODAMA, S., 2012. Oriented Collagen Scaffolds for Tissue Engineering. *Materials,* **5**(3), pp. 501-511.

ISLAM, M. and AKHTAR, A., 2001. Upregulation of Phospholipase Cγ1 Activity during EGF-Induced Proliferation of Corneal Epithelial Cells: Effect of Phosphoinositide-3 Kinase. *Investigative Opthamology and Visual Science*, **42**(7), pp. 1472-1478.

JAKUS, M.A.R.I.E.A., 1956. Studies on the cornea. II. The fine structure of Dascemet's membrane. *Journal of Biophysics and Biochemistry Cytology,* **2**(4), pp. 243-252.

JESTER, J.V., BUDGE, A., FISHER, S., HUANG, J., 2005. Corneal keratocytes: phenotypic and species differences in abundant protein expression and in vitro light-scattering. *Investigative Ophthalmology in Visual Science,* **46**(7), pp. 2369-2378.

JESTER, J.V. and JIN, H.C., 2003. Modulation of cultured corneal keratocyte phenotype by growth factors/cytokines control in vitro contractility and extracellular matrix contraction. *Experimental eye research,* **77**(5), pp. 581-592.

JESTER, J.V., LI, L., MOLAI, A. and MAURER, J.K., 2001. Extent of initial corneal injury as a basis for alternative eye irritation tests. *Toxicology in Vitro,* **15**(2), pp. 115-130.

JESTER, J.V., PETROLL, W.M., BARRY, P.A. and CAVANAGH, H.D., 1995. Expression of Alpha-Smooth Muscle (Alpha-Sm) Actin during Corneal Stromal Wound-Healing. *Investigative ophthalmology & visual science,* **36**(5), pp. 809-819.

JIANG, S.T., LIAO, K.K., LIAO, M.C. and TANG, M.J., 2000. Age effect of type I collagen on morphogenesis of Mardin-Darby canine kidney cells. *Kidney international,* **57**(4), pp. 1539-1548.

JU, B.F. and LIU, K.K., 2002. Characterizing viscoelastic properties of thin elastomeric membrane. *Mechanics of Materials,* **34**(8), pp. 485-491.

KAKAZU, A., CHANDRASEKHER, G and BAZAN, H.E.P., 2004. HGF Protects Corneal Epithelial Cells from Apoptosis by the PI-3K/Akt-1/Bad- but Not the ERK1/2-Mediated Signalling Pathway. *Investigative Opthamology and Visual Science,* **45**(10), pp. 3485-3492.

KAMMA-LORGER, C.S., BOOTE, C., HAYES, S., ALBON, J., BOULTON, M.E. and MEEK, K.M., 2009. Collagen ultrastructural changes during stromal wound healing in organ cultured bovine corneas. *Experimental eye research,* **88**(5), pp. 953-959.

KAO, W.W. and LIU, C., 2003. Roles of lumican and keratocan on corneal transparency. *Glycoconjugate journal,* **19**(4-5), pp. 275-285.

KARAMICHOS, D., BROWN, R.A. and MUDERA, V., 2007. Collagen stiffness regulates cellular contraction and matrix remodeling gene expression. *Journal of Biomedical Materials Research Part a,* **83**(3), pp. 887-894.

KARAMICHOS, D., GUO, X.Q., HUTCHEON, A.E.K. and ZIESKE, J.D., 2010. Human Corneal Fibrosis: An In Vitro Model. *Investigative ophthalmology & visual science,* **51**(3), pp. 1382-1388.

KARAMICHOS, D., HUTCHEON, A.E.K. and ZIESKE, J.D., 2011. Transforming growth factor-beta 3 regulates assembly of a non-fibrotic matrix in a 3D corneal model. *Journal of Tissue Engineering and Regenerative Medicine,* **5**(8), pp. 228-238.

KAUFMAN, D.S., HANSON, E.T., LEWIS, R.L., AUERBACH, R. and THOMSON, J.A., 2001. Hematopoietic colony-forming cells derived from human embryonic stem cells. *Proceedings of the National Academy of Sciences of the United States of America,* **98**(19), pp. 10716-10721.

KAWAKITA, T., ESPANA, E.M., HE, H., HORNIA, A., YEH, L.K., OUYANG, J., LIU, C.Y. and TSENG, S.C.G., 2005. Keratocan expression of murine keratocytes is maintained

on amniotic membrane by down-regulating transforming growth factor-beta signaling. *Journal of Biological Chemistry,* **280**(29), pp. 27085-27092.

KAWAKITA, T., ESPANA, E.M., HE, H., SMIDDY, R., PAREL, J.M., LIU, C.Y. and TSENG, S.C.G., 2006. Preservation and expansion of the primate keratocyte phenotype by downregulating TGF-beta signaling in a low-calcium, serum-free medium. *Investigative ophthalmology & visual science,* **47**(5), pp. 1918-1927.

KIM, A., ZHOU, C., LAKSHMAN, N. and PETROL, W.M., 2012. Corneal stromal cells use both high- and low-contractility migration mechanisms in 3-D collagen matrices. *Experimental cell research,* **318**(6), pp. 741-752.

KLENKLER, B. and SHEARDOWN, H., 2004. Growth factors in the anterior segment: role in tissue maintenance, wound healing and ocular pathology. *Experimental eye research,* **79**(5), pp. 677-688.

KOLLIAS, N., GILLIES, R., MORAN, M., KOCHEVAR, I. E. & ANDERSON, R. R. 1998. Endogenous skin fluorescence includes bands that may serve as quantitative markers of aging and photoaging. *Journal of investigative dermatology,* 111**,** 776-780.

KORHONEN, R.K., LAASANEN, M.S., TOYRAS, J., RIEPPO, J., HIRVONEN, J., HELMINEN, H.J. and JURVELIN, J.S., 2002. Comparison of the equilibrium response of articular cartilage in unconfined compression, confined compression and indentation. *Journal of Biomechanics,* **35**(7), pp. 903-909.

KOTECHA, A., 2007. What biomechanical properties of the cornea are relevant for the clinician? *Survey of ophthalmology,* **52**(2), pp. 109-114.

KRUEGER, R. R. & TROKEL, S. L. 1985. Quantifivation of corneal ablation by ultraviolet-laser light. *Archives of Ophthalmology,* 103**,** 1741-1742.

KRUPA, I., NEDELCEV, T., RACKO, D. and LACIK, I., 2010. Mechanical properties of silica hydrogels prepared and aged at physiological conditions: testing in the compression mode. *Journal of Sol-Gel Science and Technology,* **53**(1), pp. 107-114.

LAKSHMAN, N., KIM, A. and PETROLL, W.M., 2010. Characterization of Corneal Keratocyte Morphology and Mechanical Activity within 3-D Collagen Matrices. *Experimental Eye Research,* **90**(2), pp. 350-359.

LAKSHMAN, N. and PETROLL, W.M., 2012. Growth Factor Regulation of Corneal Keratocyte Mechanical Phenotypes in 3-D Collagen Matrices. *Investigative ophthalmology & visual science,* **53**(3), pp. 1077-1086.

LAMBERT, L.A., CHAMBERS, W.A., GREEN, S., GUPTA, K.C., HILL, R.N., HURLEY, P.M., LEE, C.C., LEE, J.K., LIU, P.T., LOWTHER, D.K., ROBERTS, C.D., SEABAUGH, V.M., SPRINGER, J.A. and WILCOX, N.L., 1993. The use of Low-Volume Dosing in the Eye Irritation Test. *Food and Chemical Toxicology,* **31**(2), pp. 99-103.

LAZARIDES, E. 1980. Intermediate filaments as mechanical integrators of cellular space. *Nature,* 283**,** 249-256.

LEVIN, A., NILSSON, F.E. VER HOEVE, J., WU, S., KAUFMAN, P.L. and ALM, A., 2011. *Adler's Physiology of the Eye.* 11th edition. Saunders Elsevier. Health Science Division, Philadelphia, USA.

LEVIS, H. and DANIELS, J.T., 2009. New technologies in limbal epithelial stem cell transplantation. *Current opinion in biotechnology,* **20**(5), pp. 593-597.

LIM, S. H. & MAO, H.-Q. 2009. Electrospun scaffolds for stem cell engineering. *Advanced Drug Delivery Reviews,* 61**,** 1084-1096.

LIM, M., YE, H., PANOSKALTSIS, N., DRAKAKIS, E.M., YUE, X.C., CASS, A.E.G., RADOMSKA, A. and MANTALARIS, A., 2007. Intelligent bioprocessing for haemotopoietic cell cultures using monitoring and design of experiments. *Biotechnology Advances,* **25**(4), pp. 353-368.

LINGELBACH, L.B., MITCHELL, A.E., RUCKER, R.B. and MCDONALD, R.B., 2000. Accumulation of advanced glycation endproducts in ageing male Fischer 344 rats during long-term feeding of various dietary carbohydrates. *Journal of Nutrition,* **130**(5), pp. 1247-1255.

LIU, K.K. and JU, B.F., 2001. A novel technique for mechanical characterization of thin elastomeric membrane. *Journal of Physics D-Applied Physics,* **34**(15), pp. 91-94.

LOPERGOLO, L. C., LUGAO, A. B. & CATALAINI, L. H. 2002. Development of a poly(N-vinyl-2-pyrrolidone)/poly (ethylene glycol) hydrogel membrane reinforced with methyl methacrylate-grafted polypropylene fibers for possible use as wound dressing. *Journal of Applied Polymer Science,* 86**,** 662-666.

LU, L., REINACH, P.S. and KAO, W.W., 2001. Corneal Epithelial Wound Healing. *Experimental Biology and Medicine,* **226**(7), pp. 653-664.

LYU, J., LEE, K. and JOO, C., 2006. Transactivation of EGFR Mediates Insulin-Stimulated ERK1/2 Activation and Enhanced Cell Migration in Human Corneal Epithelial Cells. *Molecular Vision,* **12**(157), pp. 1403-1410.

MARENZANA, M., WILSON-JONES, N., MUDERA, V. and BROWN, R., 2006. The origins and regulation of tissue tension: Identification of collagen tension-fixation process in vitro. *Experimental cell research,* **312**(4), pp. 423-433.

MATSUDA, S., HISAMA, M., SHIBAYAMA, H., ITOU, N. and IWAKI, M., 2009. Application of the Reconstructed Rabbit Corneal Epithelium Model to Assess the in Vitro Eye Irritancy Test of Chemicals. *Yakugaku Zasshi-Journal of the Pharmaceutical Society of Japan,* **129**(9), pp. 1113-1120.

MAURICE, D. M. 1957. The structure and transparency of the cornea. The *Journal of Physiology,* 136**,** 263-286.

MAURICE, D.M., 1988. Mechanics of the Cornea. In: *The Cornea: Transactions of the World Congress on the Cornea III.* 8 edition, Edited by CAVANAGH, H.D., New York: Raven Press Ltd, pp. 187.

MAYS, P., MCANULTY, R., CAMPA, J. and LAURENT, G., 1991. Age-Related-Changes in Collagen-Synthesis and Degradation in Rat-Tissues - Importance of Degradation of Newly Synthesized Collagen in Regulating Collagen Production. *Biochemical Journal,* **276**(2), pp. 307-313.

MAZZOLENI, G., DI LORENZO, D. and STEIMBERG, N., 2009. Modelling tissues in 3D: the next future of pharmaco-toxicology and food research? *Genes and Nutrition,* **4**(1), pp. 13-22.

MCLAUGHLIN, C.R., TSAI, R.J.F., LATORRE, M.A. and GRIFFITH, M., 2009. Bioengineered corneas for transplantation and in vitro toxicology. *Frontiers in Bioscience,* **14**(1), pp. 3326-3337.

MEEK, K.M. and BOOTE, C., 2004. The organization of collagen in the corneal stroma. *Experimental eye research,* **78**(3), pp. 503-512.

MEEK, K.M. and BOOTE, C., 2009. The use of X-ray scattering techniques to quantify the orientation and distribution of collagen in the corneal stroma. *Progress in retinal and eye research,* **28**(5), pp. 369-392.

MI, S., CHEN, B., WRIGHT, B. and CONNON, C.J., 2010. Ex Vivo Construction of an Artificial Ocular Surface by Combination of Corneal Limbal Epithelial Cells and a Compressed Collagen Scaffold Containing Keratocytes. *Tissue Engineering Part a,* **16**(6), pp. 2091-2100.

MIKULIKOVA, K., ECKHARDT, A., PATARIDIS, S. and MIKSIK, I., 2007. Study of posttranslational non-enzymatic modifications of collagen using capillary electrophoresis/mass spectrometry and high performance liquid chromatography/mass spectrometry. *Journal of Chromatography a,* **1155**(2), pp. 125-133.

MILLER, S.J.H. and PARSONS, J.H., 2002. *Parsons' Diseases of the Eye.* 18th Edition, Edited by: MILLER, S.J.H., Churchill Livingstone, University of California, USA.

MINAMI, Y., SUGIHARA, H. and OONO, S., 1993. Reconstruction of Cornea in 3-Dimensional Collagen Gel Matrix Culture. *Investigative ophthalmology & visual science,* **34**(7), pp. 2316-2324.

MOCAN, E., TAGADIUC, O. and NACU, V., 2011. Aspects of Collagen Isolation Procedure. *Clinical Research Studies,* **2**(320), pp. 3-5.

MOHAN, R.R., GUPTA, R., MEHAN, M.K., COWDEN, J.W. and SINHA, S., 2010. Decorin transfection suppresses profibrogenic genes and myofibroblast formation in human corneal fibroblasts. *Experimental eye research,* **91**(2), pp. 238-245.

MOHAN, R.R., TOVEY, J.C.K., GUPTA, R., SHARMA, A. and TANDON, A., 2011. Decorin Biology, Expression, Function and Therapy in the Cornea. *Current Molecular Medicine,* **11**(2), pp. 110-128.

MORONI, L., SCHOTEL, R., HAMANN, D., DE WIJN, J. R. & VAN BLITTERSWIJK, C. A. 2008. 3D Fiber-Deposited Electrospun Integrated Scaffolds Enhance Cartilage Tissue Formation. *Advanced Functional Materials,* 18**,** 53-60.

MULHOLLAND, B., TUFT, S. and KHAW, P., 2005. Matrix metalloproteinase distribution during early corneal wound healing. *Eye,* **19**(5), pp. 584-588.

MUSSELMANN, K., 2006. Developing Culture Conditions to Study Keratocyte Phenotypes in Vitro. *PhD thesis,* University of South Florida.

MUSSELMANN, K., ALEXANDROU, B., KANE, B. and HASSELL, J.R., 2005. Maintenance of the keratocyte phenotype during cell proliferation stimulated by insulin. *Journal of Biological Chemistry,* **280**(38), pp. 32634-32639.

MUSSELMANN, K., KANE, B., ALEXANDROU, B. and HASSELL, J.R., 2006. Stimulation of collagen synthesis by insulin and proteoglycan accumulation by ascorbate in bovine keratocytes in vitro. *Investigative ophthalmology & visual science,* **47**(12), pp. 5260-5266.

NAKAMURA, K., KUROSAKA, D., YOSHINO, M., OSHIMA, T. and KUROSAKA, H., 2002. Injured corneal epithelial cells promote myodifferentiation of corneal fibroblasts. *Investigative ophthalmology & visual science,* **43**(8), pp. 2603-2608.

NAKAMURA, M., KIMURA, S., KOBAYASHI, M., HIRANO, K., HOSHINO, T. & AWAYA, S. 1997. Type VI collagen bound to collagen fibrils by chondroitin/dermatan sulfate glycosaminoglycan in mouse corneal stroma. *Japanese Journal of Ophthalmology,* 41**,** 71-6.

NAKAZAWA, K., TAKAHASHI, I., OHNO, Y. and SATO, M., 1997. Modification of proteoglycan synthesis by corneal stromal cells on co-culture with either epithelial or endothelial cells. *Journal of Biochemistry,* **122**(4), pp. 851-858.

NAYLOR, E. 1953. The structure of the cornea as revealed by polarized light. *Quarterly Journal of Microscopical Science,* 3**,** 83-88.

NETTO, M.V., MOHAN, R.R., SINHA, S., SHARMA, A., DUPPS, W. and WILSON, S.E., 2006. Stromal haze, myofibroblasts, and surface irregularity after PRK. *Experimental eye research,* **82**(5), pp. 788-797.

NEWELL, F. W. 1981. Introduction to radial keratotomy. *American Journal of Ophthalmology,* 92**,** 286-286.

NEWMAN, S., CLOITRE, M., ALLAIN, C., FORGACS, G. and BEYSENS, D., 1997. Viscosity and elasticity during collagen assembly in vitro: Relevance to matrix-driven translocation. *Biopolymers,* **41**(3), pp. 337-347.

NIEDERKORN, J., 2003. The immune privilege of corneal grafts. *Journal of leukocyte biology,* **74**(2), pp. 167-171.

NICHOL, J. W., KOSHY, S. T., BAE, H., HWANG, C. M., YAMANLAR, S. & KHADEMHOSSEINI, A. 2010. Cell-laden microengineered gelatin methacrylate hydrogels. *Biomaterials,* 31**,** 5536-5544.

NISHIMURA, T., TODA, S., MITSUMOTO, T., OONO, S. and SUGIHARA, H., 1998. Effects of hepatocyte growth factor, transforming growth factor-beta 1 and epidermal growth factor on bovine corneal epithelial cells under epithelial-keratocyte interaction in reconstruction culture. *Experimental eye research,* **66**(1), pp. 105-116.

O'KEEFE, M. and KIRWAN, C., 2010. Laser epithelial keratomileusis in 2010-a review. *Clinical and Experimental Ophthalmology,* **38**(2), pp. 183-191.

ORWIN, E.J., BORENE, M.L. and HUBEL, A., 2003. Biomechanical and optical characteristics of a corneal stromal equivalent. *Journal of Biomechanical Engineering-Transactions of the Asme,* **125**(4), pp. 439-444.

ORWIN, E.J. and HUBEL, A., 2000. In vitro culture characteristics of corneal epithelial, endothelial, and keratocyte cells in a native collagen matrix. *Tissue engineering,* **6**(4), pp. 307-319.

OZDAL, M.P.C., MANSOUR, M. and DESCHENES, J., 2003. Ultrasound biomicroscopic evaluation of the traumatized eyes. *Eye,* **17**(4), pp. 467-472.

PAN, Z., SUN, C., JIE, Y., WANG, N. and WANG, L., 2007. WZS-pig is a potential donor alternative in corneal xenotransplantation. *Xenotransplantation,* **14**(6), pp. 603-611.

PANG, K., DU, L. and WU, X., 2010. A rabbit anterior cornea replacement derived from acellular porcine cornea matrix, epithelial cells and keratocytes. *Biomaterials,* **31**(28), pp. 7257-7265.

PAULING, L. 1979. Diamagnetic Anisotropy of the Peptide Group. *Proceedings of the National Academy of Science,* **76**(5), 2293-2294.

PEI, Y., REINS, R.Y. and MCDERMOTT, A.M., 2006. Aldehyde dehydrogenase (ALDH) 3A1 expression by the human keratocyte and its repair phenotypes. *Experimental eye research,* **83**(5), pp. 1063-1073.

PEI, Y., SHERRY, D.M. and MCDERMOTT, A.M., 2004. Thy-1 distinguishes human corneal fibroblasts and myofibroblasts from keratocytes. *Experimental eye research,* **79**(5), pp. 705-712.

PETROLL, W., JESTER, J., BEAN, J. and CAVANAGH, H., 1998. Myofibroblast transformation of cat corneal endothelium by transforming growth factor-beta(1), -beta(2), and -beta(3). *Investigative ophthalmology & visual science,* **39**(11), pp. 2018-2032.

PINTUCCI, S., PINTUCCI, F., CECCONI, M. and CAIAZZA, S., 1995. New Dacron Tissue Colonisable Keratoprosthesis - Clinical-Experience. *British Journal of Ophthalmology,* **79**(9), pp. 825-829.

PIRIE, A., 1976. Xerophthalmia. *Investigative ophthalmology,* **15**(5), pp. 417-422.

PRINSEN, M.K., 1996. The chicken enucleated eye test (CEET): A practical (pre)screen for the assessment of eye irritation/corrosion potential of test materials. *Food and Chemical Toxicology,* **34**(3), pp. 291-296.

PRITZ, T. 2000. Measurement methods of complex Poisson's ratio of viscoelastic materials. *Applied Acoustics,* 60**,** 279-292.

QU, L., YANG, X.Y., WANG, X., ZHAO, M., MI, S.L., DOU, Z.Y. and WANG, H.Y., 2009. Reconstruction of corneal epithelium with cryopreserved corneal limbal stem cells in a rabbit model. *Veterinary Journal,* **179**(3), pp. 392-400.

REICHL, S., BEDNARZ, J. and MULLER-GOYMANN, C.C., 2004. Human corneal equivalent as cell culture model for in vitro drug permeation studies. *British Journal of Ophthalmology,* **88**(4), pp. 560-565.

REICHL, S., DOHRING, S., BEDNARZ, J. and MULLER-GOYMANN, C.C., 2005. Human cornea construct HCC - an alternative for in vitro permeation studies? A comparison with human donor corneas. *European Journal of Pharmaceutics and Biopharmaceutics,* **60**(2), pp. 305-308.

REICHL, S. and MULLER-GOYMANN, C.C., 2001. Development of an organotypical cornea construct as an in vitro model for permeation studies. *Ophthalmologe,* **98**(9), pp. 853-858.

REICHL, S. and MULLER-GOYMANN, C.C., 2003. The use of a porcine organotypic cornea construct for permeation studies from formulations containing befunolol hydrochloride. *International journal of pharmaceutics,* **250**(1), pp. 191-201.

REISER, K. 1991. Nonenzymatic Glycation of Collagen in Aging and Diabetes. *Proceedings for the Society Experimental Biology and Medicine* ,**196**(1), pp. 17-29.

RIECK, P., ASSOULINE, M., SAVOLDELLI, M., HARTMANN, C., JACOB, C., POULIQUEN, Y. & COURTOIS, Y. 1992. Recombinany human basic fibroblast-growth factor (RH-BFGF)in 3 different wound models in rabbits -corneal wound-healing effect and pharmacology. *Experimental eye research,* 54**,** 987-998.

RIVLIN, R.S., 1948. Large Elastic Deformations of Isotropic Materials .4. further Developments of the General Theory. *Philosophical Transactions of the Royal Society of London Series A-Mathematical and Physical Sciences,* **241**(835), pp. 379-397.

ROUJEAU, J., KELLY, J., NALDI, L., RZANY, B., STERN, R., ANDERSON, T., AUQUIER, A., BASTUJIGARIN, S., CORREIA, O., LOCATI, F., MOCKENHAUPT, M., PAOLETTI, C., SHAPIRO, S., SHEAR, N., SCHOPF, E. and KAUFMAN, D., 1995. Medication use and the Risk of Stevens-Johnson Syndrome Or Toxic Epidermal Necrolysis. *New England Journal of Medicine,* **333**(24), pp. 1600-1607.

RUBERTI, J.W. and ZIESKE, J.D., 2008. Prelude to corneal tissue engineering - Gaining control of collagen organisation. *Progress in retinal and eye research,* **27**(5), pp. 549-577.

RUBERTI, J.W., ZIESKE, J.D. and TRINKAUS-RANDALL, V., 2007. Corneal-Tissue Replacement. In: *Principles of Tissue Engineering.* 3rd edition, edited by: LANZA, R.P., LANGER, R. and VACANTI, J. Elsevier Academic Press, pp. 1025.

RUBIN, A. L., PFAHL, D., SPEAKMAN, P. T., DAVISON, P. F. & SCHMITT, F. O. 1963. Tropocollagen: significance of protease-induced alterations. *Science,* 139**,** 37-9.

SACHLOS, E. and CZERNUSZKA, J.T., 2003. Making tissue engineering scaffolds work: Review on the application of solid freeform fabrication technology to the production of tissue engineering scaffolds. *European Cells & Materials,* **5**(1), pp. 29-40.

SANDEMAN, S.R., LLOYD, A.W., TIGHE, B.J., FRANKLIN, V., LI, J., LYDON, F., LIU, C.S.C., MANN, D.J., JAMES, S.E. and MARTIN, R., 2003. A model for the preliminary biological screening of potential keratoprosthetic biomaterials. *Biomaterials,* **24**(26), pp. 4729-4739.

SCHERMER, A., GALVIN, S. & SUN, T. T. 1986. Differentiation-related expression of a major 64K corneal keratin in vivo and in culture suggests limbal location of corneal epithelial stem cells. *The Journal of Cell Biology,* 103**,** 49-62.

SCHNEIDER, A.I., MAIER-REIF, K. and GRAEVE, T., 1999. Constructing an in vitro cornea from cultures of the three specific corneal cell types. *In Vitro Cellular & Developmental Biology-Animal,* **35**(9), pp. 515-526.

SCHULZE, C., WETZEL, F., KUEPER, T., MALSEN, A., MUHR, G., JASPERS, S., BLATT, T., WITTERN, K., WENCK, H. and KAS, J.A., 2012. Stiffening of human skin fibroblasts with age. *Clinics in plastic surgery,* **39**(1), pp. 9-20.

SCHULTZ, G., KHAW, P., OXFORD, K., MACAULEY, S., VANSETTEN, G. and CHEGINI, N., 1994. Growth-Factors and Ocular Wound-Healing. *Eye,* **8**(2), pp. 184-187.

SEMBA, R.D., NICKLETT, E.J. and FERRUCCI, L., 2010. Does Accumulation of Advanced Glycation End Products Contribute to the Ageing Phenotype? *Journals of Gerontology Series A-Biological Sciences and Medical Sciences,* **65**(9), pp. 963-975.

SHAO, Y., YU, Y., PEI, C. G., ZHOU, Q., LIU, Q. P., TAN, G., LI, J. M., GAO, G. P. & YANG, L. 2012. Evaluation of novel decellularizing corneal stroma for cornea tissue engineering applications. *International Journal of Ophthalmology,* 5**,** 415-8.

SHEASGREEN, J., KLAUSNER, M., KANDAROVA, H. and INGALLS, D., 2009. The MatTek Story - How the Three Rs Principles Led to 3-D Tissue Success! *Atla-Alternatives to Laboratory Animals,* **37**(6), pp. 611-622.

SINGH, R., BARDEN, A., MORI, T. and BEILIN, L., 2002. Advanced glycation end-products: a review (vol 44, pg 129, 2001). *Diabetologia,* **45**(2), pp. 293-293.

SKUTA, G.L., CANTOR, L.B. and WEISS, J.S., 2011. Refractive Surgery: Section 13 Basic and Clinical Science Course. 1st edition. Lifelong Education for the Ophthalmologist, American Academy of Ophthalmology, USA.

SOTOZONO, C., INATOMI, T., NAKAMURA, M. and KINOSHITA, S., 1995. Keratinocyte Growth-Factor Accelerates Corneal Epithelial Wound-Healing In-Vivo. *Investigative ophthalmology & visual science,* **36**(8), pp. 1524-1529.

SOTOZONO, C., KINOSHITA, S., KITA, M. and IMANISHI, J., 1994. Paracrine Role of Keratinocyte Growth-Factor in Rabbit Corneal Epithelial-Cell Growth. *Experimental eye research,* **59**(4), pp. 385-391.

SMITH, L. A., LIU, X. & MA, P. X. 2008. Tissue engineering with nano-fibrous scaffolds. *Soft Matter,* 4**,** 2144-2149.

SPARKS, D., SMITH, R., CRUZ, V., TRAN, N., CHIMBAYO, A., RILEY, D. and NAJAFI, N., 2009. Dynamic and kinematic viscosity measurements with a resonating microtube. *Sensors and Actuators A: Physical,* **149**(1), pp. 38-41.

STAMMEN, J.A., WILLIAMS, S., KU, D.N. and GULDBERG, R.E., 2001. Mechanical properties of a novel PVA hydrogel in shear and unconfined compression. *Biomaterials,* **22**(8), pp. 799-806.

STEELE, C., 1999. Corneal wound healing: a review. *Optometry today,* **40**(1), pp. 28-32.

STEVEN, F. & JACKSON, D. 1967. Purification and amino acid composition of monomeric and polymeric collagens. *Biochemical Journal,* 104**,** 534.

STEVENSON, W., CHENG, S.-F., EMAMI-NAEINI, P., HUA, J., PASCHALIS, E. I., DANA, R. & SABAN, D. R. 2012. Gamma-Irradiation Reduces the Allogenicity of Donor Corneas. *Invesigativet ophthalmology & Visual Science,* 53**,** 7151-7158.

STOOP, R., 2008. Smart biomaterials for tissue engineering of cartilage. *Injury-International Journal of the Care of the Injured, **39***(1), pp. 77-87.

SULLIVAN-MEE, M., BILLINGSLEY, S.C., PATEL, A.D., HALVERSON, K.D., ALLDREDGE, B.R. and QUALLS, C., 2008. Ocular Response Analyzer in subjects with and without glaucoma. *Optometry and Vision Science,* **85**(6), pp. 463-470.

SUNYER, R., JIN, A. J., NOSSAL, R. & SACKETT, D. L. 2012. Fabrication of hydrogels with steep stiffness gradients for studying cell mechanical response. *Plos One,* 7**,** e46107.

SUTPHIN, J.E., 2007. *External disease and cornea: 2007-2008.* San Fransisco, CA: American Academy of Opthalmology., USA.

SUURONEN, E.J., MCLAUGHLIN, C.R., STYS, P.K., NAKAMURA, M., MUNGER, R. and GRIFFITH, M., 2004. Functional innervation in tissue engineered models for in vitro study and testing purposes. *Toxicological Sciences,* **82**(2), pp. 525-533.

SUZUKI, K., Saito J, Yanai R, Yamada N, Chikama T, Seki K, Nishida T., 2003. Cell-Matrix, and Cell-Cell Interactions during Corneal Epithelial Wound Healing. *Progress in Retinal and Eye Research,* **22**(2), pp. 113-133.

TEGTMEYER, S., PAPANTONIOU, I. and MULLER-GOYMANN, C.C., 2001. Reconstruction of an in vitro cornea and its use for drug permeation studies from different formulations containing pilocarpine hydrochloride. *European Journal of Pharmaceutics and Biopharmaceutics,* **51**(2), pp. 119-125.

TEO, W.E. and RAMAKRISHNA, S., 2006. A review on electrospinning design and nanofibre assemblies. *Nanotechnology,* **17**(14), pp. 89-106.

THEN, K.Y., YANG, Y., AHEARNE, M. and EL HAJ, A.J., 2011. Effect of Microtopographical Cues on Human Keratocyte Orientation and Gene Expression. *Curr Eye Res,* **36**(2), pp. 88-93.

THYLEFORS, B., 1992. Epidemiologic Patterns of Ocular Trauma. *Australian and New Zealand Journal of Ophthalmology,* **20**(2), pp. 95-98.

TORBET, J., MALBOUYRES, M., BUILLES, N., JUSTIN, V., ROULET, M., DAMOUR, O., OLDBERG, A., RUGGIEO, F. and HULMES, D.J.S., 2007. Orthogonal scaffold of magnetically aligned collagen lamellae for corneal stroma reconstruction. *Biomaterials,* **28**, pp. 4268-4276.

TORBET, J. & RONZIERE, M. C. 1984. Magnetic Alignment of Collagen during Self-Assembly. *Biochemical Journal,* 219.

TSAKALAKOS, T., 1981. The Bulge Test - a Comparison of Theory and Experiment for Isotropic and Anisotropic Films. *Thin Solid Films,* **75**(3), pp. 293-305.

TSENG, S.C.G., 2001. Amniotic membrane transplantation for ocular surface reconstruction. *Bioscience reports,* **21**(4), pp. 481-489.

TUFT, S., GARTRY, D., RAWE, I. and MEEK, K., 1993. Photorefractive Keratectomy - Implications of Corneal Wound-Healing. *British Journal of Ophthalmology,* **77**(4), pp. 243-247.

URBAK, S.F., 1999. Ultrasound biomicroscopy. III. Accuracy and agreement of measurements. *Acta Ophthalmologica Scandinavica,* **77**(3), pp. 293-297.

VALIRON, O., PERIS, L., RIKKEN, G., SCHWEITZER, A., SAOUDI, Y., REMY, C. and JOB, D., 2005. Cellular disorders induced by high magnetic fields. *Journal of Magnetic Resonance Imaging,* **22**(3), pp. 334-340.

VRANA, N.E., BUILLES, N., JUSTIN, V., BEDNARZ, J., PELLEGRINI, G., FERRARI, B., DAMOUR, O., HULMES, D.J.S. and HASIRCI, V., 2008. Development of a Reconstructed Cornea from Collagen-Chondroitin Sulfate Foams and Human Cell Cultures. *Investigative ophthalmology & visual science,* **49**(12), pp. 5325-5331.

VRANA, N.E., ELSHEIKH, A., BUILLES, N., DAMOUR, O. and HASIRCI, V., 2007. Effect of human corneal keratocytes and retinal pigment epithelial cells on the mechanical properties of micropatterned collagen films. *Biomaterials,* **28**(29), pp. 4303-4310.

WALTON, R.S., BRAND, D.D. and CZERNUSZKA, J.Y., 2010. Influence of telopeptides, fibrils and crosslinking on physiochemical properties of Type I collagen films. *Journal of Materials Science: Materials in Medicine,* **21**(1), pp. 451-461.

WANG, J.H., GAO, C., ZHANG, Y.S. and WAN, Y.Z., 2010. Preparation and in vitro characterization of BC/PVA hydrogel composite for its potential use as artificial cornea biomaterial. *Materials Science & Engineering C-Materials for Biological Applications,* **30**(1), pp. 214-218.

WANG, L., KO, C., MEYERS, E.E., PEDROJA, B.S., PELAEZ, N. and BERNSTEIN, A.M., 2011. Concentration-dependent effects of transforming growth factor beta 1 on corneal wound healing. *Molecular Vision,* **17**(308), pp. 2835-2846.

WANG, Y., WANG, G., LUO, X., QIU, J. & TANG, C. 2012. Substrate stiffness regulates the proliferation, migration, and differentiation of epidermal cells. *Burns,* 38**,** 414-20.

WEST-MAYS JA FAU - DWIVEDI, DHRUVA,J. and DWIVEDI, D.J., 2006. The keratocyte: corneal stromal cell with variable repair phenotypes. *International Journal of Biochemistry and Cell Biology,* **38**(10), pp. 1625-1631.

WHITCHER, J., SRINIVASAN, M. and UPADHYAY, M., 2001. Corneal blindness: a global perspective. *Bulletin of the World Health Organization,* **79**(3), pp. 214-221.

WILHELMUS, K.R., 2001. The Draize eye test. *Survey of ophthalmology,* **45**(6), pp. 493-515.

WILLEMS, N.M.B.K., LANGENBACH, G.E.J., EVERTS, V., MULDER, L., GRUNHEID, T., BANK, R.A., ZENTNER, A. and VAN EIJDEN, T.M.G.J., 2011. Age-Related Changes in Collagen Properties and Mineralization in Cancellous and Cortical Bone in the Porcine Mandibular Condyle. *Calcified tissue international,* **88**(4), pp. 348-349.

WILSON, S., HE, Y., WENG, J., ZIESKE, J., JESTER, J. and SCHULTZ, G., 1994. Effect of Epidermal Growth-Factor, Hepatocyte Growth-Factor, and Keratinocyte Growth-Factor, on Proliferation, Motility and Differentiation of Human Corneal Epithelial-Cells. *Experimental eye research,* **59**(6), pp. 665-678.

WILSON, S.E., LIU, J.J. and MOHAN, R.R., 1999. Stromal-epithelial interactions in the cornea. *Progress in retinal and eye research,* **18**(3), pp. 293-309.

WILSON, S.E., NETTO, M. and AMBRÓSIO JR., R., 2003. Corneal cells: chatty in development, homeostasis,wound healing, and disease. *American Journal of Ophthalmology,* **136**(3), pp. 530-536.

WILSON, S.L., WIMPENNY, I., AHEARNE, M., RAUZ, S., HAJ, A.J.E. and YANG, Y., 2012a. Chemical and Topographical Effects on Cell Differentiation and Matrix Elasticity in a Corneal Stromal Layer Model. *Advanced Functional Materials,* **22**(17), pp. 3641-3649.

WILSON, S.L., GUILBERT, M., SULE-SUSO, J., TORBET, J., JEANNESSON, P., SOCKALINGUM, G.D. and YANG, Y., 2012b. The effect of collagen ageing on its structure and cellular behaviour. *Dynamics and Fluctuations in Biomedical Photonics ix,* **8222**(1), pp. 110-116.

WILSON, S.L., EL HAJ, A.J. and YANG, Y., 2012c. Control of Scar Tissue Formation in the Cornea: Strategies in Clinical and Corneal Tissue Engineering. *Advanced Functional Biomaterials,* **3**(3), pp. 642-687.

WORCESTER, D., 1978. Structural Origins of Diamagnetic Anisotropy in Proteins. *Proceedings of the National Academy of Sciences of the United States of America,* **75**(11), pp. 5475-5477.

WISE, J. K., YARIN, A. L., MEGARIDIS, C. M. & CHO, M. 2009. Chondrogenic Differentiation of Human Mesenchymal Stem Cells on Oriented Nanofibrous Scaffolds: Engineering the Superficial Zone of Articular Cartilage. *Tissue Engineering Part a,* 15**,** 913-921.

WRAY, L.S. and ORWIN, E.J., 2009. Recreating the Microenvironment of the Native Cornea for Tissue Engineering Applications. *Tissue Engineering Part a,* **15**(7), pp. 1463-1472.

WU, J., DU, Y., WATKINS, S.C., FUNDERBURGH, J.L. and WAGNER, W.R., 2012. The engineering of organized human corneal tissue through the spatial guidance of corneal stromal stem cells. *Biomaterials,* **33**(5), pp. 1343-1352.

XU, Y.G., XU, Y.S., HUANG, C., FENG, Y., LI, Y. and WANG, W., 2008. Development of a rabbit corneal equivalent using an acellular corneal matrix of a porcine substrate. *Molecular Vision,* **14**(253-55), pp. 2180-2189.

YANG, W.H. and HSU, K.H., 1971. Indentation of a Circular Membrane. *Journal of Applied Mechanics,* **38**(1), pp. 227-231.

YANG, Y., BAGNANINCHI, P.O., AHEARNE, M., WANG, R.K. and LIU, K.K., 2007. A novel optical coherence tomography-based micro-indentation technique for mechanical characterization of hydrogels. *Journal of the Royal Society Interface,* **4**(17), pp. 1169-1173.

YANG, Y., DUBOIS, A., QIN, X.P., LI, J., EL HAJ, A. and WANG, R.K., 2006. Investigation of optical coherence tomography as an imaging modality in tissue engineering. *Physics in Medicine and Biology,* **51**(7), pp. 1649-1659.

YANG, Y., WIMPENNY, I. and AHEARNE, M., 2011. Portable nanofiber meshes dictate cell orientation throughout three-dimensional hydrogels. *Nanomedicine-Nanotechnology Biology and Medicine,* **7**(2), pp. 131-136.

YOSHIDA, S., Shimmura S, Shimazaki J, Shinozaki N, Tsubota K., 2005. Serum-Free Spheroid Culture of Mouse Corneal Keratocytes. *Investigative Ophthalmology & Visual Science,* **46**(5), pp. 1653-1658.

ZENG, Y.J., YANG, J., HUANG, K., LEE, Z.H. and LEE, X.Y., 2001. A comparison of biomechanical properties between human and porcine cornea. *Journal of Biomechanics,* **34**(4), pp. 533-537.

ZERBE, B.L., BELIN, M.W., CIOLINO, J.B. and BOSTON TYPE 1 KERATOPROSTHESIS STU, 2006. Results from the multicenter Boston type 1 keratoprosthesis study. *Ophthalmology,* **113**(10), pp. 1779-1784.

ZHANG, Y., LIOU, G., GULATI, A. and AKHTAR, R., 1999. Expression of Phosphatidylinositol 3-Kinase during EGF-Stimulated Wound Repair in Rabbit Corneal Epithelium. *Investigative Ophthalmology & Visual Science,* **40**(12), pp. 2819-2826.

ZIESKE, J., TAKAHASHI, H., HUTCHEON, A. and DALBONE, A., 2000. Activation of epidermal growth factor receptor during corneal epithelial migration. *Investigative ophthalmology & visual science,* **41**(6), pp. 1346-1355.

Appendix

A1. Publication list

AHEARNE, M., **WILSON, S.L**., LIU, K., RAUZ, S., EL HAJ, A.J. and YANG, Y., 2010. Influence of cell and collagen concentration on the cell-matrix mechanical relationship in a corneal stroma wound healing model. *Experimental Eye Research,* **91**(5), pp. 584-591.

WILSON, S.L., WIMPENNY, I., AHEARNE, M., RAUZ, S., HAJ, A.J.E. and YANG, Y., 2012. Chemical and Topographical Effects on Cell Differentiation and Matrix Elasticity in a Corneal Stromal Layer Model. *Advanced Functional Materials,* **22**(17), pp. 3641-3649.

WILSON, S.L., GUILBERT, M., SULE-SUSO, J., TORBET, J., JEANNESSON, P., SOCKALINGUM, G.D. and YANG, Y., 2012. The effect of collagen ageing on its structure and cellular behaviour. *Dynamics and Fluctuations in Biomedical Photonics ix,* **8222**(1), pp. 110-116.

WILSON, S.L., EL HAJ, A.J. and YANG, Y., 2012. Control of Scar Tissue Formation in the Cornea: Strategies in Clinical and Corneal Tissue Engineering. *Advanced Functional Biomaterials,* **3**(3), pp. 642-687.

WILSON, S.L., SIDNEY, L.E., ROSE, J.B., DUNPHY, S. and HOPKINSON, A., 2013. Keeping an Eye on Decellularized Corneas: A Review of Methods, Characterization and Applications. *Advanced Functional Biomaterials,* **4**(3), pp 114-161

WILSON, S.L., YANG, Y. and EL HAJ, A.J., 2013. Corneal stromal cell plasticity: regulation of cell maturation through cell-cell interactions. Accepted for publication in *Tissue Engineering: Part A,* July 28, doi: 10.1089/ten.TEA.2013.0167

WILSON, S.L., GUILBERT, M., SULE-SUSO, J., TORBET, J., JEANNESSON, P., SOCKALINGUM, G.D. and YANG, Y., 2013. A microscopic and macroscopic study of ageing collagen on its molecular structure, mechanical properties, and cellular response. Accepted for publication in *FASEB J,* August 26, doi: 10.1096/fj.13-227579.

WILSON, S.L., EL HAJ, A.J. and YANG, Y. 2013. The mechanical characterisation of collagen hydrogels and their implications on molecular alterations. Book chapter submitted *Hydrogels in Cell-based Therapies,* RSCC Soft Matter Series, RSC Publishing, Series ISSN: 2048-7681.

A2. Ethical Approval

North Staffordshire Research and Development Consortium NHS

DEPARTMENT OF RESEARCH AND DEVELOPMENT
Medical Research Unit
Thornburrow Drive
Hartshill
Stoke-on-Trent
ST4 7QB
Telephone: 01782 554334
Fax: 01782 412236

Email: darren.clement@uhns.nhs.uk
katie.roebuck@uhns.nhs.uk

28th September 2007

Dr Ying Yang
Senior Lecturer in Biomaterials & Tissue engineering
Guy Hilton Centre
Thornburrow Drive
Hartshill
Stoke on Trent
Staffordshire
ST4 7QB

Dear Dr Yang,

Re: Investigation into Novel in vitro corneal model with on-line mechanical characterisation for pharmaceutical screening and tissue engineering

I can confirm that the above project has been approved by the Research & Development Department. The details of the project will be entered on to the R&D database and will be included with our next submission to the National Research Register.

I note that this research project has been designated as being SSA exempt and has been approved by the Black Country Research Ethics Committee.

If you need any further advice or guidance please do not hesitate to contact us.

Yours sincerely,

Darren Clement
R&D Manager - North Staffordshire NHS R&D Consortium